

## INFORMATION TO USERS

The most advanced technology has been used to photograph and reproduce this manuscript from the microfilm master. UMI films the text directly from the original or copy submitted. Thus, some thesis and dissertation copies are in typewriter face, while others may be from any type of computer printer.

The quality of this reproduction is dependent upon the quality of the copy submitted. Broken or indistinct print, colored or poor quality illustrations and photographs, print bleedthrough, substandard margins, and improper alignment can adversely affect reproduction.

In the unlikely event that the author did not send UMI a complete manuscript and there are missing pages, these will be noted. Also, if unauthorized copyright material had to be removed, a note will indicate the deletion.

Oversize materials (e.g., maps, drawings, charts) are reproduced by sectioning the original, beginning at the upper left-hand corner and continuing from left to right in equal sections with small overlaps. Each original is also photographed in one exposure and is included in reduced form at the back of the book. These are also available as one exposure on a standard 35mm slide or as a 17" x 23" black and white photographic print for an additional charge.

Photographs included in the original manuscript have been reproduced xerographically in this copy. Higher quality 6" x 9" black and white photographic prints are available for any photographs or illustrations appearing in this copy for an additional charge. Contact UMI directly to order.

# U·M·I

University Microfilms International  
A Bell & Howell Information Company  
300 North Zeeb Road, Ann Arbor, MI 48106-1346 USA  
313/761-4700 800/521-0600

**Order Number 9001982**

**Synthesis, reactivity and structural studies of anionic ruthenium  
and osmium polynuclear carbonyl clusters**

**Krause, Jeanette Alice, Ph.D.**

**The Ohio State University, 1989**

**Copyright ©1989 by Krause, Jeanette Alice. All rights reserved.**

**U·M·I**  
300 N. Zeeb Rd.  
Ann Arbor, MI 48106

SYNTHESIS, REACTIVITY AND STRUCTURAL STUDIES  
OF ANIONIC RUTHENIUM AND OSMIUM  
POLYNUCLEAR CARBONYL CLUSTERS

DISSERTATION

Presented in Partial Fulfillment of the Requirement for  
the Degree Doctor of Philosophy in the Graduate  
School of The Ohio State University

by

Jeanette Alice Krause, B.S. Chem, M.S.

\* \* \* \* \*

The Ohio State University

1989

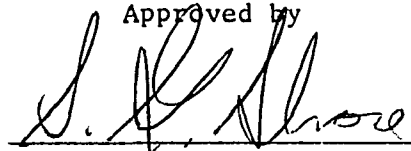
Dissertation Committee:

Dr. Daniel L. Leussing

Dr. Eugene P. Schram

Dr. Sheldon G. Shore

Approved by



Adviser  
Department of Chemistry

Copyright by  
Jeanette Alice Krause  
1989

To My Family

## ACKNOWLEDGEMENTS

I am indebted to my research director, Dr. Sheldon G. Shore, for his time, advice and instruction especially in the area of X-ray crystallography. Special thanks to Dr. Judith Gallucci and Dr. Ruth Hsu for many informative discussions in the area of crystallography.

I would like to thank the members of the research group for assistance and helpful discussions. Special thanks to Deborah McCarthy for her invaluable assistance, patience and friendship.

Most importantly, I would like to thank my family for their unwavering support and patience during both my undergraduate and graduate education. Many thanks also to Michael Richmann for his very special friendship and encouragement.

Finally, I would like to thank the Chemistry Department and The Ohio State University for their financial support.

## VITA

January 17, 1960      Born, Cleveland, Ohio

1982                B.S.Chem, University of Michigan  
Ann Arbor, Michigan

1983-1986          Graduate Teaching Associate,  
Department of Chemistry,  
The Ohio State University,  
Columbus, Ohio

1986-1989          Graduate Research Associate,  
Department of Chemistry,  
The Ohio State University,  
Columbus, Ohio

1987                M.S., The Ohio State University  
Columbus, Ohio

1987-1989          Assistant Department Crystallographer,  
Department of Chemistry,  
The Ohio State University,  
Columbus, Ohio

## PUBLICATIONS

"A Self-Stable syn-Sesquinorbornatriene. An Extreme Example of a Crystallographically Determined  $\pi$ -Pyramidalization Angle", Paquette, L. A.; Shen, C.-C.; Krause, J. A., *J. Am. Chem. Soc.* 1989, *111*, 2351.

"Synthesis of the New Boron Hydride *nido*-Undecaborane(15),  $B_{11}H_{15}$ , and the X-ray Structure fo its Conjugate Base Tetradecahydro<sup>-</sup> $B_{11}H_{14}$  undecaborate(1-),  $[B_{11}H_{14}]^-$ ", Getman, T. G.; Krause, J. A.; Shore, S. G., *Inorg. Chem.* 1988, *27*, 2398.

"Hydrogen Bonded Cluster Carboxylic Acid:  $[(\mu\text{-H})_3(\text{CO})_9\text{Os}_3(\mu_3\text{-CCOOH})_2]$ ", Krause, J. A.; Jan, D.-Y.; Shore, S. G., *J. Am. Chem. Soc.* 1987, *109*, 4416.

"Surface Organometallic Chemistry: Synthesis and X-ray Structure of  $\text{Ru}_3(\text{CO})_8(\mu\text{-OC}_6\text{H}_4\text{OMe-2})_2$ , an Oxygen Stabilized Triruthenium Cluster", Santini, C. C.; Basset, J. M.; Fontal, B.; Krause, J.; Shore, S.; Charrier, C., *J. Chem. Soc., Chem. Commun.* 1987, 512.

"Preparation and Chemistry of Some Selected Borane Anions", Shore, S. G.; Getman, T.; Wermer, J.; Krause, J.; Niedenzu, P.; Hill, T., Abstract of Papers, No. 79, *195th National Meeting of the American Chemical Society*, June 5-10, 1988, Toronto, Canada.

"Borane-Transition Metal Cluster Chemistry", Shore, S. G.; Coffy, T.; Jan, D.-Y.; Krause, J.; Workman, D., Abstract of Papers No. 705, *195th National Meeting of the American Chemical Society*, June 5-10, 1988, Toronto, Canada.

"Preparation and Chemistry of Some Selected Borane Anions", Shore, S. G.; Getman, T.; Wermer, J.; Krause, J.; Niedenzu, P.; Hill, T., Abstract of Papers No. ME53, *First Boron USA Workshop (BUSA-1)*, April 10-13, 1988, Southern Methodist University, Dallas, TX.

"Borane-Transition Metal Cluster Chemistry", Shore, S. G.; Coffy, T.; Jan, D.-Y.; Krause, J.; Workman, D., Abstract of Papers No. MM4, *First Boron USA Workshop (BUSA-1)*, April 10-13, 1988, Southern Methodist University, Dallas, TX.

"Synthesis and Reactivity Studies of  $\text{H}_2\text{Os}_3(\text{CO})_8(\text{PPh}_3)\text{BCO}$ : X-ray Crystal Structure of  $\text{H}_2\text{Os}_3(\text{CO})_8(\text{PPh}_3)\text{BCO}$ ", Jan, D.-Y.; Hsu, L.-Y.; Krause, J. A.; Workman, D. P.; Shore, S. G., Abstract of Papers No. 222, *19th Central Regional Meeting of the American Chemical Society*, June 24-26, 1987, Columbus, Ohio.

"Synthesis and X-ray Crystal Structure of a Hydrogen Bonded Carboxylic Acid:  $[(\mu\text{-H})_3\text{Os}_3(\text{CO})_9(\mu_3\text{-CCO}_2\text{H})_2]$ ", Krause, J. A.; Jan, D.-Y.; Shore, S. G., Abstract of Papers No. 223, *19th Central Regional Meeting of the American Chemical Society*, June 24-26, 1987, Columbus, Ohio.

"Synthesis and X-ray Structure of  $\text{Ru}_3(\text{CO})_8(\text{OC}_6\text{H}_4\text{OMe})_2$ , A Lightly Oxygen Stabilized Triruthenium Cluster", Santini, C.; Basset, J. M.; Fontal, B.; Krause, J. A.; Shore, S. G.; Charrier, C., Abstract of Papers No. 224, *19th Central Regional Meeting of the American Chemical Society*, June 24-26, 1988, Columbus, Ohio.

" $[B_9H_{13}]^{2-}$  an *arachno*- $[B_nH_{n+4}]^{2-}$  Dianion; Synthesis, Characterization and Molecular Structure", Getman, T. D.; Krause, J. A.; Niedenzu, P. M.; Shore, S. G., *In Press*.

"X-ray Crystallographic Analysis of the Structural Distortions Induced by Substitution and Annulation of the Dodecahedrane Nucleus", Gallucci, J. C.; Taylor, R. T.; Kobayashi, T.; Weber, J. C.; Krause, J.; Paquette, L. A., *In Press*.

"On the Mechanism of Photochemical Alkyne Insertion into  $(\eta^5-C_5H_5)_2-Fe_2(CO)_2(\mu-CO)_2$ : Crystal Structure of  $Me_2Si[(\eta^5-C_5H_4)_2Fe_2(CO)_2(\mu-CO)-\{\mu-\eta^1, \eta^3-C(O)C(C_6H_5)C(H)\}]$ ", Bursten, B. E.; Krause, J. A.; Lunder, D. M.; McKee, S. D., submitted for publication.

## FIELDS OF STUDY

Major Field: Inorganic Chemistry

Studies in Nonmetal and Organometallic Chemistry:  
Professors Sheldon G. Shore, Eugene, P. Schram,  
Andrew A. Wojcicki

Studies in Transition Metal and Bioinorganic Chemistry:  
Professors Daryle H. Busch, Bruce E. Bursten, James A.  
Cowan, Daniel L. Leussing, Devon W. Meek

## TABLE OF CONTENTS

ACKNOWLEDGEMENTS	iii
VITA	iv
LIST OF TABLES	x
LIST OF FIGURES	xii
INTRODUCTION	1
RECENT STUDIES ON METAL CLUSTERS	4
I.    STRUCTURE AND BONDING IN TRANSITION METAL CLUSTERS	7
A.    METAL-METAL BONDING	7
B.    METAL-LIGAND BONDING	10
II.   SYNTHETIC APPROACHES IN CLUSTER CHEMISTRY	10
A.    PYROLYSIS REACTIONS	13
B.    ADDITION TO COORDINATELY UNSATURATED SPECIES	16
C.    REDOX CONDENSATION REACTIONS	18
III.  PREPARATION OF CARBONYLATES	24
STATEMENT OF THE PROBLEM	28
RESULTS & DISCUSSION	29
I.    IRON/RUTHENIUM SYSTEMS	29
A.    Introduction	29
B.    Results & Discussion	34
1.    Reactions of $^{2-}[\text{Ru}_3(\text{CO})_{11}]^{2-}$ and $[\text{Ru}_4(\text{CO})_{13}]^{2-}$	34
2.    Reactions of $^{4-}[\text{Ru}_4(\text{CO})_{12}]^{4-}$ and $[\text{Ru}_4(\text{CO})_{11}]^{6-}$	39
3.    Reaction of $^{2-}[\text{Ru}_6(\text{CO})_{18}]^{2-}$	40

4. Reactions of $[\text{Ru}_6(\text{CO})_{17}]^{4-}$ and $[\text{Ru}_6(\text{CO})_{16}]^{6-}$	65
II. IRON/OSMIUM SYSTEMS	69
A. Introduction	69
B. Results & Discussion	72
1. Reaction of $[\text{Os}_3(\text{CO})_{11}]^{2-}$	73
2. Reaction of $[\text{FeOs}_3(\text{CO})_{13}]^{2-}$	75
III. RUTHENIUM/OSMIUM SYSTEMS	76
A. Introduction	76
B. Crystallographic Studies	81
1. Shore and Siriwardane	81
2. Rheingold and Gates	84
C. Results & Discussion	84
1. Reactions of $[\text{Os}_3(\text{CO})_{11}]^{2-}$ with $\text{Ru}_3(\text{CO})_{12}$ or $\text{Ru}(\text{CO})_5$	86
2. Reaction of $[\text{Ru}_3(\text{CO})_{11}]^{2-}$ with $\text{Os}_3(\text{CO})_{12}$	90
3. Crystallographic Determination of $\text{H}_2\text{RuOs}_3(\text{CO})_{13}$	99
IV. REACTIVITY STUDIES OF $\text{H}_2\text{Ru}_6(\text{CO})_{17}$	110
A. DEPROTONATION OF $\text{H}_2\text{Ru}_6(\text{CO})_{17}$	112
B. HYDROGENATION OF CARBONYLATION OF $\text{H}_2\text{Ru}_6(\text{CO})_{17}$	121
C. HYDROBORATION OF $\text{H}_2\text{Ru}_6(\text{CO})_{17}$	123
D. REACTIVITY OF $\text{H}_2\text{Ru}_6(\text{CO})_{17}$ WITH OXONIUM SALTS	125
CONCLUDING REMARKS	129
EXPERIMENTAL	
I. APPARATUS	130
A. Vacuum System	130
B. Glove Box	131
C. Glassware	131
D. Filtration Apparatus	131
E. Nuclear Magnetic Resonance Spectra	135
F. Infrared Spectra	135
G. Thin-Layer Chromatography (TLC)	136
H. High Pressure Liquid Chromatography (HPLC)	136

I. Single Crystal X-ray Diffraction	136
1. Hardware	136
2. Software	138
J. Mass Spectra	144
II. REAGENTS	144
III. SOLVENTS	150
IV. CRYSTAL GROWING	151
V. PREPARATION OF STARTING MATERIALS	153
VI. PREPARATION OF NEW COMPOUNDS	158
A. IRON/RUTHENIUM SYSTEMS	158
B. IRON/OSMIUM SYSTEMS	164
C. RUTHENIUM/OSMIUM SYSTEMS	168
VII. REACTIVITY STUDIES OF $H_2Ru_6(CO)_{17}$	171
VIII. STRUCTURE DETERMINATION OF $H_2Ru_6(CO)_{17}$	177
IX. STRUCTURE DETERMINATION OF $[PPh_4]_2[Ru_6(CO)_{18}]$	178
X. STRUCTURE DETERMINATION OF $H_2RuOs_3(CO)_{13}$	181
XI. STRUCTURE DETERMINATION OF $[PPN][HRu_6(CO)_{18}]$	182
APPENDIX	186
REFERENCES	194

## LIST OF TABLES

TABLE	PAGE
1. Crystallographic Data for $H_2Ru_6(CO)_{18}$ .	47
2. Crystallographic Data for $(\mu_3-H)_2Ru_6(\mu-CO)(CO)_{16}$ .	54
3. Selected Bond Distances (Å) and Esd's of $(\mu_3-H)_2Ru_6(\mu-CO)(CO)_{16}$ .	55
4. Selected Bond Angles (deg) and Esd's of $(\mu_3-H)_2Ru_6(\mu-CO)(CO)_{16}$ .	57
5. Crystallographic Data for $[PPh_4]_2[Ru_6(CO)_{18}]$ .	67
6. Crystallographic Data for $H_2RuOs_3(CO)_{13}$ -- Co-crystallized Systems.	82
7. Crystallographic Data for $H_2RuOs_3(CO)_{13}$ .	83
8. Crystallographic Data for $(\mu-H)_2RuOs_3(CO)_{13}$ .	101
9. Selected Bond Distances (Å) and Esd's for $(\mu-H)_2RuOs_3(CO)_{13}$ .	102
10. Selected Bond Angles (deg) and Esd's for $(\mu-H)_2RuOs_3(CO)_{13}$ .	103
11. Comparison of Semibridging Carbonyl Bond Distances and Bond Angles for $H_2RuOs_3(CO)_{13}$ , $H_2FeOs_3(CO)_{13}$ and $H_2FeRu_3(CO)_{13}$ .	107
12. Comparison of Metal Thermal Parameters in $H_2RuOs_3(CO)_{13}$ .	109
13. Crystallographic Data for $[PPN][HRu_6(CO)_{18}]$ .	119
14. Crystallographic Data for $[PPN][HRu_6(CO)_{18}]$ as Reported by Johnson and Lewis.	120

15. Classification of the Seven Crystal Systems.	140
16. Systematic Absences Caused by Translational Symmetry in the Crystal System.	142
17. Atomic Positional Parameters and Isothermal Parameters (and Esd's) for $(\mu_3\text{-H})_2\text{Ru}_6(\mu\text{-CO})(\text{CO})_{16}$ .	179
18. Atomic Positional Parameters and Isothermal Parameters (and Esd's) for $(\mu\text{-H})_2\text{RuOs}_3(\text{CO})_{13}$ .	183

## LIST OF FIGURES

FIGURE	PAGE
1. Examples from the Diverse Area of Cluster Chemistry.	2
2. Examples of Metal Clusters as Models of Surface Intermediates in Catalysis.	3
3. Supported Metal Clusters via Surface Linkages.	5
4. Model of $\text{HOs}_3(\text{CO})_{10}$ on Silica.	6
5. Geometric Configurations of Closed Polyhedra.	9
6. Geometric Arrangements of CLOSO, NIDO and ARACHNO Clusters Containing Six and Seven Skeletal Electron Bonding Pairs.	11
7. Bonding Modes of Hydrogen and Carbon Monoxide Ligands.	12
8. Examples of Unsaturated Transition Metal Complexes.	17
9. Reactivity Scheme for $\text{H}_2\text{Os}_3(\text{CO})_{10}$ .	19
10. ORTEPS of $[\text{Ru}_2(\text{CO})_8]^{2-}$ and $[\text{Os}_2(\text{CO})_8]^{2-}$ .	21
11. Synthetic Route to Mixed-Metal Clusters from Monomeric Carbonyls.	22
12. Synthetic Route to Higher Nuclearity Carbonyls.	25
13. Ketyl Reduction of $\text{Ru}_3(\text{CO})_{12}$ .	27
14. ORTEP of $\text{H}_2\text{FeRu}_3(\text{CO})_{13}$ .	31
15. ORTEP of $[\text{Fe}_4\text{Ru}_2(\text{CO})_{22}]^{2-}$ .	35
16. Proton (a) and Carbon-13 (b) NMR Spectra of $(\mu_3\text{-H})_2\text{Ru}_6(\mu\text{-CO})(\text{CO})_{16}$ .	43

17. Solution IR Spectrum of $(\mu_3\text{-H})_2\text{Ru}_6(\mu\text{-CO})(\text{CO})_{16}$ .	44
18. Solid State IR Spectrum of $(\mu_3\text{-H})_2\text{Ru}_6(\mu\text{-CO})(\text{CO})_{16}$ .	45
19. $\text{H}_2\text{Ru}_6(\text{CO})_{18}$ . Molecular Structure (a) and Probable Location of Hydrides (b).	48
20. ORTEP of $(\mu_3\text{-H})_2\text{Ru}_6(\mu\text{-CO})(\text{CO})_{16}$ .	50
21. Crystal Packing Diagram of $(\mu_3\text{-H})_2\text{Ru}_6(\mu\text{-CO})(\text{CO})_{16}$ .	51
22. Selected Views of $\text{H}_2\text{Ru}_6(\text{CO})_{17}$ Metallic Core.	52
23. Selected View of $\text{H}_2\text{Ru}_6(\text{CO})_{17}$ Metallic Core.	53
24. Molecular Structure of $\text{Os}_6(\text{CO})_{18}$ .	60
25. Intermetallic Bond Distances Within $\text{H}_2\text{Ru}_6(\text{CO})_{17}$ .	62
26. Molecular Structure of $[\text{Ru}_6(\text{CO})_{18}]^{2-}$ .	66
27. Molecular Structure of $\text{H}_2\text{FeOs}_3(\text{CO})_{13}$ .	71
28. Proton (a) and Carbon-13 (b) NMR Spectra of $\text{H}_2\text{Fe}_2\text{Os}_3(\text{CO})_{16}$ .	74
29. Molecular Structure of $\text{H}_2\text{RuOs}_3(\text{CO})_{13}$ .	85
30. Proton NMR Spectra of Inseparable (a) Penta- and (b) Tetra- nuclear Clusters.	88
31. IR (a) and Proton NMR (b) Spectra of $\text{H}_2\text{RuOs}_3(\text{CO})_{13}$ Reaction Mixture.	89
32. FT-ICR MS Spectrum of $\text{H}_2\text{RuOs}_3(\text{CO})_{13}$ Sample at $T=100^\circ\text{C}$ .	91
33. FT-ICR MS Spectrum of $\text{H}_2\text{RuOs}_3(\text{CO})_{13}$ Sample at $T=125^\circ\text{C}$ .	92
34. Proton NMR Spectrum of $\text{H}_2\text{RuOs}_3(\text{CO})_{13}$ .	94
35. IR Spectrum of $\text{H}_2\text{RuOs}_3(\text{CO})_{13}$ .	96
36. IR Spectrum of $\text{H}_2\text{Ru}_2\text{Os}_3(\text{CO})_{16}$ .	97
37. Molecular Structure of $\text{H}_2\text{Ru}_2\text{Os}_3(\text{CO})_{16}$ .	98

38.	ORTEP of $(\mu\text{-H})_2\text{RuOs}_3(\text{CO})_{13}$ .	100
39.	Structural Variations of the Ruthenium and Osmium Hexanuclear Clusters.	111
40.	Metal Crystallite Growth.	113
41.	Proton NMR Spectrum of $[\text{HRu}_6(\text{CO})_{18}]^-$ and $[\text{H}_3\text{Ru}_4(\text{CO})_{12}]^-$ .	115
42.	Carbon-13 NMR Spectrum of $[\text{HRu}_6(\text{CO})_{18}]^-$ and $[\text{H}_3\text{Ru}_4(\text{CO})_{12}]^-$ .	116
43.	Molecular structure of $[\text{HRu}_6(\text{CO})_{18}]^-$ .	117
44.	Proposed Fragmentation Pattern for $(\mu_3\text{-H})_2\text{Ru}_6(\mu\text{-CO})(\text{CO})_{16}$ .	124
45.	ORTEP of $\text{H}_3\text{Os}_3(\text{CO})_9\text{BCO}$ .	126
46.	Molecular Structure of $[\text{H}_3(\text{CO})_9\text{Os}_3(\mu_3\text{-CO})]_3(\text{B}_3\text{O}_3)$ .	127
47.	Reaction Apparatus for NMR Study.	132
48.	Vacuum Extractor.	133
49.	Filtration Apparatus.	134
50.	X,Y,Z Coordinate System and Rotation Directions on the CAD4 Kappa Geometry Deffractometer System. (Reproduced from "Enraf Nonius CAD4 Diffractometer User's Manual"; Enraf Nonius Delft: Delft, The Netherlands, 1982 by permission of Enraf Nonius Delft).	137
51.	Crystal Growing Apparatus.	152
52.	Proton NMR Spectrum of $(\mu\text{-H})_3\text{Os}_3(\text{CO})_9(\mu_3\text{-CCH}_3)$ .	190
53.	IR Spectrum of $(\mu\text{-H})_3\text{Os}_3(\text{CO})_9(\mu_3\text{-CCH}_3)$ .	191

## INTRODUCTION

In the past twenty years molecular cluster chemistry has become a rapidly expanding field in inorganic chemistry, due to its potential role in surface studies and catalysis. A cluster is defined as a definite group of metal atoms which are held together by three or more different metal-metal bonds. [1] Main group elements such as carbon, boron, phosphorous and nitrogen can also be involved as vertices in the cluster framework. Included in the diverse area of clusters [2] are polynuclear boron hydrides, metallaboranes, metal carbonyl clusters and metal halide or metal sulfide clusters a few of which are depicted in Figure 1.

Metal cluster chemistry plays an essential role in the understanding of the interaction between substrates and the metal or metal oxide surface during catalysis. The triangular bonding array of metal atoms in the cluster is said to parallel the type of binding on a metal surface, thereby providing the key to the analogy of molecular clusters as models for metal surface bound species. [3-8] (Fig. 2) Transition metal clusters have been studied not only as model systems but also as possible catalysts. Study of the catalytic behavior of transition metal clusters has been approached by two different routes. Clusters have been examined as homogenous

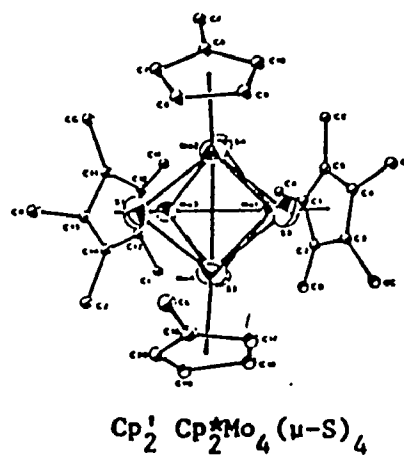
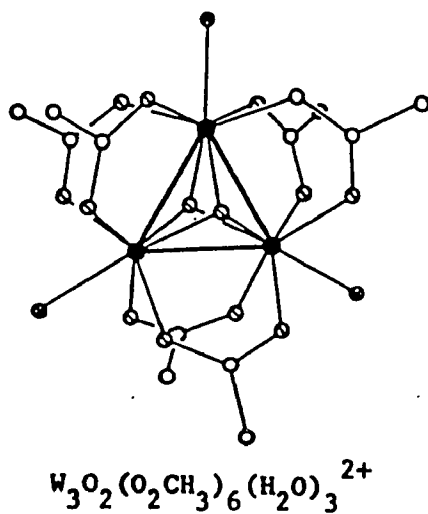
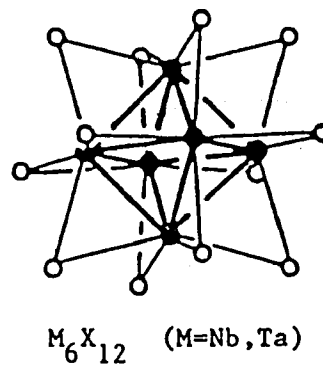
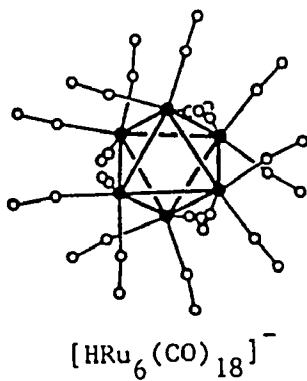
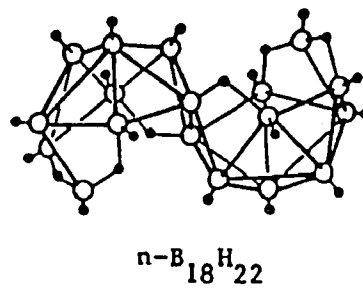
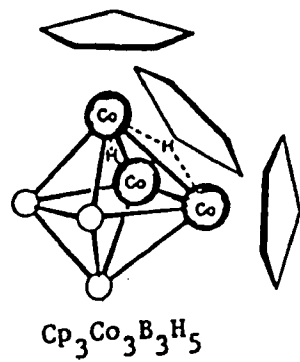


Figure 1. Examples from the Diverse Area of Cluster Chemistry.

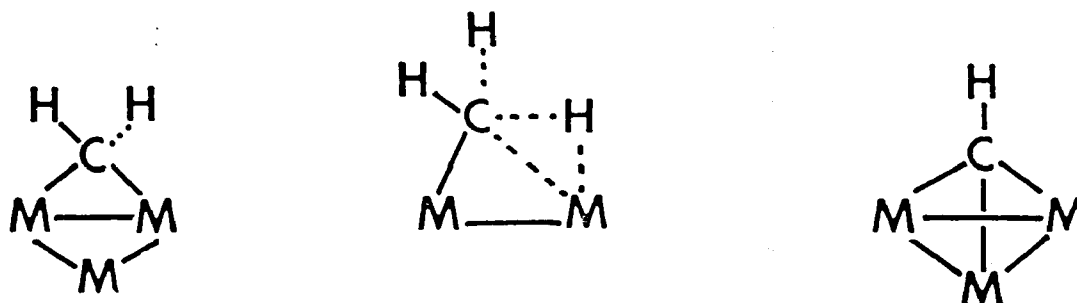


Figure 2. Examples of Metal Clusters as Models of Surface Intermediates in Catalysis.

catalysts [9,10] and have also been studied while on supports. Most supported catalyst modeling studies consist of a metal bound to a support surface; such as,  $\text{Al}_2\text{O}_3$ ,  $\text{SiO}_2$ ,  $\text{TiO}_2$ , polymers or zeolites, through surface linkages like phosphines. [3,11-18] (Fig. 3) Recently interests have turned to metal clusters bound directly to inorganic oxides *via* the oxygen atoms. [12,19-27] (Fig. 4)

### RECENT STUDIES ON METAL CLUSTERS

Metal cluster chemistry centers about the synthesis of homo- or hetero- nuclear clusters and reactivity studies of these newly synthesized clusters with  $\text{H}_2$ , CO, organic molecules, oxidizing and reducing agents. Most of these reactivity studies are seen to mimic the well established reactions of mononuclear chemistry. However, the main concern is still to develop the systematic syntheses of metal clusters and not to continue with the random approach previously observed in the earlier stages of cluster chemistry. A particular area in need of such an effort is that of the heteronuclear clusters. Although a large number of heteronuclear clusters are known, few can be synthesized in a systematic fashion. [28] The emphasis of heteronuclear cluster research is that the presence of two or more types of metal atoms in a cluster might serve to greatly enhance catalytic activity, [29] due to the advantage of cooperativity between the two adjacent, yet electronically different, metal centers.

The emphasis of this investigation has been to develop the systematic synthesis of mixed metal carbonyl clusters focusing on the

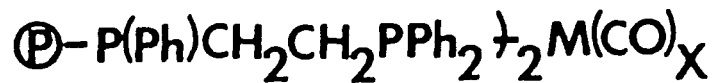
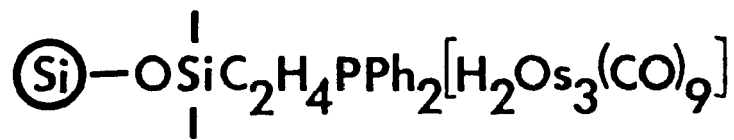
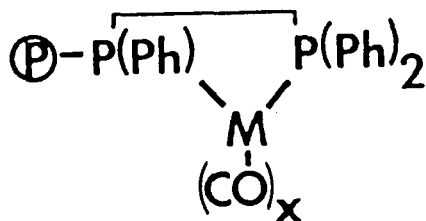
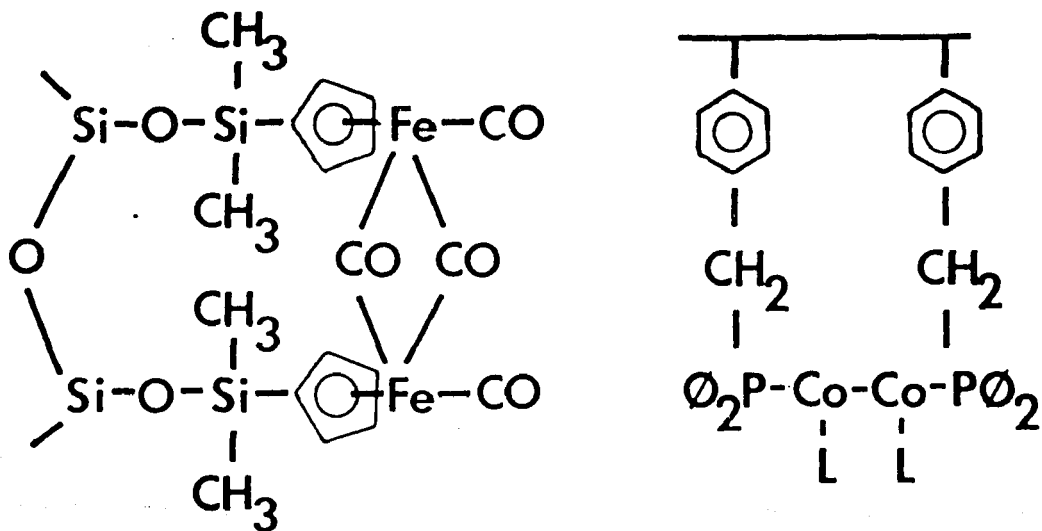


Figure 3. Supported Metal Clusters via Surface Linkages.

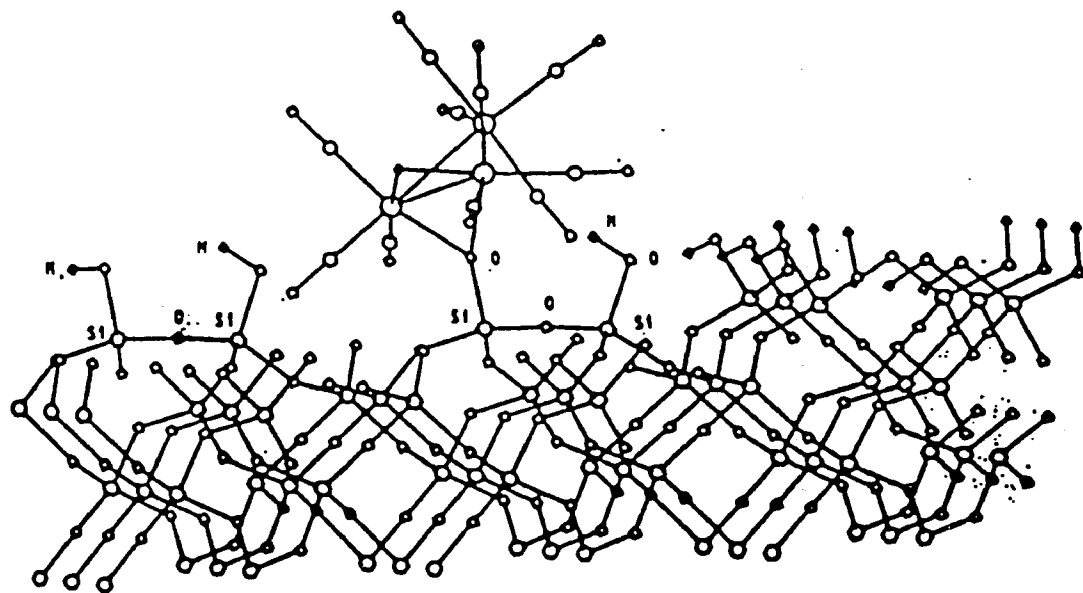


Figure 4. Model of HOS<sub>3</sub>(CO)<sub>10</sub> on Silica.

iron triad elements (Fe, Ru, Os). It is, therefore, appropriate at this time to present the groundwork already established for heteronuclear clusters, both synthetic and structural, on which the present studies are based upon.

## I. STRUCTURE AND BONDING IN TRANSITION METAL CLUSTERS

### A. METAL-METAL BONDING

There are currently two approaches taken in cluster chemistry to rationalize structures: the Effective Atomic Number Rule (EAN) and the Polyhedral Skeletal Electron Pair Theory (PSEPT). [30-34] The Effective Atomic Number Rule is essentially a valence-bond approach that allocates the skeletal bonding electrons to localized 2-center metal-metal bonds. This approach is useful in describing small clusters. [33] The Polyhedral Skeletal Electron Pair Theory, on the other hand, notes the relationship between the polyhedral shape of a cluster and the total number of skeletal electrons, instead of assigning the skeletal electrons to individual bonds. This method is useful in describing bonding occurring in the medium-sized clusters of approximately 4-12 metal atoms. [33] Extended Huckel calculations have been employed to predict the geometries of larger clusters containing up to 25 metal atoms. [35]

Initially bonding in clusters was described in terms of the Effective Number Rule until discovery of some clusters containing too many electrons to be treated in this manner brought about the need for alternate bonding descriptions. The Polyhedral Skeletal Electron Pair

Theory developed for boron hydrides and carboranes was extended to include transition metal clusters, and remains the most reliable method for predicting the geometric arrangement of metal atoms in clusters.

The metal atoms in clusters occupy positions defining polyhedra (or portions of polyhedra) with triangulated faces. The parent polyhedral arrangement from which a given cluster is derived is dependent on the number of skeletal electrons in that cluster. The skeletal electrons ( $n_e$ ) can be determined by the following relationships. [33] (Equations 1,2)

for main group fragments

$$v + x - 2 = n_e \quad (1)$$

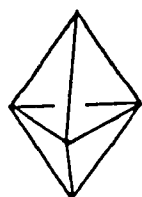
for transition metal fragments

$$v + x - 12 = n_e \quad (2)$$

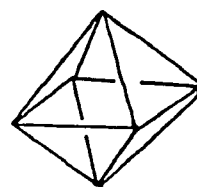
where,  $v$  = no. valence electrons of the metal element

$x$  = no. electrons contributed by the ligands

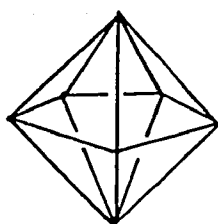
Therefore, in an  $n$ -vertex polyhedron,  $(n + 1)$  bonding molecular orbitals are generated if each atom in the skeletal framework donates three atomic orbitals for framework bonding. The metal atoms are then observed to form the closed or CLOSO polyhedral arrangements, depicted in Figure 5, if the cluster has  $(n + 1)$  skeletal bonding electron pairs. Clusters having fewer vertices but the same number of skeletal



5-vertex



6-vertex



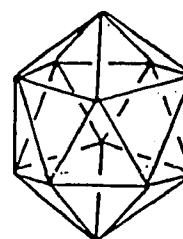
7-vertex



8-vertex



10-vertex



12-vertex

Figure 5. Geometric Configurations of Closed Polyhedra.

electron pairs as the CLOSO system have structures based upon the closed polyhedron. (Fig. 6) Clusters with one and two vertices less than the closed polyhedron are named NIDO and ARACHNO clusters, respectively.

#### B. METAL-LIGAND BONDING.

Although the aforementioned theories are useful in predicting the metal geometry in a cluster, they cannot predict the ligand arrangement about the metal atoms. The carbon monoxide and hydrogen ligands are capable of several bonding modes to the metals. They can bond in the terminal, edge-bridging and face-bridging (capping) modes illustrated in Figure 7.

Some attempts have been made to rationalize the bonding modes adopted by carbonyl groups in clusters. [36,37] It has been suggested that the carbonyl bridge is primarily a means of delocalizing negative charge in clusters. [38] There is a pronounced trend toward increasing the number of bridging carbonyls as the charge or electron density on the metal core is increased.

Attempts to predict the type of bonding for hydrogen ligands, on the other hand, has met with very limited success. [39] Hydrides have been observed to occupy the edge-bridged position most often; however, both the terminal and capping modes have been observed on occasion.

## II. SYNTHETIC APPROACHES IN CLUSTER CHEMISTRY

Although a large number of clusters have been prepared and characterized, they are often prepared *via* non-specific routes and

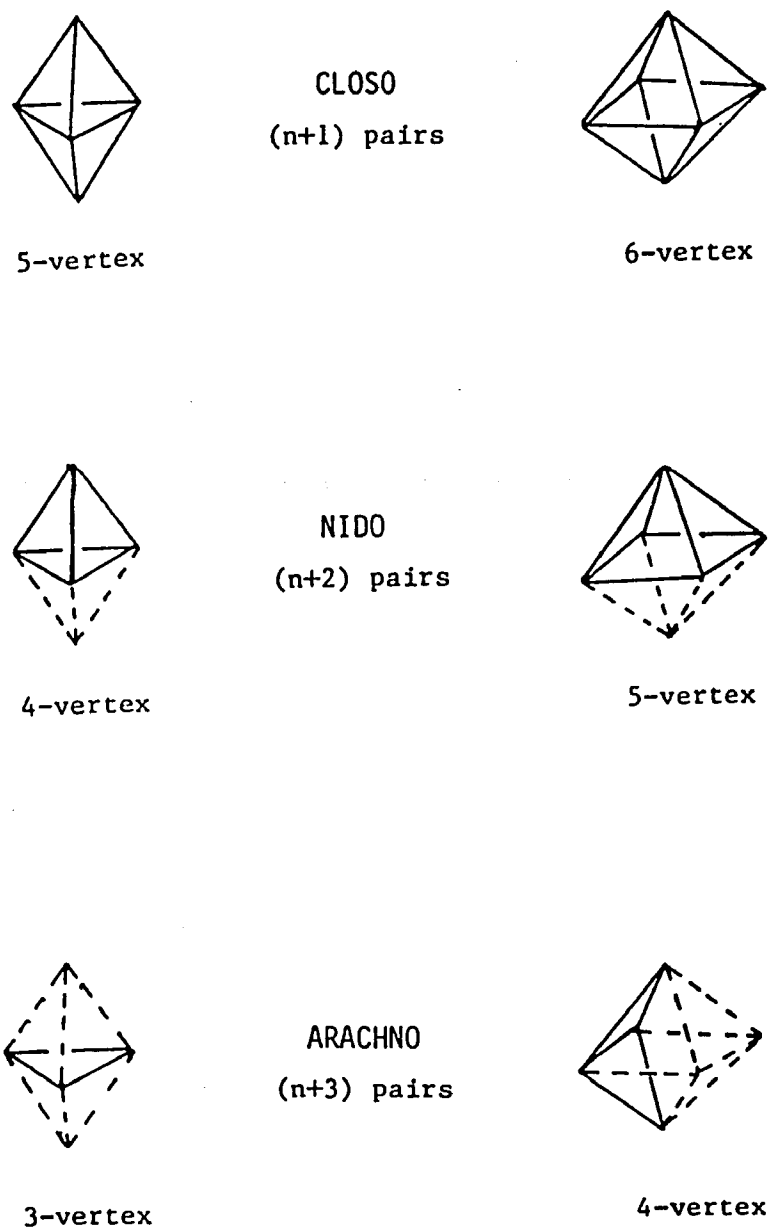


Figure 6. Geometric Arrangements of CLOSO, NIDO, and ARACHNO Clusters Containing Six and Seven Skeletal Electron Bonding Pairs.

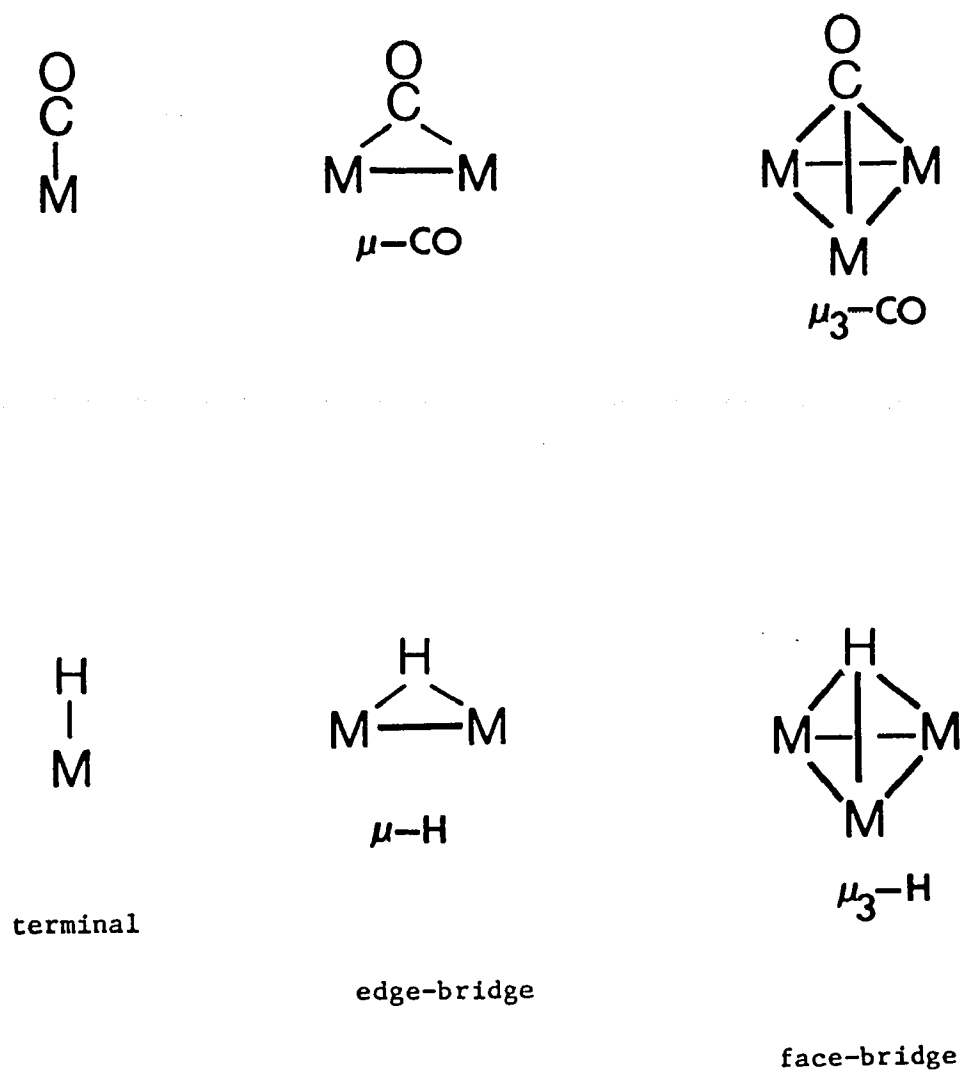
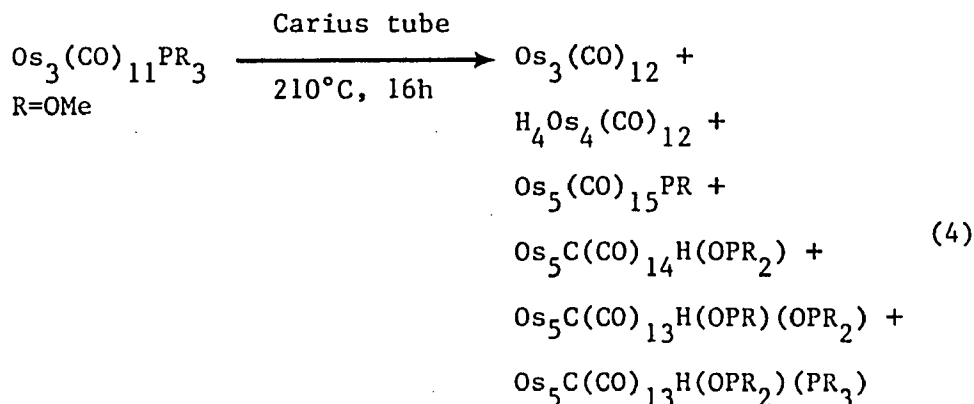
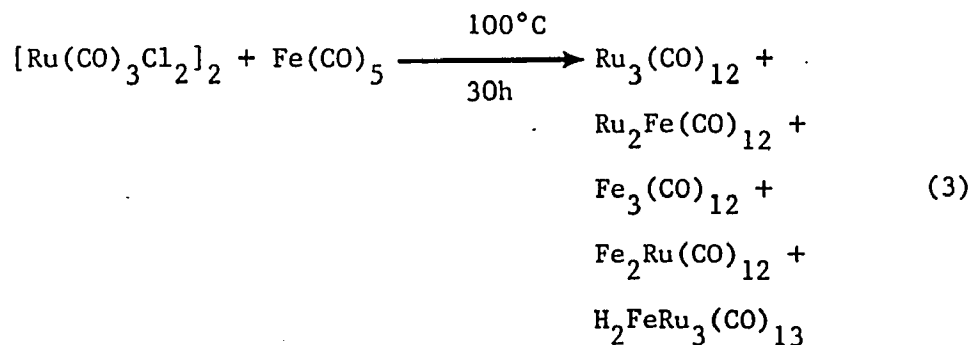


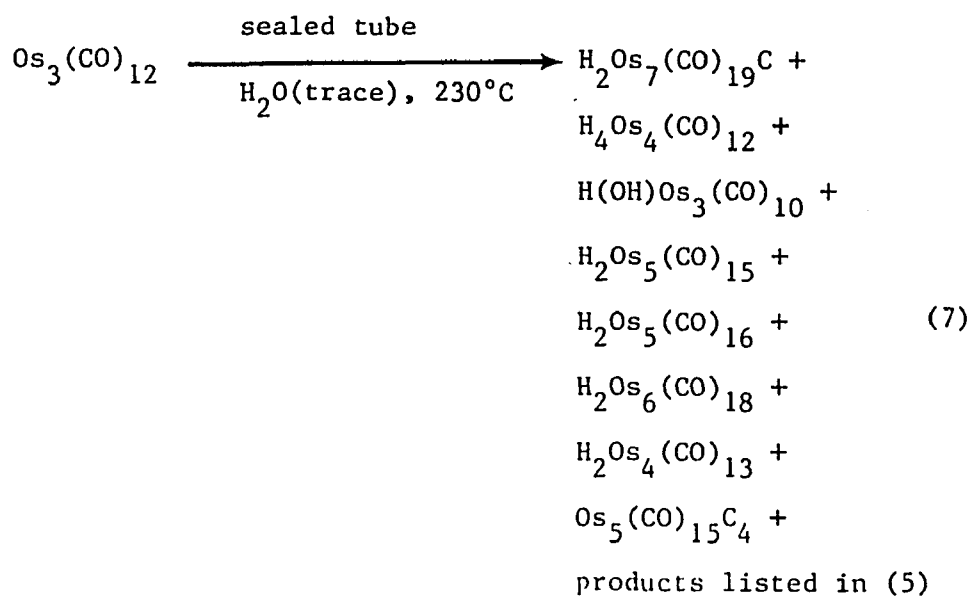
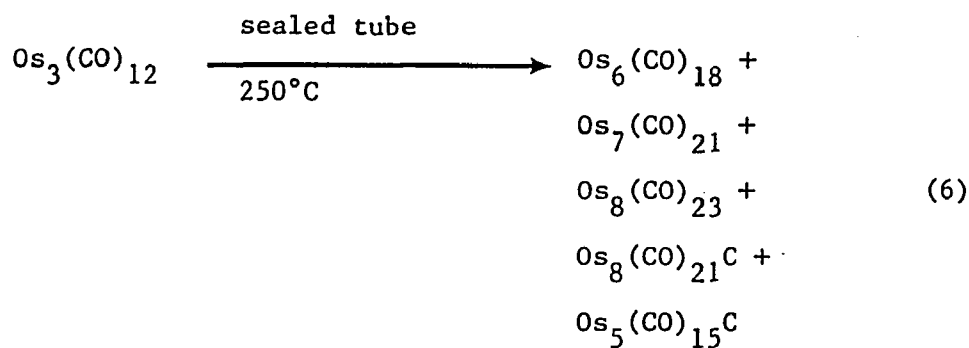
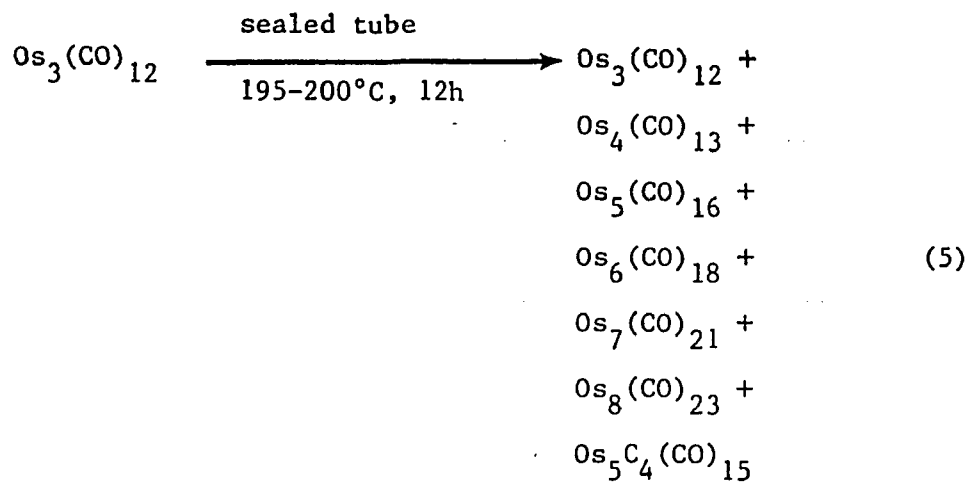
Figure 7. Bonding Modes of Hydrogen and Carbon Monoxide Ligands.

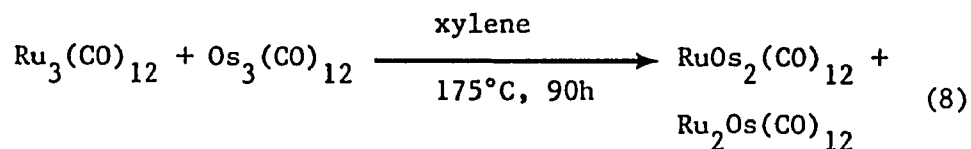
often generate complex mixtures of products. The reactions that have been employed in transition metal cluster syntheses can be broadly divided into three major categories: (1) pyrolysis, (2) addition to coordinately unsaturated species, and (3) redox condensation reactions.

#### A. PYROLYSIS REACTIONS

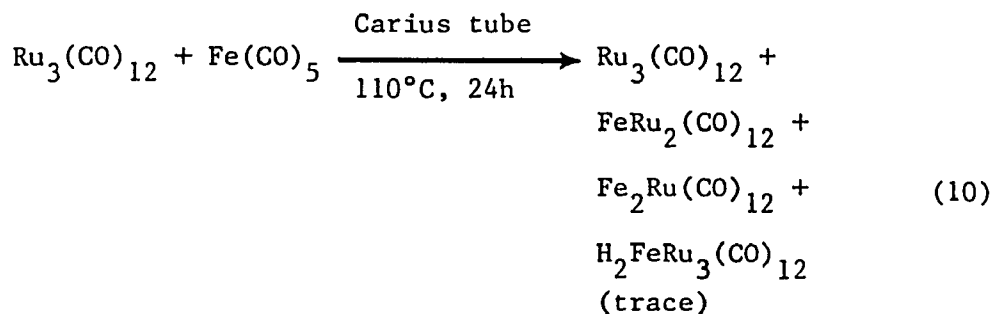
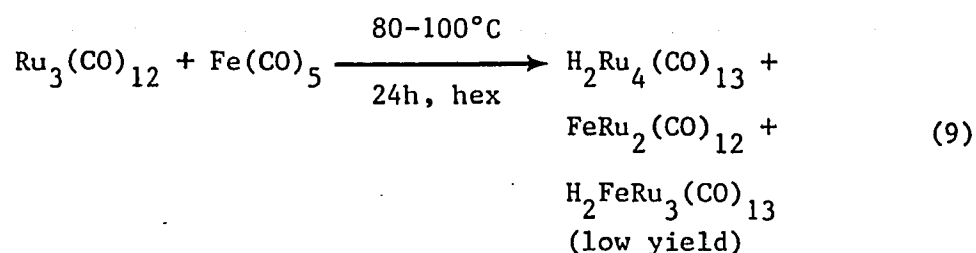
Pyrolysis reactions generally involve the heating of one or more stable compounds together to produce reactive fragments that can recombine to form higher nuclearity clusters. Recent examples of the pyrolysis method are outlined in the following reactions. [40-44]







Stone and co-workers have also demonstrated that hydrido mixed metal clusters may be formed. For example, pyrolysis of  $\text{Ru}_3(\text{CO})_{12}$  with  $\text{Fe}(\text{CO})_5$  yields  $\text{H}_2\text{FeRu}_3(\text{CO})_{13}$ ; however, product yields are again very reaction condition dependent. [40] (Equations 9,10)

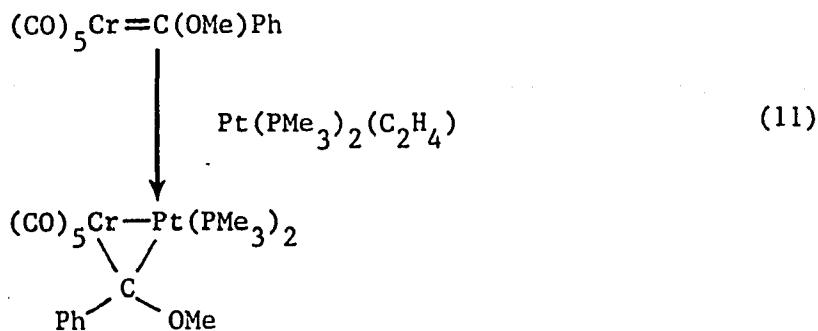


As is quite apparent from the above examples, complex mixtures are often generated in pyrolysis reactions. Prediction of products is also futile in that these preparations are very reaction condition dependent, as illustrated in Equations 5-7. The biggest disadvantage, however, is that the product mixtures require tedious chromatographic techniques to isolate pure compounds, often in very low yield.

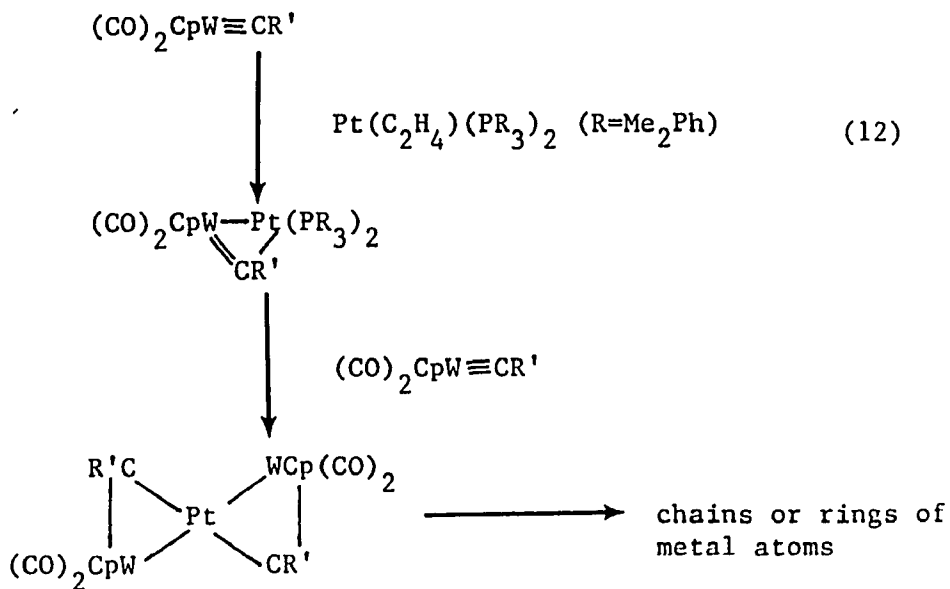
## B. ADDITION TO COORDINATELY UNSATURATED SPECIES

The discovery of unsaturated species such as those shown in Figure 8 has had a major impact on cluster synthesis. The application of this reaction type has been demonstrated by Stone [45, 47] using carbene and carbyne complexes. (Equations 11,12)

carbene



carbyne



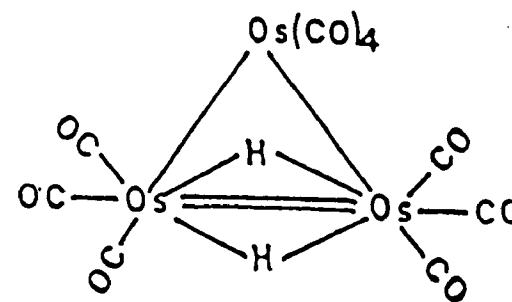
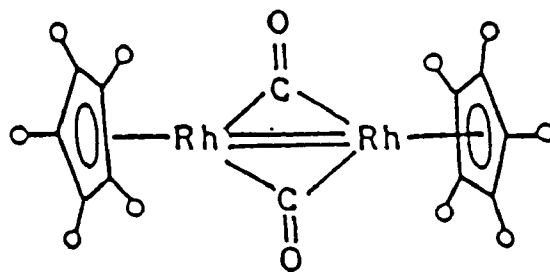
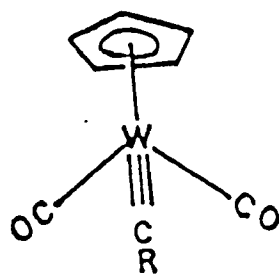
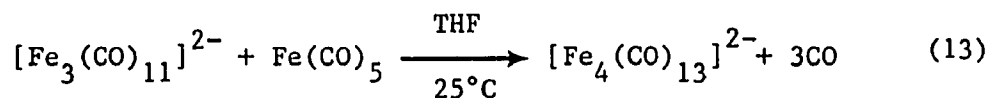


Figure 8. Examples of Unsaturated Transition Metal Complexes.

This approach has also been adopted by Shore and co-workers [48-50] in the case of  $\text{H}_2\text{Os}_3(\text{CO})_{10}$  and proved successful in making various triosmium-based tetranuclear mixed-metal clusters. (Fig. 9) The success of this technique is due to the generation of much higher yields of the cluster products especially in the area of mixed-metal systems. Finally, it appears that this reaction type is rather adaptable to designed syntheses; provided the generation of an unsaturated species is feasible.

### C. REDOX CONDENSATION REACTIONS

The reaction of carbonylates with neutral metal carbonyls or cationic metal carbonyls are labelled redox condensation reactions. [23,36a,38,51,52] The first reaction of this type was reported in 1965 by Hieber and Shubert [53] in the synthesis of  $[\text{Fe}_4(\text{CO})_{13}]^{2-}$  from  $[\text{Fe}_3(\text{CO})_{11}]^{2-}$ . (Equation 13)



The great utility of the method is due to ease of reaction and the large number of reactant combinations possible. The reaction of carbonylates with monomeric, dimeric, and higher nuclearity carbonyls has yielded many clusters of both homo- and hetero- nuclear varieties.

Work with monomeric species to form dinuclear complexes was first shown to be feasible by Ruff [54] and then Anders and Graham [55] in

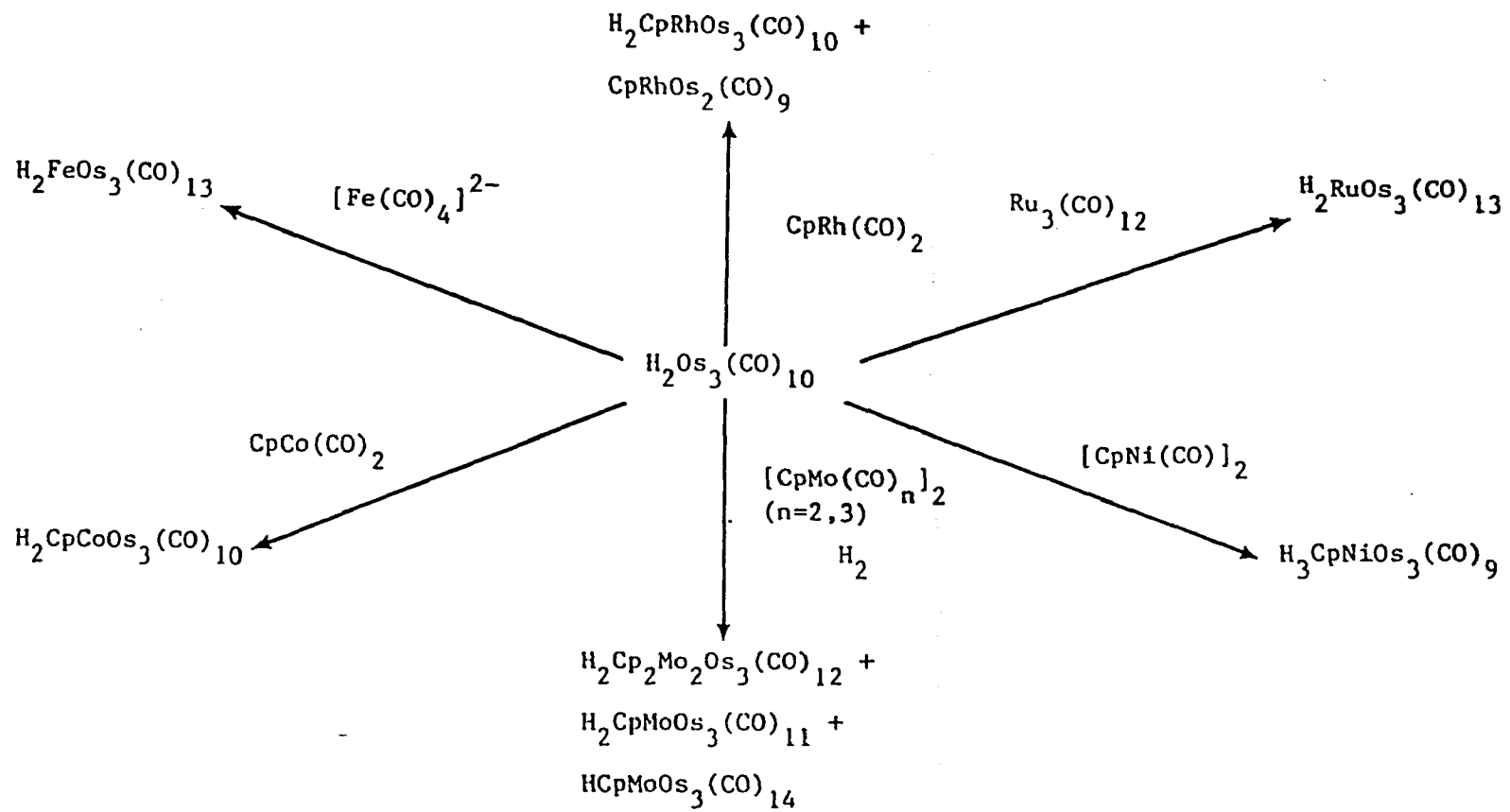


Figure 9. Reactivity Scheme for  $\text{H}_2\text{Os}_3(\text{CO})_{10}$ .



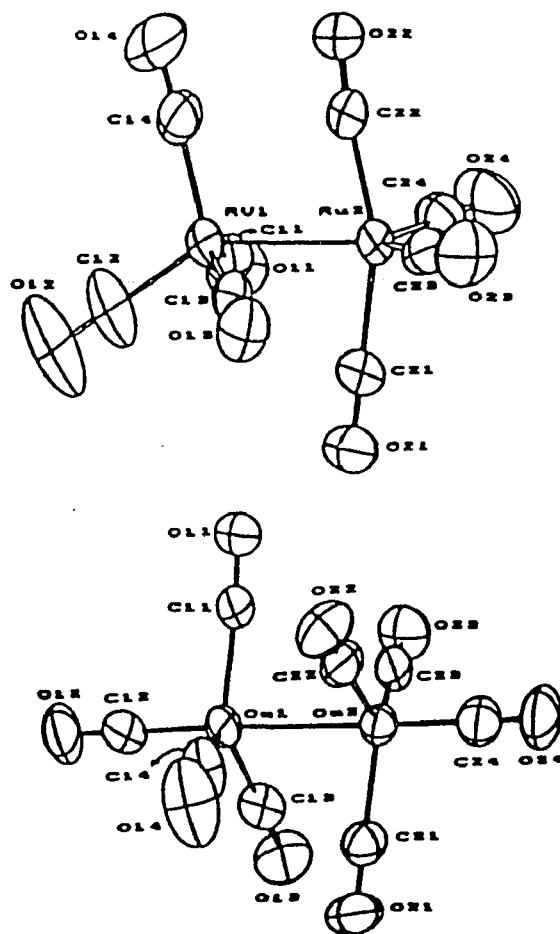


Figure 10. ORTEPS of  $[\text{Ru}_2(\text{CO})_8]^{2-}$  and  $[\text{Os}_2(\text{CO})_8]^{2-}$ .

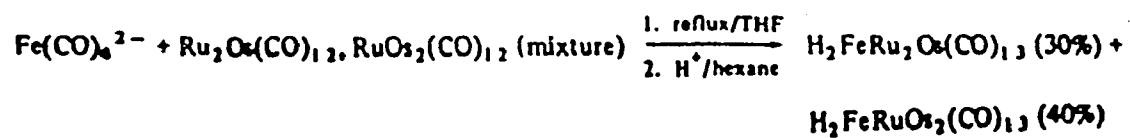
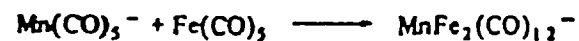
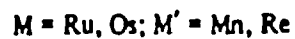
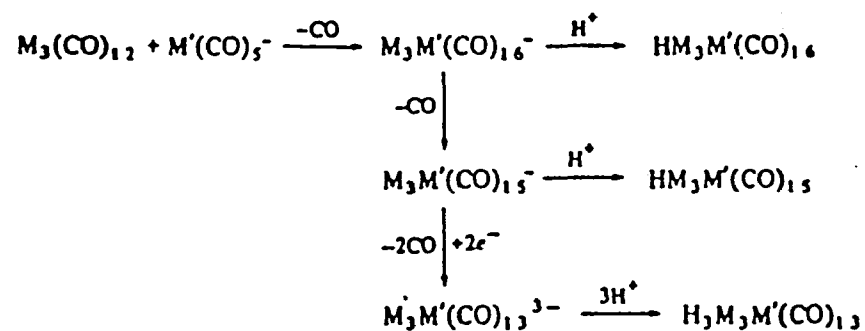
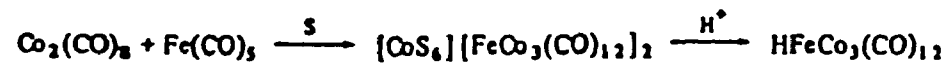
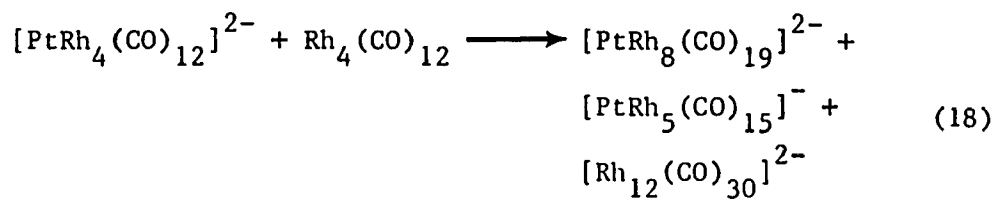
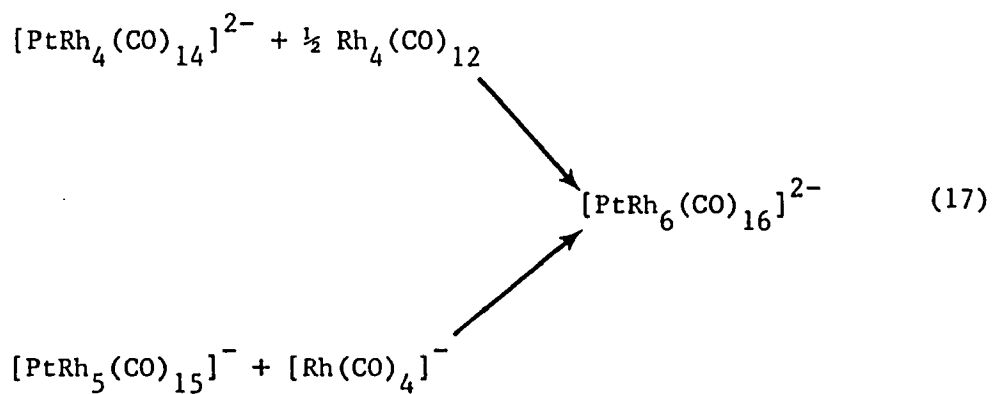
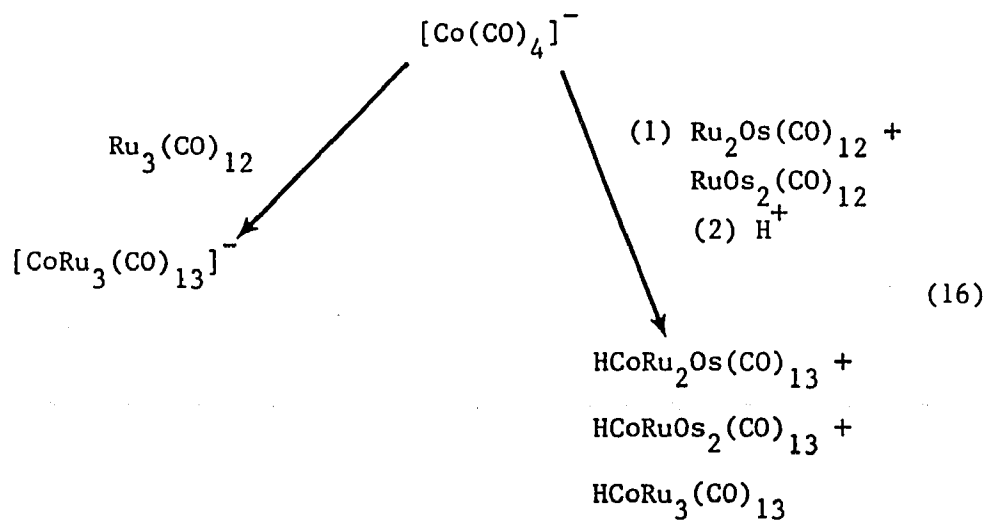
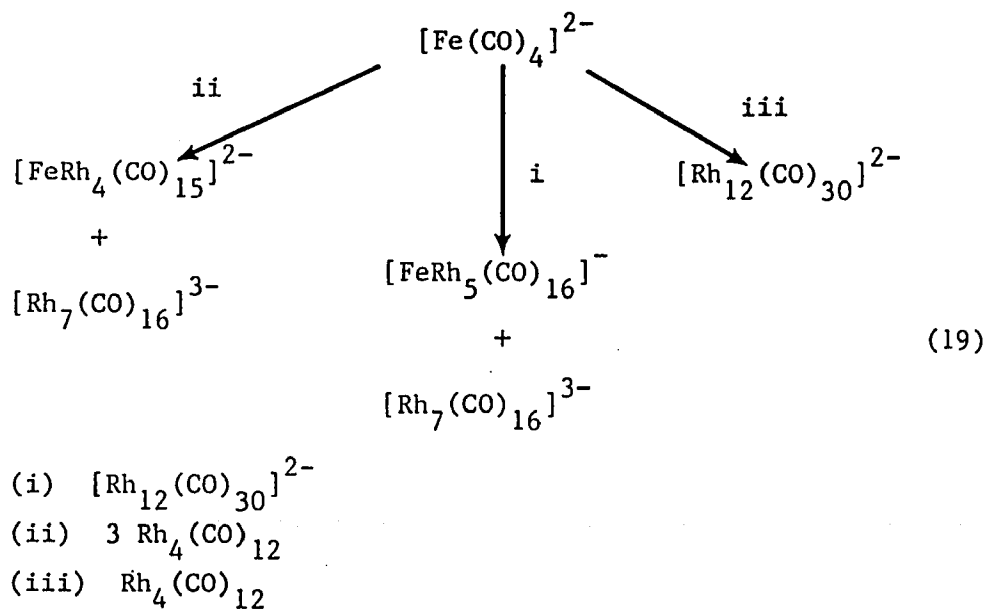


Figure 11. Synthetic Route to Mixed-Metal Clusters from Monomeric Carbonyls.

able to prepare a variety of rhodium clusters ranging from 5 to 12 metal atoms. (Equations 17-19)





As mentioned earlier, these reactions are also applicable in the synthesis of homonuclear clusters. Shore and co-workers have successfully employed this reaction type in the preparation of alkali-metal salts of higher nuclearity carbonylates in high yield. [64] (Fig. 12)

### III. PREPARATION OF CARBONYLATES

The alkali-metal carbonylates are very useful in the redox condensation method because of their higher reactivity than previously used amine and related salts. The alkali-metal carbonylates may be prepared by four basic reaction types: (1) reaction of neutral carbonyls with alkali metals, (2) reaction with alkali metal hydrides, (3) reaction with alcoholic bases, and (4) substitution reactions of carbonyl groups with anionic ligands.

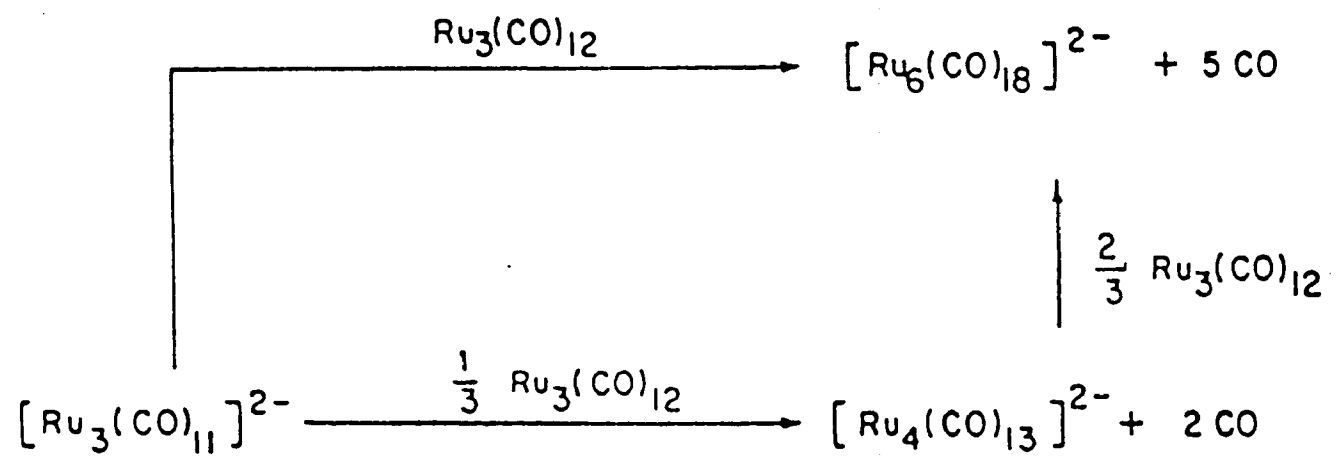


Figure 12. Synthetic Route to Higher Nuclearity Carbonylates.

Of these four, the most useful is the reduction of carbonyl complexes using alkali metals, [64-66] amalgams, [67] or alkali metal hydrides. [68] Shore and co-workers [64-66] have made extensive use of alkali-metal benzophenone ketyls to reduce cluster carbonyls, forming carbonylates in very high yield. (Fig. 13) This method is favored over the other reductions since they tend to fragment polynuclear carbonyls forming mononuclear carbonylates.

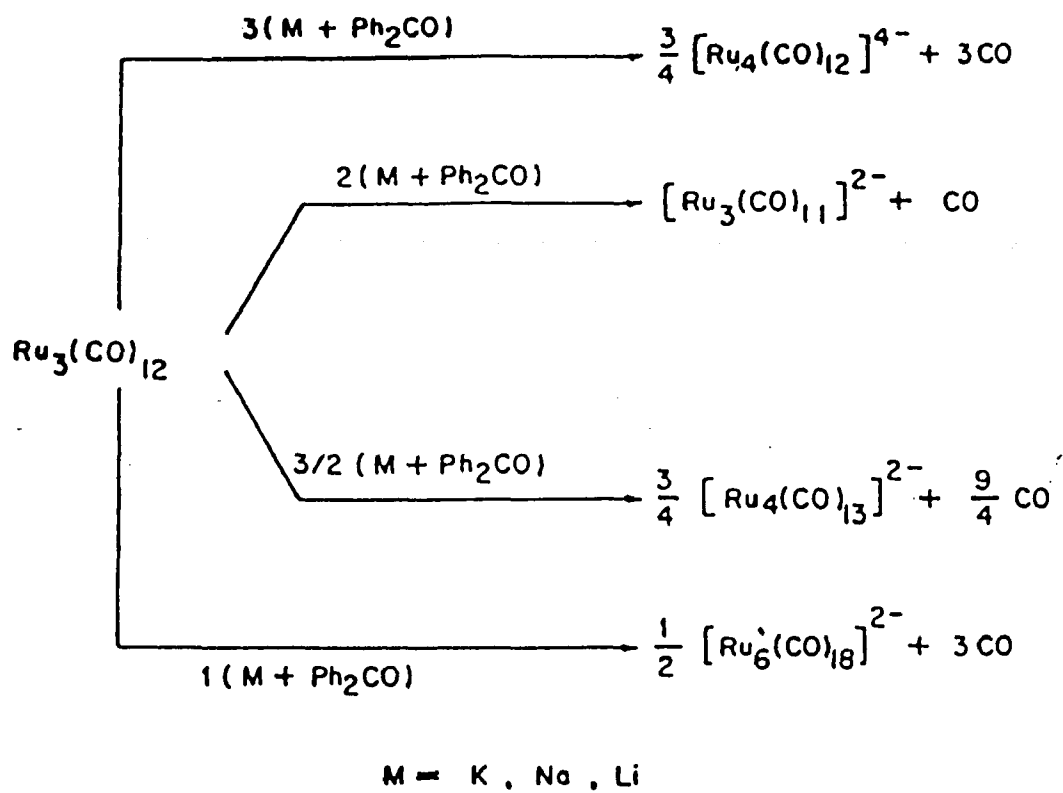


Figure 13. Ketyl Reduction of  $Ru_3(CO)_{12}$ .

## STATEMENT OF THE PROBLEM

The purpose of the present investigation is to develop systematic syntheses of mixed-metal clusters using the redox condensation method. Tetranuclear and higher nuclearity carbonyl clusters of the iron triad (Fe, Ru, Os) are of particular interest since it is this triad that has been implicated in many catalytic processes.

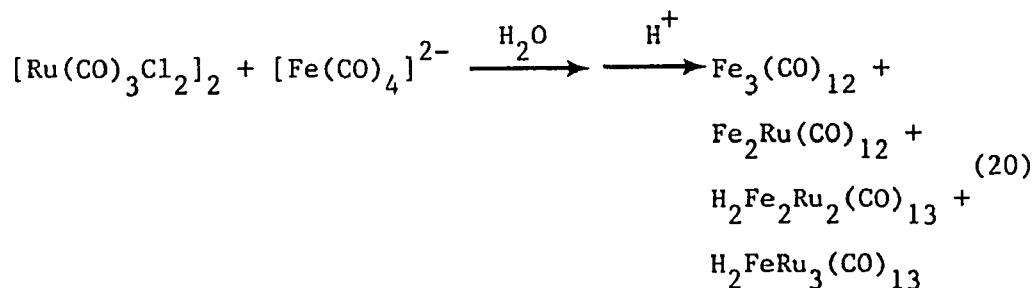
Once synthesized, structure determinations of these clusters will be undertaken. The information thus gained can be used in molecular modeling studies of these clusters on surfaces.

## RESULTS & DISCUSSION

### I. IRON/RUTHENIUM SYSTEMS

A. Introduction. The search for mixed metal clusters containing iron and ruthenium begins with the dinuclear species. As mentioned earlier, Coffy and Shore [57] have been successful in synthesizing the mixed metal dinuclear carbonylate,  $[\text{FeRu}(\text{CO})_8]^{2-}$ , using the redox condensation method. (Equation 15)

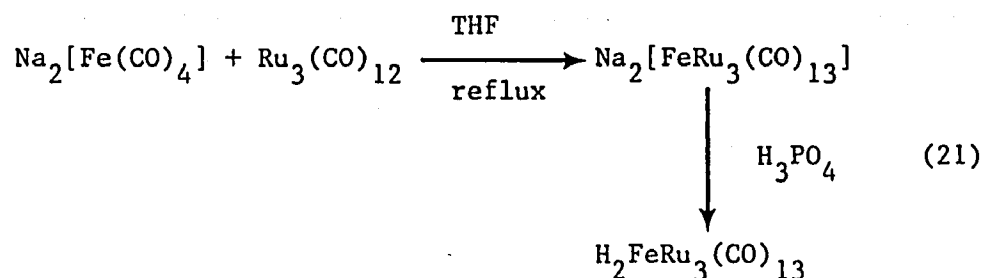
Trinuclear clusters of iron and ruthenium were first generated by Yawney and Stone [40] by the pyrolysis of  $\text{Fe}(\text{CO})_5$  with  $[\text{Ru}(\text{CO})_3\text{Cl}_2]_2$  in yields of 5-8%. (Equation 3) Generation of  $\text{Fe}_2\text{Ru}(\text{CO})_{12}$  and  $\text{FeRu}_2(\text{CO})_{12}$  is also possible from the pyrolysis of  $\text{Fe}(\text{CO})_5$  with  $\text{Ru}_3(\text{CO})_{12}$  with yields ranging from 7-11%. [40] (Equations 9,10) Recently Venalainen and Pakkanen have synthesized  $\text{Fe}_2\text{Ru}(\text{CO})_{12}$  in up to 20% yield from  $[\text{Fe}(\text{CO})_4]^{2-}$  and  $[\text{Ru}(\text{CO})_3\text{Cl}_2]_2$ . [69] (Equation 20)



Of all the possible tetranuclear iron-ruthenium combinations,

those clusters exhibiting metal ratios of 1Fe:3Ru and 2Fe:2Ru are isolable.  $\text{H}_2\text{FeRu}_3(\text{CO})_{13}$  was observed by Yawney and Stone [40a] when a ruthenium source such as  $[\text{Ru}(\text{CO})_3\text{Cl}_2]_2$  or  $\text{Ru}_3(\text{CO})_{12}$  was pyrolyzed in the presence of  $\text{Fe}(\text{CO})_5$ . (Equations 3,9,10) Yields were typically low for these syntheses ranging from trace amounts to 9%.

Geoffroy and Gladfelter [70,71] were able to synthesize  $\text{H}_2\text{FeRu}_3(\text{CO})_{13}$  in improved yields (49-56%) using the redox condensation of  $[\text{Fe}(\text{CO})_4]^{2-}$  with  $\text{Ru}_3(\text{CO})_{12}$  according to Equation 21.



Other cluster species obtained from this reaction are  $\text{H}_4\text{Ru}_4(\text{CO})_{12}$ ,  $\text{Fe}_3(\text{CO})_{12}$ ,  $\text{H}_2\text{Ru}_4(\text{CO})_{13}$ ,  $\text{FeRu}_2(\text{CO})_{12}$ , and  $\text{H}_2\text{Fe}_2\text{Ru}_2(\text{CO})_{13}$ . These may be separated using TLC or column chromatography.  $\text{H}_2\text{Fe}_2\text{Ru}_2(\text{CO})_{13}$  seems to be the only impurity which may linger to contaminate the  $\text{H}_2\text{FeRu}_3(\text{CO})_{13}$  since retention times are similar. However,  $\text{H}_2\text{Fe}_2\text{Ru}_2(\text{CO})_{13}$  is less stable to silica gel than  $\text{H}_2\text{FeRu}_3(\text{CO})_{13}$  and tends to decompose during the elution process. [70a]

The cluster  $\text{H}_2\text{FeRu}_3(\text{CO})_{13}$  has been fully characterized by IR, NMR [70-72] and X-ray crystallography. Figure 14 shows the molecular structure of  $\text{H}_2\text{FeRu}_3(\text{CO})_{13}$ . [73,74]

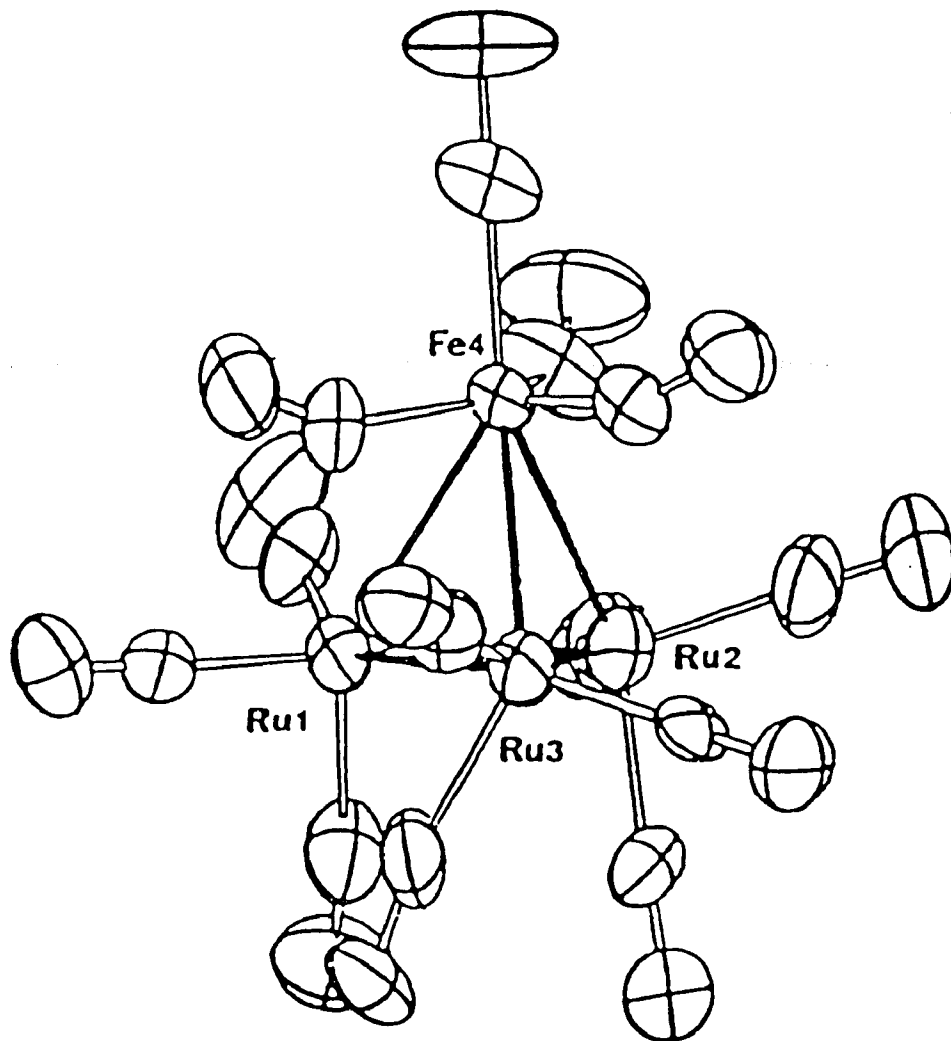
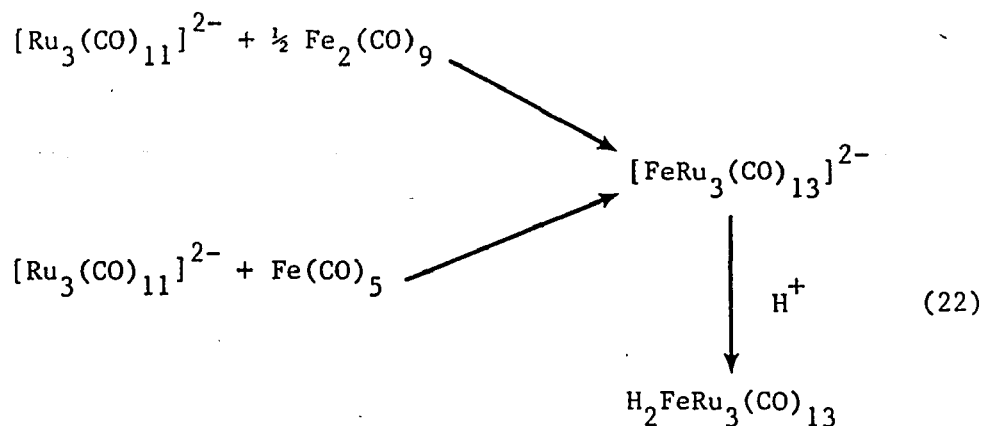


Figure 14. ORTEP of  $\text{H}_2\text{FeRu}_3(\text{CO})_{13}$ .

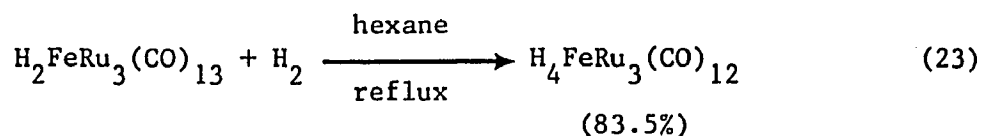
Shore and co-workers [75] have also synthesized  $\text{H}_2\text{FeRu}_3(\text{CO})_{13}$  *via* the redox condensation method. If  $[\text{Ru}_3(\text{CO})_{11}]^{2-}$  is reacted with  $1/3 \text{Fe}_3(\text{CO})_{12}$  one obtains a mixture of anions which upon protonation affords  $\text{H}_2\text{Ru}_4(\text{CO})_{13}$ ,  $\text{H}_2\text{FeRu}_3(\text{CO})_{13}$ ,  $\text{Ru}_3(\text{CO})_{12}$ ,  $\text{FeRu}_2(\text{CO})_{12}$ ,  $\text{Fe}_2\text{Ru}(\text{CO})_{12}$  and  $\text{Fe}_3(\text{CO})_{12}$ . It was found; however, that  $\text{H}_2\text{FeRu}_3(\text{CO})_{13}$  may be obtained in 80-90% when reacted according to Equation 22.



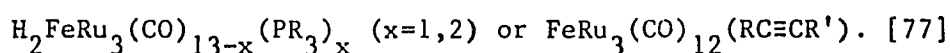
The mixed metal cluster  $\text{H}_2\text{Fe}_2\text{Ru}_2(\text{CO})_{13}$  is another tetranuclear iron-ruthenium system which is frequently synthesized along with  $\text{H}_2\text{FeRu}_3(\text{CO})_{13}$ ; however, it is most often obtained in very low yields. [70a] It is believed to be isostructural with  $\text{H}_2\text{FeRu}_3(\text{CO})_{13}$  and has been claimed to be co-crystallized with  $\text{H}_2\text{FeRu}_3(\text{CO})_{13}$  in approximately 37% occupancy. [69] It has also been claimed to be synthesized in yields of up to 20% from the reaction in Equation 20.

Reaction chemistry involving these bimetallic systems has been rather limited. Kaesz and co-workers [76] subjected  $\text{H}_2\text{FeRu}_3(\text{CO})_{13}$  under hydrogenation conditions to afford the new cluster,

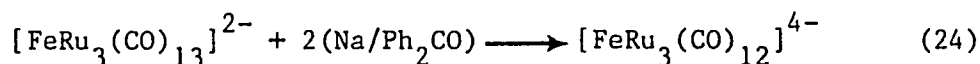
$\text{H}_4\text{FeRu}_3(\text{CO})_{12}$ . (Equation 23)



Other reactivity studies involve carbonyl ligand substitution with various phosphines or alkynes forming clusters of the type



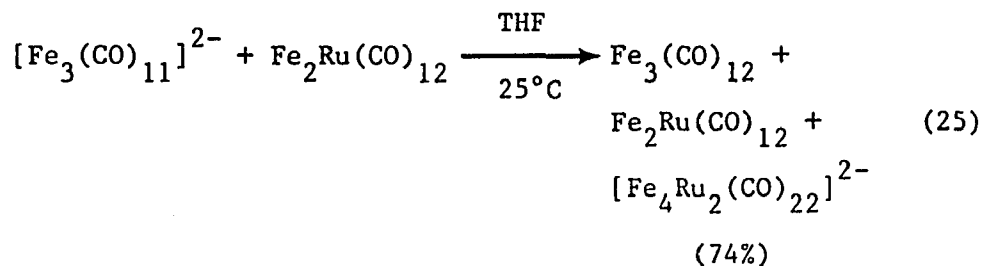
Shore and co-workers [75], on the other hand, have expended much effort on the generation of the anionic mixed-metal species,  $[\text{HFeRu}_3(\text{CO})_{13}]^-$  and  $[\text{FeRu}_3(\text{CO})_{13}]^{2-}$  *via* the reduction of the neutral cluster with either alkali metal-benzophenone ketyls or alkali metal hydrides. They have also been successful in the synthesis of the highly charged anion,  $[\text{FeRu}_3(\text{CO})_{12}]^{4-}$  by this method. (Equation 24)



Geoffroy and co-workers [77] have also generated the anions,  $[\text{HFeRu}_3(\text{CO})_{13}]^-$  and  $[\text{HFe}_2\text{Ru}_2(\text{CO})_{13}]^-$ . These clusters have been fully characterized by spectroscopic means and in the case of  $[\text{PPh}_4]_2[\text{FeRu}_3(\text{CO})_{13}]$  by X-ray crystallography. [75] These anionic clusters are then used as models for mixed-metal species on a catalytic surface. [78]

The synthesis of higher nuclearity clusters containing only iron and ruthenium seems to be a challenge. To date,  $[\text{Fe}_4\text{Ru}_2(\text{CO})_{22}]^{2-}$  is the only cluster synthesized meeting this criterion. [79]

Synthesis of this rather unique cluster is accomplished as follows. (Equation 25)



$[\text{PPN}]_2[\text{Fe}_4\text{Ru}_2(\text{CO})_{22}]$  has been spectroscopically characterized. X-ray crystallography (Fig. 15) indicates a very unusual structure. It does not adopt the expected polyhedral arrangement but rather consists of two  $\text{Fe}_2\text{Ru}$  triangles joined by a Ru-Ru bond.

B. Results & Discussion. It has been the goal of the present investigation to generate higher nuclearity clusters containing iron and ruthenium *via* the redox condensation method. The strategy employed to generate these higher nuclearity clusters was to start with a low nuclearity carbonylate and to systematically add one metal fragment to increase the nuclearity of the resulting clusters.

### 1. Reactions of $[\text{Ru}_3(\text{CO})_{11}]^{2-}$ and $[\text{Ru}_4(\text{CO})_{13}]^{2-}$

Reaction of  $[\text{Ru}_3(\text{CO})_{11}]^{2-}$  with an excess of  $\text{Fe}(\text{CO})_5$  or  $\text{Fe}_2(\text{CO})_9$  affords  $\text{Fe}_3(\text{CO})_9$ ,  $\text{H}_4\text{Ru}_4(\text{CO})_{13}$ ,  $\text{H}_2\text{FeRu}_3(\text{CO})_{13}$ , and  $\text{H}_2\text{Fe}_2\text{Ru}_2(\text{CO})_{13}$  upon protonation according to Equation 26. Each of the cluster species were isolated in pure form *via* chromatographic techniques and identified spectroscopically.

Unfortunately, the generation of higher nuclearity clusters other than the known tetranuclear clusters was not realized. Varying both

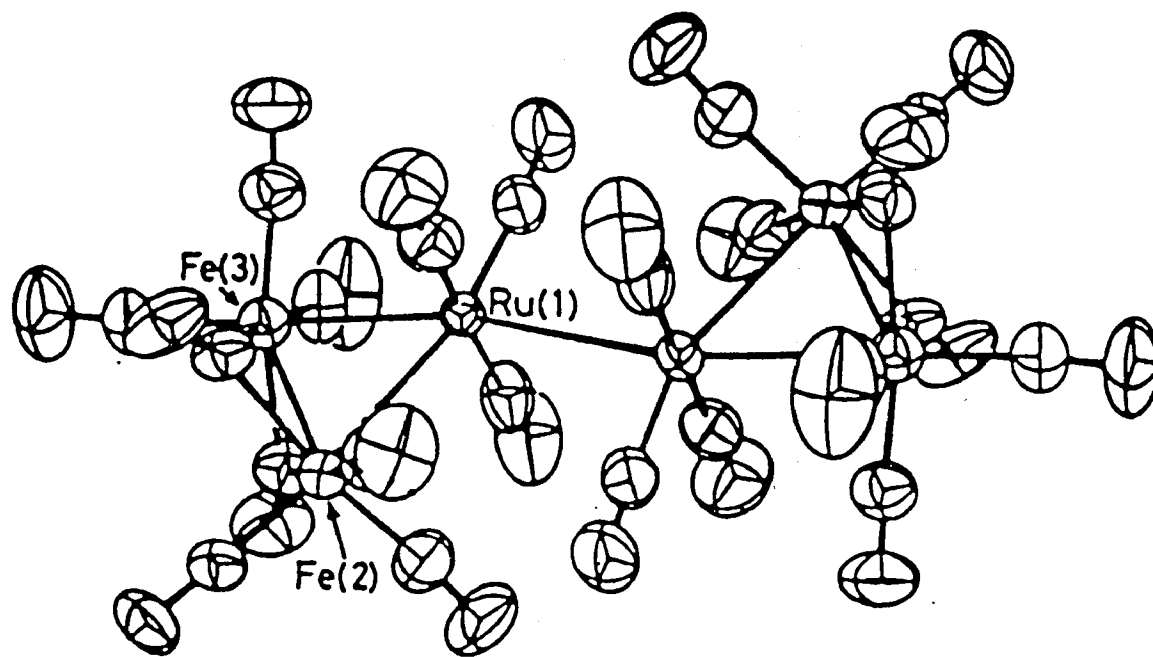
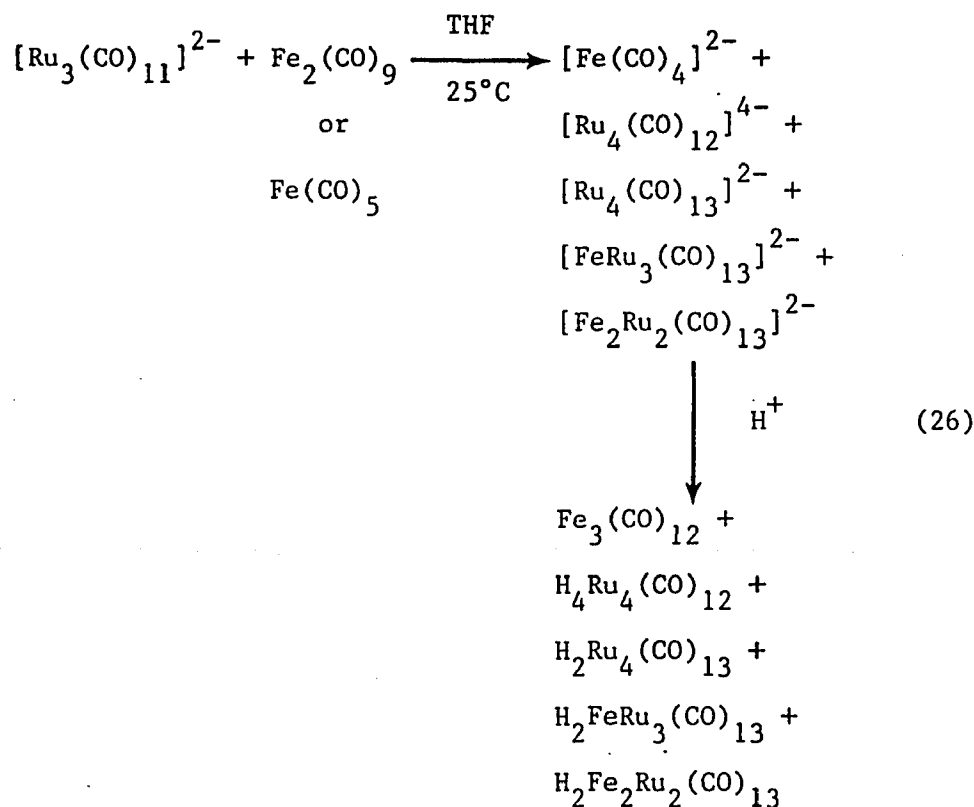


Figure 15. ORTEP of  $[\text{Fe}_4\text{Ru}_2(\text{CO})_{22}]^{2-}$ .

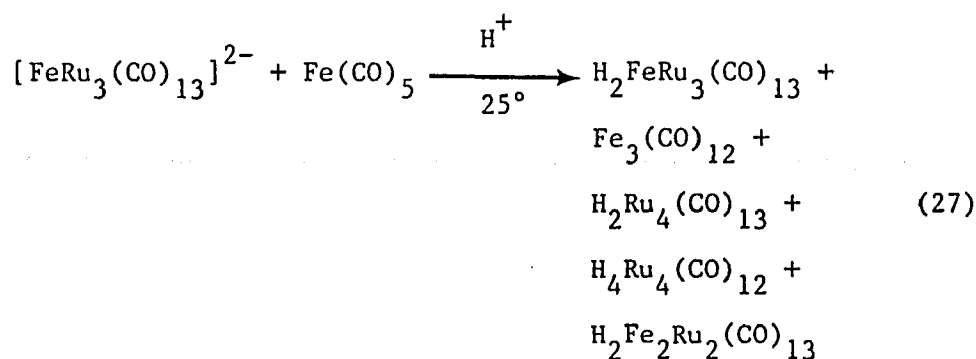


carbonylate and iron carbonyl concentrations and reaction conditions only influenced the product yields not species formed. It should also be noted that when  $\text{Fe}(\text{CO})_5$  is the neutral carbonyl employed, formation of  $\text{Fe}_3(\text{CO})_{12}$  is greatly reduced. This implies that  $\text{Fe}_2(\text{CO})_9$  dissociates into  $[\text{Fe}(\text{CO})_4]^{2-}$  and  $\text{Fe}(\text{CO})_5$  upon reaction; the  $[\text{Fe}(\text{CO})_4]^{2-}$  then recombines to form  $\text{Fe}_3(\text{CO})_{12}$  and excess  $\text{Fe}(\text{CO})_5$  can be isolated. This occurrence was observed throughout this work.

$[\text{Ru}_4(\text{CO})_{13}]^{2-}$  was reacted with iron pentacarbonyl or diiron nonacarbonyl in an attempt to synthesize the penta- or hexa- nuclear species; however, this was not achieved. Instead, the products

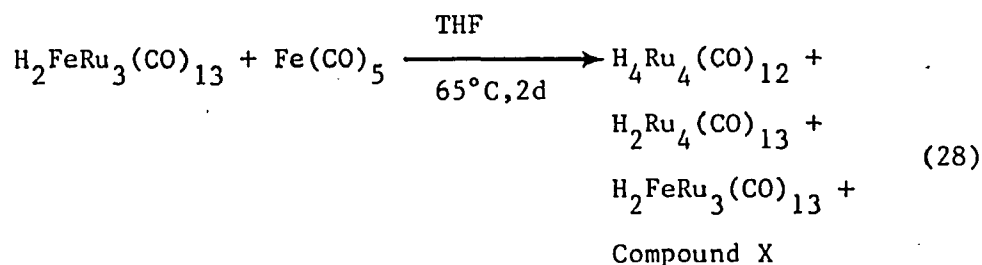
obtained were those listed in Equation 26. Again, only product yields could be altered with varying reaction conditions and concentrations.

Reaction of the mixed metal species  $[\text{FeRu}_3(\text{CO})_{13}]^{2-}$  with iron carbonyls did not produce the penta- or hexa- nuclear clusters either. (Equation 27)



In this situation most of the product yield consisted of the  $\text{FeRu}_3$  tetranuclear cluster.

If the neutral species  $\text{H}_2\text{FeRu}_3(\text{CO})_{13}$  was reacted with an excess of  $\text{Fe}(\text{CO})_5$  under more harsh conditions a small amount (8.7% by  $^1\text{H}$  NMR) of a new complex formed; (Equation 28) however, the majority of the product isolated is  $\text{H}_2\text{Ru}_4(\text{CO})_{13}$ .



The new cluster which shall be temporarily called Compound X was

been spectroscopically characterized. It is discussed fully later in this chapter (Section 3--Reaction of  $[\text{Ru}_6(\text{CO})_{18}]^{2-}$ ).

At this point it seems that the redox condensation method falls short of our expectations to be able to generate higher nuclearity clusters where  $M \geq 5$ . It seems that although the combination of a carbonylate with a neutral carbonyl species is a viable method for the direct synthesis of heteronuclear clusters with  $M \leq 4$ , several limitations cause it to fail with the larger clusters. Limitations that have been observed deal with the oxidizing/reducing ability of the carbonyl/carbonylate combination and the stability of the product with respect to the geometry of the polyhedral structure adopted.

Geoffroy [80] has commented that if the carbonylate is a strong reducing agent or if the neutral carbonyl cluster is easily oxidized, a redox reaction rather than the desired condensation reaction occurs. Therefore, greater nucleophilicity (basicity) of the carbonylate should lead to more rapid reaction with addition (ie. condensation) competing more effectively with other reaction pathways. [70a] In other words, the neutral metal carbonyl functions as a Lewis acid towards the carbonylate (the Lewis base). [81]

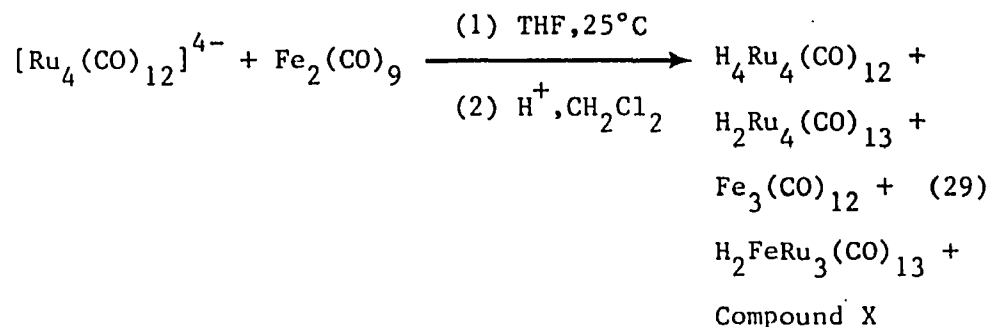
Geoffroy has also stated that the strength of the metal-carbonyl bonds in the neutral carbonyl influences the reactivity of this reaction type. [70a] One would then expect decreased reactivity and product yield going down the iron triad. However, if product did form one would expect greater product stability due to the enhanced strength.

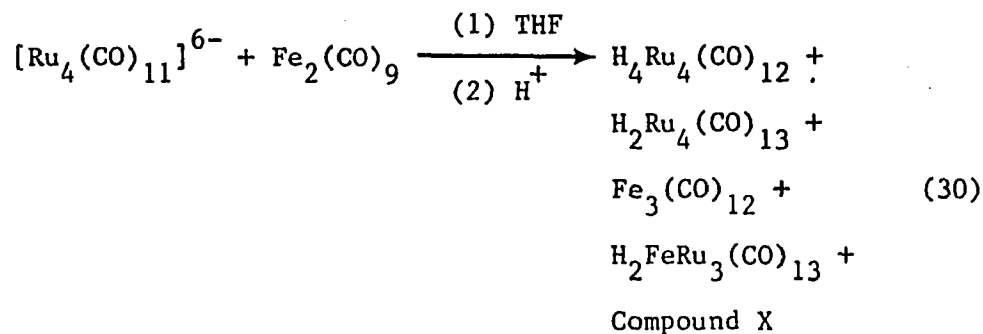
The second school of thought centers around the stability of certain polyhedral geometries. [32a,35,82,83] In particular Minot and Criado-Sancho [82a] and Mingos [82b] point out that the bond overlap within the tetrahedron is greater than that available to the octahedral geometry, thereby, implying increased stability of the former relative to the latter geometry. However, this enhanced stability is marginal and other factors are usually contributing more heavily, especially in the low nuclearity clusters where the number of valence electrons dictate the bonding characteristics.

## 2. Reactions of $[\text{Ru}_4(\text{CO})_{12}]^{4-}$ and $[\text{Ru}_4(\text{CO})_{11}]^{6-}$

In an attempt to overcome the problems encountered when the dianions were reacted with an iron carbonyl source, the highly charged clusters  $[\text{Ru}_4(\text{CO})_{12}]^{4-}$  and  $[\text{Ru}_4(\text{CO})_{11}]^{6-}$  were employed. It was hoped that the increased basicity (nucleophilicity) of these clusters would influence the condensation reaction over the other pathways possible.

Reaction of each of these clusters with diiron carbonyl (Equations 29,30); however, does not achieve the desired goal, namely, mixed metal clusters of  $M > 4$  were not observed.





In each case, isolable products are listed and are obtained in yields comparable to those in the  $[\text{Ru}_3(\text{CO})_{11}]^{2-}$  or  $[\text{Ru}_4(\text{CO})_{13}]^{2-}$  reactions with  $\text{H}_4\text{Ru}_4(\text{CO})_{12}$  being the major product under the reaction conditions described.  $^1\text{H}$  NMR also indicates formation of the new cluster Compound X in yields of up to 15% (by  $^1\text{H}$  NMR peak area integration), which was first observed in the pyrolysis reaction of  $\text{H}_2\text{FeRu}_3(\text{CO})_{13}$  with  $\text{Fe}(\text{CO})_5$ . It should be noted at this point that Compound X appears in higher yield when the hexa-anion is the carbonylate.

### 3. Reaction of $[\text{Ru}_6(\text{CO})_{18}]^{2-}$

The bond overlap may have a greater influence on the reactivity due to enhanced stability or instability of the carbonylate than the nucleophilicity does. To examine this possibility  $[\text{Ru}_6(\text{CO})_{18}]^{2-}$  (PPN,  $\text{PPh}_4$ ,  $\text{PMePh}_3$ , K, Na salts) was reacted with  $\text{Fe}_2(\text{CO})_9$  or  $\text{Fe}(\text{CO})_5$ . (Equations 31,32)

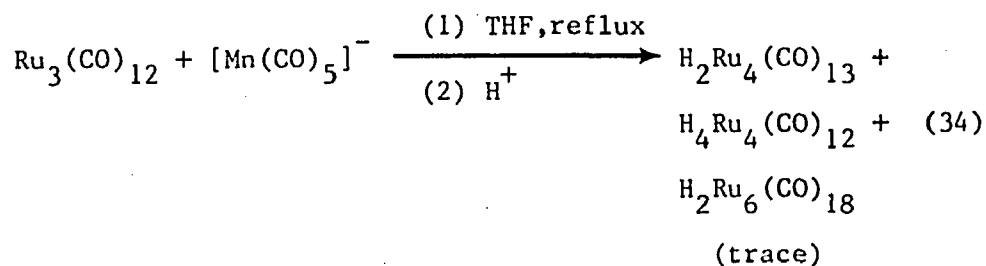
Once again the redox condensation reaction has failed to produce higher nuclearity mixed-metal species. What seems to be taking place is an oxidation/reduction reaction indicating that the carbonylate is being oxidized by the carbonyl. Evidence for this type of reaction is indicated by the formation of the new

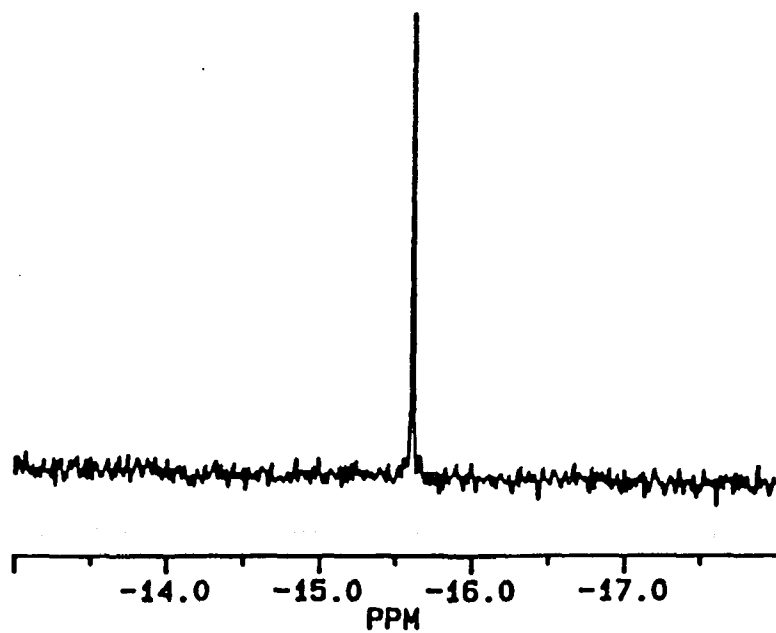


The new hexanuclear cluster  $\text{H}_2\text{Ru}_6(\text{CO})_{17}$  has been spectroscopically characterized. It exhibits a singlet in the proton NMR (Fig. 16A) at  $\delta$ -15.6 ppm which indicates the hydrides to be equivalent and having a fairly strong interaction with the metallic core as suggested by its downfield shift.  $^{13}\text{C}$  NMR (Fig. 16B) at room temperature shows a singlet in the terminal region,  $\delta$ 194.45 ppm, which implies fluxionality of the cluster. Low temperature  $^{13}\text{C}$  NMR is not possible due to the limited solubility of this cluster in organic solvents.

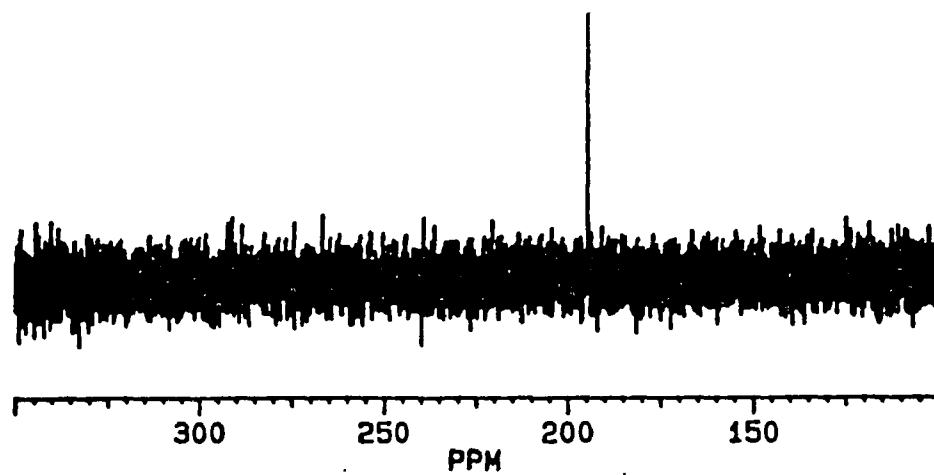
The highly symmetric structure that may be envisioned for this cluster is also indicated in the IR. The solution IR (Fig. 17) in  $\text{CH}_2\text{Cl}_2$  consists of one major band ( $2060\text{ cm}^{-1}$ ) indicating terminal carbonyls. The nujol spectrum; (Fig. 18) however, shows a weak absorption at  $1732\text{ cm}^{-1}$  indicative of a bridging carbonyl.

Upon closer examination of Equation 33, one might argue that a simple protonation is actually occurring to form the product  $\text{H}_2\text{Ru}_6(\text{CO})_{18}$ . Indeed this product has been claimed first by Knight and Mays [59a,59c,87] (Equation 34) and later by Johnson and Lewis [84-86] (Equation 35)





A



B

Figure 16. Proton (a) and Carbon-13 NMR Spectra of  $(\mu_3\text{-H})_2\text{Ru}_6(\mu\text{-CO})(\text{CO})_{16}$ .

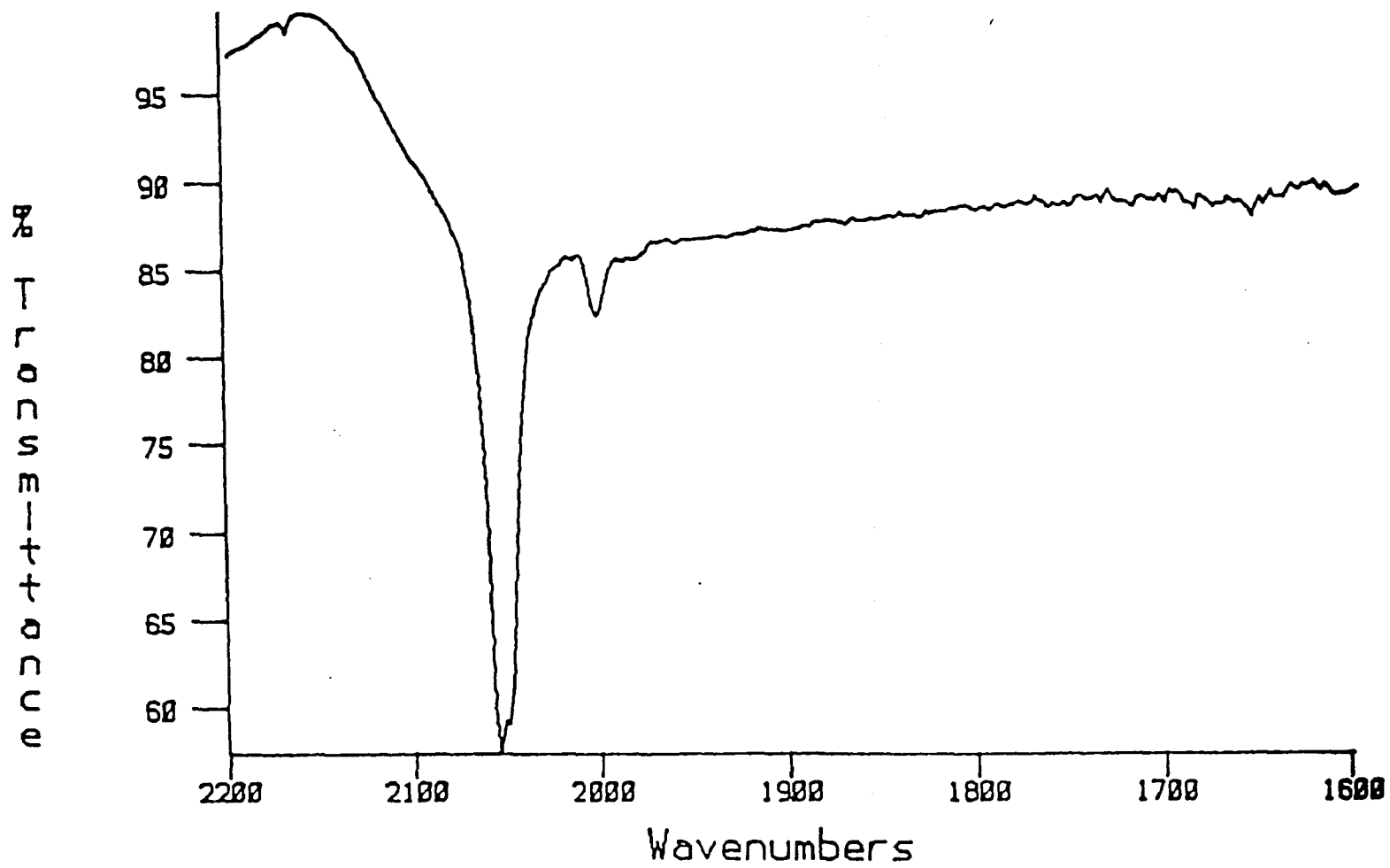


Figure 17. Solution IR Spectrum of  $(\mu_3\text{-H})_2\text{Ru}_6(\mu\text{-CO})(\text{CO})_{16}$ .

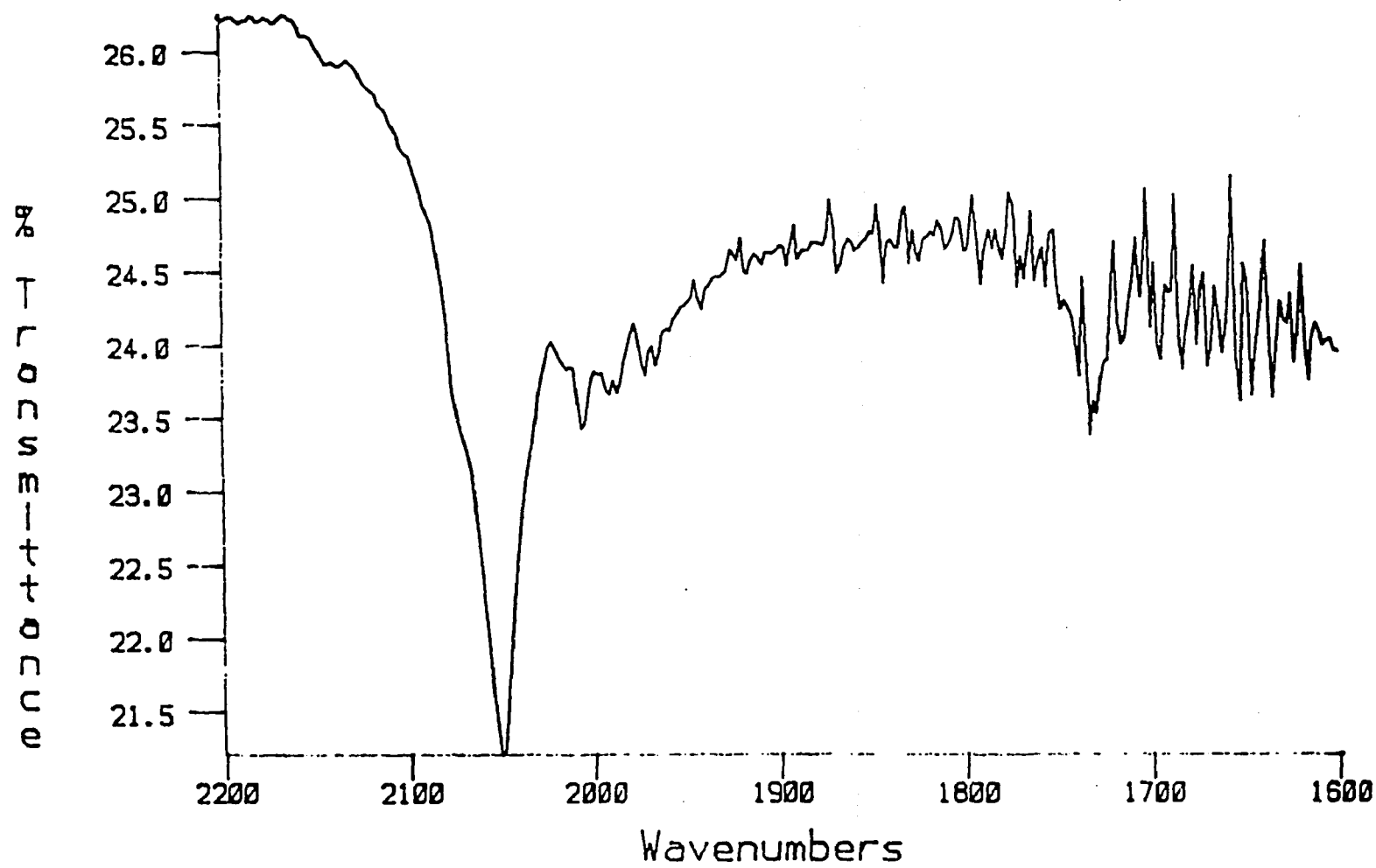
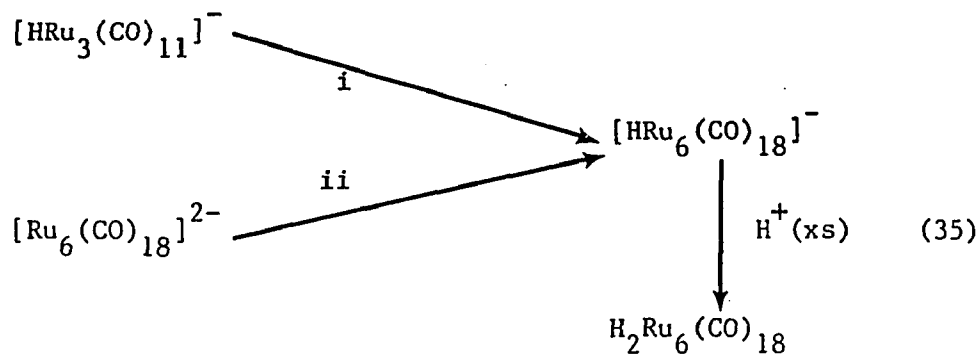


Figure 18. Solid State IR Spectrum of  $(\mu_3\text{-H})_2\text{Ru}_6(\mu\text{-CO})(\text{CO})_{16}$ .



(i) (1)  $\text{H}_2\text{SO}_4$   
 (2)  $\text{NMe}_4\text{Cl}/\text{MeOH}$

(ii) (1)  $\text{H}_2\text{SO}_4$   
 (2)  $\text{PPNCl}/\text{MeOH}$

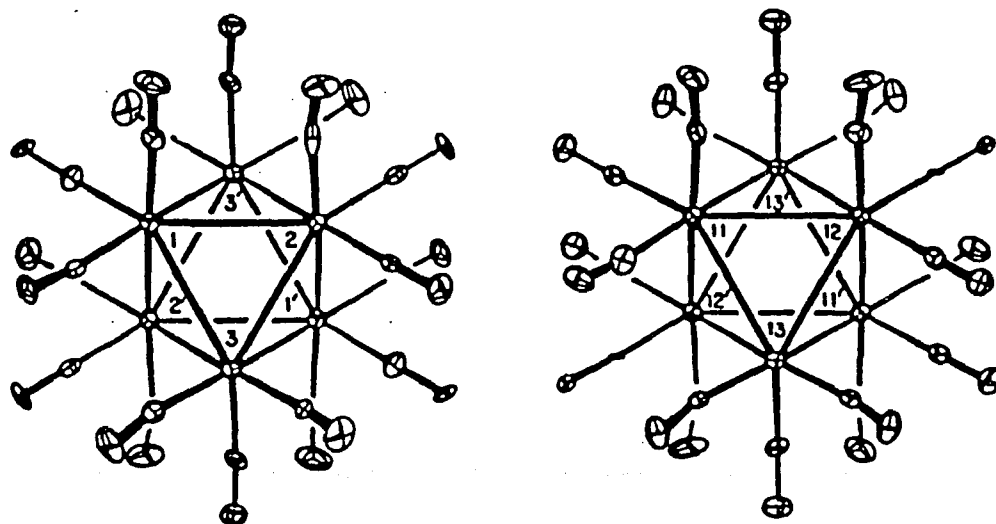
Knight and Mays claim to have obtained the  $\text{H}_2\text{Ru}_6(\text{CO})_{18}$  cluster in extremely low yields. On the other hand, Johnson and Lewis indicate yields of up to 90% are possible. Reported spectroscopic evidence is very limited from either research group; however, the IR spectra that have been reported agree with what is observed for the  $\text{H}_2\text{Ru}_6(\text{CO})_{17}$  cluster. (Fig. 17) ( $\nu_{\text{CO}}$  2058(s), 2052(s), 2003(w)  $\text{cm}^{-1}$  in  $\text{CH}_2\text{Cl}_2$  [84];  $\nu_{\text{CO}}$  2060(s), 2054(s), 2008(w)  $\text{cm}^{-1}$  in  $\text{CCl}_4$  [59a])

A crystal structure of  $\text{H}_2\text{Ru}_6(\text{CO})_{18}$  (crystal supplied by Knight and Mays [59a]) has been solved by Churchill and Wormald. [59c,87] Crystallographic data for  $\text{H}_2\text{Ru}_6(\text{CO})_{18}$  as reported by Churchill and Wormald are given in Table 1. The molecular structure of  $\text{H}_2\text{Ru}_6(\text{CO})_{18}$  is given in Figure 19A. [87]

Churchill describes the molecule as follows. [59c,87] The two crystallographically independent  $\text{H}_2\text{Ru}_6(\text{CO})_{18}$  clusters are stereochemically equivalent, each molecule having precise  $C_1$

Table 1. Crystallographic Data for  $\text{H}_2\text{Ru}_6(\text{CO})_{18}$ .

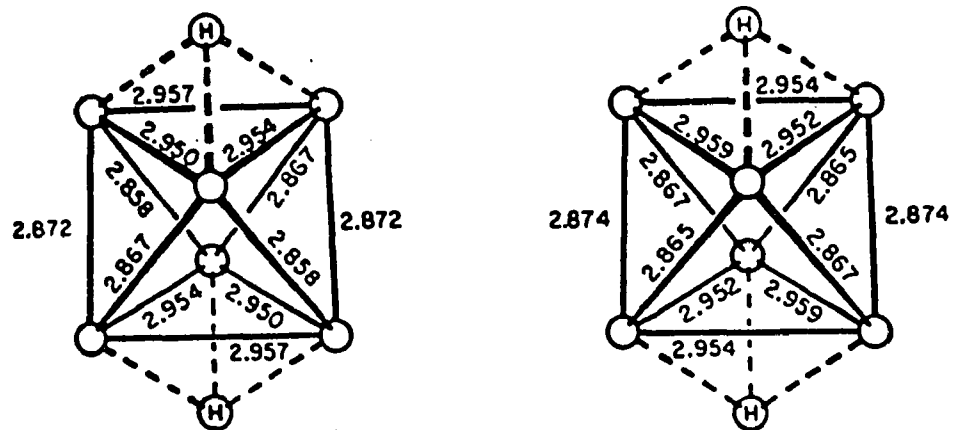
Chemical formula/Color of cryst	$\text{C}_{18}\text{H}_2\text{O}_{18}\text{Ru}_6$ /purple
Molecular wt	1113
Space group	$\text{P}2_1/c$
Molecules/unit cell	4
a, Å	16.627(23)
b, Å	9.582(5)
c, Å	19.446(19)
$\beta$ , deg	120.58(5)
Volume, unit cell Å <sup>3</sup>	2667.1
D(calcd), g cm <sup>-3</sup>	2.771
Radiation	Mo K $\alpha$ (0.710730 Å)
Diffractometer	Supper-Pace Buerger
Scan mode	$\omega$
Absorption coeff, cm <sup>-1</sup>	33.15
No. of reflctns used in structure refinement	2780
$R_f$ , %	5.72
$R_{wf}^2$ , %	2.93
GOF	1.72



A

#1

#2



B

Figure 19.  $\text{H}_2\text{Ru}_6(\text{CO})_{18}$ . Molecular Structure (a) and Probable Location of Hydrides (b).

symmetry with the six ruthenium atoms defining a distorted octahedron. Each ruthenium is associated with three terminal carbonyl ligands.

The two hydride ligand positions have not been determined in the X-ray analysis; however, their most probable locations may be derived from elongated Ru-Ru bonds and displaced carbonyls: (i) Ru-Ru distances within two opposite faces of each octahedron range from 2.950-2.959Å as opposed to other Ru-Ru bonds of 2.850-2.874Å; (ii) three carbonyls lie almost vertically above each of the six small octahedral faces, but carbonyls are spread away from truly axial positions above the two large faces of the octahedron. (Fig. 19B)

In order to determine the exact nature of the cluster formed in Equation 33, a crystal of  $\text{H}_2\text{Ru}_6(\text{CO})_{17}$  was subjected to X-ray analysis. The molecular structure of this novel cluster is shown in Figure 20 and the crystal packing diagram in Figure 21. Selected views of the metallic core displaying the compound's unique features are given in Figures 22-23. Crystallographic data for this cluster appears in Table 2. Selected bond distances and bond angles are listed in Tables 3 and 4, respectively. (The particular features with respect to the data collection and structure solution are described in the Experimental Section of this dissertation.)

The molecular structure of  $\text{H}_2\text{Ru}_6(\text{CO})_{17}$  is isostructural with  $\text{Os}_6(\text{CO})_{18}$ . [88] (Fig. 24) The cluster adopts a bicapped tetrahedral geometry where Ru(1), Ru(4), Ru(5), and Ru(6) describe the inner tetrahedron; furthermore, Ru(2) and Ru(3) cap the Ru(1)-Ru(4)-Ru(6)

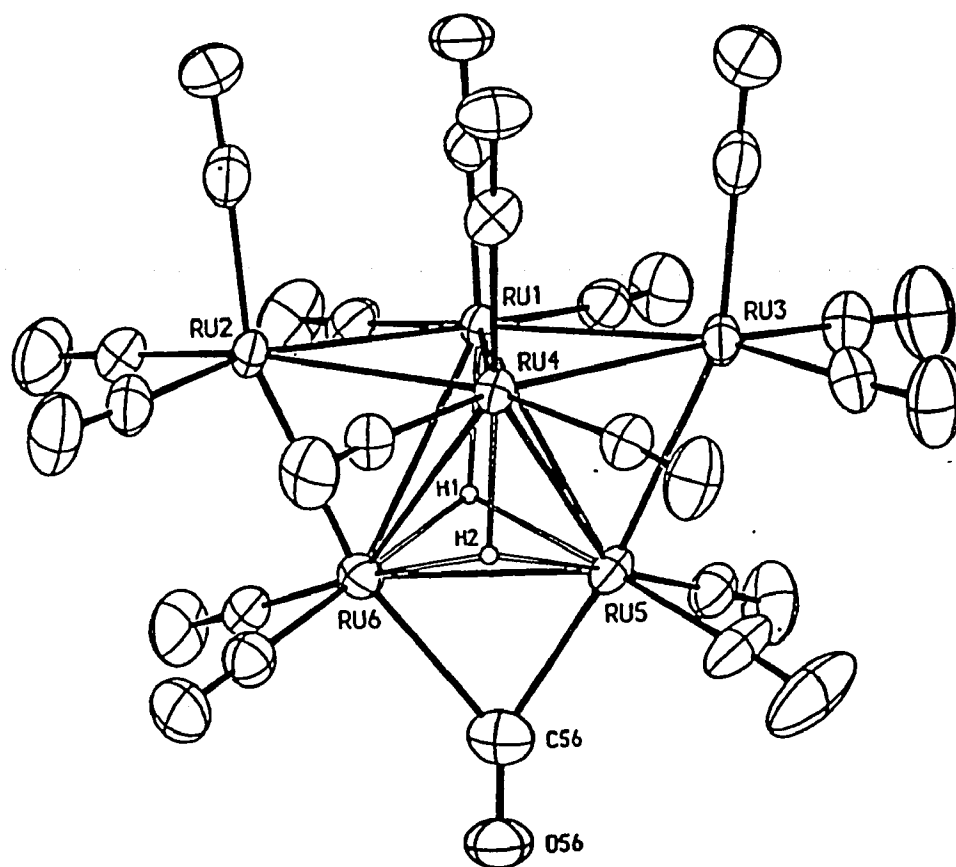


Figure 20. ORTEP of  $(\mu_3\text{-H})_2\text{Ru}_6(\mu\text{-CO})(\text{CO})_{16}$ .

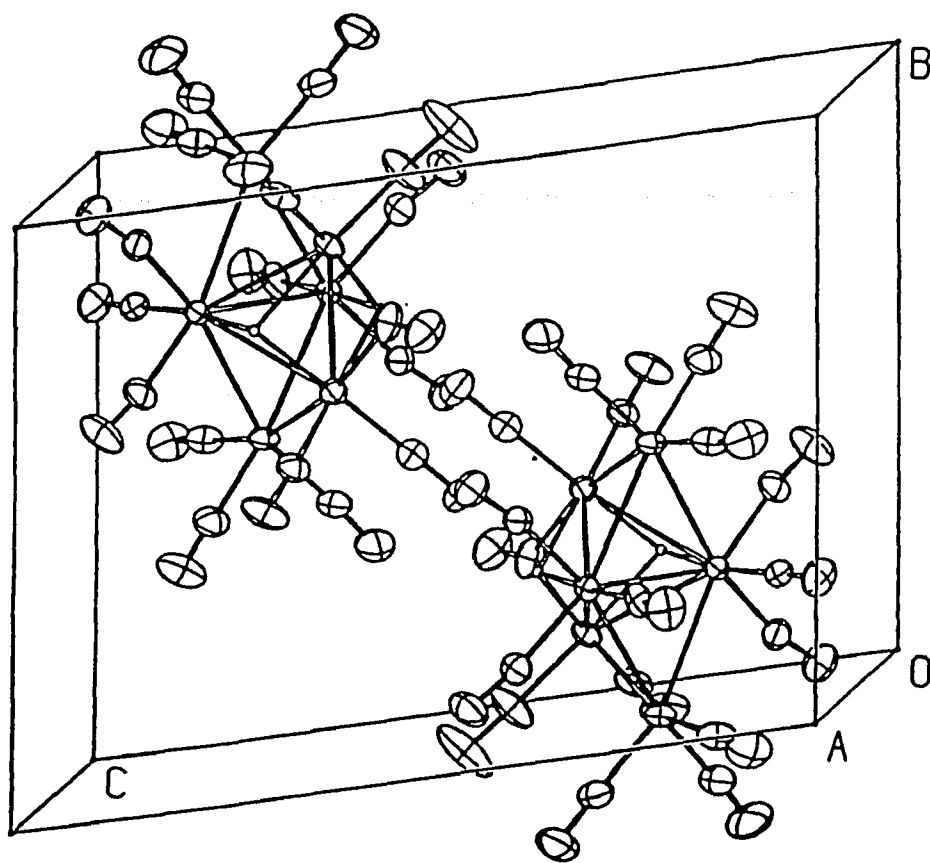


Figure 21. Crystal Packing Diagram of  $(\mu_3\text{-H})_2\text{Ru}_6(\mu\text{-CO})(\text{CO})_{16}$ .

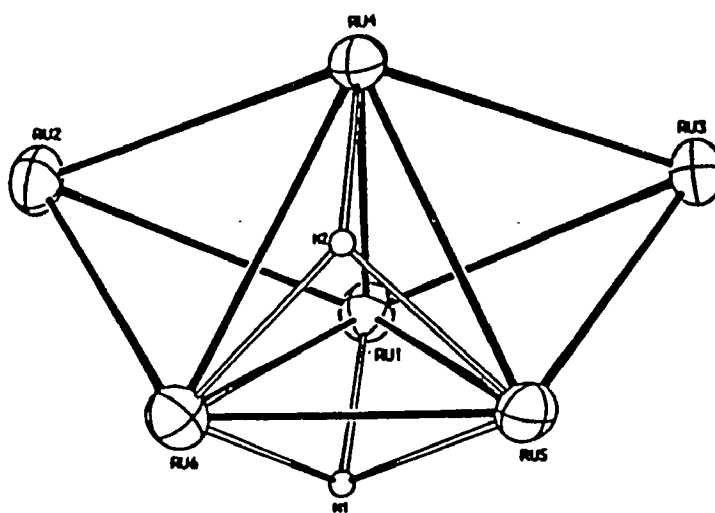
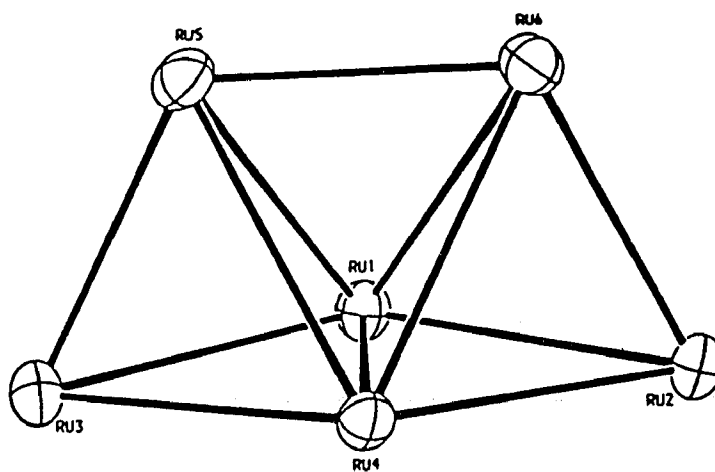


Figure 22. Selected Views of  $\text{H}_2\text{Ru}_6(\text{CO})_{17}$  Metallic Core.

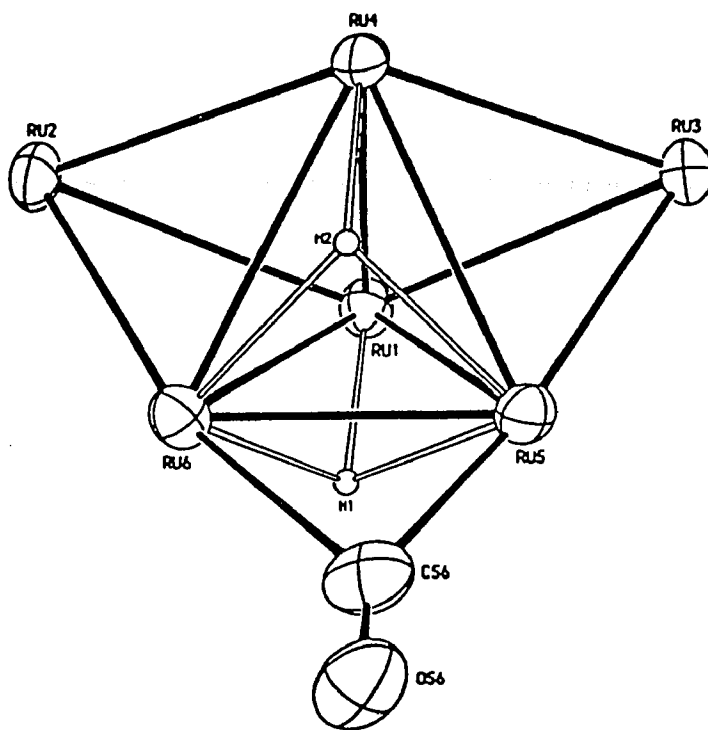


Figure 23. Selected View of  $\text{H}_2\text{Ru}_6(\text{CO})_{17}$  Metallic Core.

Table 2. Crystallographic Data for  $(\mu_3\text{-H})_2\text{Ru}_6(\mu\text{-CO})(\text{CO})_{16}$ .

Chemical formula/Color of cryst	$\text{Ru}_6\text{C}_{17}\text{O}_{17}\text{H}_2$ /purple
Molecular wt	1090
Space group	$\text{P}\bar{1}$
Molecules/unit cell	2
Temp, °C	-40
a, Å	8.131(4)
b, Å	10.996(3)
c, Å	15.350(2)
$\alpha$ , deg	93.58(2)
$\beta$ , deg	97.89(2)
$\gamma$ , deg	109.33(3)
Volume, unit cell Å <sup>3</sup>	1274.130
D(calcd), g cm <sup>-3</sup>	2.827
Radiation	Mo K $\alpha$ (0.710730 Å)
Absorptn coeff, cm <sup>-1</sup>	34.8
Max/Min transmissn, %	99.83/95.84
Scan mode	$\omega$ -2 $\theta$
Data collectn limits, deg	4-55
No. of unique reflctns	5831
No. of reflctns used in structure refinement ( $>3\sigma(I)$ )	3181
No. variable parameters	369
$R_f$	0.028
$R_{wf}/w$	0.032/0.04
GOF	0.989

Table 3. Selected Bond Distances (Å) and Esd's of  
 $(\mu_3\text{-H})_2\text{Ru}_6(\mu\text{-CO})(\text{CO})_{16}$ .

A. Metal-Metal Distances			
Ru(1)-Ru(2)	2.833(1)	Ru(2)-Ru(6)	2.690(1)
Ru(1)-Ru(3)	2.833(1)	Ru(3)-Ru(4)	2.850(1)
Ru(1)-Ru(4)	2.753(1)	Ru(3)-Ru(5)	2.708(1)
Ru(1)-Ru(5)	2.999(1)	Ru(4)-Ru(5)	2.993(1)
Ru(1)-Ru(6)	2.999(1)	Ru(4)-Ru(6)	3.009(1)
Ru(2)-Ru(4)	2.851(1)	Ru(5)-Ru(6)	2.643(1)
B. Ru-C <sub>bridge</sub> and C-O Distances			
Ru(5)-C(56)	2.102(9)	C(56)-O(56)	1.133(10)
Ru(6)-C(56)	2.282(9)		
C. Ru-C <sub>terminal</sub> Distances			
Ru(1)-C(11)	1.903(8)	Ru(3)-C(33)	1.89(1)
Ru(1)-C(12)	1.912(8)	Ru(4)-C(41)	1.922(8)
Ru(1)-C(13)	1.921(9)	Ru(4)-C(42)	1.891(8)
Ru(2)-C(21)	1.874(9)	Ru(4)-C(43)	1.936(8)
Ru(2)-C(22)	1.893(9)	Ru(5)-C(51)	1.860(9)
Ru(2)-C(23)	1.912(9)	Ru(5)-C(52)	1.865(8)
Ru(3)-C(31)	1.861(9)	Ru(6)-C(61)	1.847(9)
Ru(3)-C(32)	1.896(9)	Ru(6)-C(62)	1.848(8)
D. C-O Distances			
C(11)-O(11)	1.123(9)	C(33)-O(33)	1.14(1)
C(12)-O(12)	1.148(9)	C(41)-O(41)	1.128(9)
C(13)-O(13)	1.13(1)	C(42)-O(42)	1.130(9)
C(21)-O(21)	1.14(1)	C(43)-O(43)	1.123(9)
C(22)-O(22)	1.12(1)	C(51)-O(51)	1.14(1)
C(23)-O(23)	1.12(1)	C(52)-O(52)	1.13(1)
C(31)-O(31)	1.15(1)	C(61)-O(61)	1.14(1)
C(32)-O(32)	1.12(1)	C(62)-O(62)	1.15(1)

Table 3. Selected Bond Distances (Å) and Esd's of  
 $(\mu_3\text{-H})_2\text{Ru}_6(\mu\text{-CO})(\text{CO})_{16}$  (cont.).

---

---

E. Ru-H <sub>cap</sub> Distances			
Ru(1)-H(1)	1.81(8)	Ru(4)-H(2)	1.78(6)
Ru(5)-H(1)	2.01(7)	Ru(5)-H(2)	1.98(6)
Ru(6)-H(1)	1.86(7)	Ru(6)-H(2)	1.92(8)

---

---

Table 4. Selected Bond Angles (deg) and Esd's of  
 $(\mu_3\text{-H})_2\text{Ru}_6(\mu\text{-CO})(\text{CO})_{16}$ .

A. Angles Within $\text{Ru}_6$ Cluster			
Ru(2)-Ru(1)-Ru(3)	122.4(3)	Ru(1)-Ru(4)-Ru(3)	60.72(2)
Ru(2)-Ru(1)-Ru(4)	61.36(2)	Ru(1)-Ru(4)-Ru(5)	62.77(2)
Ru(2)-Ru(1)-Ru(5)	101.19(3)	Ru(1)-Ru(4)-Ru(6)	62.55(2)
Ru(2)-Ru(1)-Ru(6)	54.86(2)	Ru(1)-Ru(5)-Ru(3)	59.26(2)
Ru(1)-Ru(2)-Ru(4)	57.94(2)	Ru(1)-Ru(5)-Ru(4)	54.70(2)
Ru(1)-Ru(2)-Ru(6)	65.72(2)	Ru(1)-Ru(5)-Ru(6)	63.86(2)
Ru(1)-Ru(3)-Ru(4)	57.95(2)	Ru(1)-Ru(6)-Ru(2)	59.43(2)
Ru(1)-Ru(3)-Ru(5)	65.49(2)	Ru(1)-Ru(6)-Ru(4)	54.54(2)
Ru(1)-Ru(4)-Ru(2)	60.70(2)	Ru(1)-Ru(6)-Ru(5)	63.86(2)
B. Ru-Ru-C <sub>terminal</sub> Angles			
Ru(2)-Ru(1)-C(11)	86.4(2)	Ru(1)-Ru(4)-C(41)	133.2(2)
Ru(2)-Ru(1)-C(12)	165.9(3)	Ru(1)-Ru(4)-C(42)	91.8(2)
Ru(2)-Ru(1)-C(13)	78.1(3)	Ru(1)-Ru(4)-C(43)	136.3(2)
Ru(3)-Ru(1)-C(11)	92.8(2)	Ru(2)-Ru(4)-C(41)	73.1(2)
Ru(3)-Ru(1)-C(12)	71.7(3)	Ru(2)-Ru(4)-C(42)	87.9(2)
Ru(3)-Ru(1)-C(13)	159.0(3)	Ru(2)-Ru(4)-C(43)	162.1(3)
Ru(4)-Ru(1)-C(11)	94.1(3)	Ru(3)-Ru(4)-C(41)	165.7(2)
Ru(4)-Ru(1)-C(12)	132.5(3)	Ru(3)-Ru(4)-C(42)	89.1(2)
Ru(4)-Ru(1)-C(13)	138.1(3)	Ru(3)-Ru(4)-C(43)	76.5(2)
Ru(5)-Ru(1)-C(11)	146.1(2)	Ru(5)-Ru(4)-C(41)	123.9(3)
Ru(5)-Ru(1)-C(12)	86.1(2)	Ru(5)-Ru(4)-C(42)	142.5(2)
Ru(5)-Ru(1)-C(13)	120.5(2)	Ru(5)-Ru(4)-C(43)	86.6(2)
Ru(6)-Ru(1)-C(11)	140.5(2)	Ru(6)-Ru(4)-C(41)	85.6(3)
Ru(6)-Ru(1)-C(12)	125.1(2)	Ru(6)-Ru(4)-C(42)	141.0(2)
Ru(6)-Ru(1)-C(13)	86.1(3)	Ru(6)-Ru(4)-C(43)	122.9(3)
Ru(1)-Ru(2)-C(21)	162.5(3)	Ru(1)-Ru(5)-C(51)	100.6(3)
Ru(1)-Ru(2)-C(22)	104.0(3)	Ru(1)-Ru(5)-C(52)	145.9(3)
Ru(1)-Ru(2)-C(23)	97.6(3)	Ru(1)-Ru(5)-C(51)	91.0(3)

Table 4. Selected Bond Angles (deg) and Esd's of  
 $(\mu_3\text{-H})_2\text{Ru}_6(\mu\text{-CO})(\text{CO})_{16}$  (cont.).

Ru(4)-Ru(2)-C(21)	106.2(3)	Ru(3)-Ru(5)-C(52)	88.4(3)
Ru(4)-Ru(2)-C(22)	158.8(3)	Ru(4)-Ru(5)-C(51)	147.9(3)
Ru(4)-Ru(2)-C(23)	99.9(3)	Ru(4)-Ru(5)-C(52)	101.3(3)
Ru(6)-Ru(2)-C(21)	102.0(3)	Ru(6)-Ru(5)-C(51)	127.6(2)
Ru(6)-Ru(2)-C(22)	97.7(3)	Ru(6)-Ru(5)-C(52)	132.3(3)
Ru(6)-Ru(2)-C(23)	161.9(2)	Ru(1)-Ru(6)-C(61)	146.5(3)
Ru(1)-Ru(3)-C(31)	161.4(3)	Ru(1)-Ru(6)-C(62)	103.0(3)
Ru(1)-Ru(3)-C(32)	108.2(3)	Ru(2)-Ru(6)-C(61)	88.9(3)
Ru(1)-Ru(3)-C(33)	96.1(3)	Ru(2)-Ru(6)-C(62)	94.1(2)
Ru(4)-Ru(3)-C(31)	104.3(3)	Ru(4)-Ru(6)-C(61)	101.8(3)
Ru(4)-Ru(3)-C(32)	164.2(3)	Ru(4)-Ru(6)-C(62)	151.0(2)
Ru(4)-Ru(3)-C(33)	96.7(3)	Ru(5)-Ru(6)-C(61)	131.6(3)
Ru(5)-Ru(3)-C(31)	103.4(3)	Ru(5)-Ru(6)-C(62)	127.2(3)
Ru(5)-Ru(3)-C(32)	103.3(3)		
Ru(5)-Ru(3)-C(33)	158.8(3)		
C. Ru-CO <sub>bridge</sub> and Ru-CO-Ru Angles			
Ru(5)-C(56)-O(56)	147.7(8)	Ru(5)-C(56)-Ru(6)	74.0(3)
Ru(6)-C(56)-O(56)	138.3(8)		
D. Ru-CO <sub>terminal</sub> Angles			
Ru(1)-C(11)-O(11)	176.4(8)	Ru(4)-C(41)-O(41)	170.5(7)
Ru(1)-C(12)-O(12)	167.4(8)	Ru(4)-C(42)-O(42)	176.0(7)
Ru(1)-C(13)-O(13)	171.0(8)	Ru(4)-C(43)-O(42)	172.0(8)
Ru(2)-C(21)-O(21)	178.2(8)	Ru(5)-C(51)-O(51)	176.8(8)
Ru(2)-C(22)-O(22)	178.8(8)	Ru(5)-C(52)-O(52)	179.5(8)
Ru(2)-C(23)-O(23)	178.1(8)	Ru(6)-C(61)-O(61)	179.5(8)
Ru(3)-C(31)-O(31)	178.0(8)	Ru(6)-C(62)-O(62)	177.4(8)
Ru(3)-C(32)-O(32)	177.4(8)		
Ru(3)-C(33)-O(33)	177.4(8)		

Table 4. Selected Bond Angles (deg) and Esd's of  
 $(\mu_3\text{-H})_2\text{Ru}_6(\mu\text{-CO})(\text{CO})_{16}$  (cont.).

---

E. Ru-H-Ru Angles

Ru(1)-H(1)-Ru(2)	58(2)	Ru(1)-H(2)-Ru(2)	51(1)
Ru(1)-H(1)-Ru(3)	54(2)	Ru(1)-H(2)-Ru(3)	50(1)
Ru(1)-H(1)-Ru(4)	58(2)	Ru(1)-H(2)-Ru(4)	58(2)
Ru(1)-H(1)-Ru(5)	103(4)	Ru(1)-H(2)-Ru(5)	65(2)
Ru(1)-H(1)-Ru(6)	110(4)	Ru(1)-H(2)-Ru(6)	65(2)
Ru(2)-H(1)-Ru(3)	94(2)	Ru(2)-H(2)-Ru(3)	94(1)
Ru(2)-H(1)-Ru(4)	52(1)	Ru(2)-H(2)-Ru(4)	58(2)
Ru(2)-H(1)-Ru(5)	113(3)	Ru(2)-H(2)-Ru(5)	113(2)
Ru(2)-H(1)-Ru(6)	54(2)	Ru(2)-H(2)-Ru(6)	53(1)
Ru(3)-H(1)-Ru(4)	50(1)	Ru(3)-H(2)-Ru(4)	55(2)
Ru(3)-H(1)-Ru(5)	51(2)	Ru(3)-H(2)-Ru(5)	52(1)
Ru(3)-H(1)-Ru(6)	112(3)	Ru(3)-H(2)-Ru(6)	112(2)
Ru(4)-H(1)-Ru(5)	65(2)	Ru(4)-H(2)-Ru(5)	105(3)
Ru(4)-H(1)-Ru(6)	66(2)	Ru(4)-H(2)-Ru(6)	109(3)
Ru(5)-H(1)-Ru(6)	86(3)	Ru(5)-H(2)-Ru(6)	85(2)

---

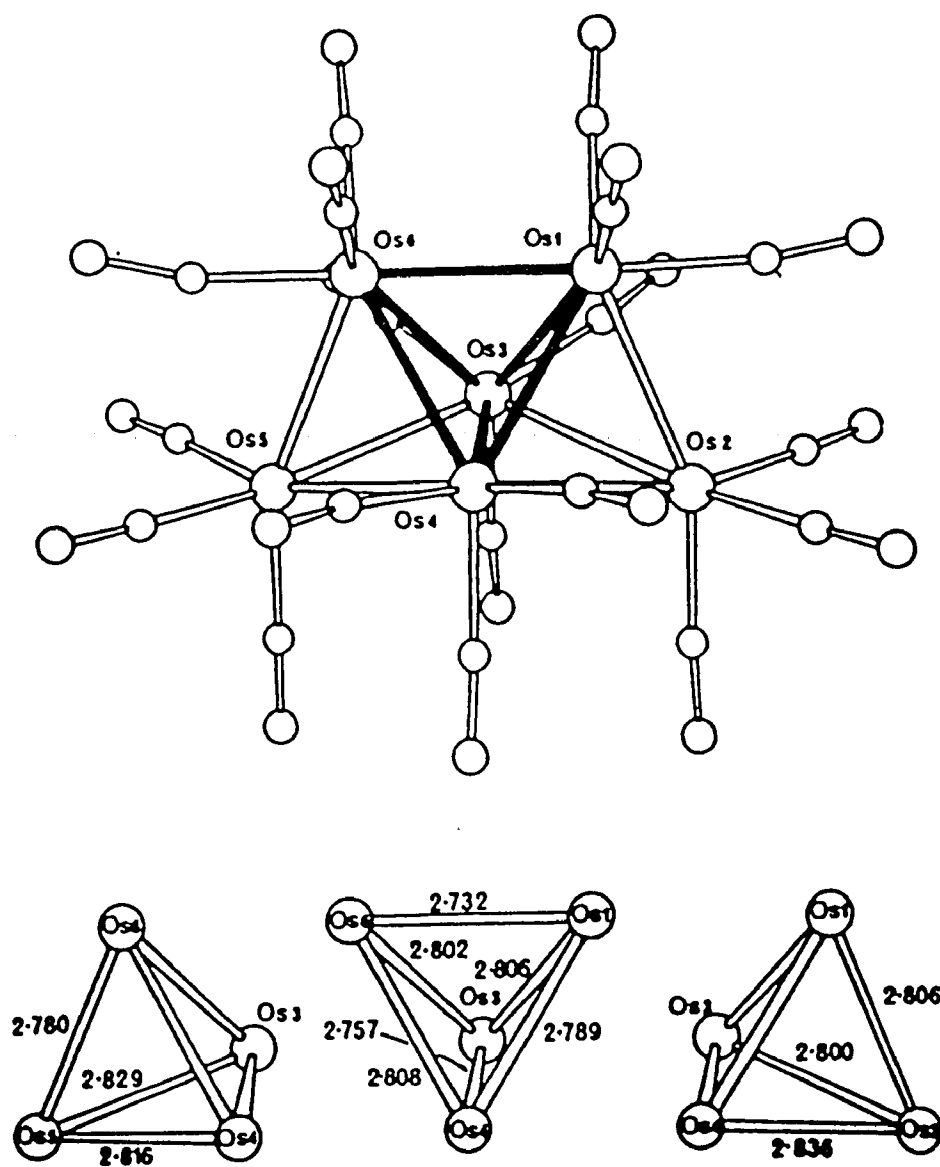


Figure 24. Molecular Structure of  $\text{Os}_6(\text{CO})_{18}$ .

and Ru(1)-Ru(4)-Ru(5) faces, respectively. The bond lengths within the inner tetrahedron range from 2.643(1)-3.009(1)Å; the capping distances range from 2.690(1)-2.851(1)Å. Ruthenium atoms Ru(1), Ru(2), Ru(3) and Ru(4) sport three terminal carbonyls; while Ru(5) and Ru(6) have two terminal carbonyls and share a bridging carbonyl. Capping hydrides H(1) and H(2), interact with the Ru(1)-Ru(5)-Ru(6) and Ru(4)-Ru(5)-Ru(6) faces, respectively.

The intermetallic distances, Fig. 25, within the cluster may be classified as: (1) "normal" ruthenium-ruthenium bond distances, (2) "short" ruthenium-ruthenium distances, and (3) "long" ruthenium-ruthenium distances. The bond distances Ru(1)-Ru(2)=2.833(1)Å, Ru(2)-Ru(4)=2.851(1)Å, Ru(1)-Ru(3)=2.833(1)Å, and Ru(3)-Ru(4)=2.850(1)Å are considered "normal", being comparable to the average Ru-Ru distance of 2.854Å in Ru<sub>3</sub>(CO)<sub>12</sub>. [89] These distances are also comparable to those in other ruthenium clusters, for example:

PPNH<sub>3</sub>Ru<sub>4</sub>(CO)<sub>12</sub> (2.937(1)Å average), [90] PPNHRu<sub>4</sub>(CO)<sub>13</sub> (2.756(1)-2.835(1)Å), [91] and PPNHRu<sub>3</sub>(CO)<sub>11</sub> (2.815(2)-2.845(3)Å). [68d]

Somewhat shorter distances associated with the outer edges of the cluster are observed, Ru(2)-Ru(6)=2.690(1)Å and Ru(3)-Ru(5)=2.708(1)Å. This may be attributed to distortion within the metal framework arising from the lengthening of the inner Ru-Ru bonds (2.993(1)-3.009(1)Å) by the capping hydrides. This distortion is exhibited by the enlarged bond angles associated with Ru(2) and Ru(3). (Ru(1)-Ru(2)-Ru(6)=65.72(2)°, Ru(4)-Ru(2)-Ru(6)=65.70(2)°, Ru(1)-Ru(3)-Ru(5)=65.49(2)°, and Ru(4)-Ru(3)-Ru(5)=65.10(2)°.)

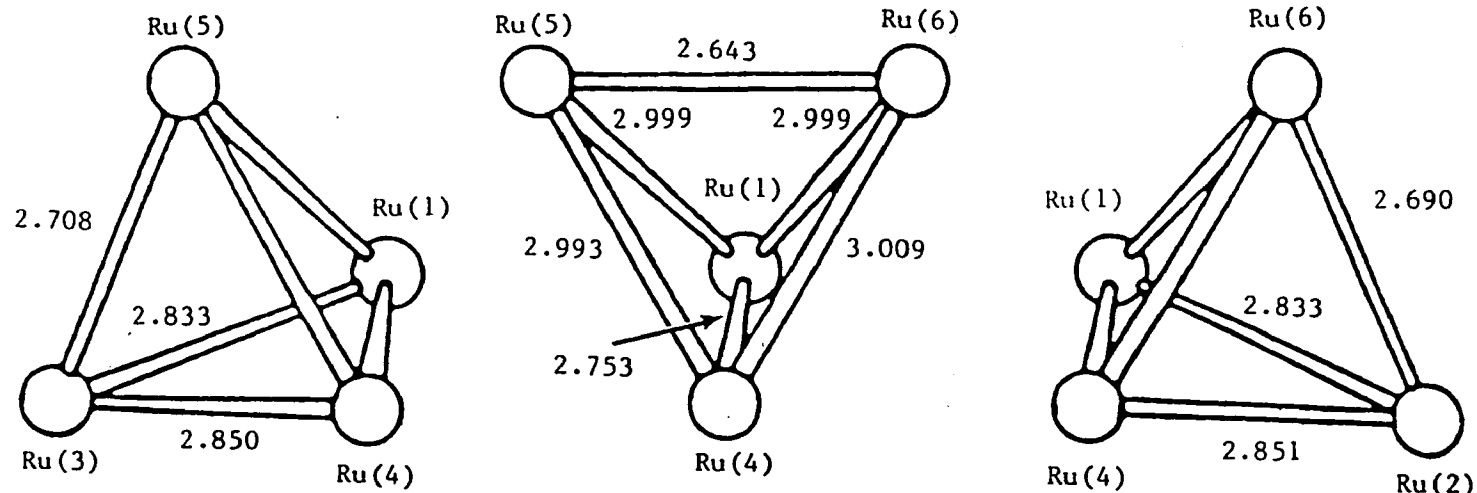


Figure 25. Intermetallic Bond Distances Within H<sub>2</sub>Ru<sub>6</sub>(CO)<sub>17</sub>.

The inner tetrahedral bonds  $\text{Ru}(1)\text{-Ru}(5)=2.999(1)\text{\AA}$ ,  $\text{Ru}(1)\text{-Ru}(6)=2.999(1)\text{\AA}$ ,  $\text{Ru}(4)\text{-Ru}(5)=2.993(1)\text{\AA}$  and  $\text{Ru}(4)\text{-Ru}(6)=3.009(1)\text{\AA}$  are lengthened appreciably relative to the non-bridged distances discussed previously. This is consistent with the presence of  $\mu_2^-$  or  $\mu_3^-$  hydride ligands. [49,55,59a,70a,92-100] The capping hydrides were found directly from the X-ray analysis and the metal-hydride distances ranging from  $1.78(6)\text{-}2.01(7)\text{\AA}$  are comparable to those reported in the literature. [95-100]

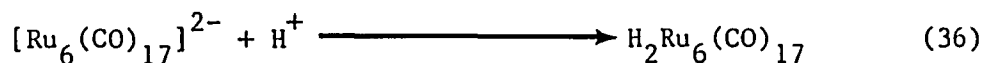
A particularly interesting feature of  $\text{H}_2\text{Ru}_6(\text{CO})_{17}$  is the extremely short  $\text{Ru}(5)\text{-Ru}(6)$  distance of  $2.643(1)\text{\AA}$ . One could argue that this bond is shortened due to the metals being in the formal oxidation state of 0 as Mason [88] notes for the  $\text{Os}_6(\text{CO})_{18}$  cluster,  $\text{Os}(1)\text{-Os}(6)=2.732\text{\AA}$ . (Fig. 24) He argues that the  $\text{Os}(3)\text{-Os}(4)$  distance of  $2.757\text{\AA}$  is also shortened due to the metals involved being in a formal oxidation state of +1. However, one should immediately observe that the  $\text{Ru}(5)\text{-Ru}(6)$  distance is  $0.089\text{\AA}$  shorter than the corresponding bond in  $\text{Os}_6(\text{CO})_{18}$ . This distance is greater than can be accounted for by the differences in the covalent radii between Os ( $1.255\text{\AA}$ ) and Ru ( $1.241\text{\AA}$ ). Also, if the covalent radii or formal oxidation states played a *substantial* role then one would expect the  $\text{Ru}(1)\text{-Ru}(4)$  distance of  $2.753(1)\text{\AA}$  to also be severely shortened and this is not observed. (compare to  $\text{Os}(3)\text{-Os}(4)=2.757\text{\AA}$ )

Another possibility for the shortened bond is the presence of the bridging carbonyl ligand. There is substantial evidence that bridging hydride ligands lengthen metal-metal bonds as noted above; however, a

bridging hydride supported by another bridging ligand may either lengthen or shorten the metal-metal bond depending on the nature of the other bridging ligand. [101] However, comparisons between bridged and non-bridged Ru-Ru distances are usually less than 0.05Å. For example, a comparison between the two types of bonding situations in  $\text{HRu}_3(\text{CO})_{10}(\text{CNMe}_2)$  is 0.027Å [101] and in  $[\text{HRu}_3(\text{CO})_{11}]^-$  is 0.029Å. [68] The Ru(5)-Ru(6) bond is, therefore, considered double bonded in character; similar to that observed in  $\text{H}_2\text{Os}_3(\text{CO})_{10}$  (2.683Å). [95,99, 100]

The bridging carbonyl group is asymmetric, with Ru(5)-C(56)=2.102(9)Å, Ru(6)-C(56)=2.282(9)Å, and the angles Ru(5)-C(56)-O(56)=147.7(8)°, and Ru(6)-C(56)-O(56)=138.3(8)°. The distances and angles associated with the terminal carbonyls are considered normal.

The questions which come to mind at this point are: (1) What is the likelihood of simple protonation *vs.* redox behavior with respect to the carbonyl/carboxylate combination? (2) Is it possible that the carbonylate used in these reactions is really  $[\text{Ru}_6(\text{CO})_{17}]^{2-}$ , and that we do only observe protonation according to Equation 36?



In an attempt to answer these questions especially that concerned with the identity of the starting material, the carbonylate was subjected to an X-ray diffraction experiment.

The molecular structure of this carbonylate proved to be the same as that reported by Shore and Hsu [102] for the  $[\text{PPh}_4]^+$  salt and

Johnson and Lewis [85] for the  $[\text{PMePh}_3]^+$  salt. Figure 26 gives the molecular structure as reported by Johnson and Lewis. Table 5 gives crystallographic data comparing the results obtained in this X-ray study (Column I) with that obtained by Shore and Hsu. (Column II) (The particular details with respect to the data collection and structure solution are outlined in the Experimental Section of this dissertation.) Therefore, one may conclude that a redox reaction is occurring and not just a simple protonation.

However, this conclusion is challenged by the observations of Johnson and Lewis [84-86] (Equation 35) where they report reaction of a strong acid,  $\text{H}_2\text{SO}_4$ , with  $[\text{PPN}]_2[\text{Ru}_6(\text{CO})_{18}]$  results in formation of  $\text{H}_2\text{Ru}_6(\text{CO})_{18}$ . A re-investigation of their experimental procedures result in  $\text{H}_2\text{Ru}_6(\text{CO})_{17}$  formation (in this investigator's hands) as identified by NMR, IR and elemental analysis. A re-investigation of the procedure reported by Knight and Mays [59a,59c,87] (Equation 34) also gives  $\text{H}_2\text{Ru}_6(\text{CO})_{17}$ . It can only be concluded, at this point in time, that perhaps a *very* small amount of  $\text{H}_2\text{Ru}_6(\text{CO})_{18}$  is formed in these reactions and that the crystal Knight and Mays obtained was not indicative of the bulk compound.  $\text{H}_2\text{Ru}_6(\text{CO})_{17}$  seems to be the bulk species formed in the reaction of  $[\text{Ru}_6(\text{CO})_{18}]^{2-}$  as shown by elemental analysis. (see Experimental Section)

#### 4. Reactions of $[\text{Ru}_6(\text{CO})_{17}]^{4-}$ and $[\text{Ru}_6(\text{CO})_{16}]^{6-}$

As noted in Section 2, when the carbonylate was a highly charged species formation of a new cluster; namely,  $\text{H}_2\text{Ru}_6(\text{CO})_{17}$  was observed.

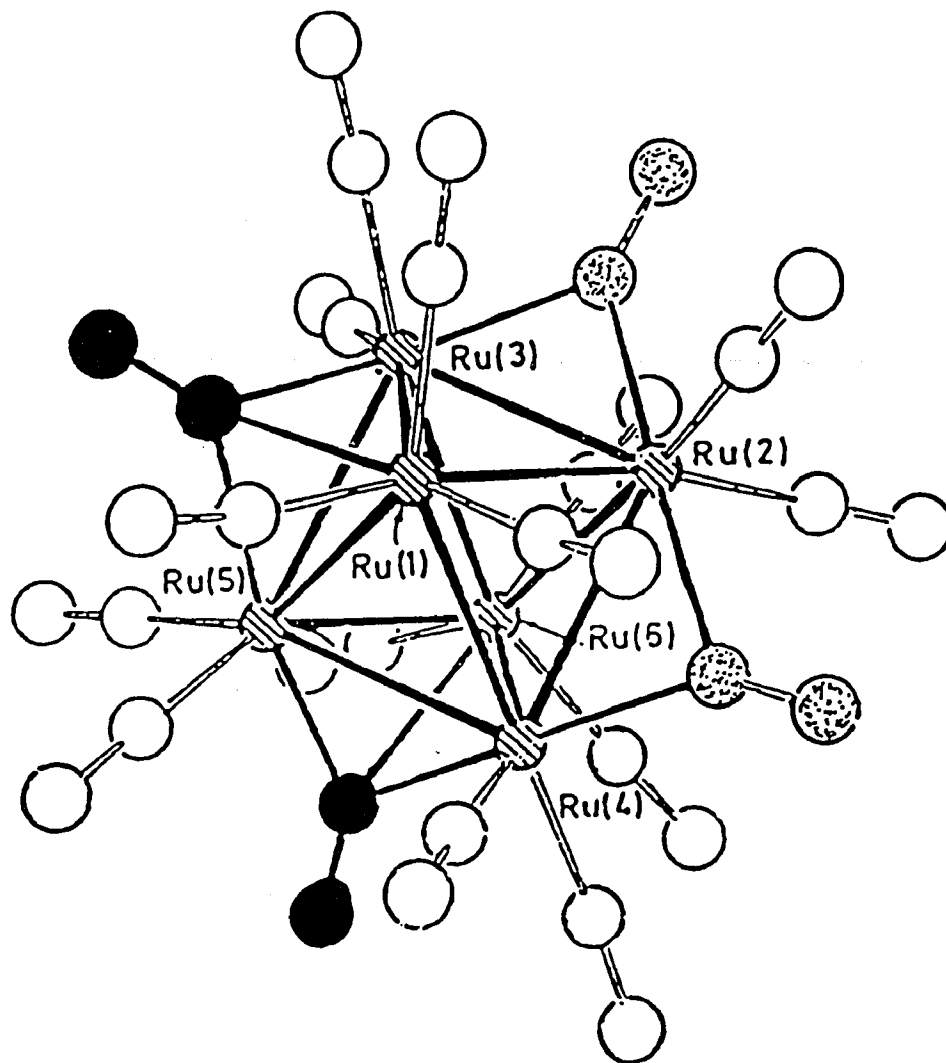


Figure 26. Molecular Structure of  $[\text{Ru}_6(\text{CO})_{18}]^{2-}$ .

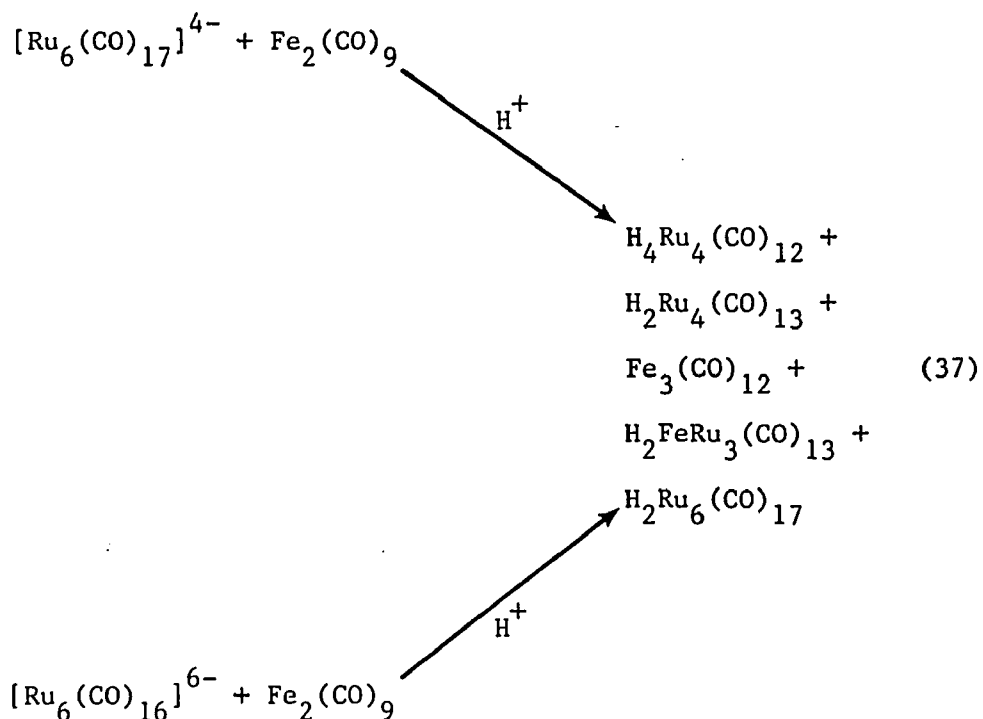
Table 5. Crystallographic Data for  $[\text{PPh}_4]_2[\text{Ru}_6(\text{CO})_{18}]$ .

Chemical formula	$\text{C}_{66}\text{H}_{40}\text{Ru}_6\text{P}_2\text{O}_{18}$ <sup>a</sup>	$\text{C}_{66}\text{H}_{40}\text{Ru}_6\text{P}_2\text{O}_{18}$ <sup>b</sup>
Color of cryst	dark brown	
Molecular wt	1788.622	
Space group	$P2_1/c$	$P2_1/c$
Z	4	4
Temp, °C	25	25
a, Å	22.878(3)	22.854(2)
b, Å	14.241(1)	14.257(2)
c, Å	19.706(3)	19.655(3)
$\beta$ , deg	90.93(1)	90.65(1)
Volume, Å <sup>3</sup>	6419.6	6403.5
D(calcd), g cm <sup>-3</sup>	1.851	
Absorptn coeff, cm <sup>-1</sup>	14.7	14.6
Scan mode	$\omega$ -2 $\theta$	$\omega$ -2 $\theta$
Data collectn limits, deg	4-40	4-50
No. of unique reflctns	5965	6188
No. of reflctns used in structure refinement	3525 ( $>2\sigma(I)$ )	4766 ( $>3\sigma(I)$ )
$R_f$		0.069
$R_{wf}$		0.078

<sup>a</sup>this work<sup>b</sup>Shore and Hsu [102]

Since a tetranuclear cluster reactant resulted in a hexanuclear product one may assume a cluster building pathway is functional, whose activity is possibly influenced by the basicity of the carbonylate. It was hoped that increasing the basicity of the hexanuclear carbonylate would perhaps result in formation of either a hetero- or homo- nuclear species with  $M \geq 6$ .

Reaction of either  $[\text{Ru}_6(\text{CO})_{17}]^{4-}$  or  $[\text{Ru}_6(\text{CO})_{16}]^{6-}$  with  $\text{Fe}_2(\text{CO})_9$  (Equation 37) resulted in  $\text{H}_4\text{Ru}_4(\text{CO})_{12}$ ,  $\text{Fe}_3(\text{CO})_{12}$ ,  $\text{H}_2\text{Ru}_4(\text{CO})_{13}$ ,  $\text{H}_2\text{FeRu}_3(\text{CO})_{13}$  and  $\text{H}_2\text{Ru}_6(\text{CO})_{17}$  after protonation with a strong acid.

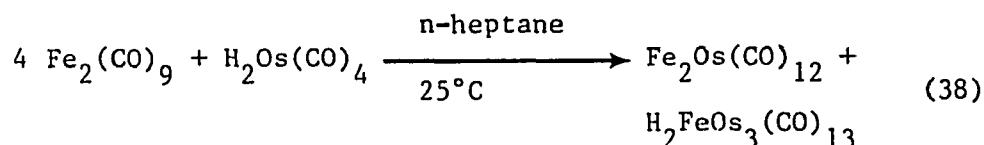


When  $[\text{Ru}_6(\text{CO})_{16}]^{6-}$  was reacted with  $\text{Fe}_2(\text{CO})_9$  the yield of  $\text{H}_2\text{Ru}_6(\text{CO})_{17}$  was observed to be 2-3 times that formed when  $[\text{Ru}_6(\text{CO})_{17}]^{4-}$  was employed (by  $^1\text{H}$  NMR); however, the major products isolated were  $\text{H}_4\text{Ru}_4(\text{CO})_{12}$  and  $\text{H}_2\text{Ru}_4(\text{CO})_{13}$ .

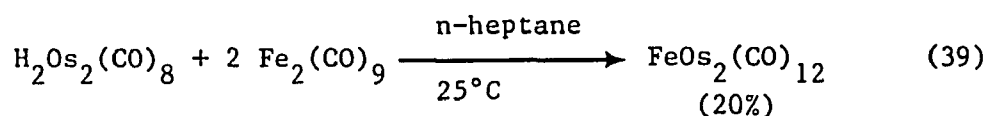
## II. IRON/OSMIUM SYSTEMS

A. Introduction. Mixed-metal clusters containing iron and osmium have also been synthesized and characterized. One sees examples ranging from the dinuclear species,  $[\text{FeOs}(\text{CO})_8]^{2-}$ , [57] (Equation 15) through a pentanuclear cluster,  $\text{H}_2\text{Fe}_2\text{Os}_3(\text{CO})_{16}$ . [50a]

Moss and Graham [103-105] reported the first synthesis of iron-osmium trinuclear clusters,  $\text{Fe}_2\text{Os}(\text{CO})_{12}$  and  $\text{FeOs}_2(\text{CO})_{12}$ , under mild conditions. (Equations 38,39) Heretofore, harsh pyrolysis conditions were used in the synthesis of the FeRu and RuOs trimers. [40,44] (Equations 3-10)

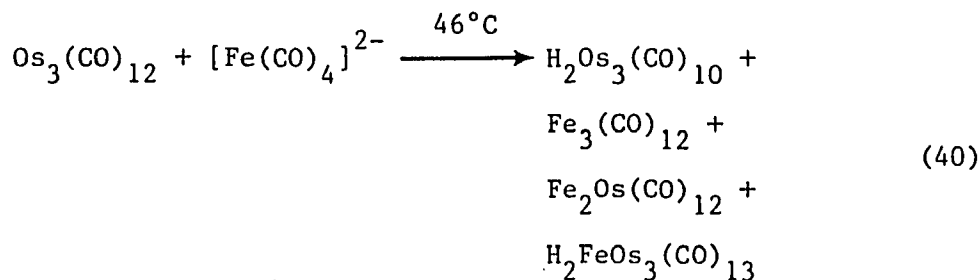


$\text{Fe}_2\text{Os}(\text{CO})_{12}$  is formed in 70% yield while  $\text{H}_2\text{FeOs}_3(\text{CO})_{13}$  is only observed in 6%.

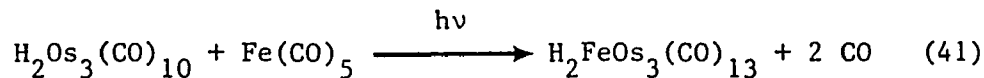


As with the iron-ruthenium clusters, iron-osmium tetranuclear clusters have also been prepared and fully characterized. As noted in Equation 38, formation of  $\text{H}_2\text{FeOs}_3(\text{CO})_{13}$  is possible, albeit in low yield. Since this reaction reported by Moss and Graham, several research groups have succeeded in synthesizing this cluster in yields > 90%.

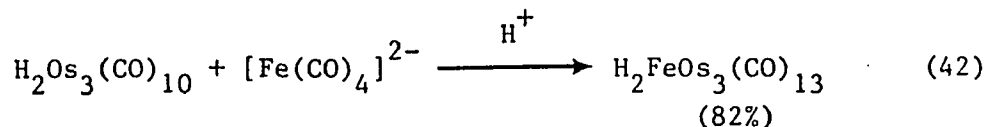
Various methods are utilized in order to achieve formation of this tetranuclear cluster. For example, Geoffroy first synthesized  $\text{H}_2\text{FeOs}_3(\text{CO})_{13}$  in yields of 9% according to Equation 40. [70a]



He later achieved yields of up to 95% using  $\text{H}_2\text{Os}_3(\text{CO})_{10}$  in a photolysis reaction. [71] (Equation 41)



Shore and co-workers [50a] have also made use of the unsaturation in  $\text{H}_2\text{Os}_3(\text{CO})_{10}$  to form mixed-metal clusters containing three osmium atoms. In their syntheses, they made use of the versatility  $\text{H}_2\text{Os}_3(\text{CO})_{10}$  possesses with respect to Lewis acid/base character. In Equation 42,  $\text{H}_2\text{Os}_3(\text{CO})_{10}$  functions as an apparent Lewis acid reacting with the very nucleophilic iron carbonylate  $[\text{Fe}(\text{CO})_4]^{2-}$ .



The X-ray crystal structure of  $\text{H}_2\text{FeOs}_3(\text{CO})_{13}$  has been solved by Churchill [94] and is depicted in Figure 27.

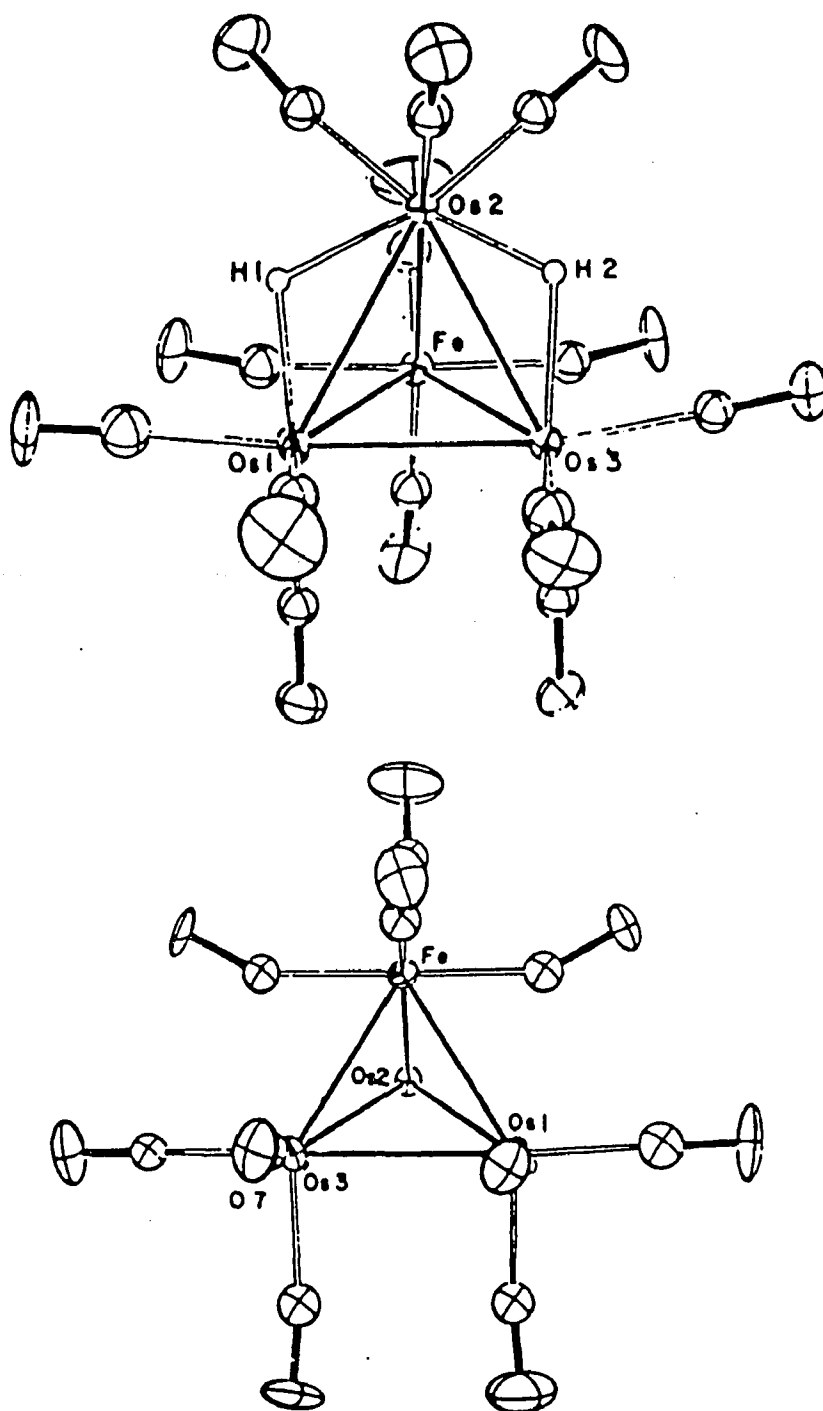
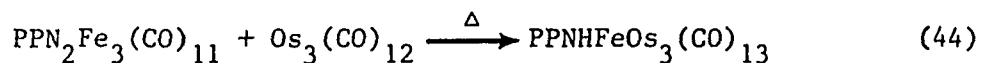
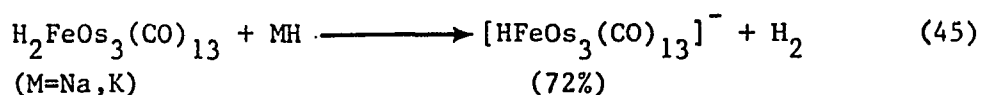


Figure 27. Molecular Structure of  $\text{H}_2\text{FeOs}_3(\text{CO})_{13}$ .

The anionic  $[\text{HFeOs}_3(\text{CO})_{13}]^-$  cluster has also been prepared and structurally characterized using the redox condensation method as outlined below. [106] (Equation 44)



Shore [75,107] has used the neutral  $\text{H}_2\text{FeOs}_3(\text{CO})_{13}$  cluster as a source of  $[\text{HFeOs}_3(\text{CO})_{13}]^-$  formation *via* an alkali-hydride reduction. (Equation 45)



As with the iron-ruthenium clusters, these mixed-metal clusters particularly the anions are then used as models for cluster species on metal supports. [78]

B. Results & Discussion. As was alluded to in the introduction, a pentanuclear cluster  $\text{H}_2\text{Fe}_2\text{Os}_3(\text{CO})_{16}$  has been synthesized by Plotkin and Shore. [50a] The complex is a very minor side-product (< 2%) of the reaction outlined in Equation 43.

The objective of this investigation has been to synthesize higher nuclearity clusters. In this case, it was hoped to increase the yield of the pentanuclear cluster and to possibly extend the nuclearity of this species to six or more metals using the redox condensation method. Perhaps the increased bond strength associated with osmium atoms would stabilize the higher nuclearity complex formed,



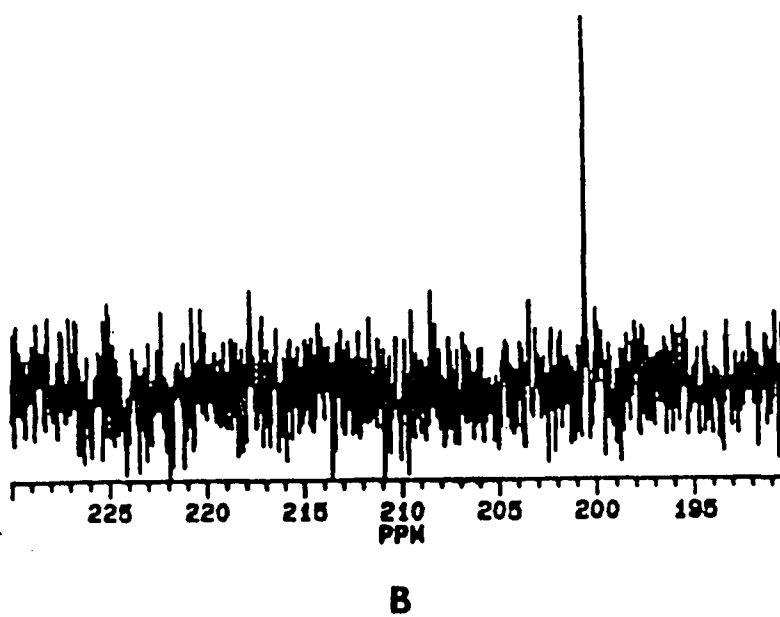
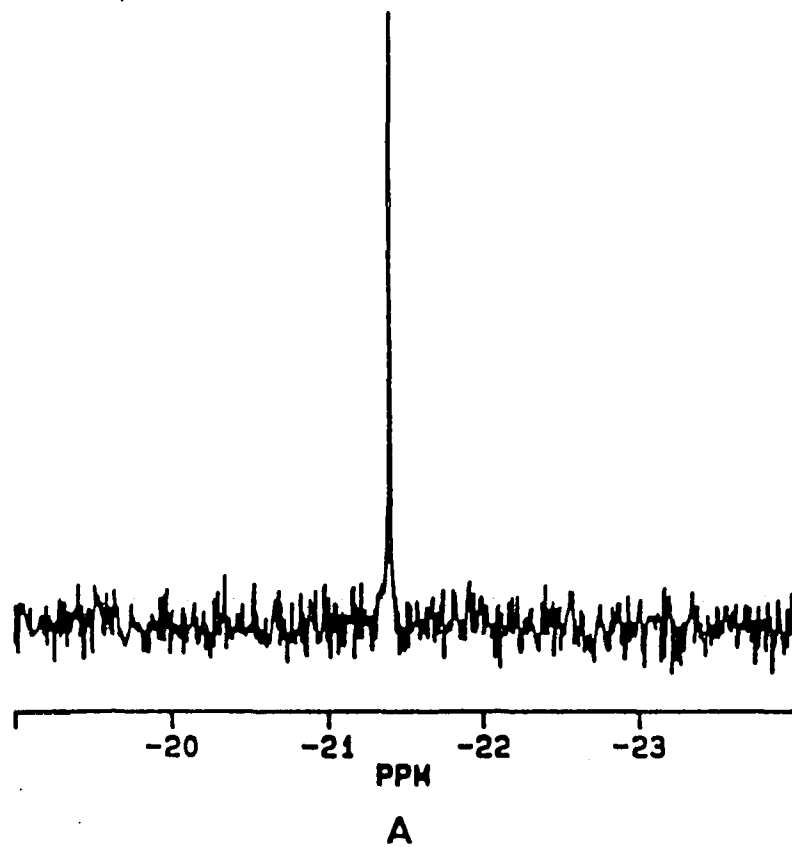


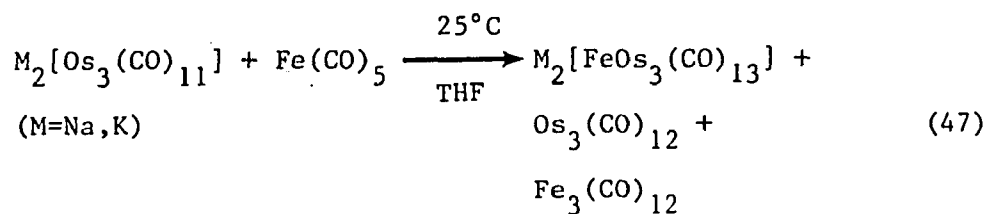
Figure 28. Proton (a) and Carbon-13 (b)  
NMR Spectra of  $\text{H}_2\text{Fe}_2\text{Os}_3(\text{CO})_{16}$ .

up to 7%. If the temperature of the reaction is lowered to 0°C the rate of reactivity is decreased but yields between 13-15% are observed. (see Experimental Section for details)

This cluster does not exhibit great stability in air or moisture. If the reaction is worked-up with improperly dried solvents or TLC plates which have not been activated thoroughly or if small amounts of O<sub>2</sub> are present during the reaction period, formation of HOs<sub>3</sub>(CO)<sub>10</sub>OH and Os<sub>3</sub>(CO)<sub>12</sub> are observed. Furthermore, upon standing in solution (ie. during the course of crystal growth) decomposition of H<sub>2</sub>Fe<sub>2</sub>Os<sub>3</sub>(CO)<sub>16</sub> to form Os<sub>3</sub>(CO)<sub>12</sub> and possibly Fe<sub>2</sub>Os(CO)<sub>12</sub> is detected. The Os<sub>3</sub>(CO)<sub>12</sub> has been identified by X-ray analysis and the IR shows peaks due to Fe<sub>2</sub>Os(CO)<sub>12</sub> and Os<sub>3</sub>(CO)<sub>12</sub>.

## 2. Reaction of [FeOs<sub>3</sub>(CO)<sub>13</sub>]<sup>2-</sup>

In an attempt to determine the sequence of events which lead to the formation of the pentanuclear cluster, the reaction of [FeOs<sub>3</sub>(CO)<sub>13</sub>]<sup>2-</sup> with Fe(CO)<sub>5</sub> should be carried out to see if the formation of [Fe<sub>2</sub>Os<sub>3</sub>(CO)<sub>16</sub>]<sup>2-</sup> can be detected. In order to do this, the heretofore unknown dianion [FeOs<sub>3</sub>(CO)<sub>13</sub>]<sup>2-</sup> was synthesized. The preparation was accomplished as follows. (Equation 47)



Reaction of  $[\text{FeOs}_3(\text{CO})_{13}]^{2-}$  with  $\text{Fe}(\text{CO})_5$  does not afford  $\text{H}_2\text{Fe}_2\text{Os}_3(\text{CO})_{13}$  upon protonation, only  $\text{H}_2\text{FeOs}_3(\text{CO})_{13}$  and  $\text{Fe}_3(\text{CO})_{12}$  are isolated. From this result one may conclude that the pentanuclear cluster is formed when an intact  $\text{Fe}_2$  unit combines with  $[\text{Os}_3(\text{CO})_{11}]^{2-}$  in a concerted fashion, rather than a step-wise addition of one iron unit. This mechanism is similar to that proposed by Adams [108] for the reaction of  $\text{Ru}_3(\text{CO})_9(\mu_3\text{-CO})(\mu_3\text{-S})$  with  $[\text{CpMo}(\text{CO})_2]_2$  forming  $\text{Cp}_2\text{Mo}_2\text{Ru}_3(\text{CO})_{10}(\mu\text{-CO})(\mu_4\text{-S})$ .

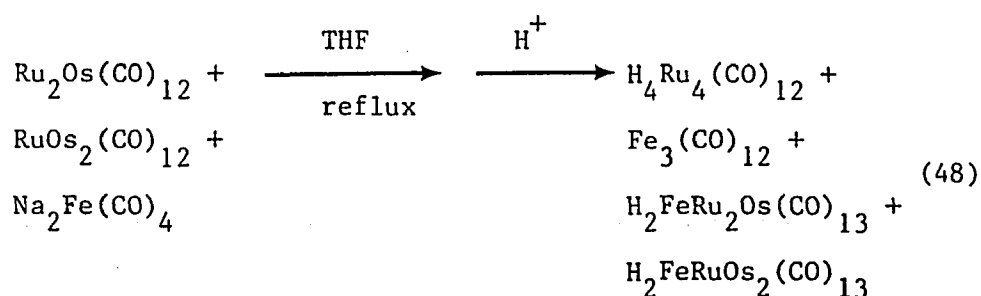
Unfortunately, the formation of mixed-metal clusters with  $M > 5$  was not realized in these syntheses. It may at this point be advantageous to explore the reactivity of  $[\text{Os}_6(\text{CO})_{18}]^{2-}$  or other higher nuclearity systems in an attempt to isolate the larger cluster systems.

### III. RUTHENIUM/OSMIUM SYSTEMS

A. Introduction. To complete the study of mixed-metal clusters of the iron triad, ruthenium-osmium systems must be considered. Mixed-metal clusters containing ruthenium-osmium should exhibit increased stability over the iron-ruthenium and iron-osmium clusters studied thus far; due to the increased metal-metal bond strengths as one goes down the triad.

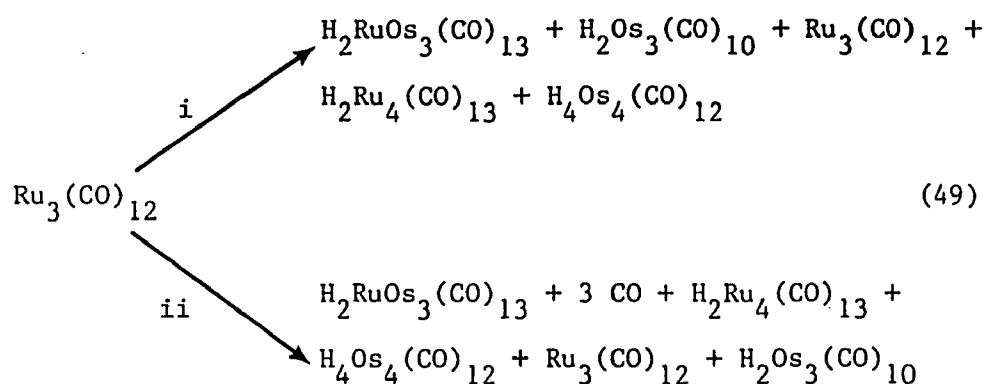
As with the other systems studied, the synthetic strategy is to build up clusters one metal fragment at a time using the redox condensation method. Again, this has been employed in this research group to successfully synthesize the mixed dimer  $[\text{RuOs}(\text{CO})_8]^{2-}$ . [57] (Equation 15)

As outlined in Equation 8, the pyrolysis of  $\text{Ru}_3(\text{CO})_{12}$  with  $\text{Os}_3(\text{CO})_{12}$  is the source for ruthenium-osmium trimetallic clusters. [42] These clusters have been used by Geoffroy and co-workers [70] to generate tetranuclear clusters containing three different metal atoms. (Equation 48)



The new clusters,  $\text{H}_2\text{FeRu}_2\text{Os}(\text{CO})_{13}$  and  $\text{H}_2\text{FeRuOs}_2(\text{CO})_{13}$ , may be isolated in yields of 30% and 40%, respectively. They have been fully characterized in solution by  $^1\text{H}$  and  $^{13}\text{C}$  NMR [72] and appear to be highly fluxional with respect to bridging carbonyl and hydride ligands.

The tetranuclear system of particular interest to this research is  $\text{H}_2\text{RuOs}_3(\text{CO})_{13}$ . Several synthetic routes to this cluster have been devised. Geoffroy *et al.* [71,109] first synthesized  $\text{H}_2\text{RuOs}_3(\text{CO})_{13}$  using the unsaturated cluster  $\text{H}_2\text{Os}_3(\text{CO})_{10}$  as shown in Equation 49. Depending on the stoichiometry of the  $\text{H}_2\text{Os}_3(\text{CO})_{10}$  added one may influence the yield of  $\text{H}_2\text{RuOs}_3(\text{CO})_{13}$  obtained. When 1 equivalent is employed 23%  $\text{H}_2\text{RuOs}_3(\text{CO})_{13}$  is isolated; whereas, increasing the reactant to 3 equivalents increases the isolated yield of  $\text{H}_2\text{RuOs}_3(\text{CO})_{13}$  to 53%. The reported clusters are obtained in pure form using column



(i) 1 eq  $\text{H}_2\text{Os}_3(\text{CO})_{10}$ , hv, 70h

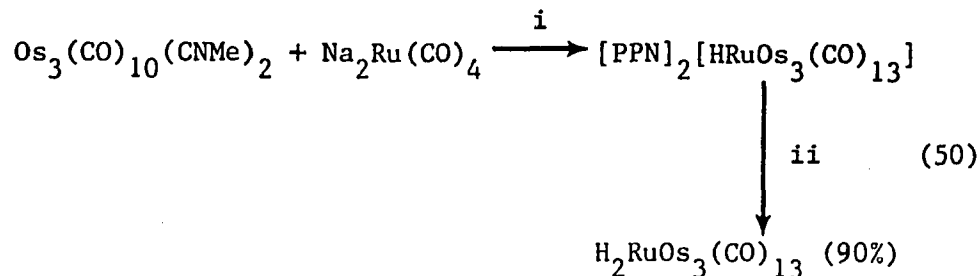
(ii) 3 eq  $\text{H}_2\text{Os}_3(\text{CO})_{10}$ , hv, 70h

chromatography (silica gel, hexane as eluent) and have been fully characterized by common spectroscopic methods.

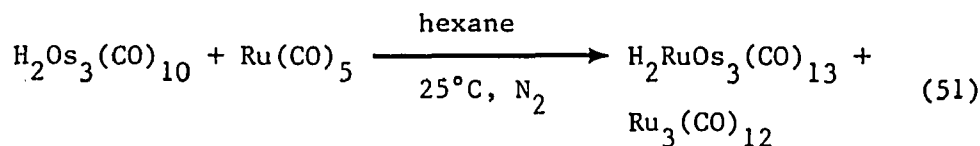
Johnson and Lewis [110-112] adopt a somewhat different approach using the di-substituted osmium carbonyl,  $\text{Os}_3(\text{CO})_{10}(\text{CNMe})_2$ , and reacting it with the mononuclear dianion  $[\text{Ru}(\text{CO})_4]^{2-}$ . (Equation 50)

Yet another approach to  $\text{H}_2\text{RuOs}_3(\text{CO})_{13}$  is employed by Gates *et al.* [113,114] In this preparation the highly reactive mononuclear carbonyl,  $\text{Ru}(\text{CO})_5$ , is utilized according to Equation 51.  $\text{H}_2\text{RuOs}_3(\text{CO})_{13}$  was purified by column chromatography using hexane as the eluent and isolated in yields of 30-45%. This cluster has been fully characterized including the X-ray crystal structure. [115]

Shore and Siriwardane [75] utilized the redox condensation reaction method to generate  $\text{H}_2\text{RuOs}_3(\text{CO})_{13}$ . If  $[\text{Ru}_3(\text{CO})_{11}]^{2-}$  is reacted with  $1/3 \text{Os}_3(\text{CO})_{12}$  one obtains upon protonation the mixture of neutral clusters  $\text{H}_2\text{Ru}_4(\text{CO})_{13}$ ,  $\text{H}_2\text{RuOs}_3(\text{CO})_{13}$  and  $\text{H}_2\text{Os}_4(\text{CO})_{13}$ . If the stoichiometry of  $\text{Os}_3(\text{CO})_{12}$  is raised to  $2/3$  equivalents, one

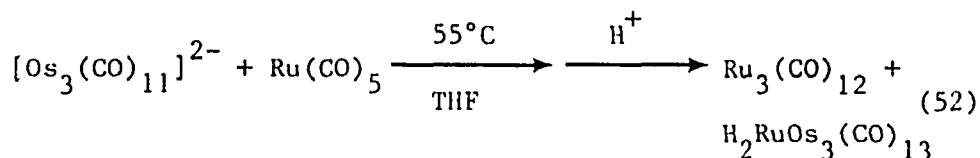


- (i) (1) THF, 25°C  
 (2) PPNC1, CH<sub>2</sub>Cl<sub>2</sub>, 25°C  
 (3) TLC (50:10:40 CH<sub>2</sub>Cl<sub>2</sub>:acetone:cyclohexane)
- (ii) (1) CH<sub>2</sub>Cl<sub>2</sub>, 25°C, excess concentrated H<sub>2</sub>SO<sub>4</sub>  
 (2) TLC (20:80 CH<sub>2</sub>Cl<sub>2</sub>:cyclohexane)



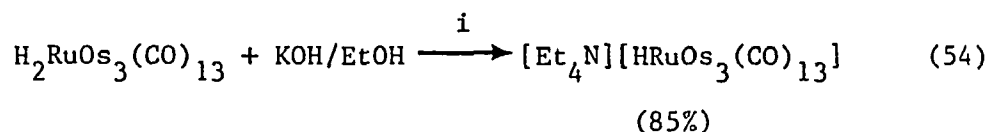
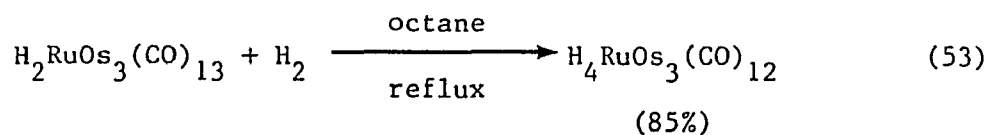
obtains the aforementioned products along with the pentanuclear species  $\text{H}_2\text{Ru}_2\text{Os}_3(\text{CO})_{16}$  and  $\text{H}_2\text{Os}_5(\text{CO})_{16}$ . Finally, if one equivalent of  $\text{Os}_3(\text{CO})_{12}$  is reacted with one equivalent of  $\text{Ru}_3(\text{CO})_{12}$  all five species above are again observed with the higher nuclearity clusters being formed in increased yields.

A second approach in an attempt to eliminate the large number of side products observed in the reaction of  $[\text{Ru}_3(\text{CO})_{11}]^{2-}$  with  $\text{Os}_3(\text{CO})_{12}$ , was to react  $[\text{Os}_3(\text{CO})_{11}]^{2-}$  with  $\text{Ru}(\text{CO})_5$  as shown below. [75] (Equation 52)

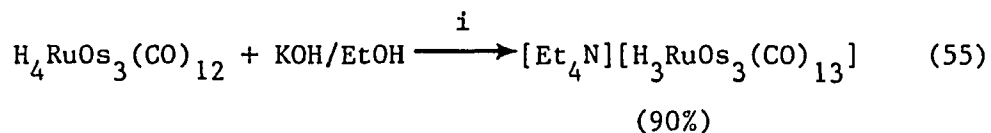


The mixed-metal cluster obtained from both reaction types was fully characterized including a crystal structure. [75]

Reactivity studies of  $\text{H}_2\text{RuOs}_3(\text{CO})_{13}$  center around the preparation of the tetrahydrido cluster  $\text{H}_4\text{RuOs}_3(\text{CO})_{12}$  (Equation 53) and the related monoanions,  $[\text{HRuOs}_3(\text{CO})_{13}]^-$  (Equation 54) and  $[\text{H}_3\text{RuOs}_3(\text{CO})_{12}]^-$ . [113,114] (Equation 55)



- (i) (1) 55°C  
(2)  $\text{Et}_4\text{NBr}$ , -8°C



- (i) (1) 55°C  
(2)  $\text{Et}_4\text{NBr}$ , -8°C

Shore [75] has also shown that deprotonation with NaH leads to formation of  $[\text{H}_3\text{RuOs}_3(\text{CO})_{12}]^-$  and  $[\text{HRuOs}_3(\text{CO})_{13}]^-$ . A cleaner deprotonation reaction can be achieved by using PPNC1 to generate  $[\text{PPN}][\text{HRuOs}_3(\text{CO})_{13}]$  in approximately 70%. These clusters have subsequently been used by Gates [114] in surface and catalytic studies by attachment to  $\gamma\text{-Al}_2\text{O}_3$  supports.

## B. Crystallographic Studies.

1. Shore and Siriwardane. The first X-ray analyses of  $\text{H}_2\text{RuOs}_3(\text{CO})_{13}$  were reported by Shore and Siriwardane. [75] Crystals for these studies were obtained from the reaction of  $[\text{Ru}_3(\text{CO})_{11}]^{2-}$  with  $2/3$  equivalent  $\text{Os}_3(\text{CO})_{12}$ . The first set of crystals obtained were shown to be a co-crystallized\* single crystal of  $\text{H}_2\text{Os}_4(\text{CO})_{13}$ ,  $\text{H}_2\text{RuOs}_3(\text{CO})_{13}$  and  $\text{H}_2\text{Ru}_4(\text{CO})_{13}$  in the ratio 60:20:20%. The second set of crystals obtained were shown to be a co-crystallized single crystal of  $\text{H}_2\text{Os}_4(\text{CO})_{13}$  and  $\text{H}_2\text{RuOs}_3(\text{CO})_{13}$  in the ratio of 20:80%. Table 6 gives crystallographic data comparing the results of the two studies described above.

In light of the co-crystallization of the mixed-metal cluster with the homonuclear clusters from this particular reaction, a new synthetic route for  $\text{H}_2\text{RuOs}_3(\text{CO})_{13}$  was devised. A crystal for the third crystallographic study was obtained from the reaction of  $[\text{Os}_3(\text{CO})_{11}]^{2-}$  with  $\text{Ru}(\text{CO})_5$ . (Equation 52) Table 7 (Column I) gives crystallographic data for  $\text{H}_2\text{RuOs}_3(\text{CO})_{13}$  for the third X-ray analysis. The molecule is described as consisting of a  $\text{RuOs}_3$  tetrahedron. Each osmium atom sports three terminal carbonyls; while the ruthenium atom has two terminal carbonyls and two semibridging carbonyls ( $d(\text{Ru}-\text{C}_{\text{sb}})=1.955\text{\AA}$  (ave),  $d(\text{Os}-\text{C}_{\text{sb}})=2.505\text{\AA}$  (ave)). The

---

\*Co-crystallization: Crystallization of two or more chemically different isostructural molecules which occupy equivalent sites in the lattice of the crystal in a random distribution.

Table 6. Crystallographic Data for  $\text{H}_2\text{RuOs}_3(\text{CO})_{13}$ ---Co-crystallized Systems.

Crystal Composition	$\text{H}_2\text{Os}_4(\text{CO})_{13}$ (60%) $\text{H}_2\text{RuOs}_3(\text{CO})_{13}$ (20%) $\text{H}_2\text{Ru}_4(\text{CO})_{13}$ (20%)	$\text{H}_2\text{RuOs}_3(\text{CO})_{13}$ (80%) $\text{H}_2\text{Os}_4(\text{CO})_{13}$ (20%)
Space Group	P1 bar	$P2_1/c$
Z	4	8
a, Å	9.146(2)	23.082(5)
b, Å	26.650(7)	9.082(4)
c, Å	9.303(3)	19.296(5)
$\alpha$ , deg	92.00(2)	
$\beta$ , deg	112.30(3)	90.86(2)
$\gamma$ , deg	81.76(2)	
Volume, Å <sup>3</sup>	2014.87	4046.07
Data collectn limits, deg	4-50	4-46
No. of unique reflctns	9210	7095
No. of reflctns used in structure refinement ( $>3\sigma(I)$ )	7096	4583
$R_f$	0.061	0.051
$R_{wf}$	0.076	0.067
GOF	2.121	1.647

Table 7. Crystallographic Data for  $\text{H}_2\text{RuOs}_3(\text{CO})_{13}$ .

Chemical formula	$\text{C}_{13}\text{O}_{13}\text{Os}_3\text{RuH}_2^{\text{a}}$	$\text{C}_{13}\text{O}_{13}\text{Os}_3\text{RuH}_2^{\text{b}}$
Color of cryst	orange	orange
Solvent system	$\text{CH}_2\text{Cl}_2$ (25°C)	pentane (25°C)
Space group	$\text{P}2_1/\text{c}$	$\text{P}1$ bar
Z	8	4
Temp, °C	25	22
a, Å	23.091(9)	9.046(4)
b, Å	9.083(7)	9.140(4)
c, Å	19.332(7)	26.560(9)
$\alpha$ , deg		81.88(3)
$\beta$ , deg	90.81(4)	91.81(3)
$\gamma$ , deg		112.07(3)
Volume, Å <sup>3</sup>	4052.25	2014.1
D(calcd), g cm <sup>-3</sup>	3.40	3.42
Radiation	Mo K $\alpha$ (0.710730Å)	Mo K $\alpha$ (0.710730Å)
Diffractometer	CAD-4	Nicolet R3
Absorptn coeff, cm <sup>-1</sup>	195.7	196.8
Scan mode	$\omega$ -2 $\theta$	$\omega$ (full profile)
Data collectn limits, deg	4-50	4-46
No. of unique reflctns	6882	5397
No. of reflctns used in structure refinement ( $>3\sigma(I)$ )	4587	4576
$R_f$	0.048	0.0491
$R_{wf}/w$	0.066/0.06	0.0485
GOF	1.971	1.379

<sup>a</sup>Shore and Siriwardane [75]<sup>b</sup>Rheingold and Gates [115]

bridging hydrides were located directly from the X-ray analysis and are bridging the osmium base as expected from their  $^1\text{H}$  NMR chemical shifts.

2. Rheingold and Gates. Crystals of  $\text{H}_2\text{RuOs}_3(\text{CO})_{13}$  for this particular X-ray investigation were obtained from the reaction of  $\text{Ru}(\text{CO})_5$  and  $\text{H}_2\text{Os}_3(\text{CO})_{10}$  in hexane at ambient temperature. (Equation 51) Table 7 (Column II) gives crystallographic data for  $\text{H}_2\text{RuOs}_3(\text{CO})_{13}$  as reported by Rheingold and Gates. [115]

The basic structure of this cluster is analogous to that of Shore and Siriwardane and is shown in Figure 29. The difference arises in the interpretation of the structure refinement. Refinement of the metal site occupancies show that in Molecule A Ru(1) is 100% Ru in character; whereas, Molecule B is only 79% Ru in character at that site and the residual 21% Ru is evenly distributed among the Os sites. Rheingold subsequently attributes this to disordering\* of the metal atom identities; presumably because only one molecule exhibits this behavior. As opposed to the phenomenon observed by Shore and Siriwardane where both molecules showed identical behavior (within experimental error).

C. Results & Discussion. Examination of the reported structural studies of  $\text{H}_2\text{RuOs}_3(\text{CO})_{13}$  by Shore *et al.* [75] and Rheingold *et al.*

---

\* Disorder: Crystallization of a pure molecule which exhibits random orientation of the molecule throughout the crystal lattice.

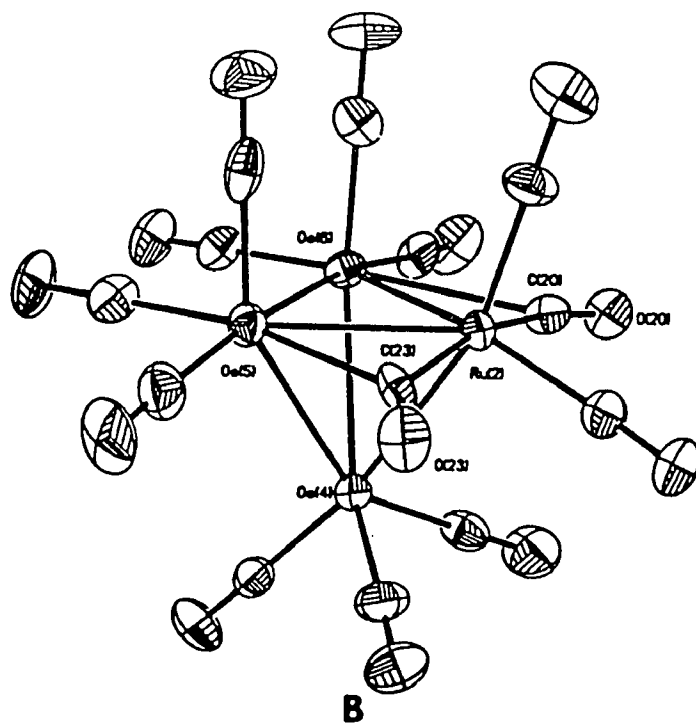
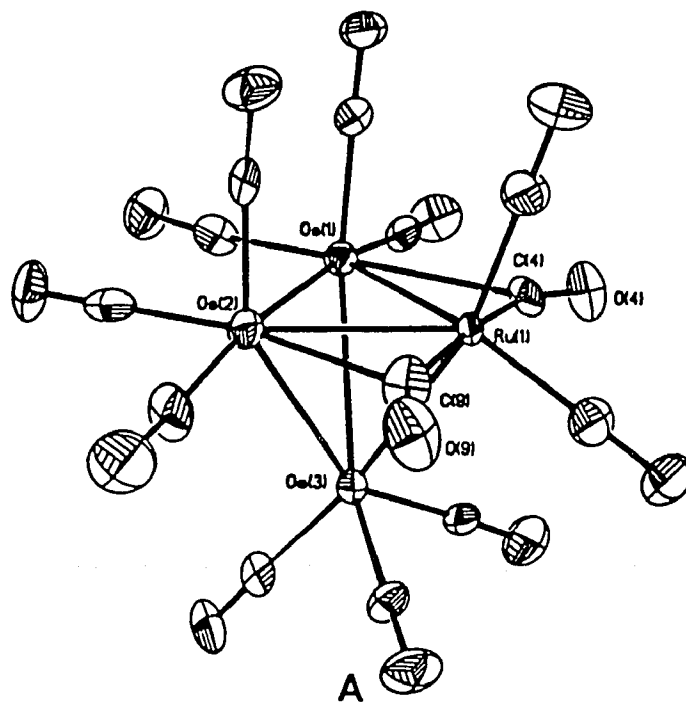


Figure 29. Molecular Structure of  $\text{H}_2\text{RuOs}_3(\text{CO})_{13}$ .



$\text{H}_2\text{Os}_4(\text{CO})_{13}$  and  $\text{H}_2\text{RuOs}_3(\text{CO})_{13}$ . These cluster species were identified as being a mixture by  $^1\text{H}$  NMR. (Fig. 30)

Due to the inseparable mixtures obtained in the above reactions, a more suitable route to the preparation of pure  $\text{H}_2\text{RuOs}_3(\text{CO})_{13}$  is needed. Shore and Siriwardane apparently synthesized pure  $\text{H}_2\text{RuOs}_3(\text{CO})_{13}$  according to Equation 52. The spectroscopic evidence they cite is as follows:  $^1\text{H}$  NMR  $\delta$ -21.0 ppm; IR  $\nu_{\text{CO}}$  2110(vw), 2082(vs), 2067(vs), 2056(vs), 2029(m), 2025(m), 1870(w,br)  $\text{cm}^{-1}$ ; FT-ICR MS m/e 1044.

A re-investigation of their experimental procedure results in formation of the inseparable mixture  $\text{H}_2\text{RuOs}_3(\text{CO})_{13}$  and  $\text{H}_2\text{Os}_4(\text{CO})_{13}$ . IR spectroscopic characterization of this mixture can be rather misleading. As one may notice, the IR spectra of  $\text{H}_2\text{RuOs}_3(\text{CO})_{13}$  and  $\text{H}_2\text{Os}_4(\text{CO})_{13}$  are very similar. ( $\text{H}_2\text{RuOs}_3(\text{CO})_{13}$ :  $\nu_{\text{CO}}$  2081(vs), 2068(vs), 2056(vs), 2027(m,sh), 2023(m,sh), 2018(m), 2006(w,sh)  $\text{cm}^{-1}$  in hexane [this work];  $\nu_{\text{CO}}$  2081(vs), 2066(vs), 2055(vs), 2017(m,br), 1852 (w,br)  $\text{cm}^{-1}$  in  $\text{CH}_2\text{Cl}_2$  [110];  $\nu_{\text{CO}}$  2081(vs), 2066(vs), 2055(vs), 2028(m), 2023(m), 2017(s), 2007(w), 1868 (w,br)  $\text{cm}^{-1}$  in hexane [114]) ( $\text{H}_2\text{Os}_4(\text{CO})_{13}$ :  $\nu_{\text{CO}}$  2081(vs), 2064(vs), 2056(vs), 2019(s,br)  $\text{cm}^{-1}$  in  $\text{CH}_2\text{Cl}_2$  [110];  $\nu_{\text{CO}}$  2084(vs), 2070(vs), 2060(vs), 2021(vs), 2005(w), 1860 (w,br)  $\text{cm}^{-1}$  [75];  $\nu_{\text{CO}}$  2090(s), 2062(s), 2053(s), 2041(w), 2020(vs), 1998(w), 1987(w)  $\text{cm}^{-1}$  in cyclohexane [100b,114]) Figure 31A shows the IR spectrum of the reaction mixture ( $\nu_{\text{CO}}$  2081(s), 2076(m,sh), 2066(vs), 2056(s), 2034(w,sh), 2025(s), 2017(m,sh), 2010(w,sh), 1993(vw), 1989(vw)  $\text{cm}^{-1}$  in hexane) which was further identified to be a mixture

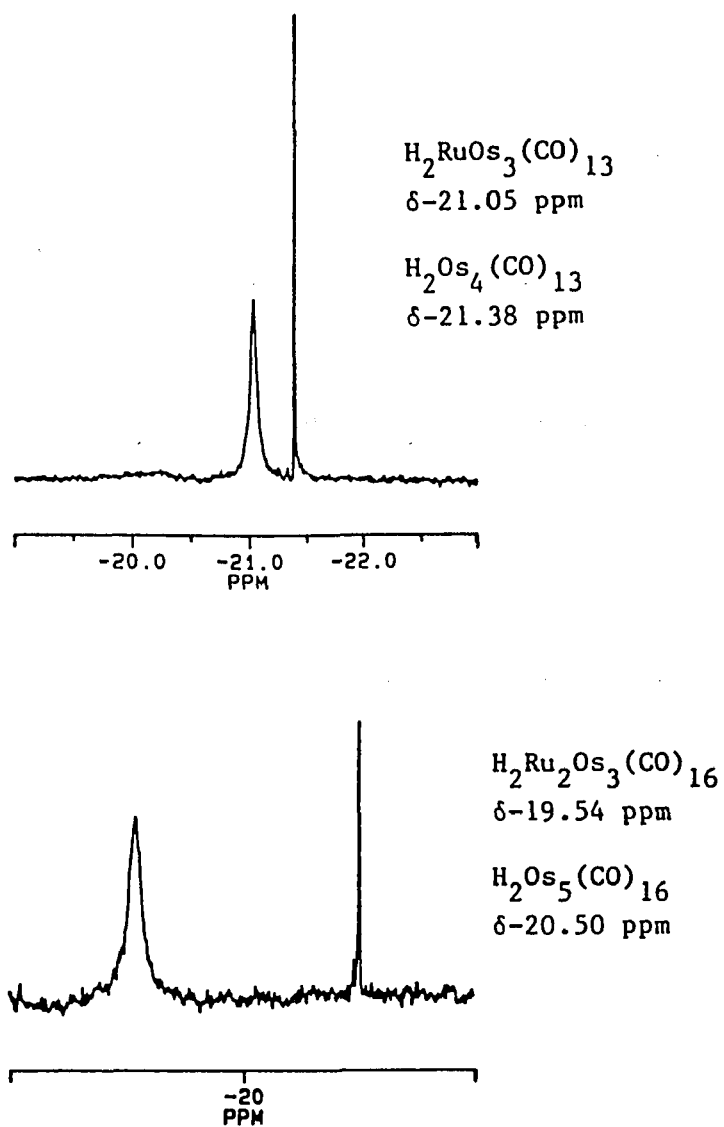


Figure 30. Proton NMR Spectra of Inseparable (a) Penta- and (b) Tetra- nuclear Clusters.

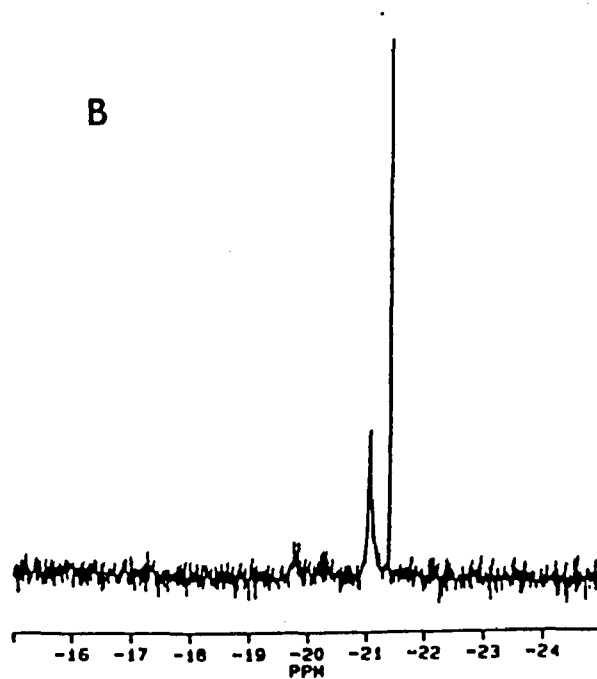
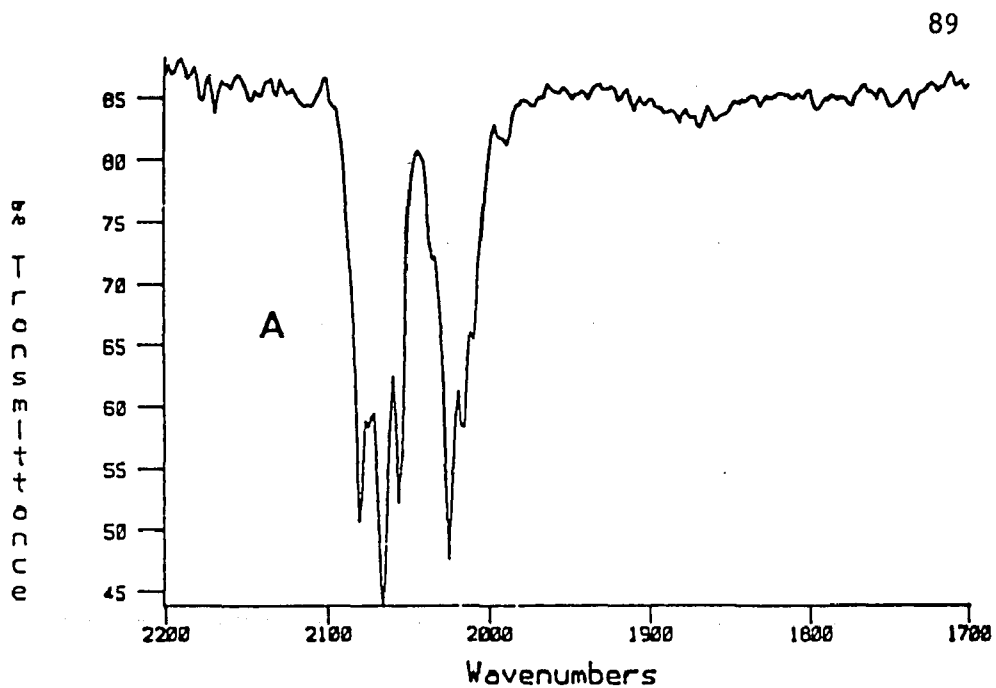


Figure 31. IR (a) and Proton NMR (b) Spectra of  $\text{H}_2\text{RuOs}_3(\text{CO})_{13}$  Reaction Mixture.

by  $^1\text{H}$  NMR. (Fig. 31B) ( $\text{H}_2\text{RuOs}_3(\text{CO})_{13}$   $\delta$ -21.04 ppm,  $\text{H}_2\text{Os}_4(\text{CO})_{13}$   $\delta$ -21.38 ppm in  $\text{CDCl}_3$ )

Another method of product characterization used widely in cluster chemistry is mass spectroscopy. In this particular case, the results obtained may lead to an erroneous conclusion. The product mixture described above was subjected to an FT-ICR MS study. The results of this study show that at  $100^\circ\text{C}$  the product appears to be pure  $\text{H}_2\text{RuOs}_3(\text{CO})_{13}$ . (Fig. 32) The parent peak occurs at  $m/e$  1044 and the sequential loss of 13 carbonyls and 2 hydrides are readily observed. However, if the same sample is run at  $125^\circ\text{C}$  both  $\text{H}_2\text{Os}_4(\text{CO})_{13}$  and  $\text{H}_2\text{RuOs}_3(\text{CO})_{13}$  are present. (Fig. 33) The parent peaks of  $\text{H}_2\text{RuOs}_3(\text{CO})_{13}$  and  $\text{H}_2\text{Os}_4(\text{CO})_{13}$  occur at  $m/e$  1044 and  $m/e$  1134, respectively. The loss of 13 carbonyls and 2 hydrides from each cluster can be identified. Therefore,  $\text{H}_2\text{RuOs}_3(\text{CO})_{13}$  is more volatile than  $\text{H}_2\text{Os}_4(\text{CO})_{13}$  and can be made to look pure depending on which temperature the spectrum is run at.

Further purification of the reaction mixture using multiple column, TLC and HPLC chromatographic techniques does not succeed in product separation. The conclusion can be made that once  $\text{H}_2\text{Os}_4(\text{CO})_{13}$  and  $\text{H}_2\text{RuOs}_3(\text{CO})_{13}$  are formed in the reaction, they are inseparable. Therefore, one must be cautious in devising a reaction scheme which eliminates the possibility of  $\text{H}_2\text{Os}_4(\text{CO})_{13}$  formation.

## 2. Reaction of $[\text{Ru}_3(\text{CO})_{11}]^{2-}$ with $\text{Os}_3(\text{CO})_{12}$

The product mixture obtained when  $[\text{Ru}_3(\text{CO})_{11}]^{2-}$  is reacted with 1/2 equivalent  $\text{Os}_3(\text{CO})_{12}$  is somewhat different (Equation 57) than that

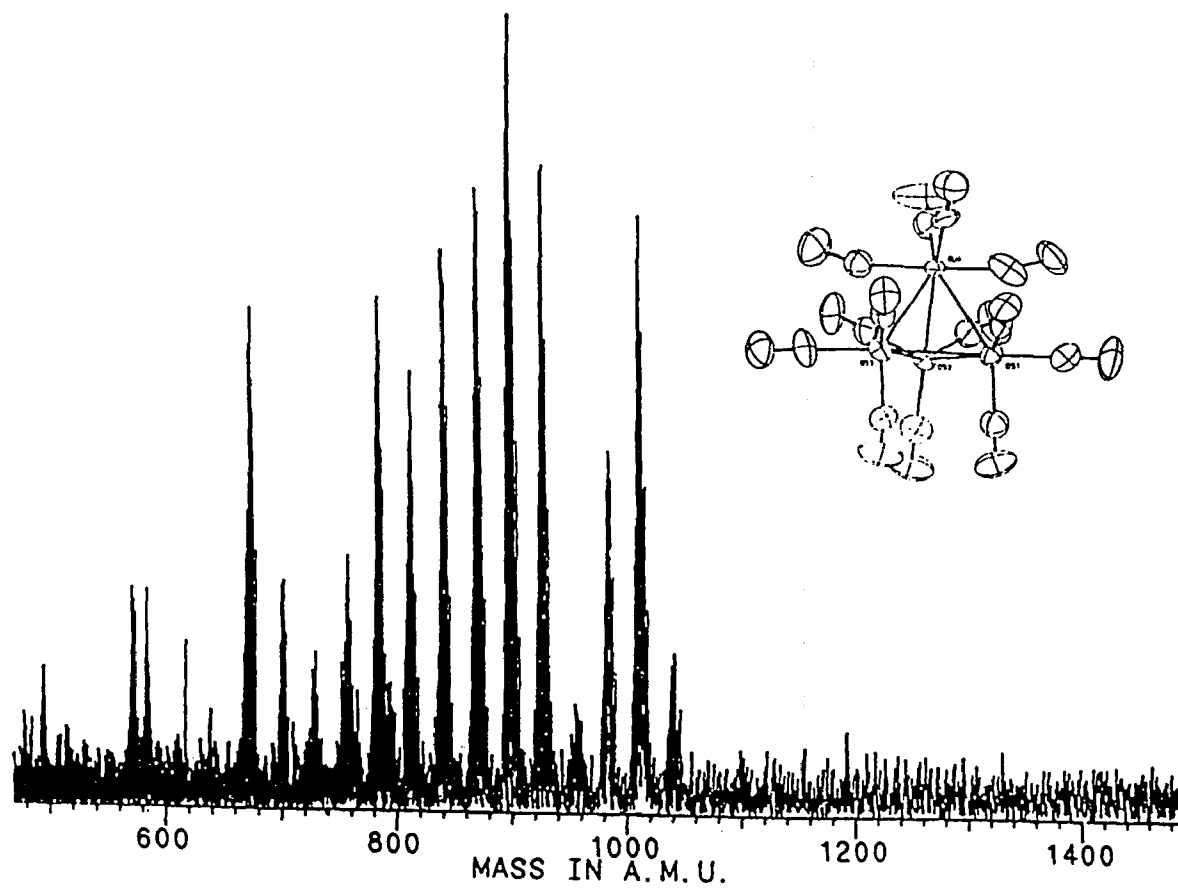


Figure 32. FT-ICR MS Spectrum of  $\text{H}_2\text{RuOs}_3(\text{CO})_{13}$  Sample at  $T=100^\circ\text{C}$ .

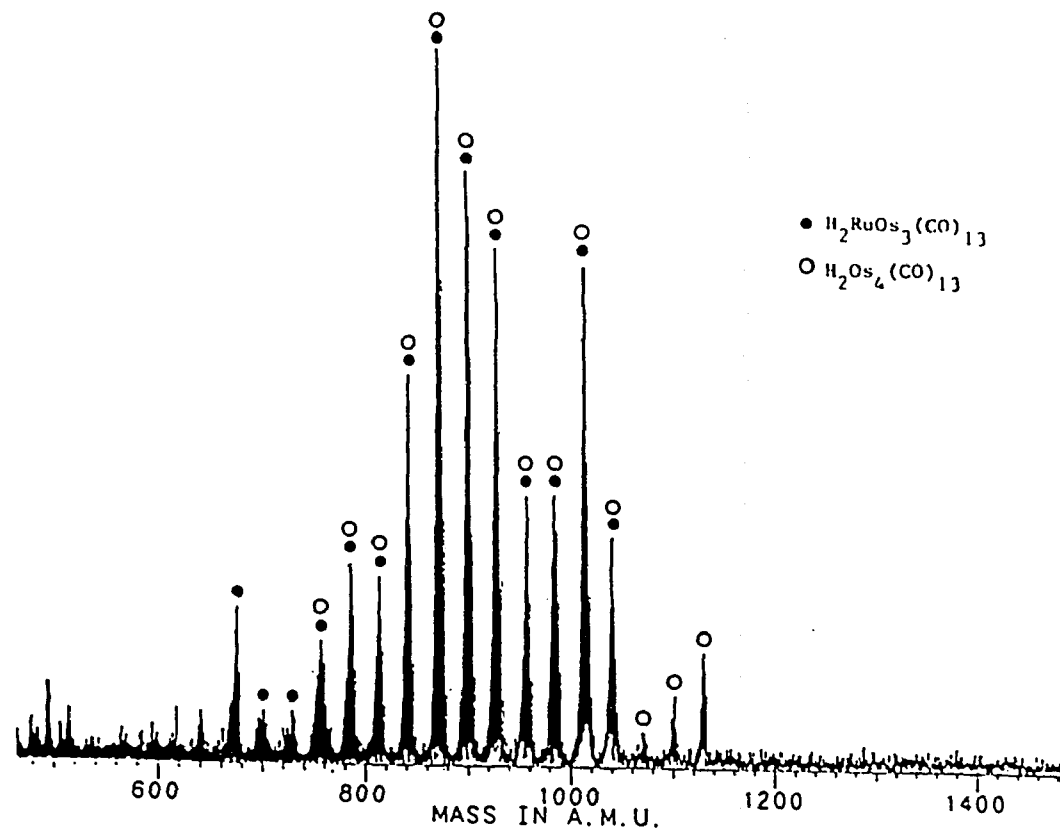
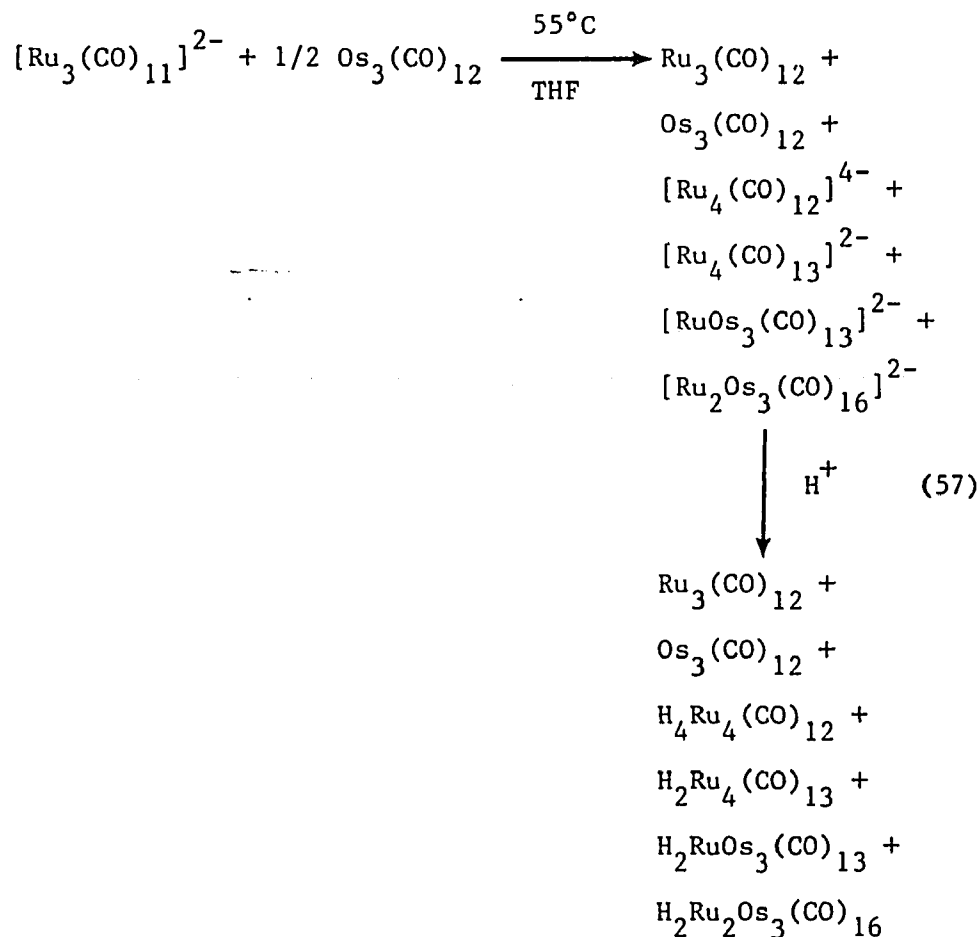


Figure 33. FT-ICR MS Spectrum of  $\text{H}_2\text{RuOs}_3(\text{CO})_{13}$  Sample at  $T=125^\circ\text{C}$ .

obtained when  $[\text{Os}_3(\text{CO})_{11}]^{2-}$  is reacted with  $1/2 \text{Ru}_3(\text{CO})_{12}$  (Equation 56) as previously described.



Separations using column, TLC and HPLC chromatographic techniques are successful in obtaining the pure mixed-metal products  $\text{H}_2\text{RuOs}_3(\text{CO})_{13}$  and  $\text{H}_2\text{Ru}_2\text{Os}_3(\text{CO})_{16}$ . This success is possible because the isostructural, homonuclear clusters  $\text{H}_2\text{Os}_4(\text{CO})_{13}$  and  $\text{H}_2\text{Os}_5(\text{CO})_{16}$  are not formed.

The tetranuclear cluster  $\text{H}_2\text{RuOs}_3(\text{CO})_{13}$  has been spectroscopically characterized. It exhibits a broad singlet in the proton NMR (Fig. 34)

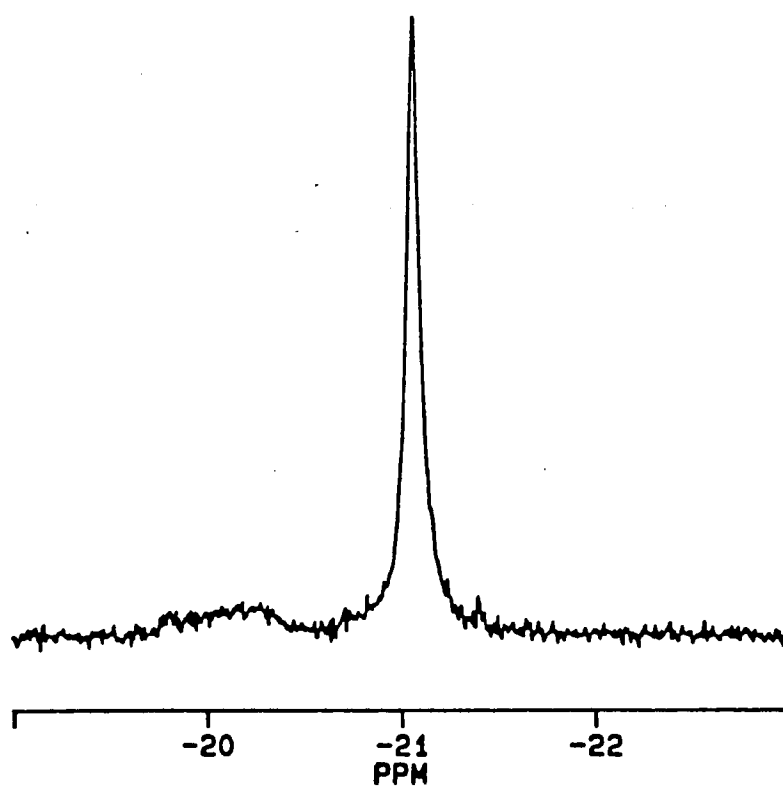


Figure 34. Proton NMR Spectrum of  $\text{H}_2\text{RuOs}_3(\text{CO})_{13}$ .

at approximately  $\delta$ -21.0 ppm (slightly solvent dependent, see Experimental Section) which indicates the equivalence of the hydrides. The upfield occurrence also indicates the position of the hydrides to be bridging two osmium atoms as opposed to a heteronuclear bridge.

The IR spectrum shows a rather simple pattern indicative of a fairly symmetrical structure. (Fig. 35) Comparison of this spectrum with the spectra of  $\text{H}_2\text{FeRu}_3(\text{CO})_{13}$  and  $\text{H}_2\text{FeOs}_3(\text{CO})_{13}$  shows that these are indeed an isostructural series.

The pentanuclear cluster  $\text{H}_2\text{Ru}_2\text{Os}_3(\text{CO})_{16}$  may also be isolated in its pure form from this synthetic route. The proton NMR is a singlet at  $\delta$ -19.54 ppm indicative of a heteronuclear bridging position (Ru-H-Os). The IR spectrum (Fig. 36) is similar to that reported for  $\text{H}_2\text{Os}_5(\text{CO})_{16}$  ( $\nu_{\text{CO}}$  2126(w), 2088(s), 2066(s), 2053(s), 2045(m,sh), 2038(w), 2013(m)  $\text{cm}^{-1}$  in cyclohexane [44a]) and  $\text{H}_2\text{Fe}_2\text{Os}_3(\text{CO})_{16}$  ( $\nu_{\text{CO}}$  2086(vs), 2070(vs), 2062(vs), 2040(w), 2030(s), 2005(m), 1983(w)  $\text{cm}^{-1}$  [50a]) confirming their isostructural character.

Shore and Siriwardane [75] first synthesized  $\text{H}_2\text{Ru}_2\text{Os}_3(\text{CO})_{16}$  from the reaction of  $[\text{Ru}_3(\text{CO})_{11}]^{2-}$  and  $2/3 \text{Os}_3(\text{CO})_{12}$ . They showed through X-ray crystallography that this system is also plagued with co-crystallization problems. In this case, the isostructural clusters  $\text{H}_2\text{Ru}_2\text{Os}_3(\text{CO})_{16}$  and  $\text{H}_2\text{Os}_5(\text{CO})_{16}$  exhibit this phenomenon. Figure 37 depicts the structure as reported by Shore and Siriwardane. The positions labelled Ru(1) and Ru(2) are the sites of co-crystallization with the cluster occupancies actually being  $\text{H}_2\text{Ru}_2\text{Os}_3(\text{CO})_{16}$  and  $\text{H}_2\text{Os}_5(\text{CO})_{16}$  in a ratio of 75%:25%.

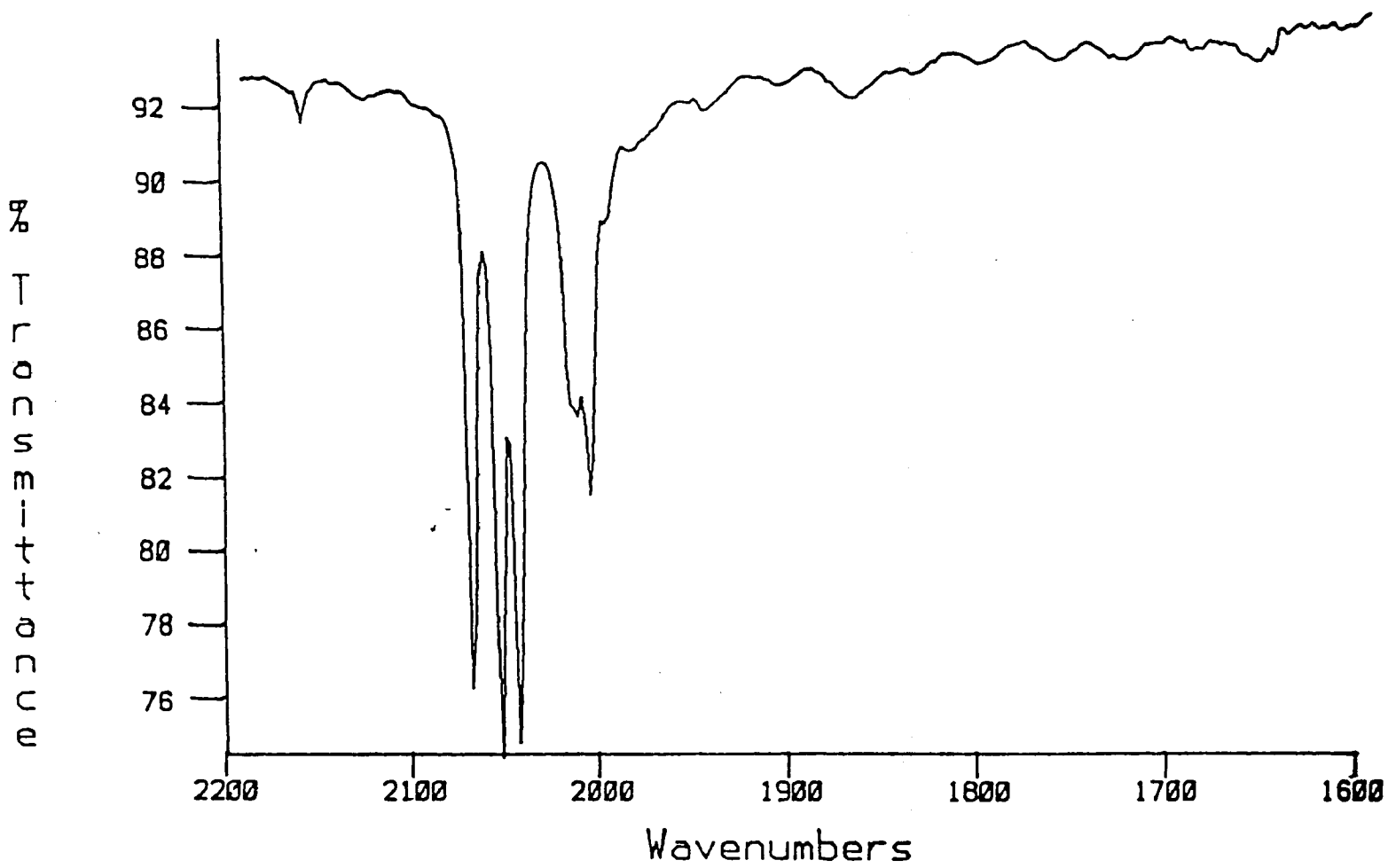


Figure 35. IR Spectrum of  $\text{H}_2\text{RuOs}_3(\text{CO})_{13}$ .

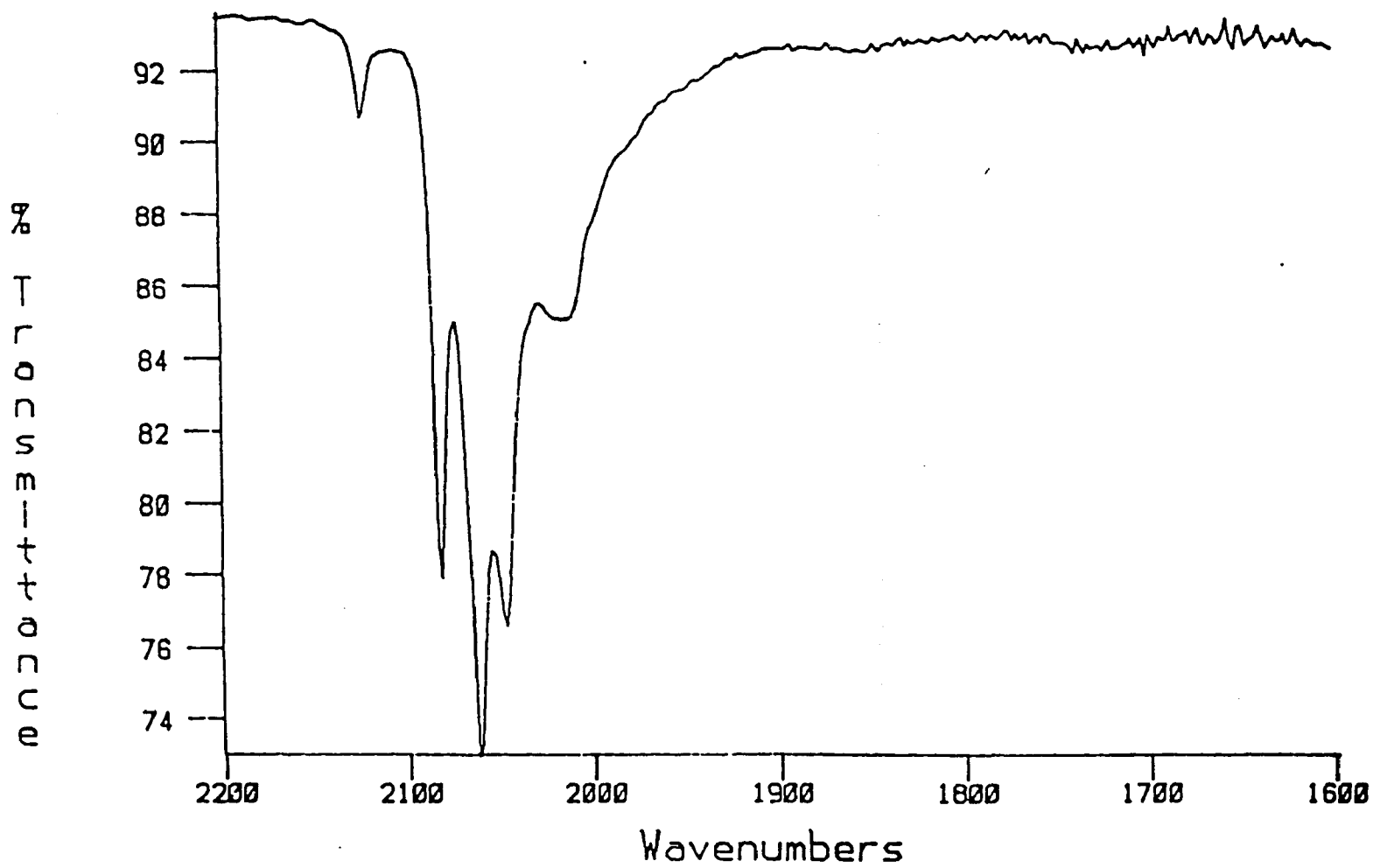


Figure 36. IR Spectrum of  $\text{H}_2\text{Ru}_2\text{Os}_3(\text{CO})_{16}$ .

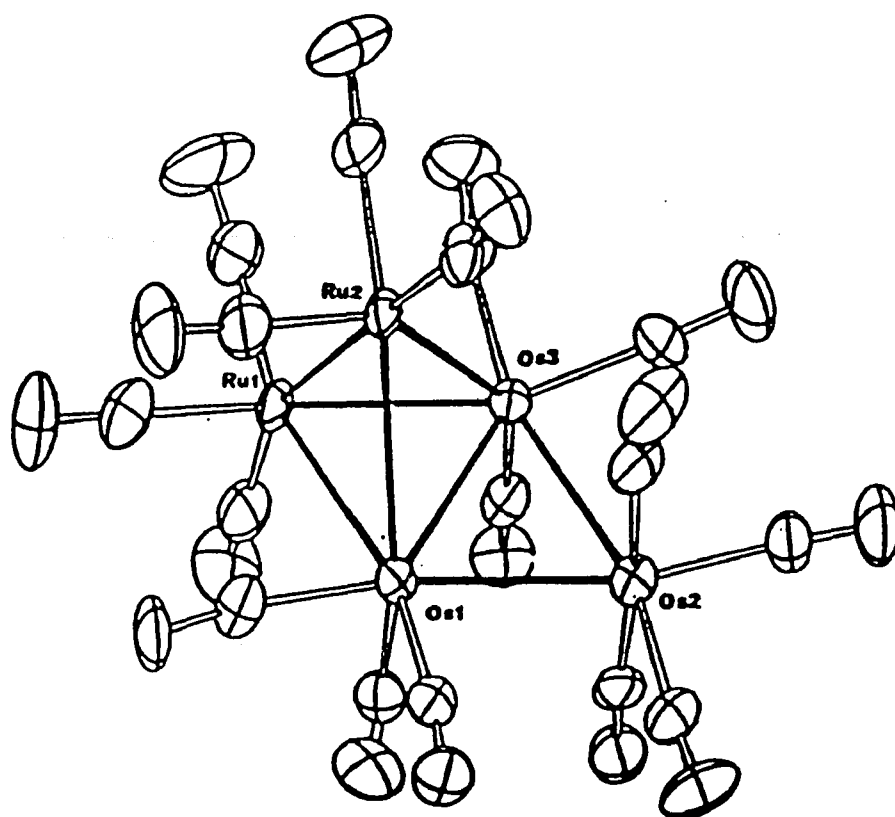


Figure 37. Molecular Structure of  $\text{H}_2\text{Ru}_2\text{Os}_3(\text{CO})_{16}$ .

It seems that reaction of  $[\text{Ru}_3(\text{CO})_{11}]^{2-}$  with  $1/2 \text{Os}_3(\text{CO})_{12}$  is a desirable synthetic route to the mixed-metal tetra- and penta-nuclear systems; however, the yields obtained are quite low.

### 3. Crystallographic Determination of $\text{H}_2\text{RuOs}_3(\text{CO})_{13}$

Several structural studies on  $\text{H}_2\text{RuOs}_3(\text{CO})_{13}$  were discussed previously (Section B--Crystallographic Studies) and displayed marked differences. These differences warranted the re-determination of the structure which is presented below.

The molecular structure of  $\text{H}_2\text{RuOs}_3(\text{CO})_{13}$  is shown in Figure 38. Crystallographic data for this particular structural determination appears in Table 8. Tables 9 and 10 list selected bond distances and bond angles, respectively. (The particular features with respect to the data collection and structure solution are described in the Experimental Section of this dissertation.)

The molecular structure of this cluster is isostructural with  $\text{H}_2\text{FeRu}_3(\text{CO})_{13}$  [74] (Fig. 14) and  $\text{H}_2\text{FeOs}_3(\text{CO})_{13}$ . [94] (Fig. 27) The cluster adopts a distorted tetrahedral metal arrangement where a ruthenium atom caps an  $\text{Os}_3$  triangle. Each osmium atom is associated with three terminal carbonyls, whereas the ruthenium atoms bonds to two terminal and two semibridging carbonyls.

The intermetallic distances within the cluster may be classified as: (1) "normal" osmium-osmium bond distances, (2) "long" osmium-osmium distances, and (3) ruthenium-osmium distances. The bond distance  $\text{Os}(1)-\text{Os}(3)=2.839(2)\text{\AA}$  is considered "normal", being comparable

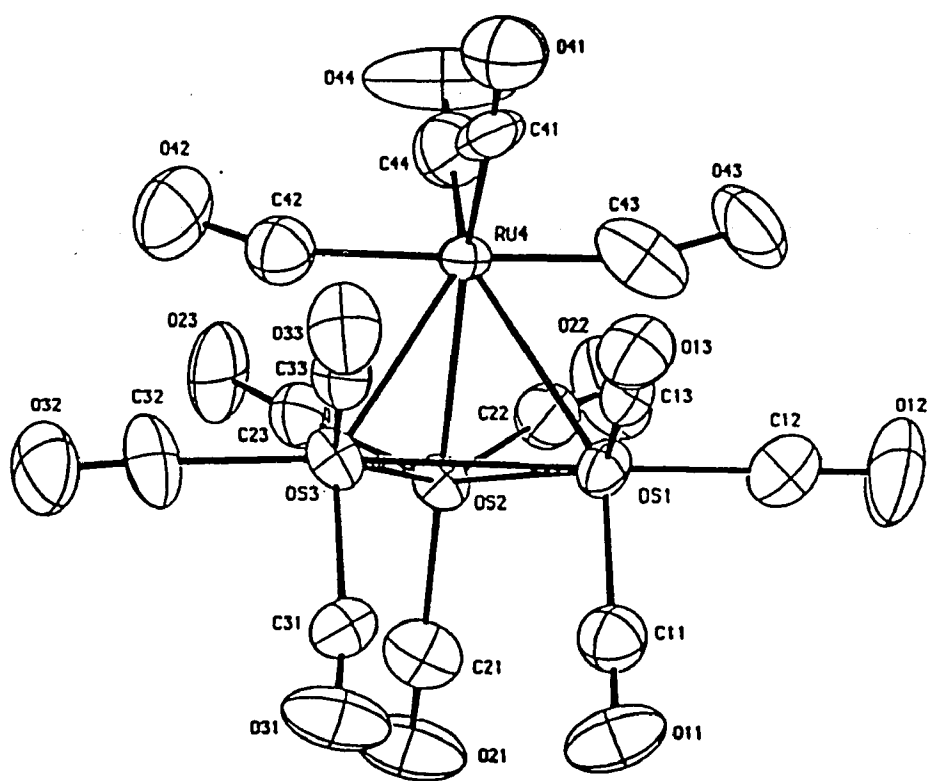


Figure 38. ORTEP of  $(\mu\text{-H})_2\text{RuOs}_3(\text{CO})_{13}$ .

Table 8. Crystallographic Data for  $(\mu\text{-H})_2\text{RuOs}_3(\text{CO})_{13}$ .

Chemical formula	$\text{RuOs}_3\text{C}_{13}\text{O}_{13}\text{H}_2^{\text{a}}$	$\text{RuOs}_3\text{C}_{13}\text{O}_{13}\text{H}_2^{\text{b,c}}$
Molecular wt	1044	1044
Space group	C2/c	
Molecules/unit cell	8	
Temp, °C	25	25
a, Å	31.856(4)	23.044(5)
b, Å	9.774(1)	9.070(8)
c, Å	13.953(2)	19.306(3)
$\beta$ , deg	110.83(1)	90.82(2)
Volume, Å <sup>3</sup>	4060.7	4034.8
D(calcd), g cm <sup>-3</sup>	3.395	
Radiation	Mo K $\alpha$ (0.710730Å)	
Absorptn coeff, cm <sup>-1</sup>	195.2	
Transmissn coeff, %	max. 99.67 min. 9.80	
Scan mode	$\omega$ -2 $\theta$	
Data collectn limits, deg	4-55	
No. of unique reflctns	4065	
No. of reflctns used in structure refinement (>3 $\sigma$ (I))	2371	
No. variable parameters	252	
R <sub>f</sub>	0.064	
R <sub>wf</sub> /w	0.076/0.05	
GOF	2.065	
extinctn coeff	refined	

<sup>a</sup>from pentane<sup>b</sup>from CH<sub>2</sub>Cl<sub>2</sub><sup>c</sup>low angle data only (< 24° 2 $\theta$ )

Table 9. Selected Bond Distances (Å) and Esd's for  $(\mu\text{-H})_2\text{RuOs}_3(\text{CO})_{13}$ .

---



---

A. Metal-Metal Distances			
Os(1)-Os(2)	2.946(2)	Os(1)-Ru(4)	2.795(3)
Os(1)-Os(3)	2.839(2)	Os(2)-Ru(4)	2.787(2)
Os(2)-Os(3)	2.950(1)	Os(3)-Ru(4)	2.794(2)
B. M-C <sub>terminal</sub> Distances			
Os(1)-C(11)	1.90(3)	Os(3)-C(31)	1.95(3)
Os(1)-C(12)	1.91(4)	Os(3)-C(32)	1.90(4)
Os(1)-C(13)	1.88(3)	Os(3)-C(33)	1.88(3)
Os(2)-C(21)	1.94(3)	Ru(4)-C(41)	1.87(3)
Os(2)-C(22)	1.89(3)	Ru(4)-C(42)	1.94(4)
Os(2)-C(23)	1.90(4)	Ru(4)-C(43)	1.85(4)
		Ru(4)-C(44)	1.84(4)
C. M-C <sub>semibridge</sub> Distances			
Os(1)-C(43)	2.50(3)	Os(3)-C(42)	2.49(3)
D. C-O Distances			
C(11)-O(11)	1.15(4)	C(31)-O(31)	1.09(3)
C(12)-O(12)	1.15(5)	C(32)-O(32)	1.12(5)
C(13)-O(13)	1.13(3)	C(33)-O(33)	1.14(3)
C(21)-O(21)	1.08(3)	C(41)-O(41)	1.21(4)
C(22)-O(22)	1.13(3)	C(42)-O(42)	1.19(5)
C(23)-O(23)	1.15(5)	C(43)-O(43)	1.23(4)
		C(44)-O(44)	1.20(5)

---

Table 10. Selected Bond Angles (deg) and Esd's for  $(\mu\text{-H})_2\text{RuOs}_3(\text{CO})_{13}$ .

A. Angles Within $\text{RuOs}_3$ Core			
$\text{Os}(2)\text{-Os}(1)\text{-Os}(3)$	61.28(4)	$\text{Os}(1)\text{-Os}(2)\text{-Ru}(4)$	58.29(6)
$\text{Os}(2)\text{-Os}(1)\text{-Ru}(4)$	58.02(5)	$\text{Os}(3)\text{-Os}(2)\text{-Ru}(4)$	58.20(5)
$\text{Os}(3)\text{-Os}(1)\text{-Ru}(4)$	59.44(5)	$\text{Os}(1)\text{-Os}(3)\text{-Os}(2)$	61.14(4)
$\text{Os}(1)\text{-Os}(2)\text{-Os}(3)$	57.58(4)	$\text{Os}(1)\text{-Os}(3)\text{-Ru}(4)$	59.50(6)
		$\text{Os}(2)\text{-Os}(3)\text{-Ru}(4)$	57.99(4)
B. $\text{M-M-C}_{\text{terminal}}$ Angles			
$\text{Os}(2)\text{-Os}(1)\text{-C}(11)$	106(1)	$\text{Os}(1)\text{-Os}(3)\text{-C}(31)$	87.7(9)
$\text{Os}(2)\text{-Os}(1)\text{-C}(12)$	113(1)	$\text{Os}(1)\text{-Os}(3)\text{-C}(32)$	170.2(8)
$\text{Os}(2)\text{-Os}(1)\text{-C}(13)$	145.8(9)	$\text{Os}(1)\text{-Os}(3)\text{-C}(33)$	95(1)
$\text{Os}(3)\text{-Os}(1)\text{-C}(11)$	93(1)	$\text{Os}(2)\text{-Os}(3)\text{-C}(31)$	106.6(7)
$\text{Os}(3)\text{-Os}(1)\text{-C}(12)$	174(1)	$\text{Os}(2)\text{-Os}(3)\text{-C}(32)$	109.3(8)
$\text{Os}(3)\text{-Os}(1)\text{-C}(13)$	90.5(9)	$\text{Os}(2)\text{-Os}(3)\text{-C}(33)$	147.1(8)
$\text{Ru}(4)\text{-Os}(1)\text{-C}(11)$	152(1)	$\text{Ru}(4)\text{-Os}(3)\text{-C}(31)$	147.2(9)
$\text{Ru}(4)\text{-Os}(1)\text{-C}(12)$	117(1)	$\text{Ru}(4)\text{-Os}(3)\text{-C}(32)$	118.4(9)
$\text{Ru}(4)\text{-Os}(1)\text{-C}(13)$	92.0(8)	$\text{Ru}(4)\text{-Os}(3)\text{-C}(33)$	91.3(7)
$\text{Os}(1)\text{-Os}(2)\text{-C}(21)$	114(1)	$\text{Os}(1)\text{-Ru}(4)\text{-C}(41)$	103(1)
$\text{Os}(1)\text{-Os}(2)\text{-C}(22)$	103(1)	$\text{Os}(1)\text{-Ru}(4)\text{-C}(42)$	121.5(9)
$\text{Os}(1)\text{-Os}(2)\text{-C}(23)$	148.0(8)	$\text{Os}(1)\text{-Ru}(4)\text{-C}(44)$	141(1)
$\text{Os}(3)\text{-Os}(2)\text{-C}(21)$	112.6(8)	$\text{Os}(2)\text{-Ru}(4)\text{-C}(41)$	165(1)
$\text{Os}(3)\text{-Os}(2)\text{-C}(22)$	148.9(9)	$\text{Os}(2)\text{-Ru}(4)\text{-C}(42)$	89.4(9)
$\text{Os}(3)\text{-Os}(2)\text{-C}(23)$	98.6(8)	$\text{Os}(2)\text{-Ru}(4)\text{-C}(43)$	91.1(9)
$\text{Ru}(4)\text{-Os}(2)\text{-C}(21)$	169.6(9)	$\text{Os}(2)\text{-Ru}(4)\text{-C}(44)$	95(1)
$\text{Ru}(4)\text{-Os}(2)\text{-C}(22)$	91.2(8)	$\text{Os}(3)\text{-Ru}(4)\text{-C}(41)$	104.7(9)
$\text{Ru}(4)\text{-Os}(2)\text{-C}(23)$	91.7(8)	$\text{Os}(3)\text{-Ru}(4)\text{-C}(43)$	122.(1)
		$\text{Os}(3)\text{-Ru}(4)\text{-C}(44)$	140(1)
C. $\text{M-M-C}_{\text{semibridge}}$ Angles			
$\text{Os}(1)\text{-Ru}(4)\text{-C}(43)$	61(1)	$\text{Os}(3)\text{-Ru}(4)\text{-C}(42)$	60.4(9)

Table 10. Selected Bond Angles (deg) and Esd.'s for  $(\mu\text{-H})_2\text{RuOs}_3(\text{CO})_{13}$   
(cont.).

---



---

D. M-CO <sub>terminal</sub> Angles			
Os(1)-C(11)-O(11)	177(3)	Os(3)-C(31)-O(31)	172(3)
Os(1)-C(12)-O(12)	176(3)	Os(3)-C(32)-O(32)	177(3)
Os(1)-C(13)-O(13)	177(3)	Os(3)-C(33)-O(33)	177(2)
Os(2)-C(21)-O(21)	178(4)	Ru(4)-C(41)-O(41)	178(3)
Os(2)-C(22)-O(22)	174(2)	Ru(4)-C(44)-O(44)	179(3)
Os(2)-C(23)-O(23)	176(2)		
E. M-CO <sub>semibridge</sub> and M-CO-M Angles			
Ru(4)-C(42)-O(42)	159(3)	Ru(4)-C(42)-Os(3)	77(1)
Ru(4)-C(43)-O(43)	160(3)	Ru(4)-C(43)-Os(1)	78(1)

---

to the distances found in  $\text{Os}_3(\text{CO})_{12}$  ( $d(\text{Os}-\text{Os})_{\text{ave}}=2.877(3)\text{\AA}$  [100a]) or the unbridged osmium-osmium bonds in  $\text{H}_2\text{Os}_3(\text{CO})_{10}$  ( $2.857(7)\text{\AA}$  [95,99, 100]),  $\text{H}_2\text{FeOs}_3(\text{CO})_{13}$  ( $2.847(1)\text{\AA}$  [94]),  $\text{H}_4\text{Os}_4(\text{CO})_{11}(\text{CNMe})$  ( $2.822(1)\text{\AA}$  [116]),  $\text{HCpWOs}_3(\text{CO})_{12}$  ( $2.784(2)$ - $2.799(2)\text{\AA}$  [117]) or  $\text{H}_3\text{CpWOs}_3(\text{CO})_{11}$  ( $2.825(2)$ - $2.827(2)\text{\AA}$  [92]). Comparison of the corresponding distance with that reported by Shore *et al.* ( $2.816(1)\text{\AA}$  for Molecule 1,  $2.823(1)\text{\AA}$  for Molecule 2 [75]) or Rheingold *et al.* ( $2.850(1)\text{\AA}$  for Molecule 1,  $2.842(1)\text{\AA}$  for Molecule 2 [115]) shows no significant difference.

Somewhat longer distances are associated with Os(2),  $\text{Os}(1)-\text{Os}(2)=2.946(2)\text{\AA}$  and  $\text{Os}(2)-\text{Os}(3)=2.950(1)\text{\AA}$ . This lengthening is consistent with the presence of bridging hydride ligands; [49,55,59a,70a,92-100] however, the hydrides were not directly located in this study. These bond lengths are comparable to those found in  $\text{H}_2\text{FeOs}_3(\text{CO})_{13}$  ( $2.934(1)\text{\AA}$ ,  $2.937(1)\text{\AA}$  [94]) or those reported for  $\text{H}_2\text{RuOs}_3(\text{CO})_{13}$  in the previous studies. (Shore:  $2.929(1)$ - $2.947(1)\text{\AA}$  [75]; Rheingold:  $2.945(1)$ - $2.963(1)\text{\AA}$  [115])

The heterometallic distances  $\text{Ru}(4)-\text{Os}(1)=2.795(3)\text{\AA}$ ,  $\text{Ru}(4)-\text{Os}(2)=2.787(2)\text{\AA}$  and  $\text{Ru}(4)-\text{Os}(3)=2.794(2)\text{\AA}$  are consistent with those reported by Shore ( $2.786(1)$ - $2.825(1)\text{\AA}$  [75]) and Rheingold ( $2.787(2)$ - $2.817(2)\text{\AA}$  [115]) for  $\text{H}_2\text{RuOs}_3(\text{CO})_{13}$ .

Two semibridging carbonyls are associated with Ru(4) which exhibit typical metal-carbon and carbon-oxygen bond distances as tabulated in Table 9. In the isostructural clusters,  $\text{H}_2\text{FeRu}_3(\text{CO})_{13}$  [74] and  $\text{H}_2\text{FeOs}_3(\text{CO})_{13}$  [94] a slight contraction of the metal-metal bond is observed. Examination of the heterometallic distances associated

with the semibridging carbonyl in all the  $\text{H}_2\text{RuOs}_3(\text{CO})_{13}$  studies does not reveal a similar trend. Bond angles associated with these carbonyls are also typical and similar to those reported for the isostructural analogs. (Table 11)

The final difference Fourier map calculated for  $\text{H}_2\text{RuOs}_3(\text{CO})_{13}$  shows two peaks around Os(1) with  $5.8 \text{ EA}^{-3}$  about 0.9-1.0Å away, Os(2) with two peaks with  $4.6 \text{ EA}^{-3}$  about 0.9-1.0Å away, Os(3) with one peak with  $5.2 \text{ EA}^{-3}$  about 1.0Å away and Ru(4) with one peak  $4.0 \text{ EA}^{-3}$  about 0.9Å away. This may suggest some type of orientational disorder of the molecule, microscopic twinning or perhaps more likely due to the marginal quality of the crystal used in this study. The quality of the crystal being less than ideal is also observed in the presence of thermal parameters going negative upon anisotropic refinement of carbons C(11), C(22), C(42) and C(44). The presence of high electron density peaks around the metal atoms was also observed by Shore and Siriwardane [75] and Rheingold and Gates [115] for  $\text{H}_2\text{RuOs}_3(\text{CO})_{13}$ . Yawney *et al.* [119] observed this for  $\text{H}_2\text{Ru}_4(\text{CO})_{13}$  and similar occurrences were noted by Churchill [87] and Dahl [120] for other polynuclear metal carbonyl species.

Comparison of all the  $\text{H}_2\text{RuOs}_3(\text{CO})_{13}$  structures discussed thus far lead one to believe that two crystalline polymorphs\* exist for this cluster, a monoclinic form and a triclinic form. Rheingold [115]

---

\* Polymorphism: Property of crystallizing in two or more forms with distinct structures. [118]

Table 11. Comparison of Semibridging Carbonyl Bond Distances and Bond Angles for  $\text{H}_2\text{RuOs}_3(\text{CO})_{13}$ ,  $\text{H}_2\text{FeOs}_3(\text{CO})_{13}$  and  $\text{H}_2\text{FeRu}_3(\text{CO})_{13}$ .

	$\text{H}_2\text{RuOs}_3(\text{CO})_{13}$ <sup>a</sup>	$\text{H}_2\text{FeOs}_3(\text{CO})_{13}$ <sup>b</sup>	$\text{H}_2\text{FeRu}_3(\text{CO})_{13}$ <sup>c</sup>
$\text{M}'\text{-C}$ (Å) <sup>d</sup>	2.50(3)	2.34(2)	2.334(5)
	2.49(3)	2.35(2)	2.299(5)
$\text{M}'\text{-M-C}$ (deg)	61(1)	58.9(7)	58.9(2)
	60.4(9)	58.9(6)	58.5(2)
$\text{M-C-O}$ (deg)	159(3)	152.5(2)	154.7(5)
	160(3)	153.6(2)	152.5(4)
$\text{M-C}\dots\text{M}'$ (deg)	77(1)	79.3(8)	78.8(2)
	78(1)	78.6(7)	79.1(2)

<sup>a</sup>this work

<sup>b</sup>Ref. 94

<sup>c</sup>Ref. 74

<sup>d</sup>M denotes apex metal, M' denotes metals in triangular unit

suggests the polymorphs arise due to crystallization from different solvent systems. Apparently crystallization from pentane favors the triclinic crystal system; whereas,  $\text{CH}_2\text{Cl}_2$  favors the monoclinic system. (Table 7)

As part of this structural analysis, the effect of the solvent on crystallization was studied. Crystals were grown from pentane or  $\text{CH}_2\text{Cl}_2$  using  $\text{H}_2\text{RuOs}_3(\text{CO})_{13}$  obtained from the same synthetic mixture which was shown to be pure by  $^1\text{H}$  NMR, IR and HPLC. Crystals were grown under identical environmental conditions in order to ensure effects; such as, temperature did not play a *substantial* role in the crystallization process. Unit cell parameters for these two samples are collected in Table 8. One sees that the different solvents cause a change in space groups; however, the crystal system remains the same (ie. monoclinic).

Upon closer examination of Tables 6-8, one may draw the conclusion that incorporation of a high ratio of  $\text{H}_2\text{Os}_4(\text{CO})_{13}^*$  into the single crystal would tend to cause crystallization in the triclinic crystal system. Large amounts of  $\text{H}_2\text{RuOs}_3(\text{CO})_{13}$  or  $\text{H}_2\text{Ru}_4(\text{CO})_{13}^{**}$  would favor crystallization in the monoclinic system.

Examination of the metal thermal parameters for all the  $\text{H}_2\text{RuOs}_3(\text{CO})_{13}$  structure analyses are tabulated in Table 12 (excluding

\*Crystallization Data for  $\text{H}_2\text{Os}_4(\text{CO})_{13}$  [75]

$a=9.129(4)\text{\AA}$	$\alpha=91.95(4)^\circ$	P1 bar (Z=4)
$b=26.552(6)\text{\AA}$	$\beta=112.27(4)^\circ$	$D_c=3.46\text{ g cm}^{-3}$
$c=9.025(5)\text{\AA}$	$\gamma=81.76(3)^\circ$	

Table 12. Comparison of Metal Thermal Parameters in  $H_2RuOs_3(CO)_{13}$ .

(A) $B_{iso}$				
	This Work		Shore & Siriwardane <sup>a</sup>	
Os	2.87(2)		2.92(2)	3.26(2)
Os	2.64(2)		2.84(2)	2.87(2)
Os	2.94(2)		2.97(2)	3.31(2)
Ru	2.14(2)		2.19(3)	2.37(3)
(B) $B_{iso}$ <sup>b</sup> from $U_{iso}$				
	$U_{iso}$ Rheingold & Gates <sup>c</sup>		$B_{iso}$ Rheingold & Gates	
Os	35(1)	41(1)	2.81	3.29
Os	34(1)	43(1)	2.73	3.45
Os	38(1)	42(1)	3.05	3.37
Ru	25(1)	34(1)	2.00	2.73
(C) $U_{iso}$ <sup>d</sup> from $B_{iso}$				
	This Work		Shore & Siriwardane	
Os	36		36	41
Os	33		35	36
Os	37		37	41
Ru	27		27	30

<sup>a</sup> data corresponding to structure solution in Table 7-Column I

<sup>b</sup> calculated as  $B_{iso} = U_{iso} (2\pi^2 a^{*2})$  where  $a^*$  = reciprocal of a axis since  $B_{iso} = B_{11} = B_{22} = B_{33}$  [118,142] (a axis chosen since has largest reciprocal value)

<sup>c</sup> data corresponding to structure solution in Table 7-Column II

<sup>d</sup> calculated as  $U_{iso} = B_{iso} / 2\pi^2 A^{*2}$

the co-crystallized situations). Normally an abnormal value would be observed for the ruthenium atom if co-crystallization were occurring at this position; however, the data here does not give conclusive evidence for or against co-crystallization.

A re-investigation of the experimental procedures cited by Rheingold and Gates [113-115] (Equation 51) results in formation of the inseparable mixture  $\text{H}_2\text{RuOs}_3(\text{CO})_{13}$  and  $\text{H}_2\text{Os}_4(\text{CO})_{13}$  (in this investigator's hands) as identified by  $^1\text{H}$  NMR, IR and HPLC. Therefore, based upon the chemical and structural studies performed here, the conclusion is made that  $\text{H}_2\text{RuOs}_3(\text{CO})_{13}$  in its *pure* form crystallizes in the monoclinic system and any type of co-crystallization *not* disorder influences crystal growth and is exhibited as the triclinic form.

#### IV. REACTIVITY STUDIES OF $\text{H}_2\text{Ru}_6(\text{CO})_{17}$

As mentioned earlier, the overall geometry adopted by  $\text{H}_2\text{Ru}_6(\text{CO})_{17}$  is a bicapped tetrahedron. This type of metal framework is rare for a hexanuclear cluster, for example,  $[\text{Ru}_6(\text{CO})_{18}]^{2-}$ , which usually exhibits an octahedral arrangement according to classical electron counting rules, [31,33,34a,121-122] as depicted in Figure 39 for related ruthenium and osmium clusters. If one counts electrons for

---

\*\* Crystallization Data for  $\text{H}_2\text{Ru}_4(\text{CO})_{13}$  [119]

a=9.534(10)Å    β=90.29(3)°

b=9.032(9)Å    P2<sub>1</sub>/c (Z=8)

c=47.44(4)Å

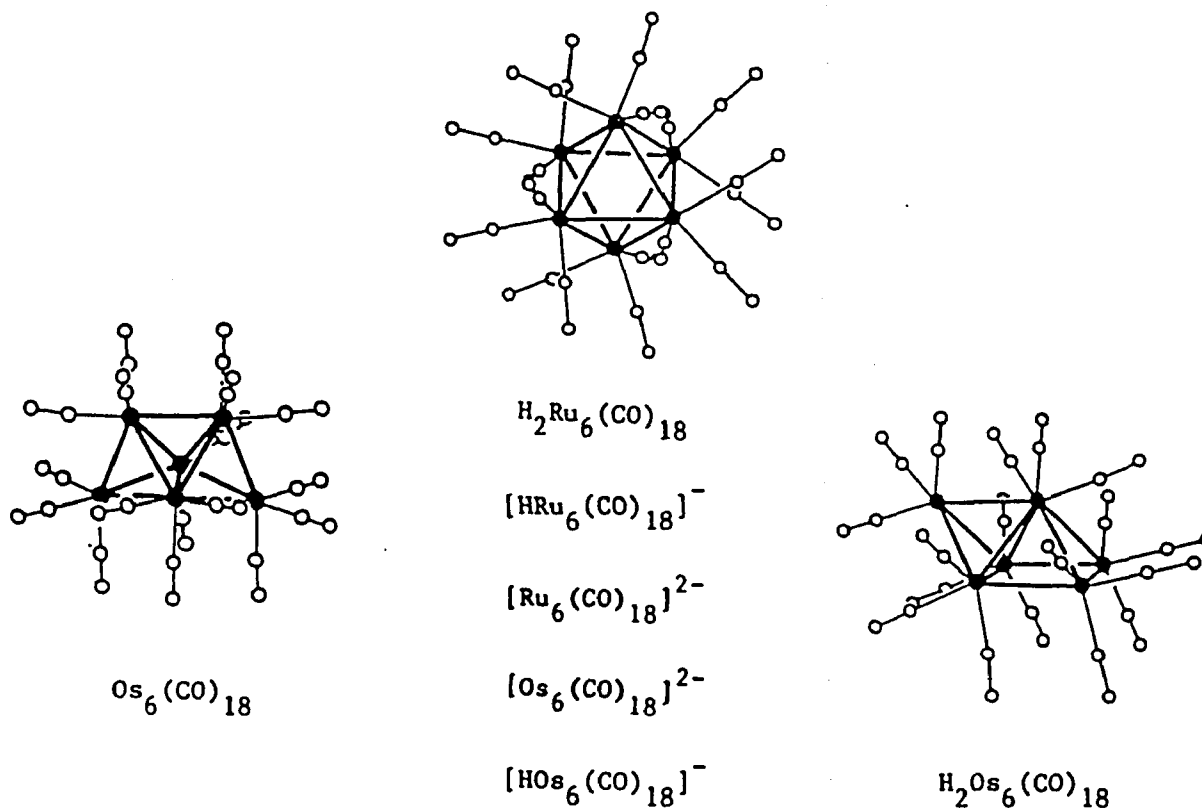


Figure 39. Structural Variations of the Ruthenium and Osmium Hexanuclear Clusters.

$[\text{Ru}_6(\text{CO})_{18}]^{2-}$  one arrives at the "magic number" of 86 electrons for a stable octahedral arrangement; however, for  $\text{H}_2\text{Ru}_6(\text{CO})_{17}$  only 84 electrons are present. This electron-deficiency determines the outcome of the framework geometry and one may predict a bicapped tetrahedron when the Capping Principle developed by Mingos [32a,123] is invoked. Surface science also recognizes this geometry as a logical progression to metal crystallite formation. [124,125] (Fig. 40)

The electron deficiency of the  $\text{H}_2\text{Ru}_6(\text{CO})_{17}$  cluster may also be described as being "localized" at the site of the Ru(5)-Ru(6) bond. This description is similar to arguments used with respect to the electron deficiency (44 electrons) and multiple bond character of  $\text{H}_2\text{Os}_3(\text{CO})_{10}$ . The possible importance of the unsaturation in  $\text{H}_2\text{Ru}_6(\text{CO})_{17}$  regarding reactivity is discussed in the following sections.

#### A. DEPROTONATION OF $\text{H}_2\text{Ru}_6(\text{CO})_{17}$

In an ongoing attempt to study cluster species on supports, it has become necessary to independently synthesize and fully characterize anionic cluster species, in order to elucidate events occurring on the support.

It has been shown by Lavigne and Kaesz [126] that PPNC1 is capable of deprotonating hydrido complexes selectively forming the monoanion under mild conditions. Deprotonation reactions using PPNC1 were employed in the attempt to generate the monoanion,  $[\text{HRu}_6(\text{CO})_{17}]^-$ .

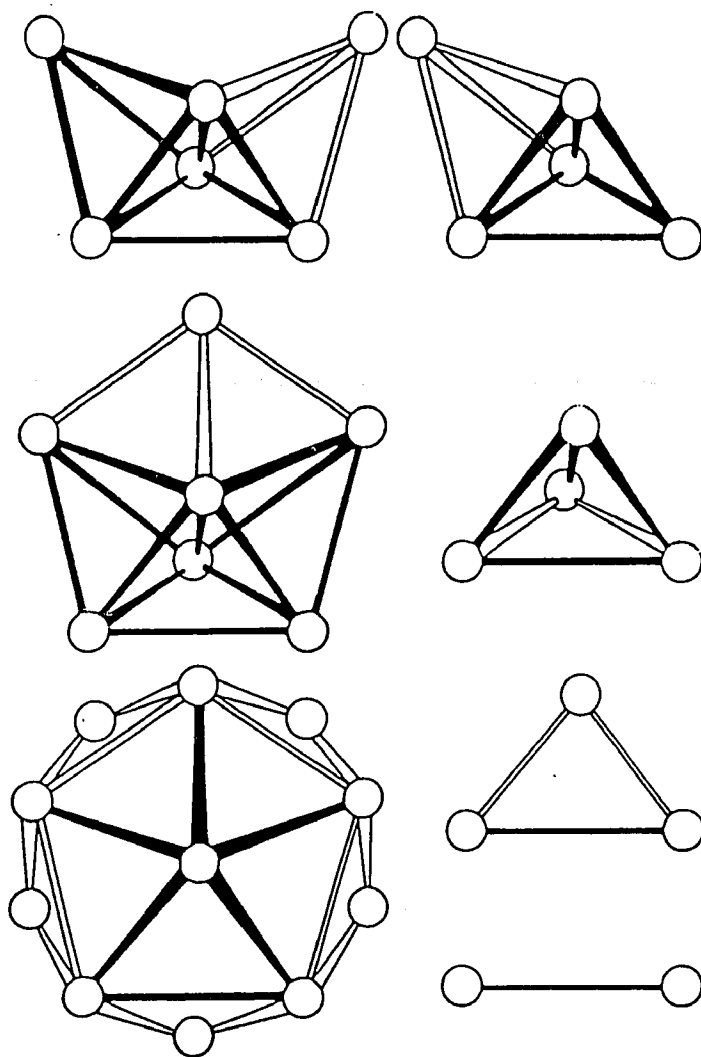
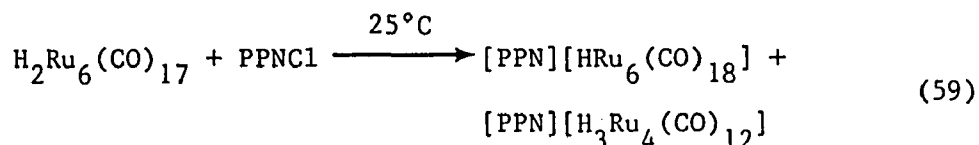


Figure 40. Metal Crystallite Growth.

This anion would be rather interesting in that it, too, is an 84 electron, unsaturated species. Unfortunately, this reaction does not proceed as planned; instead, formation of  $[\text{HRu}_6(\text{CO})_{18}]^-$  and  $[\text{H}_3\text{Ru}_4(\text{CO})_{12}]^-$  is observed. (Equation 59)



The formation of  $[\text{PPN}][\text{H}_3\text{Ru}_4(\text{CO})_{12}]$  is readily identified by  $^1\text{H}$  NMR ( $\delta$ -17.04 ppm) (Fig. 41) and  $^{13}\text{C}$  NMR ( $\delta$ 198.17 ppm) (Fig. 42) [68a]; the  $[\text{PPN}][\text{HRu}_6(\text{CO})_{18}]$ , on the other hand, is not. The saturated monoanion,  $[\text{HRu}_6(\text{CO})_{18}]^-$ , exhibits a singlet in the  $^{13}\text{C}$  NMR at  $\delta$ 202.01 ppm which indicates equivalent terminal carbonyls. (Fig. 42) The proton spectrum at first glance does not indicate any hydrides associated with this cluster. However, if the downfield region between  $\delta$ 20 to 10 ppm is magnified a resonance at  $\delta$ 16.4 ppm is detected. This signal does not always appear cleanly in the  $^1\text{H}$  NMR, most time severe magnification is necessary. A signal this deshielded suggests the presence of an interstitial hydride [127] which agrees well with that reported by Johnson and Lewis for this monoanion. [84-86]. However, one may doubt the existence of this peak due to its lack of intensity and haphazard appearance.

In order to determine the true nature of the monoanion, an X-ray analysis was performed. The molecular structure of this anion proved to be the same as reported by Johnson and Lewis [84,86] for one of the crystalline forms they observed. Figure 43 gives the molecular

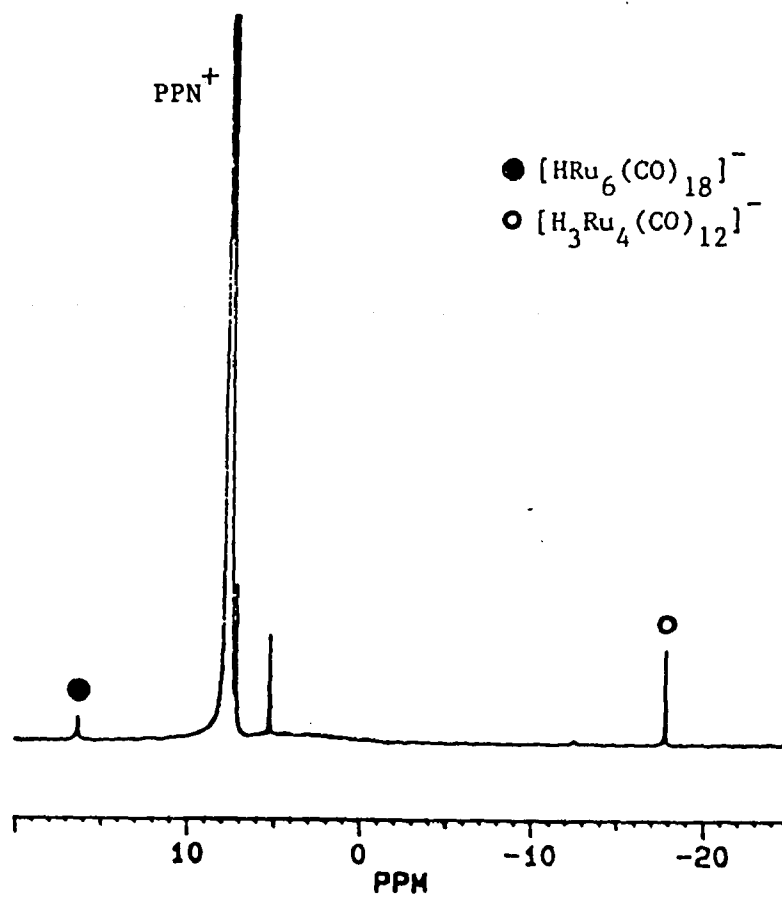


Figure 41. Proton NMR Spectrum of  $[\text{HRu}_6(\text{CO})_{18}]^-$  and  $[\text{H}_3\text{Ru}_4(\text{CO})_{12}]^-$ .

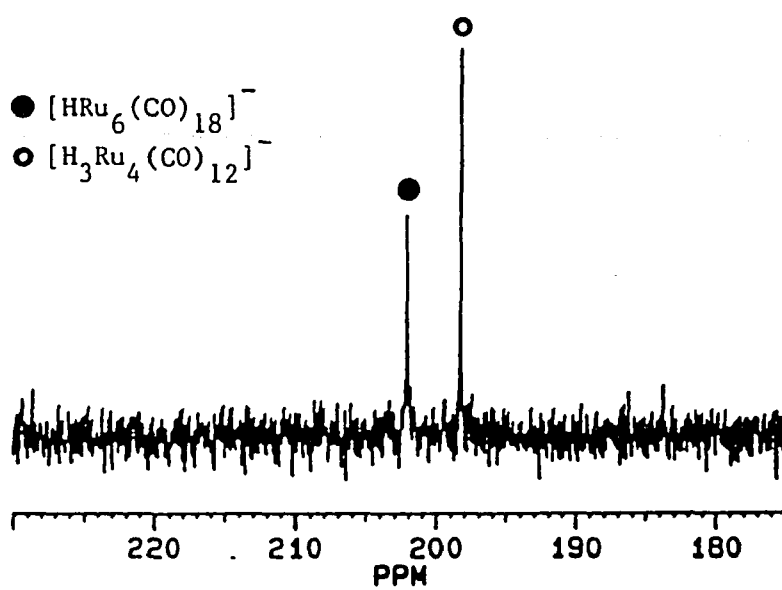


Figure 42. Carbon-13 NMR Spectrum of  $[\text{HRu}_6(\text{CO})_{18}]^-$  and  $[\text{H}_3\text{Ru}_4(\text{CO})_{12}]^-$ .

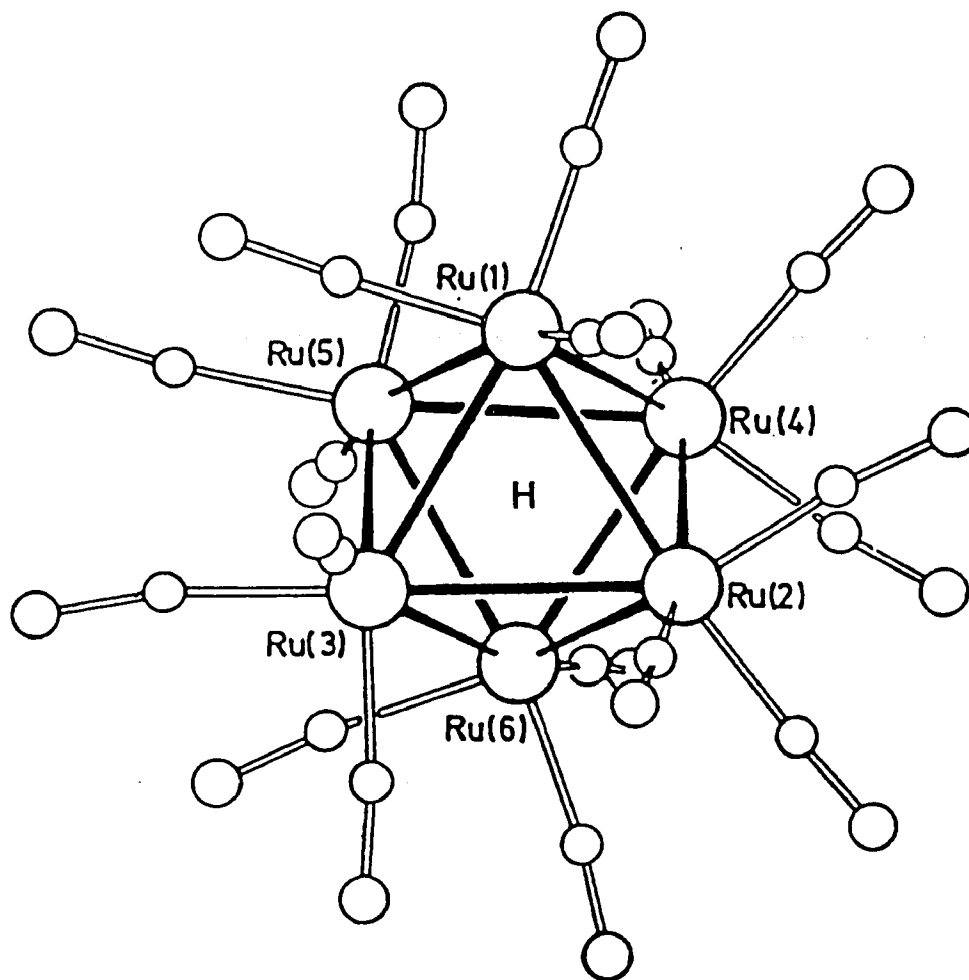
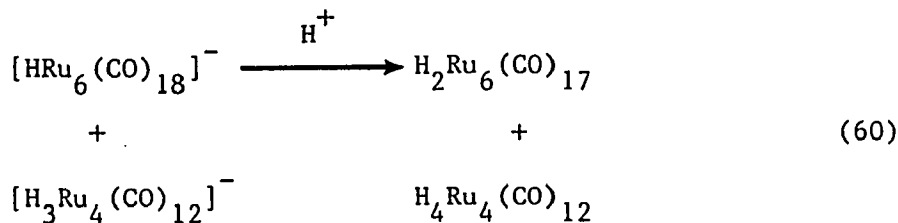


Figure 43. Molecular Structure of  $[\text{HRu}_6(\text{CO})_{18}]^-$ .

structure of  $[\text{PPN}][\text{HRu}_6(\text{CO})_{18}]$  as reported by Johnson and Lewis. Table 13 gives crystallographic data obtained in this study. Table 14 gives the crystallographic data obtained by Johnson and Lewis. (The particular details with respect to this data collection and structure solution are outlined in the Experimental Section.) As with the previous analysis, location of the interstitial hydride was not possible.

Once it became apparent that the product in this deprotonation was actually  $[\text{PPN}][\text{HRu}_6(\text{CO})_{18}]$ , the most logical concerns were: (1) Is CO being liberated in the reaction so that  $[\text{HRu}_6(\text{CO})_{18}]^-$  is being formed instead of the desired  $[\text{HRu}_6(\text{CO})_{17}]^-$ ? (2) Could the neutral unsaturated cluster be regenerated by protonation of the  $[\text{HRu}_6(\text{CO})_{18}]^-$  or would the product obtained by  $\text{H}_2\text{Ru}_6(\text{CO})_{18}$ ?

In a series of experiments it was shown that CO is indeed given off during the reaction as identified by gas mass spectra. It was also shown that  $\text{H}_2\text{Ru}_6(\text{CO})_{17}$  may be regenerated according to the reaction below; (Equation 60) however, yields of  $\text{H}_2\text{Ru}_6(\text{CO})_{17}$  are disappointingly low.



Note that this result is in disagreement with what Johnson and Lewis [84-86] claimed as outlined in Equation 35.

Table 13. Crystallographic Data for [PPN][HRu<sub>6</sub>(CO)<sub>18</sub>].

Chemical formula/Color of cryst	C <sub>54</sub> H <sub>33</sub> P <sub>2</sub> NRu <sub>6</sub> O <sub>18</sub> /orange-red
Molecular wt	1655.55
Space group	P $\bar{1}$
Molecules/unit cell	4
Temp, °C	-50
a, Å	18.004(4)
b, Å	19.002(3)
c, Å	19.170(3)
$\alpha$ , deg	62.39(1)
$\beta$ , deg	77.95(2)
$\gamma$ , deg	83.13(2)
Volume, unit cell Å <sup>3</sup>	5681.36
D(calcd), g cm <sup>-3</sup>	1.787
Absorptn coeff, cm <sup>-1</sup>	16.4
Max/Min transmissn, %	99.95/87.69
Scan mode	$\omega$ -2 $\theta$
Data collectn limits, deg	4-45
No. of unique reflctns	15398
No. of reflctns used in structure refinement ( $>3\sigma(I)$ )	9623

Table 14. Crystallographic Data for [PPN][HRu<sub>6</sub>(CO)<sub>18</sub>] as Reported by Johnson and Lewis.

Space group	P $\bar{1}$ <sup>a</sup>	P2 <sub>1</sub> /n <sup>b</sup>
Molecules/unit cell	4	12
a, Å	18.083(4)	33.82(8)
b, Å	19.101(4)	52.55(10)
c, Å	19.238(5)	9.832(2)
$\alpha$ , deg	117.70(4)	
$\beta$ , deg	78.13(2)	
$\gamma$ , deg	97.05(2)	
Volume, unit cell Å <sup>3</sup>	5767	17452
D(calcd), g cm <sup>-3</sup>	1.90	1.88
No. of reflctns used in structure refinement ( $>3\sigma(I)$ )	9165	
R <sub>f</sub>	0.068	0.23
Scan mode	$\theta$ -2 $\theta$	
Radiation	Mo K $\alpha$ (0.710730Å)	
Diffractionmeter	Philips PW1100	

<sup>a</sup> triclinic cell converted to C $\bar{1}$  cell in actual structure solution

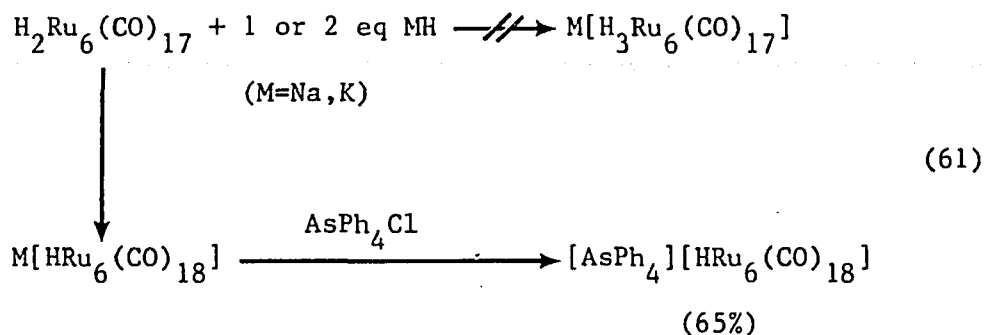
a=19.248(4)Å       $\alpha$ =91.23(2)°

b=33.912(8)Å       $\beta$ =101.86(3)°

c=18.081(4)Å       $\gamma$ =92.53(2)°

<sup>b</sup> only Ru atoms refined

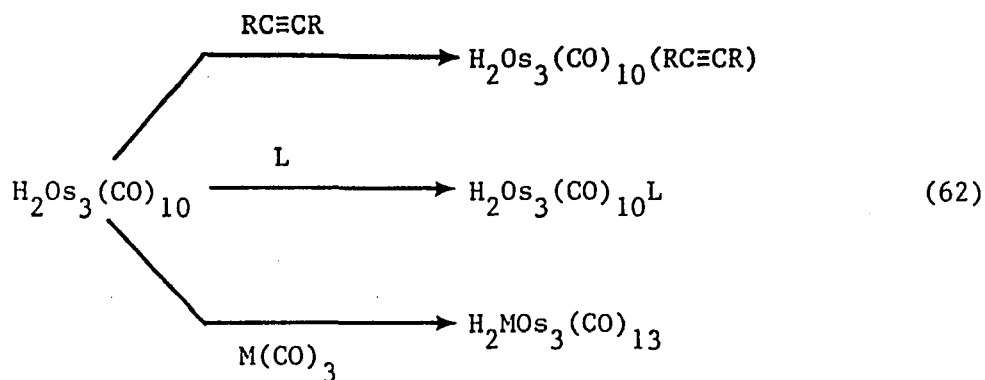
The analogy has been made between  $\text{H}_2\text{Os}_3(\text{CO})_{10}$  and  $\text{H}_2\text{Ru}_6(\text{CO})_{17}$  with respect to the unsaturation within the cluster framework. It has been shown by Kennedy [48] that reaction of  $\text{H}_2\text{Os}_3(\text{CO})_{10}$  with an alkali-metal hydride results in the saturated, 48 electron anionic cluster  $[\text{H}_3\text{Os}_3(\text{CO})_{10}]^-$ . Perhaps the  $\text{H}_2\text{Ru}_6(\text{CO})_{17}$  cluster in the presence of a hydride source; such as KH, would also display similar reactivity. (Equation 61)



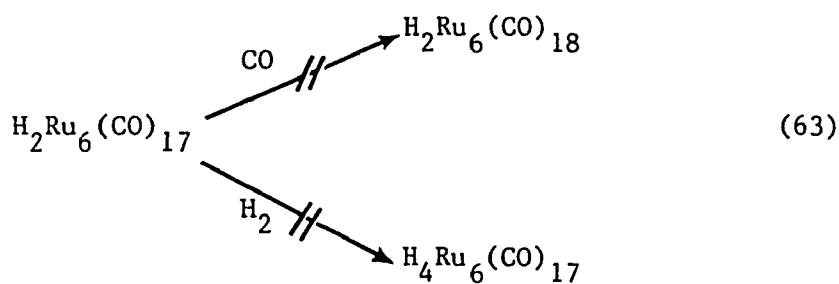
As is outlined above, formation of  $[\text{H}_3\text{Ru}_6(\text{CO})_{17}]^-$  is not realized, only the aforementioned  $[\text{HRu}_6(\text{CO})_{18}]^-$  species is isolable. It has been noted by Johnson and Lewis [84] and Shapley [67] that  $[\text{HRu}_6(\text{CO})_{18}]^-$  does not readily deprotonate even under strongly basic conditions.

## B. HYDROGENATION OR CARBONYLATION OF $\text{H}_2\text{Ru}_6(\text{CO})_{17}$

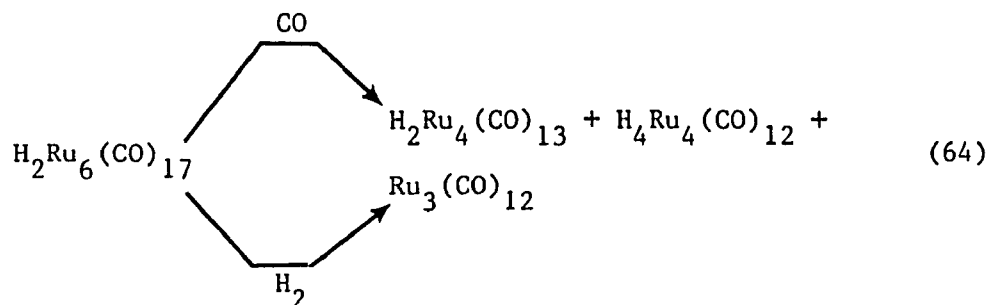
$\text{H}_2\text{Os}_3(\text{CO})_{10}$  readily undergoes addition reactions with two-electron donors; such as, CO,  $\text{PR}_3$ , isocyanides and halides. Unsaturated hydrocarbons and transition metal fragments are also incorporated into this highly reactive cluster [48-51,128] (Equation 62). Since  $\text{H}_2\text{Ru}_6(\text{CO})_{17}$  displays a site of unsaturation one would hope that similar reactions could be carried out.



The reaction of  $\text{H}_2\text{Ru}_6(\text{CO})_{17}$  with  $\text{H}_2$  or  $\text{CO}$  under various conditions does not lead to addition of the  $\text{H}_2$  or  $\text{CO}$  relieving the cluster of its unsaturation as shown in Equation 63.

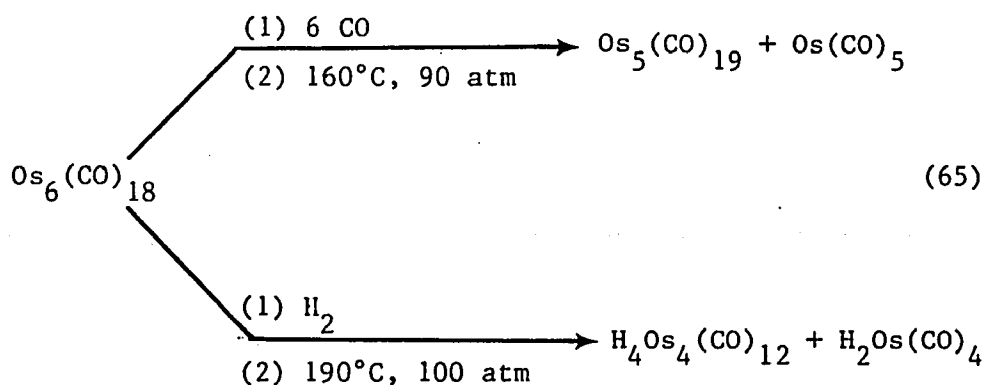


Instead, fragmentation of the cluster is observed. (Equation 64)\*



\* Reaction conditions ranging from 1 eq reactant gas to 1 atm reactant gas over the cluster solution or bubbling of gas through the cluster solution at temperatures ranging from  $-10^\circ\text{C}$  to  $40^\circ\text{C}$ .

This fragmentation pattern is similar to that displayed by  $\text{Os}_6(\text{CO})_{18}$  in the presence of strong bases; such as,  $\text{OH}^-$ ,  $\text{OMe}^-$  or  $\text{CN}^-$ . [129] Fragmentation of  $\text{Os}_6(\text{CO})_{18}$  is also obtained when reacted with CO or  $\text{H}_2$  under high pressures and temperatures. [130] (Equation 65)



The fragmentation of  $\text{H}_2\text{Ru}_6(\text{CO})_{17}$  may be envisioned as depicted in Figure 44 where one sees successive loss of " $\text{Ru}(\text{CO})_3$ " units. Loss of the first  $\text{Ru}(\text{CO})_3$  capping unit results in generation of a reactive, unstable  $\text{Ru}_5$  species which is not detectable by  $^1\text{H}$  NMR. Loss of a second  $\text{Ru}(\text{CO})_3$  unit generates the stable  $\text{Ru}_4$  species. It should be noted that in the hydrogenation reaction the major cluster isolated is  $\text{H}_4\text{Ru}_4(\text{CO})_{12}$ . If the carbonylation reaction is carried out,  $\text{H}_2\text{Ru}_4(\text{CO})_{13}$  constitutes the major yield.  $\text{Ru}_3(\text{CO})_{12}$  may be generated from combination of the reactive " $\text{Ru}(\text{CO})_3$ " fragments.

### C. HYDROBORATION OF $\text{H}_2\text{Ru}_6(\text{CO})_{17}$

Hydroboration of unsaturated organic compounds is a useful reductive method and has been extensively studied by Brown and co-workers. [131] The concept of hydroboration has been extended to

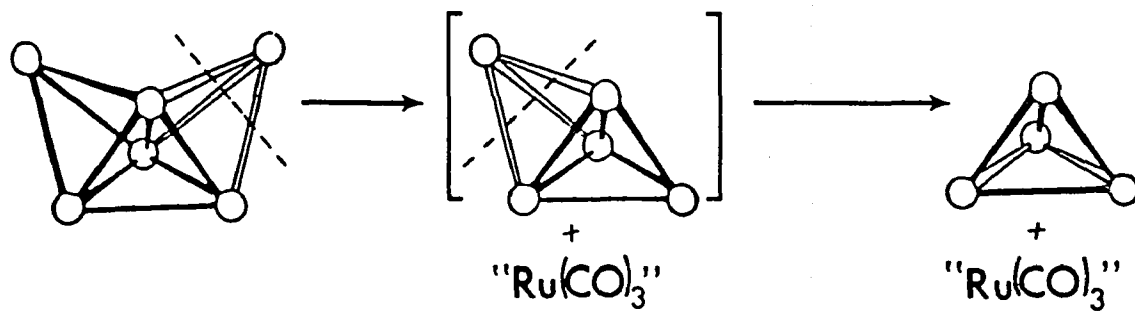
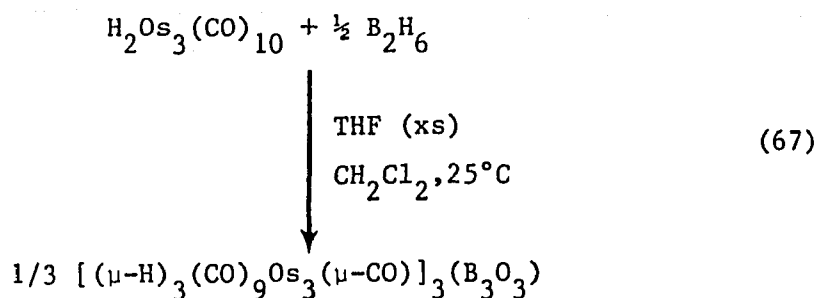
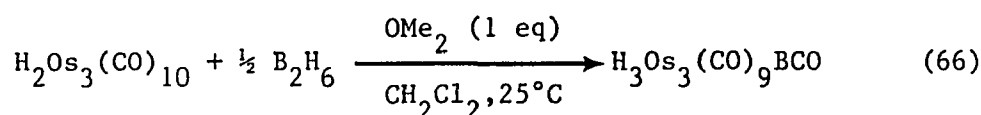


Figure 44. Proposed Fragmentation Pattern  
for  $(\mu_3\text{-H})_2\text{Ru}_6(\mu\text{-CO})(\text{CO})_{16}$ .

unsaturated transition metal complexes, namely  $\text{H}_2\text{Os}_3(\text{CO})_{10}$ , by Shore and co-workers. [48,49,50h,50i] They were able to show that reactions conducted under different conditions can lead to two very unique cluster systems: a triosmium borylidyne carbonyl (Equation 66) (Fig. 45) and a boroxine-supported oxymethylidyne carbonyl. (Equation 67) (Fig. 46)



The intent here was to generate a hexanuclear analog of the  $\text{H}_3\text{Os}_3(\text{CO})_9\text{BCO}$  cluster.  $\text{H}_2\text{Ru}_6(\text{CO})_{17}$  was reacted with 1/2 equivalent  $\text{B}_2\text{H}_6$  and 1 equivalent  $\text{Me}_2\text{O}$  in  $\text{CH}_2\text{Cl}_2$  in a manner similar to that shown in Equation 66 for  $\text{H}_2\text{Os}_3(\text{CO})_{10}$ .  $^{11}\text{B}$  NMR indicates formation of  $\text{B}_2\text{O}_3$  ( $\delta 21.54(\text{s})$  ppm in  $d_8$ -acetone). The proton NMR shows formation of  $\text{H}_4\text{Ru}_4(\text{CO})_{12}$  ( $\delta -17.74$  ppm in  $\text{CD}_2\text{Cl}_2$ ) along with hydride signals between  $\delta -18.0$  to  $-18.5$  ppm. However, upon purification by TLC the only isolable product proved to be  $\text{H}_4\text{Ru}_4(\text{CO})_{12}$ .

#### D. REACTIVITY OF $\text{H}_2\text{Ru}_6(\text{CO})_{17}$ WITH OXONIUM SALTS

The lack of reactivity of  $\text{H}_2\text{Ru}_6(\text{CO})_{17}$  could be caused by the presence of the bridging carbonyl spanning the doubly bonded

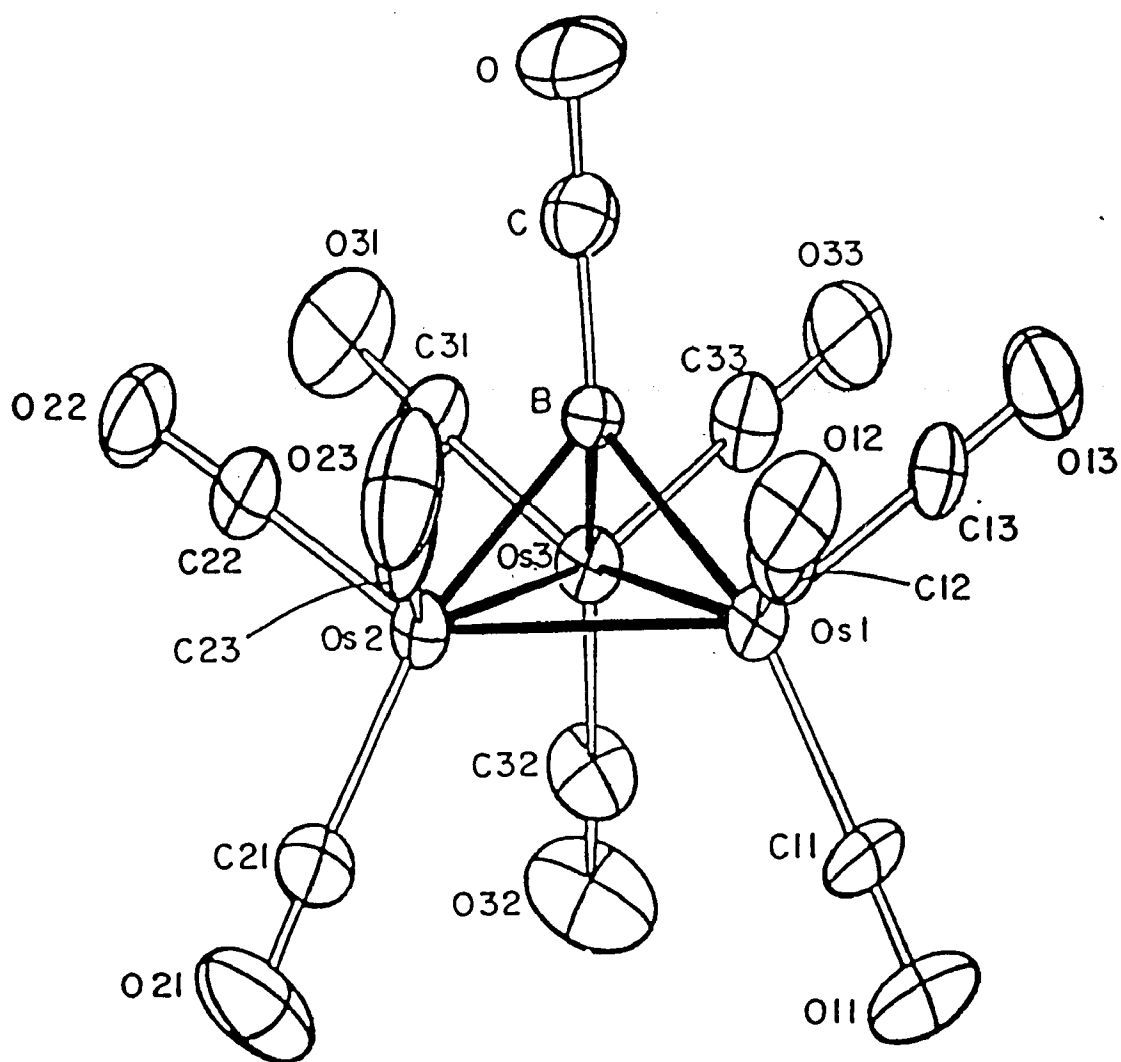


Figure 45. ORTEP of  $\text{H}_3\text{Os}_3(\text{CO})_9\text{BCO}$ .

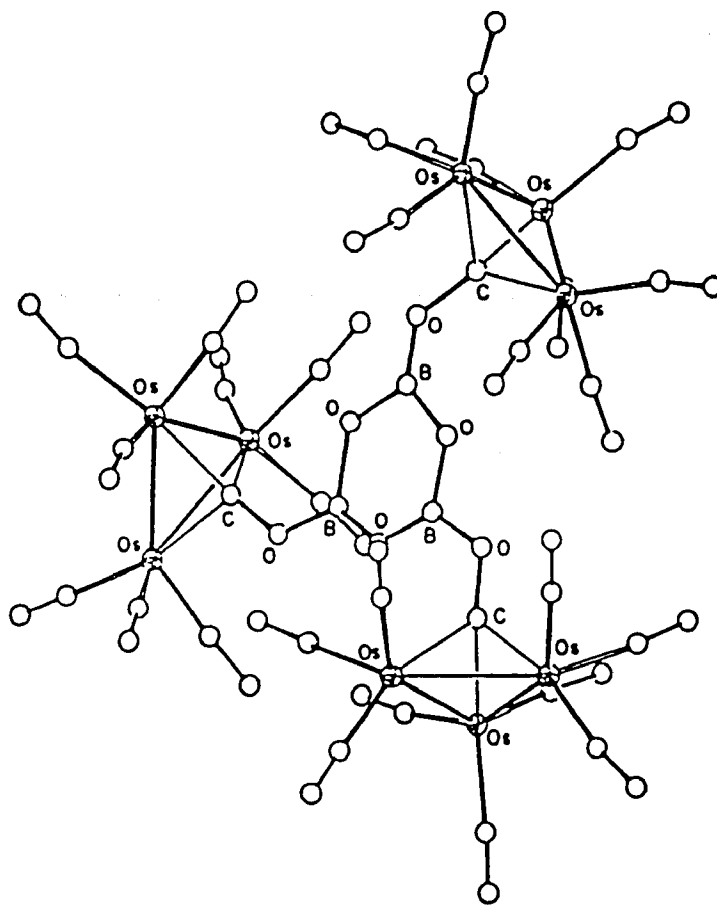


Figure 46. Molecular Structure of  
 $[\text{H}_3(\text{CO})_9\text{Os}_3(\mu_3\text{-CO})]_3(\text{B}_3\text{O}_3)$ .

Ru(5)-Ru(6) bond. Perhaps reactivity of this cluster could be induced through the bridging carbonyl unit. If the bond order of the bridging carbonyl is reduced that site should then be more susceptible to attack. This type of reactivity is observed for the trimetallic systems  $[\text{HM}_3(\mu\text{-CO})(\text{CO})_{10}]^-$  (M=Ru,Os). [132-136]

However if  $\text{H}_2\text{Ru}_6(\text{CO})_{17}$  is reacted with either  $\text{Me}_3\text{OBF}_4$  or  $\text{Et}_3\text{OPF}_6$  no signal due to a  $\mu\text{-COMe}$  moiety could be detected by proton NMR. In the case of  $\text{Me}_3\text{OBF}_4$  one observes a signal at  $\delta 12.22$  ppm which may be the result of an interstitial hydride. Using  $\text{Et}_3\text{OPF}_6$  a signal at  $\delta 8.83$  ppm grows in which may be due to an interstitial hydride rearrangement but is more likely due to  $\mu_3\text{-CH}$  formation. In either case the region between  $\delta 0$  to  $-35$  ppm is void of any hydride signals. Further purification to isolate these species was futile. Other products obtained in low yields were  $\text{H}_2\text{Ru}_4(\text{CO})_{13}$  and  $\text{H}_4\text{Ru}_4(\text{CO})_{12}$ , most of the product mixture consisted of unreacted  $\text{H}_2\text{Ru}_6(\text{CO})_{17}$ .

## CONCLUDING REMARKS

The primary goal of this investigation was to develop systematic syntheses of mixed-metal clusters using the redox condensation method. Using this method, the higher nuclearity clusters  $\text{H}_2\text{Os}_5(\text{CO})_{16}$ ,  $\text{H}_2\text{Fe}_2\text{Os}_3(\text{CO})_{16}$  and  $\text{H}_2\text{Ru}_2\text{Os}_3(\text{CO})_{16}$  were generated. Tetranuclear clusters,  $\text{H}_2\text{Fe}_2\text{Ru}_2(\text{CO})_{13}$ ,  $\text{H}_2\text{FeRu}_3(\text{CO})_{13}$ ,  $\text{H}_2\text{FeOs}_3(\text{CO})_{13}$  and  $\text{H}_2\text{RuOs}_3(\text{CO})_{13}$  were also observed.

In the course of this investigation the novel, unsaturated, hexanuclear cluster,  $(\mu_3\text{-H})_2\text{Ru}_6(\mu\text{-CO})(\text{CO})_{16}$ , was synthesized and structurally characterized. Reactivity studies of  $(\mu_3\text{-H})_2\text{Ru}_6(\mu\text{-CO})(\text{CO})_{16}$  with small molecules showed that there is little tendency to oxidatively add two-electron donors. Fragmentation of the metallic core to give tetranuclear clusters was observed.

Additionally, the structure of  $\text{H}_2\text{RuOs}_3(\text{CO})_{13}$  was re-determined. It exists in the monoclinic crystal system when pure and in the triclinic system when co-crystallized with  $\text{H}_2\text{Os}_4(\text{CO})_{13}$ . Also,  $[\text{PPh}_4]_2[\text{Ru}_6(\text{CO})_{18}]$  and  $[\text{PPN}][\text{HRu}_6(\text{CO})_{18}]$  were structurally characterized.

## EXPERIMENTAL

### I. APPARATUS

#### A. VACUUM SYSTEM

A Pyrex glass high-vacuum system similar to that described by Shriver [137] was used for manipulation of volatile compounds. The vacuum line consists of two reaction manifolds, McLeod gauge, and distillation train. The entire system was evacuated to a pressure of  $10^{-5}$  torr by a two-stage mercury diffusion pump and a Welch Duo-Seal high-speed mechanical pump, which were protected by traps cooled to  $-196^{\circ}\text{C}$  (liquid nitrogen) and  $-78^{\circ}\text{C}$  (dry ice/isopropanol), respectively.

One reaction manifold contains five inlets consisting of two Fischer-Porter 9-mm Solv-Seal joints and three 14/35 standard taper joints, equipped with Fischer-Porter Teflon stopcocks. The other manifold consists of five 14/35 standard taper joints equipped with Fischer-Porter Teflon stopcocks. Mercury blowouts were attached to each of the inlets and were used for monitoring reaction pressures.

The distillation train consists of four U-traps with 4-mm bore ground glass stopcocks, an isolated mercury manometer, a 14/35 standard taper joint inlet, and a 9/18 ball joint inlet.

## B. GLOVE BOX

Manipulation of non-volatile air-sensitive compounds was conducted in a Vacuum Atmospheres glove box. A nitrogen atmosphere (Matheson) in the range of 10 ppm oxygen was maintained by continual circulation of pre-purified nitrogen through a purification tower which contains Ridox oxygen scavenger (Fischer Scientific Co.) and Linde 13-X molecular sieves. The nitrogen atmosphere was monitored by mass spectral analysis, the titanocene test and also by exposing a freshly-cut piece of potassium. Design and operation of the glove box has been described previously. [138]

## C. GLASSWARE

Pyrex and Kimax round-bottom flasks with 9-mm or 15-mm Fischer-Porter Solv-Seal joints were utilized. These vessels were connected to the vacuum line by glass adaptors with Teflon stopcocks. Sidearm flasks and tiptubes were used for addition of various non-volatile reactants to the reaction mixture and also for removal of samples for NMR. A typical reaction apparatus for an NMR study is illustrated in Figure 47. Filtrations were carried out using vacuum extractors as shown in Figure 48.

## D. FILTRATION APPARATUS

For filtrations requiring removal of very fine particulate matter from solution (ie. HPLC) the filtration apparatus shown in Figure 49 was employed. It consisted of a Teflon PFA inline filter purchased

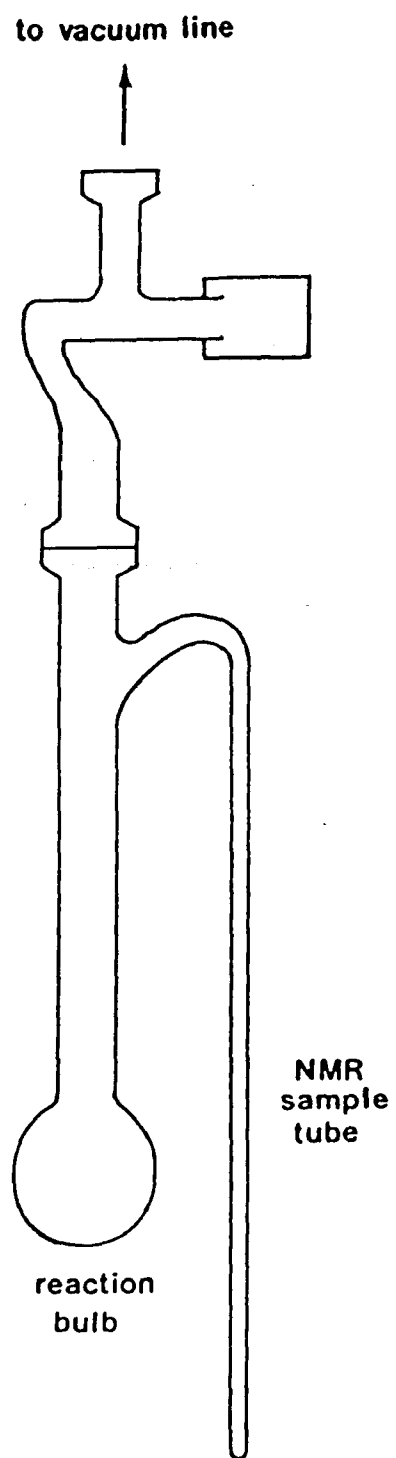


Figure 47. Reaction Apparatus for NMR Study.

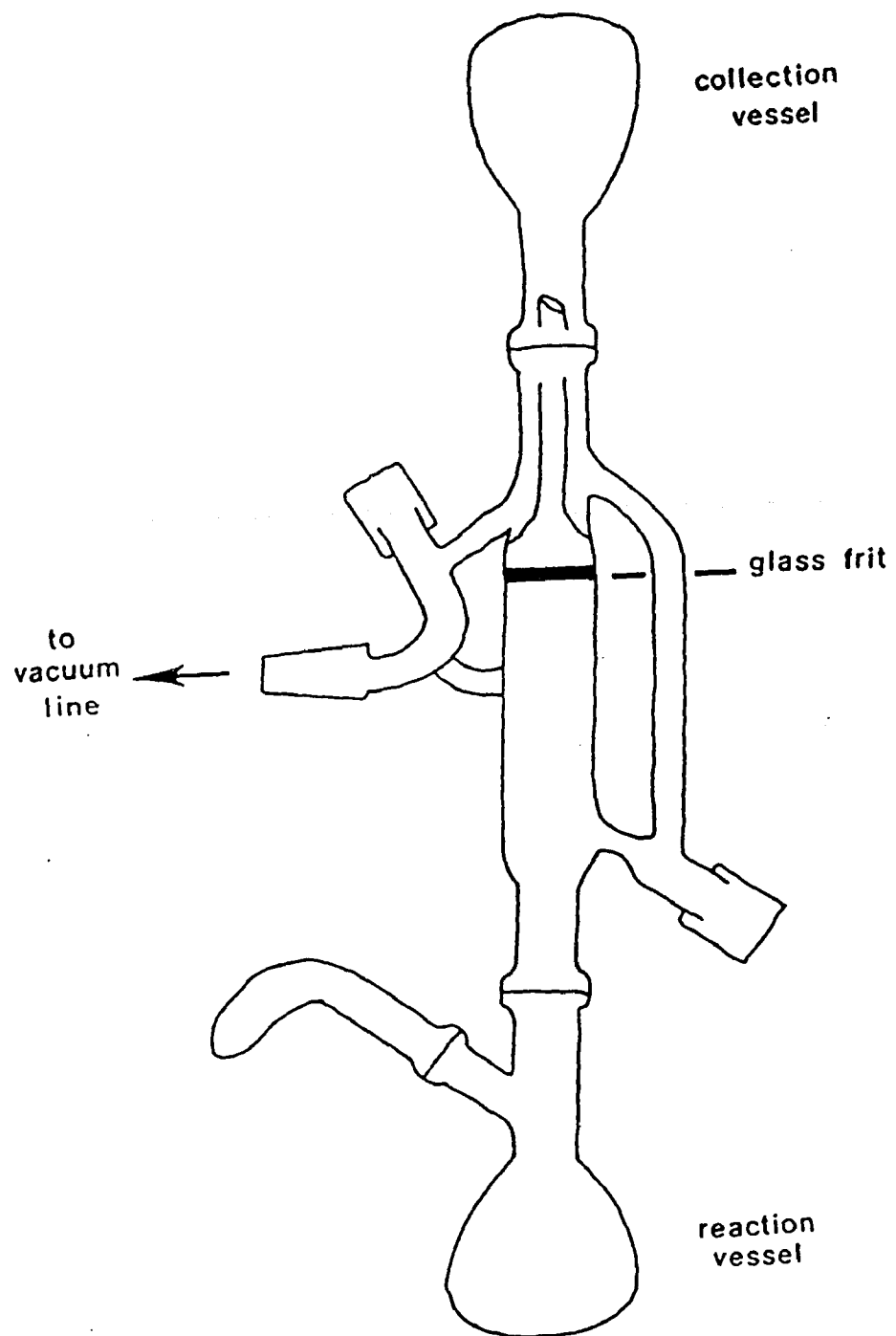


Figure 48. Vacuum Extractor.

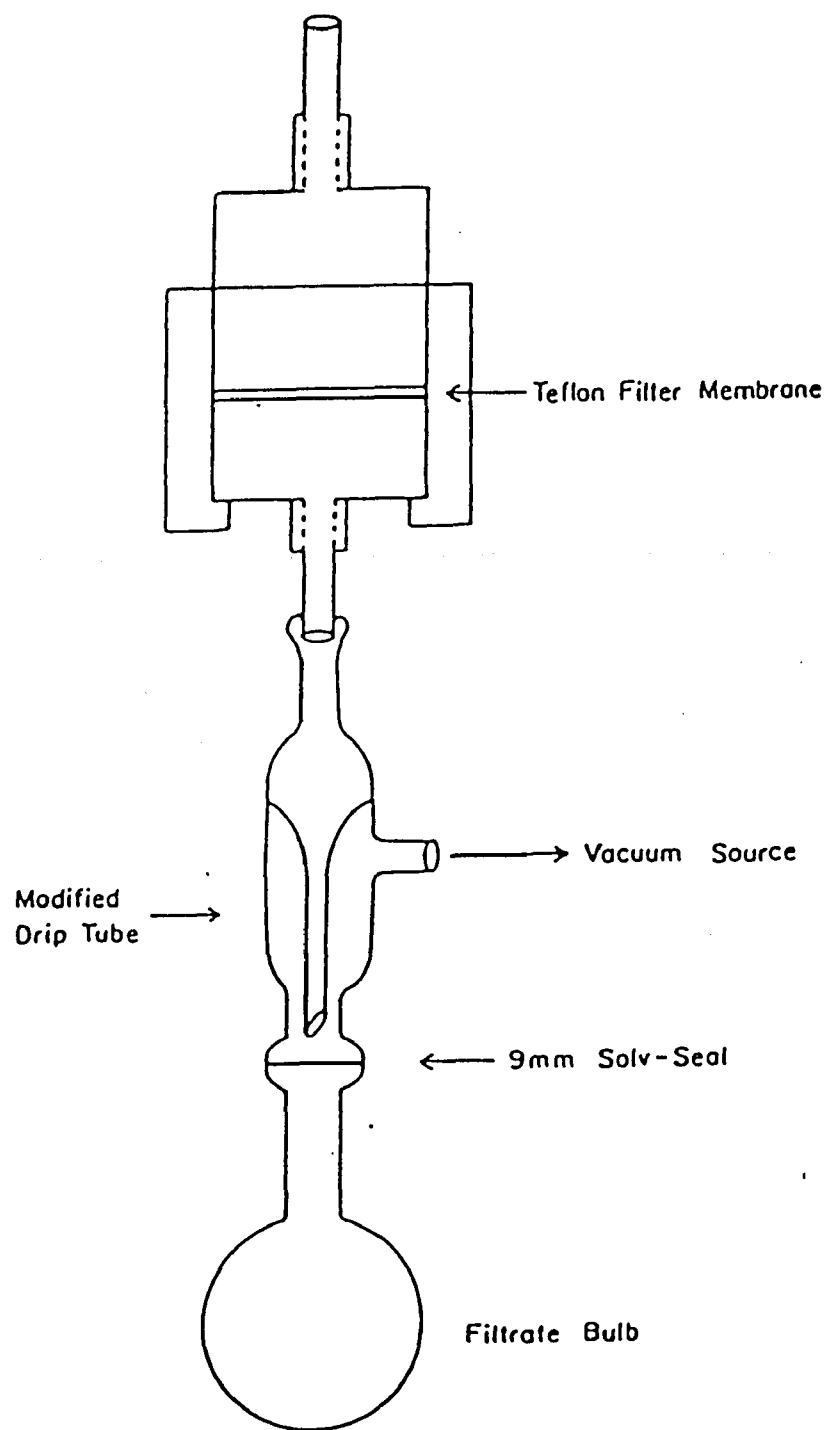


Figure 49. Filtration Apparatus.

from Cole-Parmer International with certain modifications. Design of this apparatus has been described previously. [139]

#### E. NUCLEAR MAGNETIC RESONANCE SPECTRA

Nuclear Magnetic Resonance spectra were obtained on Bruker AM-500, Bruker WH-300, Bruker MSL-300, Bruker AM-250 and Bruker WP-200 spectrometers operating in the FT mode. The spectrometers were equipped with variable temperature and heteronuclear decoupling capabilities. The operating frequency, MHz, of each spectrometer is listed below:

<u>SPECTROMETER</u>	<u><math>^1\text{H}</math></u>	<u><math>^{11}\text{B}</math></u>	<u><math>^{13}\text{C}</math></u>
Bruker AM-500	500.14		125.75
Bruker WH-300	300.13	96.27	75.48
Bruker MSL-300		96.30	
Bruker AM250	250.13	80.25	62.90
Bruker WP-200	200.13		

Proton and carbon-13 shifts are reported in  $\delta$  units referenced to tetramethylsilane (TMS) at 0.00 ppm. Boron-11 chemical shifts are relative to  $\text{Et}_2\text{O}/\text{BF}_3$  at 0.00 ppm.

#### F. INFRARED SPECTRA

Infrared spectra were obtained with a Matteson Cygnus-25 FT spectrometer. Solution spectra were obtained in matched Perkin-Elmer liquid cells with 0.1- or 0.5-mm Teflon spacers and KBr or NaCl windows.

## G. THIN-LAYER CHROMATOGRAPHY (TLC)

The plates used were made by first mixing silica gel,  $\text{CaSO}_4$ , and  $\text{H}_2\text{O}$  in a 30:8:80 ratio by weight. The paste was then deposited on 20 x 20 cm glass plates forming a homogenous layer of 2-mm thickness. The plates were then stored in a closed space for a week to control the drying process. The plates were activated by heating in an oven at 90-100°C for 7 hours before use.

## H. HIGH PRESSURE LIQUID CHROMATOGRAPHY (HPLC)

A Perkin-Elmer high pressure liquid chromatograph equipped with an analytical column (PEO 258-0051) was used to analyze neutral cluster complexes for qualitative analysis. A preparative silica column (PEO 258-5002) was also used for preparative scale separations. Heptane and methylene chloride were used to elute samples. Chromatograms were plotted on a Linear plotter as a variation of absorbance at 255 nm UV radiation produced by a deuterium lamp.

## I. SINGLE CRYSTAL X-RAY DIFFRACTION

### 1. Hardware

All data was collected using the Enraf-Nonius Delft CAD4 Kappa Axis Diffractometer system. (Fig. 50) This system consists of the Diffractis 586 Generator and CAD4 Kappa Geometry Goniostat equipped with a microscope (75x magnification) attached to the Omega base with a standard crystal-to-detector distance of 173 mm.

The power to the X-ray tube was supplied by a 3 kW constant potential X-ray generator and the X-ray source consisted of a Mo



target emitting graphite-monochromated Mo K $\alpha$  radiation at  $\lambda=0.710730 \text{ \AA}$ . The X-ray tube was operated at 20 mA and 45 kV.

The crystals were cooled in a continuous stream of air using an FTS Systems refrigeration unit. Collected data was processed on a Digital PDP 11/44 minicomputer interfaced to the diffractometer. The operations of the diffractometer were controlled by input from a LA 34 lineprinter which has a speed of 30 characters/second. The movements of the kappa goniostat can also be controlled manually using a pocket terminal. The steps up to the data collection were carried out using the pocket terminal and the LA 34 lineprinter. The PDP 11/44 computer is also interfaced to a LA 120 lineprinter with a speed of 180 characters/second, a VT100 video terminal, and a VT330 graphics terminal. The data reduction, structure solution and refinement were carried out on these peripherals using the Structure Determination Package (SDP). [140]

Molecular structure orientations using the program ORTEP [141] or PLUTO [140] were monitored on an ESPRIT EXECUTIVE 10/102 graphics terminal or the VT330 graphics terminal. The final ORTEP plots were drawn on a TEKTRONIX 4662 Interactive Digital plotter or an Evans & Sutherland PS300 graphics terminal using the computer program PSORTEP. [142]

## 2. Software

The programs discussed below are part of the CAD4 data collection package [143] and SDP (Structure Determination Package) [140] written for use with this system.

The automated SEARCH program is used to scan the crystal's reciprocal space to find and center observable reflections. This program is then followed by SETANG which actually centers the reflections previously located in the SEARCH program, since now the angle settings of  $\phi$ ,  $2\theta$ ,  $\omega$  and  $\kappa$  are known, approximately.

After several reflections (usually 25) have been centered, an initial orientation matrix is calculated and the unit cell dimensions are determined. Optimized angular values from the initial orientation matrix are subsequently used in a least squares refinement program, LS, to ensure the crystal's proper orientation and a final orientation matrix is generated and used in the computation of the positions of the reflections during the data collection.

Using information from the final orientation matrix and unit cell dimensions, the crystal's reflections are classified as belonging to one of the seven crystal systems. Hence, knowing the crystal system influences the amount of data collected. (Table 15)

The data collection method utilized in the intensity data acquisition is normally the  $\omega$ - $2\theta$  scan mode, where both the crystal and detector are in motion. Parameters pertaining to this collection mode such as, maximum and minimum  $2\theta$ , scan width, scan rate and the time for background intensity measurements are specified in DATCIN, depending on the size and shape of the diffraction peaks based on a few trial scans. The stability of the crystal and diffractometer

Table 15. Classification of the Seven Crystal Systems.

<u>CRYSTAL SYSTEM</u>	<u>PARAMETERS</u>
Triclinic	$a \neq b \neq c; \alpha \neq \beta \neq \gamma$
Monoclinic	$a \neq b \neq c; \alpha = \gamma = 90^\circ; \beta \neq 90^\circ$
Orthorhombic	$a \neq b \neq c; \alpha = \beta = \gamma = 90^\circ$
Tetragonal	$a = b \neq c; \alpha = \beta = \gamma = 90^\circ$
Rhombohedral	$a = b = c; \alpha = \beta = \gamma \neq 90^\circ$
Hexagonal	$a = b \neq c; \alpha = \beta = 90^\circ; \gamma = 120^\circ$
Cubic	$a = b = c; \alpha = \beta = \gamma = 90^\circ$

electronics are also monitored in this scan mode by measuring the intensities of several standard reflections after every batch of 500 reflections.

The Structure Determination Package (SDP) processes the X-ray data and applies appropriate polarization and absorption corrections, solves and refines the structure and produces the tables and drawings for publication. Described below is a brief account of the program sequence used in data reduction and structure solution.

The programs GENESIS and BEGIN initialize the data reduction sequence by creating the STRUC.NME file. This file is a general parameter file in which all preliminary information pertaining to the crystal and data collection are stored.

The data, at this point, may be corrected for intensity decay using the program DECAY. A numerical or graphical display of the crystal's decay pattern as indicated by the intensity of the standard reflections may be calculated using the program STDPLT.

The program PSI is the initial step of the empirical absorption correction routine using  $\Psi$  scan data taken from the PSI.DAT file. Program EAC actually applies the empirical absorption correction to the reflection data using the crystal's orientation matrix and the psi data from program PSI.

Space group requirements must also be taken into consideration when applying corrections to the data. First, reflections which are considered to be unobserved or systematically absent are removed *via* the program REJECT. Table 16 lists absent reflection requirements of

Table 16. Systematic Absences Caused by Translational Symmetry in the Crystal System.

<u>SYMMETRY ELEMENT</u>	<u>AFFECTED REFLECTION</u>	<u>CONDITION FOR ABSENCE</u>
2-fold screw ( $2_1$ )	h00 0k0 00l	$h = 2n + 1 = \text{odd}$ $k = 2n + 1$ $l = 2n + 1$
Glide plane $\perp$ a	0kl	
b glide		$k = 2n + 1$
c glide		$l = 2n + 1$
n glide		$k + l = 2n + 1$
d glide		$k + l = 4n + 1, 2, \text{ or } 3$
Glide plane $\perp$ b	h0l	
a glide		$h = 2n + 1$
c glide		$l = 2n + 1$
n glide		$h + l = 2n + 1$
d glide		$h + l = 4n + 1, 2, \text{ or } 3$
Glide plane $\perp$ c	hk0	
a glide		$h = 2n + 1$
b glide		$k = 2n + 1$
n glide		$h + k = 2n + 1$
d glide		$h + k = 4n + 1, 2, \text{ or } 3$
A-centered (A)	hkl	$k + l = 2n + 1$
B-centered (B)		$h + l = 2n + 1$
C-centered (C)		$h + k = 2n + 1$
F-centered (F)		$h + k = 2n + 1$ } not all $h + l = 2n + 1$ } even or $k + l = 2n + 1$ } odd
Body-centered (I)		$h + k + l = 2n + 1$

of the 230 crystallographic space groups. [144] Secondly, the data is averaged in PAINT to remove equivalent reflections due to the Friedel pair relationship,  $F_{hkl} = F_{-h-k-l}$ .

Having the reduced structure factor data, the phase angles must be calculated by one of several methods. The direct methods program MULTAN is most often used. In the subsequent programs EXFFT and DMS, simple stereochemical restraints concerning bond lengths and bond angles are applied to produce a "sensible" structure. In the case where direct methods failed to give a true solution, a Patterson map, PATTERSON, could be used to attempt to solve the structure.

The Structure Determination Package (SDP) has a rather flexible set of programs to analyze the geometry of the peaks obtained from either MULTAN or PATTERSON. The most widely used SEARCH program uses the electron density peaks to produce a line-printer plot of the molecular units as well as giving a complete listing of bond distances and angles. The program DMS may also be used for this purpose but is most often restricted to bond distances of up to 2.0Å.

The ATOMS program is the main utility for modifying atomic parameters obtained. It is used for adding/deleting, sorting, renaming etc. of the atoms or electron density peaks. It is also used to modify thermal parameter options in the subsequent least squares refinement, LSFM.

Finally, ESD and the set of programs PTA, BTA, and FTA complete

the structure solution by calculating the bond distances and angles (with standard deviations) to produce the final tables for publication.

## J. MASS SPECTRA

Mass spectra (CI, FAB) were obtained at the OSU Chemical Instrument Center by using a VG 70-250S mass spectrometer. FT-ICR (Fourier Transform Ion Cyclotron Resonance) mass spectra were obtained on a Nicolet FT-MS-1000 spectrometer equipped with a 1-inch cubic cell and a 3.022 Tesla coil. Mass spectra of all gas samples were run on either a modified AEI MS-10 spectrometer or a Balzers QME 112 Quadrupole mass spectrometer with a Faraday cup detector.

## II. REAGENTS

### A. ACETYL CHLORIDE

Acetyl chloride was obtained from Mallinckrodt. Purification of the acetyl chloride involved refluxing it over  $\text{PCl}_5$  for several hours and then distilling it. It was then re-distilled from quinoline and subsequently fractionated in a series of traps at  $-31^\circ\text{C}$ ,  $-78^\circ\text{C}$ , and  $-196^\circ\text{C}$ . The acetyl chloride was collected in the  $-78^\circ\text{C}$  trap.

### B. AMMONIA

Ammonia was obtained from Matheson Scientific Products. It was purified by condensation onto metallic Na followed by stirring for several hours. Purified ammonia was transferred into a thick-walled Pyrex tube equipped with a 4-mm Kontes stopcock and stored at  $-78^\circ\text{C}$ .

### C. BENZOPHENONE

Benzophenone was purchased from Fischer Scientific Co. and used as received.

### D. BIS(TRIPHENYLPHOSPHORANYLIDENE)AMMONIUM CHLORIDE

Bis(triphenylphosphoranylidene)ammonium chloride was obtained from Aldrich Chemical Co. It was dried at 110°C overnight and stored in a glove box prior to use.

### E. CARBON DIOXIDE

Carbon dioxide was obtained from Matheson Scientific Products. It was purified by fractionation through successive U-traps at -78°C, -111°C, and -126°C and stored in a thick-walled Pyrex tube equipped with a 4-mm Kontes stopcock at -78°C.

### F. CARBON MONOXIDE

Carbon monoxide, 99.9%, was obtained from Matheson Gas Products and used as received.

### G. CARBON MONOXIDE (99% <sup>13</sup>C ENRICHED)

Carbon monoxide, 99% <sup>13</sup>C enriched, was purchased from Monsanto (Mound Laboratory, OH) and used as received.

### H. DIBORANE

Diborane was kindly donated by Dr. Joseph Wermer, Mr. Timothy Coffy and Mr. David Workman.

### I. DIIRON NONACARBONYL

Diiron nonacarbonyl was purchased from Aldrich Chemical Co. and used as received.

### J. DIMETHYL ETHER

Dimethyl ether was kindly donated by Dr. Thomas Getman and Mr. Philipp Niedenzu.

### K. ETHYLENE

Ethylene was obtained from Matheson Scientific Products and used as received.

### L. HYDROGEN

Hydrogen (pre-purified) was obtained from Union Carbide Corp. Linde Division and used as received.

### M. HYDROGEN BROMIDE

Hydrogen bromide was obtained from Matheson Scientific Products. It was purified by fractionation through a  $-140^{\circ}\text{C}$  trap and stored in a thick-walled Pyrex tube equipped with a Kontes stopcock at  $-78^{\circ}\text{C}$ .

### N. HYDROGEN CHLORIDE

Hydrogen chloride was obtained from Matheson Scientific Products. It was purified by fractionation through a series of traps at  $-78^{\circ}\text{C}$ ,  $-111^{\circ}\text{C}$ , and  $-126^{\circ}\text{C}$  and stored in a thick-walled Pyrex tube equipped with a Kontes stopcock at  $-78^{\circ}\text{C}$ .

## O. IRON PENTACARBONYL

Iron pentacarbonyl was purchased from Aldrich Chemical Co. It was vacuum distilled into a lightproof storage tube and stored at  $-15^{\circ}\text{C}$ .

## P. LITHIUM TRIETHYLBOROHYDRIDE, 1.0M IN TETRAHYDROFURAN

Lithium triethylborohydride, 1.0M in THF, was obtained from Aldrich Chemical Co. and used in the glove box.

## Q. POTASSIUM

Potassium metal in mineral oil was purchased from Mallinckrodt. It was washed with hexane and cut into pieces and stored in the glove box.

## R. POTASSIUM HYDRIDE

Potassium hydride in mineral oil was purchased from Alfa Products Ventron Division. It was washed with either hexane or pentane and stored in the glove box prior to use.

## S. RUTHENIUM(III) CHLORIDE

Ruthenium(III) chloride was purchased from Aldrich Chemical Co. and used as received. It was stored in the glove box.

## T. SILICA GEL FOR COLUMN CHROMATOGRAPHY

Silica gel for this purpose, Grade H type 100-200 mesh size was obtained from Davison Chemical or Grade 60 type 0.063-0.1000 mm particle size was obtained from EM Science, and used as received.

## U. SILICA GEL FOR THIN-LAYER CHROMATOGRAPHY

Silica gel for this purpose, 60 PF<sub>254</sub>, was obtained from EM Reagents and used as received.

## V. SODIUM

Sodium metal in mineral oil was purchased from Mallinckrodt. Preparation prior to use of this alkali metal is identical to that of potassium metal. It was stored in the glove box prior to use.

## W. SULFUR (SUBLIMED)

Sulfur (sublimed) was purchased from Mallinckrodt and used as received.

## X. SULFURIC ACID

Sulfuric acid (aqueous) was used as received from Mallinckrodt.

## Y. TETRAPHENYLARSONIUM CHLORIDE

Tetraphenylarsonium chloride was purchased from Aldrich Chemical Co. or J. T. Baker Chemical Co. It was dried at 100°C under vacuum and stored in a glove box prior to use.

## Z. TETRAPHENYLPHOSPHONIUM BROMIDE

Tetraphenylphosphonium bromide was purchased from Aldrich Chemical Co. and used as received.

## AA. TRIETHYL OXONIUM HEXAFLUOROPHOSPHATE

Triethyl oxonium hexafluorophosphate was purchased from Aldrich Chemical Co. and used as received. It was stored at -15°C in a glove box.

## BB. TRIETHYLBORON

Triethylboron was kindly donated by Dr. Thomas Getman and Mr. David Workman.

## CC. TRIFLUOROACETIC ACID

Trifluoroacetic acid was purchased from Alfa Products Ventron Division. It was stored in the dark at  $-15^{\circ}\text{C}$  and degassed prior to use.

## DD. TRIIRON DODECACARBONYL

Triiron dodecacarbonyl was purchased from Strem Chemical, Inc. It was recrystallized from  $\text{CH}_2\text{Cl}_2$  and dried under vacuum at  $25^{\circ}\text{C}$  and stored under  $\text{N}_2$  at  $-15^{\circ}\text{C}$ .

## EE. TRIMETHYL OXONIUM TETRAFLUOROBORATE

Trimethyl oxonium tetrafluoroborate was obtained from Alfa Products Ventron Division. It was stored under  $\text{N}_2$  at  $-15^{\circ}\text{C}$  and used in the glove box.

## FF. TRIMETHYLAMINE N-OXIDE DIHYDRATE

Trimethylamine N-oxide dihydrate was purchased from Aldrich Chemical Co. and sublimed prior to use.

## GG. TRIMETHYLBORON

Trimethylboron was kindly donated by Dr. Martin Payne and Dr. Thomas Getman.

## HH. TRIOSMIUM DODECACARBONYL

Triosmium dodecacarbonyl was purchased from Strem Chemical, Inc. and used as received.

## II. TRIPHENYLMETHYLPHOSPHONIUM TETRAFLUOROBORATE

Triphenylmethylphosphonium tetrafluoroborate was purchased from Alfa Products Ventron Division and used in the glove box.

## JJ. TRIRUTHENIUM DODECACARBONYL

Triruthenium dodecacarbonyl was purchased from Strem Chemical, Inc. and used as received.

## III. SOLVENTS

Pentane, hexane and cyclohexane were dried over  $\text{CaH}_2$  at elevated temperatures for a minimum of 24 hours. They were then vacuum distilled into solvent storage bulbs. Methylene chloride and acetonitrile were dried over either  $\text{CaH}_2$  or  $\text{P}_2\text{O}_5$  at room temperature for a minimum of 48 hours and then vacuum distilled into solvent storage bulbs. Dimethyl ether, benzene and toluene were dried over  $\text{CaCl}_2$  or sodium-benzophenone ketyl at elevated temperatures for a minimum of 24 hours and subsequently distilled into solvent storage bulbs containing sodium-benzophenone ketyl. Tetrahydrofuran and diethyl ether were dried over sodium-benzophenone ketyl at elevated temperatures for a minimum of 24 hours and vacuum distilled into storage bulbs containing sodium metal and benzophenone. Methanol was dried by refluxing over magnesium methoxide [143] and vacuum

distilled into a storage bulb. Deuterated solvents were dried and stored in the same manner as the proton-containing analog.

#### IV. CRYSTAL GROWING

Crystal growing procedures and conditions are intrinsically a matter of trial and error and have varied for the different compounds reported here. A basic starting point to obtain suitable crystals for diffraction is outlined below. For air-stable compounds, the preferred procedure is as follows.

The desired compound is dissolved in a minimum amount of a less polar solvent to which a more polar solvent is added. The more polar solvent is added in a dropwise manner to the solution so as not to agitate the culture tube. The tube is flushed with nitrogen and then quickly sealed and left undisturbed in a refrigerator (-15°C) until crystals appear on the sides of the tube.

A similar procedure is adapted to grow crystals of air-sensitive compounds by using a diffusion apparatus. (Fig. 51) In the glove box, the compound is again dissolved in a solvent; however, this time the desired solvent is the more polar solvent. The solution is placed in the removable tube of the apparatus. The apparatus is then removed from the glove box and evacuated on the vacuum line. A less polar solvent is then transferred *via* the vacuum line to the other tube of this apparatus. The apparatus is placed in an undisturbed place which is free of large temperature fluctuations. The stopcock between the two tubes is opened and adjusted so that an observable change in the solvent levels occurs only after 3-5 hours. When the crystals

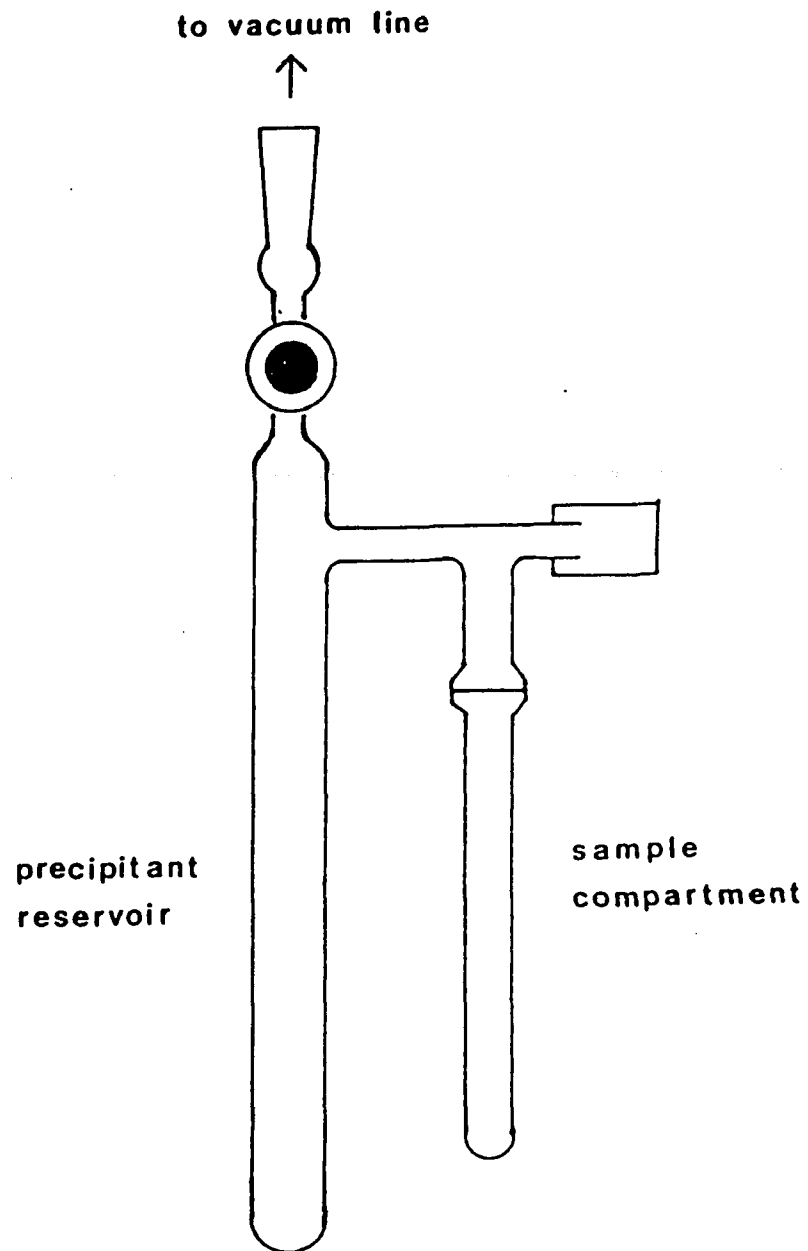


Figure 51. Crystal Growing Apparatus.

are observed on the walls of the removable tube, the solvent is decanted to the other side leaving the crystals behind. The crystals may then be removed from the tube and sealed in glass capillaries.

## V. PREPARATION OF STARTING MATERIALS

### A. $M_2Os_3(CO)_{11}$ (M=Na,K)

$M_2Os_3(CO)_{11}$  was prepared by the method of Shore and co-workers. [146]

### B. $M_2Os_3(^{13}CO)_{11}$ (M=Na,K)

$M_2Os_3(^{13}CO)_{11}$  was enriched by equilibration of 1 atm  $^{13}CO$  over a THF solution of the anion at room temperature.

### C. $[PPN]_2[Os_3(CO)_{11}]$

Metathesis of  $K_2Os_3(CO)_{11}$  with  $PPNCl$  afforded  $[PPN]_2[Os_3(CO)_{11}]$ .

### D. $[PPN]_2[Os_3(CO)_9CCO]$

$[PPN]_2[Os_3(CO)_9CCO]$  was prepared in a similar manner to that of its analogs,  $[PPN]_2[Fe_3(CO)_9CCO]$  [147] and  $[PPN]_2[Ru_3(CO)_9CCO]$ . [148]

### E. $HOs_3(CO)_{10}COCH_3$

$HOs_3(CO)_{10}COCH_3$  was prepared as described by Keister and co-workers. [149] Another method was also employed using a slight modification [98] of the procedure described by Johnson [150] for the synthesis of  $HRu_3(CO)_{10}COCH_3$ .

### F. $HOs_3(CO)_{10}CH$

$HOs_3(CO)_{10}CH$  was prepared by the literature method of Shapley. [149]

G.  $\text{KHos}_3(\text{CO})_{11}$ 

$\text{KHos}_3(\text{CO})_{11}$  was prepared by the method developed by Bricker. [152]

H.  $\text{K}[\text{BR}_3\text{H}]$  (R=Me,Et)

$\text{K}[\text{BR}_3\text{H}]$  was prepared by the method developed by Nagel [153] or a slight variation thereof.

I.  $\text{H}_2\text{Os}_3(\text{CO})_9\text{CCH}_2$ 

$\text{H}_2\text{Os}_3(\text{CO})_9\text{CCH}_2$  was prepared by the method developed by Deeming. [154]

J.  $\text{H}_2\text{Os}_3(\text{CO})_9\text{CCO}$ 

$\text{H}_2\text{Os}_3(\text{CO})_9\text{CCO}$  may be accomplished by two methods. [98] The first method involves the protonation of  $[\text{PPN}]_2[\text{Os}_3(\text{CO})_9\text{CCO}]$ . [155] The alternative method involves thermal conversion of the osmium methylidyne cluster,  $\text{Hos}_3(\text{CO})_{10}\text{CH}$ . [8,156]

K.  $\text{M}_2[\text{Ru}(\text{CO})_4]$  (M=Na,K)

$\text{M}_2[\text{Ru}(\text{CO})_4]$  was prepared by the method of Stone and co-workers. [112]

L.  $\text{M}_2[\text{Os}(\text{CO})_4]$  (M=Na,K)

$\text{M}_2[\text{Os}(\text{CO})_4]$  was prepared by the method of Stone and co-workers. [112]

M.  $M_2[Ru_6(CO)_{18}]$  (M=Na,K,PPN)

$M_2[Ru_6(CO)_{18}]$  was prepared by modification of one of the methods developed by Shore [64], Johnson and Lewis [84] or Shapley [67] as outlined below.

Prep I.

A flask was charged with  $Ru_3(CO)_{12}$  (0.5000g, 0.7824 mmoles), K (0.0315g, 0.8057 mmoles) and  $Ph_2CO$  (0.1432g, 0.7859 mmoles) to which THF was introduced. The mixture was stirred at 60–65°C for 38 hours during which time the solution turned deep red. The THF was removed and  $CH_2Cl_2$  was introduced to precipitate out  $K_2Ru_6(CO)_{18}$ .

NOTE: If the reaction temperature is reduced to 55–60°C the reaction slows and is complete within 65 hours. Also when Na is the counterion the reaction rate is slowed.

Prep II.

$Ru_3(CO)_{12}$  (0.0965g, 0.1509 mmoles) was dissolved in 20 mL THF. KOH (0.2603g, 4.5762 mmoles) was dissolved in 0.1 mL  $H_2O$  and 2 mL THF. The  $Ru_3(CO)_{12}$  solution was slowly dripped into the aqueous KOH solution over a period of 30 minutes. During the course of 1½ hours at room temperature the solution turned dark red-brown. The solvent was removed and MeOH added. To this solution was added PPNCl (0.1018g, 0.1173 mmoles) and again stirred at room temperature for 3½ hours. Filtration to remove unreacted PPNCl afforded  $[PPN]_2[Ru_6(CO)_{18}]$  as a dark brown solid.

## Prep III.

A flask was charged with  $K_2Ru_4(CO)_{13}$  (0.1000g, 0.1181 mmoles),  $Ru_3(CO)_{12}$  (0.0503g, 0.0787 mmoles) and THF. The solution was stirred at 60-65°C for 53 hours. After this reaction period the THF was removed and the product was precipitated using  $CH_2Cl_2$ .

NOTE: Preparation of  $K_2Ru_6(CO)_{18}$  can also be accomplished by reacting  $K_2Ru_3(CO)_{11}$  with  $Ru_3(CO)_{12}$  in a 1:1 stoichiometric ratio. [64] (Fig. 12)

N.  $M'_2[Ru_6(CO)_{18}]$  ( $M'=PMePh_3, PPh_4$ )

Metathesis of  $K_2Ru_6(CO)_{18}$  with  $Ph_4PBr$  or  $Ph_3MePBF_4$  afforded  $M'_2[Ru_6(CO)_{18}]$ .

O.  $M_2[Ru_6(^{13}CO)_{18}]$  ( $M=Na, K$ )

$M_2[Ru_6(^{13}CO)_{18}]$  was enriched by equilibration of 1 atm  $^{13}CO$  over a THF solution of the anion at room temperature.

P.  $M_2[Ru_4(CO)_{13}]$  ( $M=Na, K$ )

$M_2[Ru_4(CO)_{13}]$  was prepared by the method of Shore and co-workers. [64]

Q.  $M_2[Ru_3(CO)_{11}]$  ( $M=Na, K$ )

$M_2[Ru_3(CO)_{11}]$  was prepared by the method of Shore and co-workers. [64]

R.  $Na_6[Ru_4(CO)_{11}]$ 

$Na_6[Ru_4(CO)_{11}]$  was prepared by the method of Shore and co-workers. [65]

S.  $K_4[Ru_6(CO)_{17}]$ 

$K_4[Ru_6(CO)_{17}]$  was prepared by the method of Shore and co-workers. [65]

T.  $K_6[Ru_6(CO)_{16}]$ 

$K_6[Ru_6(CO)_{16}]$  was prepared by the method of Shore and co-workers. [65]

U.  $Ru_3(CO)_{12}$ 

$Ru_3(CO)_{12}$  that was prepared from  $RuCl_3$  and CO was accomplished with a slight modification [139] of the literature procedure. [84]

In the glove box, 5g of  $RuCl_3$  was weighed into a small vial and was sealed with parafilm. About 150 mL of fresh MeOH and a Teflon-coated stir bar were added to the glass jacket in the bomb and the  $RuCl_3$  was immediately added. The bomb was sealed and the atmosphere over the solution was flushed several times with CO gas from the cylinder. The bomb was then pressurized to 750 psi CO and heated to 125°C. The bomb was allowed to stir for 8-9 hours. After this time period the bomb was slowly cooled to room temperature, vented and opened to the air. Orange crystals of  $Ru_3(CO)_{12}$  were filtered using the mother liquor to wash the crystals. Usually the crystals could be used without further purification. If, however, the crystals had impurities they were crystallized from hot toluene. Average yield was 3.4g (84%)

V.  $\text{K}_2\text{FeRu}_3(\text{CO})_{13}$ 

$\text{K}_2\text{FeRu}_3(\text{CO})_{13}$  was prepared by the method developed by Siriwardane. [75]

W.  $\text{H}_2\text{Os}_4(\text{CO})_{13}$ 

$\text{H}_2\text{Os}_4(\text{CO})_{13}$  was prepared by the method developed by Siriwardane. [75]

## VI. PREPARATION OF NEW COMPOUNDS

## A. IRON/RUTHENIUM SYSTEMS

1. Reaction of  $[\text{Ru}_3(\text{CO})_{11}]^{2-}$ 

$\text{K}_2\text{Ru}_3(\text{CO})_{11}$  (0.0996g, 0.144 mmoles) and  $\text{Fe}_2(\text{CO})_9$  (0.2649g, 0.7281 mmoles) were placed in a flask. THF was introduced and the mixture stirred at room temperature for 6 hours. The solvent was removed leaving behind a dark green-brown residue. The residue was dissolved in  $\text{CH}_2\text{Cl}_2$ , protonated with HCl (0.5069 mmoles) and stirred at room temperature for 7 hours. Filtration afforded a greyish-white precipitate and a dark brown filtrate. Purification of the filtrate by TLC (silica gel, hexane) yielded four bands (in order of decreasing  $R_f$ ): yellow, green, purple, and orange-brown. The compounds were identified as  $\text{H}_4\text{Ru}_4(\text{CO})_{12}$  (11.4%) [34b,76],  $\text{Fe}_3(\text{CO})_{12}$  (11.7%),  $\text{H}_2\text{Ru}_4(\text{CO})_{13}$  (17.0%) [110,157], and  $\text{H}_2\text{FeRu}_3(\text{CO})_{13}$  (10-20%) [40a,60,71], respectively, by IR or NMR spectroscopy.

2. Reaction of  $[\text{Ru}_4(\text{CO})_{13}]^{2-}$ 

A flask attached to the vacuum line was charged with  $\text{K}_2\text{Ru}_4(\text{CO})_{13}$  (0.1005g, 0.1187 mmoles) and  $\text{Fe}_2(\text{CO})_9$  (0.2138g, 0.5877 mmoles). THF

was condensed in and the solution stirred at room temperature for 6 hours. The solvent was removed and  $\text{CH}_2\text{Cl}_2$  introduced. Protonation using HCl (0.4816 mmoles) was stirred at room temperature for 7 hours and subsequent purification *via* TLC (silica gel, hexane) afforded four bands; yellow, green, purple, and orange-brown. Spectroscopic data ( $^1\text{H}$  NMR and IR) indicate formation of  $\text{H}_4\text{Ru}_4(\text{CO})_{12}$  [34b,76],  $\text{Fe}_3(\text{CO})_{12}$ ,  $\text{H}_2\text{Ru}_4(\text{CO})_{12}$  [110,157], and  $\text{H}_2\text{FeRu}_3(\text{CO})_{13}$  [40a,60,71], respectively. A minor amount of  $\text{H}_2\text{Fe}_2\text{Ru}_2(\text{CO})_{13}$  [69,70a] is also formed which is partially inseparable from  $\text{H}_2\text{FeRu}_3(\text{CO})_{13}$ .

NOTE: In the above reactions one may substitute  $\text{Fe}(\text{CO})_5$  for  $\text{Fe}_2(\text{CO})_9$ . If this is done, formation of  $\text{Fe}_3(\text{CO})_{12}$  is severely depressed or even eliminated indicating that  $\text{Fe}_2(\text{CO})_9$  disproportionates in solution to give  $\text{Fe}(\text{CO})_5$  and  $[\text{Fe}(\text{CO})_4]^{2-}$  under these reaction conditions. Further evidence for this occurrence is that when  $\text{Fe}_2(\text{CO})_9$  is employed one recovers unreacted  $\text{Fe}(\text{CO})_5$  while removing the solvent, THF, prior to protonation.

NOTE: Changing reaction conditions (ie. reaction time for both the initial redox condensation and the protonation, solvents, etc.) and reactant concentrations only influences the product yields not the species formed.

### 3. Reaction of $[\text{Ru}_4(\text{CO})_{12}]^{4-}$

$\text{K}_4\text{Ru}_4(\text{CO})_{12}$  (0.0728g, 0.0808 mmoles) and  $\text{Fe}_2(\text{CO})_9$  (0.1489g, 0.4093 mmoles) were combined in a flask and THF condensed in. The solution was stirred at room temperature for 20 hours. The solvent was removed. Protonation of the resulting dark purple-brown residue

with HCl (0.4331 mmoles) in  $\text{CH}_2\text{Cl}_2$  at room temperature afforded  $\text{H}_4\text{Ru}_4(\text{CO})_{12}$  (3.1%) [34b,76],  $\text{Fe}_3(\text{CO})_{12}$  (9.6%),  $\text{H}_2\text{Ru}_4(\text{CO})_{13}$  (2.4%) [110,157],  $\text{H}_2\text{FeRu}_3(\text{CO})_{13}$  (7.3%) [40a,60,71], and  $\text{H}_2\text{Fe}_2\text{Ru}_2(\text{CO})_{13}$  (trace) [69,70a] after TLC (silica gel, hexane).

#### 4. Reaction of $[\text{FeRu}_3(\text{CO})_{13}]^{2-}$

A flask was charged with  $\text{K}_2\text{FeRu}_3(\text{CO})_{13}$  (0.0665g, 0.0827 mmoles) and THF was introduced.  $\text{Fe}(\text{CO})_5$  (0.1103 mmoles) was condensed into the flask and the reaction mixture stirred at  $55^\circ\text{C}$  for 25 hours. THF was removed,  $\text{CH}_2\text{Cl}_2$  introduced and HCl (0.4689 mmoles) condensed onto the reaction mixture. The solution was stirred at room temperature for 4 hours and purification by TLC (silica gel, hexane) afforded  $\text{H}_4\text{Ru}_4(\text{CO})_{12}$  [34b,76],  $\text{Fe}_3(\text{CO})_{12}$ ,  $\text{H}_2\text{Ru}_4(\text{CO})_{13}$  [110,157],  $\text{H}_2\text{FeRu}_3(\text{CO})_{13}$  [40a,60,71], and trace amounts of  $\text{H}_2\text{Fe}_2\text{Ru}_2(\text{CO})_{13}$  [69,70a]. The major product was  $\text{H}_2\text{FeRu}_3(\text{CO})_{13}$ .

#### 5. Reduction of $\text{H}_2\text{FeRu}_3(\text{CO})_{13}$

$\text{H}_2\text{FeRu}_3(\text{CO})_{13}$  (0.0312g, 0.0430 mmoles) and K (0.0038g, 0.097 mmoles) and  $\text{Ph}_2\text{CO}$  (0.0158g, 0.0867 mmoles) were combined in a flask. THF was added and the reaction stirred at room temperature for 36 hours. Within several minutes the reaction turned from red-orange to dark red. The reaction was filtered to remove a greyish-white precipitate and the filtrate analyzed *via*  $^1\text{H}$  NMR.  $^1\text{H}$  NMR indicates formation of  $\text{KH}_3\text{Ru}_4(\text{CO})_{12}$  [68a],  $\text{H}_2\text{Ru}_4(\text{CO})_{13}$  [110,157],  $\text{H}_4\text{Ru}_4(\text{CO})_{12}$  [34b,76] and mostly unreacted  $\text{H}_2\text{FeRu}_3(\text{CO})_{13}$ .

6. Reaction of  $[\text{Ru}_4(\text{CO})_{11}]^{6-}$ 

$\text{Na}_6\text{Ru}_4(\text{CO})_{11}$  (0.0262g, 0.0307 mmoles) was reacted with  $\text{Fe}_2(\text{CO})_9$  (0.0566g, 0.156 mmoles) in THF. The mixture was stirred at room temperature for 14 hours at which time the solution turned purple. The THF was removed and the residue taken up in  $\text{CH}_2\text{Cl}_2$ . Protonation with HBr (0.3722 mmoles) afforded  $\text{H}_4\text{Ru}_4(\text{CO})_{12}$  [34b,76],  $\text{Fe}_3(\text{CO})_{12}$ ,  $\text{H}_2\text{Ru}_4(\text{CO})_{13}$  [110,157],  $\text{H}_2\text{FeRu}_3(\text{CO})_{13}$  [40a,60,71] and small amounts of  $\text{H}_2\text{Ru}_6(\text{CO})_{17}$ . These compounds were purified *via* TLC (silica gel, hexane) and identified by standard spectral means.

7. Reaction of  $[\text{Ru}_6(\text{CO})_{17}]^{4-}$ 

$\text{K}_4\text{Ru}_6(\text{CO})_{17}$  (0.0249g, 0.0200 mmoles) and  $\text{Fe}_2(\text{CO})_9$  (0.0424g, 0.117 mmoles) were reacted in THF at room temperature for 14 hours at which time the solution turned purple. Protonation in  $\text{CH}_2\text{Cl}_2$  with HBr (0.1933 mmoles) afforded  $\text{H}_4\text{Ru}_4(\text{CO})_{12}$  [34b,76],  $\text{Fe}_3(\text{CO})_{12}$ ,  $\text{H}_2\text{Ru}_4(\text{CO})_{13}$  [110,157],  $\text{H}_2\text{FeRu}_3(\text{CO})_{13}$  [40a,60,71] and fairly low yields of  $\text{H}_2\text{Ru}_6(\text{CO})_{17}$ .

8. Reaction of  $[\text{Ru}_6(\text{CO})_{16}]^{6-}$ 

$\text{K}_6\text{Ru}_6(\text{CO})_{16}$  (0.0254g, 0.0196 mmoles) was reacted with  $\text{Fe}_2(\text{CO})_9$  (0.0418g, 0.115 mmoles) in THF. The mixture was stirred at room temperature for 14 hours at which time the solution turned purple as in the above cases. The THF was removed and the residue taken up in  $\text{CH}_2\text{Cl}_2$ . Protonation with HBr (0.2577 mmoles) and purification as above afforded the same products in comparable yields.

9. Reaction of  $[\text{Ru}_6(\text{CO})_{18}]^{2-}$ 

$\text{K}_2\text{Ru}_6(\text{CO})_{18}$  (0.110g, 0.0921 mmoles) and  $\text{Fe}_2(\text{CO})_9$  (0.1730g, 0.4755 mmoles) were added to a flask to which THF was introduced. The mixture was stirred at room temperature for 25 hours. The solvent was removed and the purple residue taken up in  $\text{CH}_2\text{Cl}_2$ .  $\text{HCl}$  (0.3364 mmoles) was added and the reaction was stirred at room temperature for 4 hours. The solution was filtered to remove a greyish-white precipitate assumed to be  $\text{KCl}$ .  $\text{CH}_2\text{Cl}_2$  removal from the filtrate and introduction of hexane precipitated out  $\text{H}_2\text{Ru}_6(\text{CO})_{17}$  as a dark purple solid in 55% yield. Hexane was removed from the filtrate and  $\text{CH}_2\text{Cl}_2$  introduced. This fraction was then purified by TLC (silica gel, hexane) to give the previously observed clusters  $\text{H}_4\text{Ru}_4(\text{CO})_{12}$  (< 5%) [34b,76],  $\text{Fe}_3(\text{CO})_{12}$  (10%),  $\text{H}_2\text{Ru}_4(\text{CO})_{13}$  (< 5%) [110,157],  $\text{H}_2\text{FeRu}_3(\text{CO})_{13}$  (10%) [40a,60,71] and trace amounts of  $\text{H}_2\text{Fe}_2\text{Ru}_2(\text{CO})_{13}$  [69,70a].

Spectral Characterization of  $\text{H}_2\text{Ru}_6(\text{CO})_{17}$ .

$^1\text{H}$  NMR ( $\text{CDCl}_3$ , 30°C)  $\delta$ -15.61 (s,2H) ppm

( $\text{CD}_2\text{Cl}_2$ , 30°C)  $\delta$ -15.56 (s,2H) ppm

$^{13}\text{C}$  NMR ( $\text{CDCl}_3$ , 30°C)  $\delta$ 194.45 (s) ppm

IR ( $\text{CH}_2\text{Cl}_2$ , 30°C)  $\nu_{\text{CO}}$  2060(vs), 2055(s,sh), 2006(w), 1983(vw,sh)  $\text{cm}^{-1}$

(nujol, 30°C)  $\nu_{\text{CO}}$  2050(s,br), 2006(w), 1732(w,br)  $\text{cm}^{-1}$

Elemental Analysis: Calcd for  $\text{C}_{17}\text{H}_2\text{O}_{17}\text{Ru}_6$ .

Calcd: C, 18.76; H, 0.18

Found: C, 18.78; H, 0.21

Crystallographic quality crystals were grown from slow evaporation of a  $\text{CH}_2\text{Cl}_2$ /hexane solution at room temperature. Suitable crystals may also be grown from slow evaporation of concentrated  $\text{CH}_2\text{Cl}_2$  solutions at either room or lower temperatures.

10. Reaction of  $[\text{Ru}_6(\text{CO})_{18}]^{2-}$

$\text{K}_2\text{Ru}_6(\text{CO})_{18}$  (0.111g, 0.0935 mmoles) were reacted with  $\text{Fe}(\text{CO})_5$  (0.1545 mmoles, 1.65 eq) in THF at  $55^\circ\text{C}$  for 25 hours. Removal of THF and protonation with HCl (0.4259 mmoles) in  $\text{CH}_2\text{Cl}_2$  afforded  $\text{H}_2\text{Ru}_6(\text{CO})_{17}$  (30%) along with minor amounts of  $\text{H}_4\text{Ru}_4(\text{CO})_{12}$  [34b,76] and  $\text{H}_2\text{Ru}_4(\text{CO})_{13}$  [110,157].

11.  $^{13}\text{C}$  Enrichment of  $\text{H}_2\text{Ru}_6(\text{CO})_{17}$

$\text{K}_2\text{Ru}_6(\text{CO})_{18}$  (0.101g, 0.0852 mmoles) and  $\text{Fe}_2(\text{CO})_9$  (0.1654g, 0.4546 mmoles) were combined in a flask which was attached to the vacuum line. THF was condensed in and the reaction was stirred at room temperature for  $3\frac{1}{2}$  hours.  $^{13}\text{CO}$  (1.4 atm) was transferred to the reaction vessel at  $-196^\circ\text{C}$  and the reaction was warmed to room temperature. The reaction was stirred for an additional 10 hours. THF was removed and  $\text{CH}_2\text{Cl}_2$  introduced. HCl (0.3293 mmoles) was added and stirred at room temperature for 2 hours. The solution was filtered to remove a greyish-white precipitate. The filtrate was dried and subsequently taken up in hexane to precipitate out  $\text{H}_2\text{Ru}_6(^{13}\text{CO})_{17}$ .

NOTE: Enrichment of  $\text{H}_2\text{Ru}_6(\text{CO})_{17}$  can also be accomplished using  $\text{K}_2\text{Ru}_6(^{13}\text{CO})_{18}$ . Percentage enrichment for  $\text{H}_2\text{Ru}_6(\text{CO})_{17}$  is slightly better than the above method.

## 12. Pyrolysis of $\text{H}_2\text{FeRu}_3(\text{CO})_{13}$

$\text{H}_2\text{FeRu}_3(\text{CO})_{13}$  (0.0115g, 0.0159 mmoles) was placed into a flask to which was condensed THF and  $\text{Fe}(\text{CO})_5$  (0.1718 mmoles, 10.8 eq). The reaction was stirred at 65°C for 2 days. During this time the original orange solution underwent discoloration until it was yellowish brown in color. At this time the solvent was removed and no  $\text{Fe}(\text{CO})_5$  was observed with the volatiles.  $\text{CH}_2\text{Cl}_2$  was added and the solution filtered.  $^1\text{H}$  NMR of this solution indicated formation of  $\text{H}_4\text{Ru}_4(\text{CO})_{12}$  [34b,76],  $\text{H}_2\text{Ru}_4(\text{CO})_{13}$  [110,157], unreacted  $\text{H}_2\text{FeRu}_3(\text{CO})_{13}$  and  $\text{H}_2\text{Ru}_6(\text{CO})_{17}$  (9% based on peak area).

## 13. Protonation of $[\text{Ru}_6(\text{CO})_{18}]^{2-}$

$\text{K}_2\text{Ru}_6(\text{CO})_{18}$  (0.1491g, 0.1254 mmoles) was protonated with HCl (0.4259 mmoles) in  $\text{CH}_2\text{Cl}_2$ . The solution was stirred at room temperature for 19 hours and then  $\text{CH}_2\text{Cl}_2$  was removed.  $^1\text{H}$  NMR of the residue showed formation of  $\text{H}_4\text{Ru}_4(\text{CO})_{12}$ ,  $\text{H}_2\text{Ru}_4(\text{CO})_{13}$  and  $\text{H}_2\text{Ru}_6(\text{CO})_{17}$ .  $\text{H}_2\text{Ru}_6(\text{CO})_{17}$  was isolated in 40.1% yield from this reaction.

## B. IRON/OSMIUM SYSTEMS

### 1. Preparation of $\text{Na}_2\text{FeOs}_3(\text{CO})_{13}$

An extractor was charged with  $\text{Na}_2\text{Os}_3(\text{CO})_{11}$  (0.2002g, 0.2153 mmoles) and THF condensed in.  $\text{Fe}(\text{CO})_5$  (0.4634 mmoles) was condensed into the flask and the solution stirred at room temperature for 7 hours. The THF and excess  $\text{Fe}(\text{CO})_5$  was pumped away and  $\text{CH}_2\text{Cl}_2$  added to precipitate  $\text{Na}_2\text{FeOs}_3(\text{CO})_{13}$  (33%).  $[\text{FeOs}_3(\text{CO})_{13}]^{2-}$  was

characterized by comparison of its IR spectrum with that of  $[\text{FeRu}_3(\text{CO})_{13}]^{2-}$ . [75] Other products obtained in this reaction were  $\text{Os}_3(\text{CO})_{12}$  and  $\text{Fe}_3(\text{CO})_{12}$ .

The potassium salt was prepared using  $\text{K}_2\text{Os}_3(\text{CO})_{11}$  and generally was produced in approx. 50% yield when the same reaction conditions described above are employed.

### 2. Reaction of $[\text{FeOs}_3(\text{CO})_{13}]^{2-}$

$\text{Na}_2\text{FeOs}_3(\text{CO})_{13}$  (0.0756g, 0.0726 mmoles) was reacted with  $\text{Fe}(\text{CO})_5$  (0.1103 mmoles) in THF at 55°C for 25 hours. Solvent removal and protonation with HCl (0.3944 mmoles) in  $\text{CH}_2\text{Cl}_2$  afforded  $\text{Fe}_3(\text{CO})_{12}$  (60%) and  $\text{H}_2\text{FeOs}_3(\text{CO})_{13}$  (37%). [50a,71]

### 3. Reaction of $[\text{Os}_3(\text{CO})_{11}]^{2-}$

$\text{K}_2\text{Os}_3(\text{CO})_{11}$  (0.0975g, 0.102 mmoles) and  $\text{Fe}_2(\text{CO})_9$  (0.2215g, 0.6089 mmoles) were combined and THF introduced. The reaction was stirred at 0°C for 3-4 days then at room temperature for 1 hour. The solvent was removed and the residue protonated with HCl (0.4331 mmoles) in  $\text{CH}_2\text{Cl}_2$  and stirred at room temperature for 1½ hours. Purification *via* multiple TLC runs (silica gel, 4:1 hexane:toluene) afforded  $\text{H}_2\text{Os}_3(\text{CO})_{10}$  [76,100b],  $\text{Fe}_3(\text{CO})_{12}$ ,  $\text{H}_2\text{FeOs}_3(\text{CO})_{13}$ , [50a,71]  $\text{Fe}_2\text{Os}(\text{CO})_{12}$  [40,42,103,105] and  $\text{H}_2\text{Fe}_2\text{Os}_3(\text{CO})_{16}$  (13-15%). [50a]

Spectral Characterization of  $\text{H}_2\text{Fe}_2\text{Os}_3(\text{CO})_{16}$ .

$^1\text{H}$  NMR ( $\text{CDCl}_3$ , 30°C)  $\delta$ -21.39 (s,2H) ppm

( $d_8$ -toluene, 30°C)  $\delta$ -21.52 (s,2H) ppm

$^{13}\text{C}$  NMR ( $\text{CDCl}_3$ ,  $30^\circ\text{C}$ )  $\delta 200.57$  (s) ppm

The IR spectrum matches that reported by Plotkin and Shore. [50a]

FAB MS shows a parent peak which corresponds to the molecular

formula  $^1\text{H}_2\ ^{56}\text{Fe}_2\ ^{192}\text{Os}_3\ ^{12}\text{C}_{16}\ ^{16}\text{O}_{16}$  m/z(obsd) 1138, m/z(calcd) 1138.

NOTE: The above preparation gives optimum yields of  $\text{H}_2\text{Fe}_2\text{Os}_3(\text{CO})_{16}$  when run at  $0^\circ\text{C}$  for 4 days with a 5-6 molar excess of  $\text{Fe}_2(\text{CO})_9$ . If the reaction conditions are varied one may obtain the yields as indicated below.

Fe Eq	T, $^\circ\text{C}$	Time	%I	%II	%III	%IV	%V
2	25	22h	--	--	11.4	1.5	24.2
5	25	12h	trace	--	> 20	< 5	9.9
5	25	22h	--	trace	19.2	6.8	44.6
5	0	16h	2.1	trace	9.9	13-15	xx
	25	12h					
5	0	3d	--	trace	8.8	12-15	> 22
	25	1h					
5	0	4d	--	trace	15.1	13-15	9.5-30
	25	1h					

I =  $\text{H}_2\text{Os}_3(\text{CO})_{10}$

-- = not observed

II =  $\text{Fe}_2\text{Os}(\text{CO})_{12}$

xx = not measured

III =  $\text{Fe}_3(\text{CO})_{12}$

IV =  $\text{H}_2\text{Fe}_2\text{Os}_3(\text{CO})_{16}$

V =  $\text{H}_2\text{FeOs}_3(\text{CO})_{13}$

NOTE: If solvents are not thoroughly dried or if the TLC plates are not properly activated,  $\text{H}_2\text{Fe}_2\text{Os}_3(\text{CO})_{16}$  is not observed to form or is formed in extremely low yield. The product which is formed instead is  $\text{HOs}_3(\text{CO})_{10}\text{OH}$  and  $\text{Os}_3(\text{CO})_{12}$ .

Crystals were grown by slow evaporation of either the mixed solvent system  $\text{CH}_2\text{Cl}_2$ /hexane or the pure solvent  $\text{CH}_2\text{Cl}_2$  at room temperature. Crystals were not observed to form at lower temperatures or in other solvent systems. During the course of crystal growth which was a rather long time (3-6 weeks approximately) the product  $\text{H}_2\text{Fe}_2\text{Os}_3(\text{CO})_{16}$  decomposed forming  $\text{Os}_3(\text{CO})_{12}$  and most likely  $\text{Fe}_2\text{Os}(\text{CO})_{12}$ .

#### 4. $^{13}\text{C}$ Enrichment of $\text{H}_2\text{Fe}_2\text{Os}_3(\text{CO})_{16}$

$\text{K}_2\text{Os}_3(\text{CO})_{11}$  (0.1001g, 0.1046 mmoles) and  $\text{Fe}_2(\text{CO})_9$  (0.2039g, 0.5605 mmoles) were combined and THF introduced. The reaction was stirred at  $0^\circ\text{C}$  for 2 days.  $^{13}\text{CO}$  (1.7 atm) was transferred to the reaction vessel at  $-196^\circ\text{C}$  and the reaction was then warmed to  $0^\circ\text{C}$  and stirred for an additional  $1\frac{1}{2}$  days and then at room temperature for 1 hour. The solvent was removed and the residue protonated with  $\text{HCl}$  (0.3722 mmoles) in  $\text{CH}_2\text{Cl}_2$  and stirred at room temperature for 2 hours. Purification *via* TLC (silica gel, 4:1 hexane:toluene) afforded  $\text{H}_2\text{Fe}_2\text{Os}_3(^{13}\text{CO})_{16}$  along with enriched  $\text{H}_2\text{Os}_3(\text{CO})_{10}$ ,  $\text{Fe}_3(\text{CO})_{12}$ ,  $\text{H}_2\text{FeOs}_3(\text{CO})_{13}$  and  $\text{Fe}_2\text{Os}(\text{CO})_{12}$ .

NOTE: Enrichment can also be accomplished using  $\text{K}_2\text{Os}_3(^{13}\text{CO})$ .

Enrichment by this second method is slightly better than that above depending on the degree of enrichment of the  $\text{K}_2\text{Os}_3(\text{CO})_{11}$ .

#### 5. Reduction of $\text{H}_2\text{FeOs}_3(\text{CO})_{13}$

$\text{H}_2\text{FeOs}_3(\text{CO})_{13}$  (0.0398g, 0.0401 mmoles) and  $\text{K}$  (0.0033g, 0.084 mmoles) and  $\text{Ph}_2\text{CO}$  (0.0149g, 0.0818 mmoles) were combined in a flask.

THF was added and the reaction stirred at room temperature for 36 hours. Within several minutes the reaction turned from orange-yellow to red-orange. The reaction was filtered to remove a greyish-white precipitate. The filtrate was taken up in hexane and subsequently filtered giving a red precipitate and a yellow filtrate. The red precipitate was shown to be  $\text{KHFeOs}_3(\text{CO})_{13}$  [110] by  $^1\text{H}$  NMR. The yellow filtrate was identified as  $\text{Os}_3(\text{CO})_{12}$ .

### C. RUTHENIUM/OSMIUM SYSTEMS

#### 1. Reaction of $[\text{Os}_3(\text{CO})_{11}]^{2-}$ with $\text{Ru}_3(\text{CO})_{12}$

A THF solution of  $\text{K}_2\text{Os}_3(\text{CO})_{11}$  (0.1013g, 0.1059 mmoles) was slowly dripped into a THF solution of  $\text{Ru}_3(\text{CO})_{12}$  (0.0339g, 0.0530 mmoles) which was maintained at 55°C. The reaction was stirred at 55°C for 24 hours. The THF was removed and  $\text{CH}_2\text{Cl}_2$  introduced. Protonation using HCl (0.1933 mmoles) and purification by column chromatography (silica gel, hexane) afforded four bands in order of elution: yellow, yellow-orange, orange-brown and dark brown. The yellow band was identified as  $\text{H}_4\text{Ru}_4(\text{CO})_{12}$  [34b,76] which also contained minor quantities of  $\text{H}_2\text{Os}_3(\text{CO})_{10}$ ,  $\text{H}_2\text{Ru}_2\text{Os}_3(\text{CO})_{16}$  [75] and  $\text{H}_2\text{Os}_5(\text{CO})_{16}$ . [44a] Purification of the orange-brown band by TLC or HPLC yielded  $\text{H}_2\text{Ru}_2\text{Os}_3(\text{CO})_{16}$  and  $\text{H}_2\text{Os}_5(\text{CO})_{16}$  as inseparable mixtures. The yellow-orange band consisted of the chromatographically inseparable mixture  $\text{H}_2\text{RuOs}_3(\text{CO})_{13}$  and  $\text{H}_2\text{Os}_4(\text{CO})_{13}$ .

## 2. Reaction of $[\text{Os}_3(\text{CO})_{11}]^{2-}$ with $\text{Ru}(\text{CO})_5$

A two-neck flask was charged with  $\text{Na}_2\text{Ru}(\text{CO})_4$  (0.0537g, 0.207 mmoles) in THF. A driptube was connected which contained a THF solution of  $\text{K}_2\text{Os}_3(\text{CO})_{11}$  (0.2010g, 0.2101 mmoles).  $\text{CO}_2$  (1.0308 mmoles) was condensed onto the  $\text{Na}_2\text{Ru}(\text{CO})_4$  solution at  $-196^\circ\text{C}$  and the reaction vessel was then covered with aluminum foil to exclude all light. The reaction was stirred at  $-22^\circ\text{C}$  for 3 hours and then brought down to  $-78^\circ\text{C}$ . Excess  $\text{CO}_2$  was removed by pumping on the reaction mixture for at least 15 minutes while keeping it at  $-78^\circ\text{C}$ . The  $\text{K}_2\text{Os}_3(\text{CO})_{11}$  solution was slowly added as the mixture was stirred at  $0^\circ\text{C}$ . The reaction was maintained at  $0^\circ\text{C}$  while stirring for 3 hours and then warmed to room temperature and placed in an oil bath maintained at  $55^\circ\text{C}$ . The reaction was stirred at  $55^\circ\text{C}$  for 4 hours, cooled to room temperature and subsequently protonated with HCl (0.9931 mmoles). Purification *via* TLC (3:1 hexane: $\text{CH}_2\text{Cl}_2$ , silica gel) afforded three bands (purple, yellow, and orange in decreasing R value). The purple and yellow bands were identified as  $\text{H}_2\text{Os}_3(\text{CO})_{10}$  (13%) [76,100b] and  $\text{H}_4\text{Ru}_4(\text{CO})_{12}$  (7%) [34b,76], respectively, by  $^1\text{H}$  NMR and IR. Further purification of the orange band by numerous HPLC runs (10%:90%  $\text{CH}_2\text{Cl}_2$ :n-heptane, normal phase, silica gel) and TLC (silica gel, 3:1 hexane: $\text{CH}_2\text{Cl}_2$ ) gave  $\text{H}_2\text{RuOs}_3(\text{CO})_{13}$  [71,75,110] and  $\text{H}_2\text{Os}_4(\text{CO})_{13}$  [44a,110] as an inseparable mixture.

## 3. Reaction of $[\text{Ru}_3(\text{CO})_{11}]^{2-}$ with $\text{Os}_3(\text{CO})_{12}$

A THF solution of  $\text{K}_2\text{Ru}_3(\text{CO})_{11}$  (0.1500g, 0.2175 mmoles) was slowly dripped into a THF solution of  $\text{Os}_3(\text{CO})_{12}$  (0.0980g, 0.108 mmoles)

which was maintained at 55°C. The reaction mixture was stirred at 55°C for 22 hours and then protonated using HCl (0.3865 mmoles) in CH<sub>2</sub>Cl<sub>2</sub>. Purification *via* column chromatography (silica gel, hexane) afforded four bands. These bands were in order of elution: yellow, orange-red, orange-brown and dark brown. The yellow band was identified as a mixture of Os<sub>3</sub>(CO)<sub>12</sub> and H<sub>4</sub>Ru<sub>4</sub>(CO)<sub>12</sub>. [34b,76] The orange-red band was H<sub>2</sub>Ru<sub>4</sub>(CO)<sub>13</sub>. [110,157] The orange-brown band was identified as a mixture of H<sub>2</sub>Ru<sub>4</sub>(CO)<sub>13</sub> and H<sub>2</sub>RuOs<sub>3</sub>(CO)<sub>13</sub>. Finally the dark brown band was identified as a mixture of H<sub>2</sub>RuOs<sub>3</sub>(CO)<sub>13</sub> and H<sub>2</sub>Ru<sub>2</sub>Os<sub>3</sub>(CO)<sub>16</sub>. [75] Further purification of the orange-brown band *via* TLC (silica gel, hexane) gave two bands: orange-red and yellow-orange. The orange-red band was identified as H<sub>2</sub>Ru<sub>4</sub>(CO)<sub>13</sub> and the yellow-orange band as H<sub>2</sub>RuOs<sub>3</sub>(CO)<sub>13</sub> (13%). Further purification of the dark brown band by TLC (silica gel, 5:1 hexane:CH<sub>2</sub>Cl<sub>2</sub>) gave H<sub>2</sub>Ru<sub>2</sub>Os<sub>3</sub>(CO)<sub>16</sub> (6%) and minor amounts of the products Ru<sub>3</sub>(CO)<sub>12</sub> and Os<sub>3</sub>(CO)<sub>12</sub>.

Spectral Characterization of H<sub>2</sub>RuOs<sub>3</sub>(CO)<sub>13</sub>.

<sup>1</sup>H NMR (C<sub>6</sub>D<sub>6</sub>, 30°C) δ-21.21 (s,2H) ppm

(CDCl<sub>3</sub>, 30°C) δ-21.05 (s,2H) ppm

(CD<sub>2</sub>Cl<sub>2</sub>, 30°C) δ-20.96 (s,2H) ppm

IR (hexane, 30°C) ν<sub>CO</sub> 2081(vs), 2068(vs), 2056(vs), 2027(m,sh),  
2023(m,sh), 2018(m), 2006(w,sh) cm<sup>-1</sup>

FT-ICR MS shows a parent ion peak which corresponds to the molecular formula <sup>1</sup>H<sub>2</sub><sup>102</sup>Ru<sup>192</sup>Os<sub>3</sub><sup>12</sup>C<sub>13</sub><sup>16</sup>O<sub>13</sub> m/z(obsd) 1044, m/z(calcd) 1044. The sequential loss of each of the 13 carbonyls and the 2 hydrides from

the molecular ion was observed. Crystallographic quality crystals were grown from slow evaporation of a  $\text{CH}_2\text{Cl}_2$  solution or from pentane solution at either room or lower temperatures.

Spectral Characterization of  $\text{H}_2\text{Ru}_2\text{Os}_3(\text{CO})_{16}$ .

$^1\text{H}$  NMR ( $\text{CDCl}_3$ ,  $30^\circ\text{C}$ )  $\delta$ -19.54 (s, 2H) ppm

IR ( $\text{CH}_2\text{Cl}_2$ ,  $30^\circ\text{C}$ )  $\nu_{\text{CO}}$  2123(w), 2081(s), 2061(vs), 2047(s),  
2016(w,sh)  $\text{cm}^{-1}$

## VII. REACTIVITY STUDIES OF $\text{H}_2\text{Ru}_6(\text{CO})_{17}$

### A. DEPROTONATION OF $\text{H}_2\text{Ru}_6(\text{CO})_{17}$ WITH $\text{PPNCl}$

$\text{H}_2\text{Ru}_6(\text{CO})_{17}$  (0.0187g, 0.0172 mmoles) and  $\text{PPNCl}$  (0.0098g, 0.017 mmoles) were combined in an extractor and THF introduced. The reaction was stirred at room temperature for 2 hours during which time the reaction changed from purple to deep orange-red. The solvent was removed and hexane added to precipitate out a dark red-orange solid in 63% yield. This compound was identified on the basis of  $^1\text{H}$  NMR ( $\delta$ 16.38 ppm ( $\text{CDCl}_3$ ),  $\delta$ 16.46 ppm ( $d_8$ -THF)),  $^{13}\text{C}$  NMR ( $\delta$ 202.01 ppm ( $d_8$ -THF)) and X-ray analysis as  $\text{PPNHu}_6(\text{CO})_{18}$ . The X-ray and  $^1\text{H}$  NMR are in accord with that reported by Johnson and Lewis. [86] Johnson and Lewis have reported that the  $^{13}\text{C}$  NMR exhibits a sharp singlet at room temperature; however, failed to report the chemical shift. The other product in the reaction is  $\text{PPNH}_3\text{Ru}_4(\text{CO})_{12}$  as identified by  $^1\text{H}$  NMR ( $\delta$ -17.04 ppm ( $\text{CDCl}_3$ )) and  $^{13}\text{C}$  NMR ( $\delta$ 198.17 ppm ( $d_8$ -THF)). [68a] Suitable crystals for X-ray analysis were grown from slow diffusion of hexane into  $\text{CH}_2\text{Cl}_2$  at room temperature.

### B. DEPROTONATION OF $\text{H}_2\text{Ru}_6(\text{CO})_{17}$ WITH NaH

$\text{H}_2\text{Ru}_6(\text{CO})_{17}$  (0.0585g, 0.0536 mmoles) and NaH (0.0020g, 0.083 mmoles) were combined in a flask and THF introduced. The reaction was stirred at 55°C for 24 hours. THF was removed and  $\text{Ph}_4\text{AsCl}$  (0.0290g, 0.0692 mmoles) was added to the residue. A mixed solvent system of  $\text{CH}_2\text{Cl}_2/\text{THF}$  was condensed in. The reaction was stirred at room temperature for 8½ hours. The mixed solvent was removed and the flask taken into a glove box where an extractor was attached. Fresh  $\text{CH}_2\text{Cl}_2$  was condensed in to precipitate out  $\text{Ph}_4\text{AsHRu}_6(\text{CO})_{18}$  in 65% yield. The filtrate was identified as  $\text{Ph}_4\text{AsH}_3\text{Ru}_4(\text{CO})_{12}$  on the basis of  $^1\text{H}$  NMR.

The potassium salt was generated using KH in place of NaH. The reaction conditions were as follows: One or two equivalents of KH were reacted with one equivalent of  $\text{H}_2\text{Ru}_6(\text{CO})_{17}$ . The solution was stirred at 55°C for 12 hours.

NOTE: CO was observed to be liberated in these reduction reactions as identified by mass spectral analysis.

### C. PROTONATION OF $[\text{HRu}_6(\text{CO})_{18}]^-/[\text{H}_3\text{Ru}_4(\text{CO})_{12}]^-$ REACTION MIXTURES

Protonation of the product mixtures from either Reaction A or B in  $\text{CH}_2\text{Cl}_2$  or THF at room temperature with a strong acid ( $\text{H}_3\text{PO}_4$ , HCl, HBr, or  $\text{H}_2\text{SO}_4$ ) results in formation of  $\text{H}_2\text{Ru}_6(\text{CO})_{17}$  and  $\text{H}_4\text{Ru}_4(\text{CO})_{12}$  as identified by  $^1\text{H}$  NMR.

NOTE:  $\text{H}_4\text{Ru}_4(\text{CO})_{12}$  can be isolated from the above reaction in approximately 25%; therefore, approximately 1 equivalent CO is

liberated upon deprotonation. This liberated CO then reacts to form  $[\text{HRu}_6(\text{CO})_{18}]^-$ .

#### D. HYDROGENATION OF $\text{H}_2\text{Ru}_6(\text{CO})_{17}$

##### 1. With 1 atm $\text{H}_2$

An atmosphere of  $\text{H}_2$  was expanded over a  $\text{CH}_2\text{Cl}_2$  solution of  $\text{H}_2\text{Ru}_6(\text{CO})_{17}$  (0.010g, 0.0092 mmoles). This solution was stirred at room temperature for 6 hours. During this period the solution turned from purple to red-orange. Spectroscopic analysis indicated cluster fragmentation to give  $\text{H}_4\text{Ru}_4(\text{CO})_{12}$  (major product),  $\text{H}_2\text{Ru}_4(\text{CO})_{13}$  and trace amounts of  $\text{Ru}_3(\text{CO})_{12}$ .

##### 2. With 1 equivalent $\text{H}_2$ --NMR Study

The reaction was studied in a 5-mL reaction vessel with a sidearm connected to an NMR tube.  $\text{H}_2$  (0.0137 mmoles, 1.3eq) was measured using a calibrated bulb and then expanded over a  $\text{CD}_2\text{Cl}_2$  (dried, degassed) solution of  $\text{H}_2\text{Ru}_6(\text{CO})_{17}$  (0.0111g, 0.0102 mmoles) which was kept at  $-196^\circ\text{C}$ . The sample was then sealed under high vacuum. NMR data was collected at room temperature every 20 minutes over a period of 12 hours. During this reaction period no change in the NMR spectrum was observed. After 24 hours at room temperature the cluster was observed to fragment forming  $\text{H}_4\text{Ru}_4(\text{CO})_{12}$ . The IR spectrum of the solution indicated the presence of  $\text{Ru}_3(\text{CO})_{12}$  in trace amounts.

##### 3. With Bubbling $\text{H}_2$

$\text{H}_2\text{Ru}_6(\text{CO})_{17}$  (0.010g, 0.0095 mmoles) was dissolved in  $\text{CH}_2\text{Cl}_2$  and maintained at  $40^\circ\text{C}$ .  $\text{H}_2$  was bubbled through the solution for 2

hours. Spectroscopic analysis revealed  $\text{H}_4\text{Ru}_4(\text{CO})_{12}$  to be the as the major product.

If the reaction above is run at  $-10^\circ\text{C}$  for 4 hours, the products formed are  $\text{H}_4\text{Ru}_4(\text{CO})_{12}$  (major),  $\text{H}_2\text{Ru}_4(\text{CO})_{13}$  and trace amounts of  $\text{Ru}_3(\text{CO})_{12}$ .

#### E. CARBONYLATION OF $\text{H}_2\text{Ru}_6(\text{CO})_{17}$

##### 1. With 1 atm CO

An atmosphere of CO was expanded over a  $\text{CH}_2\text{Cl}_2$  solution of  $\text{H}_2\text{Ru}_6(\text{CO})_{17}$  (0.0206g, 0.0189 mmoles). This solution was stirred at room temperature over a period of 5 hours. During the course of the reaction the solution changed from purple to red to orange-red to orange and finally yellow-orange. Removal of the solvent and purification by TLC (silica gel,  $\text{CH}_2\text{Cl}_2$ ) gave  $\text{H}_2\text{Ru}_4(\text{CO})_{13}$  and  $\text{Ru}_3(\text{CO})_{12}$  as identified by  $^1\text{H}$  NMR and IR.

If the reaction is run for 1-1½ hours as opposed to 5 hours, formation of  $\text{H}_4\text{Ru}_4(\text{CO})_{12}$  in addition to the  $\text{H}_2\text{Ru}_4(\text{CO})_{13}$  and  $\text{Ru}_3(\text{CO})_{12}$  is observed.

##### 2. With 1 equivalent CO--NMR Study

The reaction was studied in a 5-mL reaction vessel with a sidearm connected to an NMR tube. CO (0.0106 mmoles, 1.1eq) was measured using a calibrated bulb and then expanded over a  $\text{CD}_2\text{Cl}_2$  (dried, degassed) solution of  $\text{H}_2\text{Ru}_6(\text{CO})_{17}$  (0.0104g, 0.0095 mmoles) which was kept at  $-196^\circ\text{C}$ . The sample was then sealed under high vacuum. NMR data was collected at room temperature every 20 minutes over a period

of 12 hours. (The initial spectrum was taken after the sample equilibrated to room temperature, approx. 5 minutes.) During this reaction period no change in the NMR spectrum was observed. After 48 hours at room temperature and continuing for an additional 7 days the cluster was observed to fragment forming  $\text{H}_4\text{Ru}_4(\text{CO})_{12}$  (major), and  $\text{H}_2\text{Ru}_4(\text{CO})_{13}$  (minor).  $\text{Ru}_3(\text{CO})_{12}$  was also observed *via* IR.

### 3. With Bubbling CO

$\text{H}_2\text{Ru}_6(\text{CO})_{17}$  (0.011g, 0.0098 mmoles) was dissolved in  $\text{CH}_2\text{Cl}_2$  and maintained at  $40^\circ\text{C}$ . CO was bubbled through this solution for 2 hours. Removal of the  $\text{CH}_2\text{Cl}_2$  and subsequent spectroscopic analysis indicated cluster fragmentation as previously observed.

If the reaction is run for 5 hours at  $-10^\circ\text{C}$  cluster fragmentation is still observed.

### F. HYDROBORATION OF $\text{H}_2\text{Ru}_6(\text{CO})_{17}$

$\text{H}_2\text{Ru}_6(\text{CO})_{17}$  (0.0420g, 0.0385 mmoles) was dissolved in  $\text{CH}_2\text{Cl}_2$  and frozen at  $-196^\circ\text{C}$ .  $\text{B}_2\text{H}_6$  (0.0211 mmoles, 0.55eq) and  $\text{Me}_2\text{O}$  (0.0423 mmoles, 1.1eq) were condensed over into the reaction flask and the flask covered with foil. The reaction was then stirred at room temperature for 3 days. A white precipitate formed which was filtered off and subsequently identified as  $\text{B}_2\text{O}_3$  by  $^{11}\text{B}$  NMR ( $\delta 21.54$  (s) ppm ( $d_6$ -acetone)). Removal of the solvent after filtration afforded a red-brown residue which exhibited hydride signals between  $\delta -18.0$  to  $-18.5$  ppm along with some  $\text{H}_4\text{Ru}_4(\text{CO})_{12}$  ( $\delta -17.74$  ppm

( $\text{CD}_2\text{Cl}_2$ ). The residue decomposed upon purification by TLC (silica gel, cyclohexane) to give  $\text{H}_4\text{Ru}_4(\text{CO})_{12}$  as the only isolable product.

#### G. REACTION OF $\text{H}_2\text{Ru}_6(\text{CO})_{17}$ WITH OXONIUM SALTS

##### 1. With $\text{Me}_3\text{OBF}_4$

$\text{H}_2\text{Ru}_6(\text{CO})_{17}$  (0.0093g, 0.0085 mmoles) and  $\text{Me}_3\text{OBF}_4$  (0.0368g, 0.248 mmoles) were combined in a flask to which  $\text{CH}_2\text{Cl}_2$  was introduced. The reaction was allowed to stir at room temperature for 3 days. The  $\text{CH}_2\text{Cl}_2$  was removed and the residue taken up in  $\text{CD}_2\text{Cl}_2$ .  $^1\text{H}$  NMR indicates formation of  $\text{H}_2\text{Ru}_4(\text{CO})_{13}$  presumably from the decomposition of  $\text{H}_2\text{Ru}_6(\text{CO})_{17}$ .  $^1\text{H}$  NMR also exhibits a singlet at  $\delta 12.22$  ppm which could be indicative of a species with an interstitial hydride similar to that found for  $[\text{HRu}_6(\text{CO})_{18}]^-$  ( $\delta 16.43$  ppm). [86] Treatment by TLC led to decomposition products that could not be removed from the silica gel. Purification by fractional crystallization techniques did not prove to be fruitful either.

##### 2. With $\text{Et}_3\text{OPF}_6$

Reaction with  $\text{Et}_3\text{OPF}_6$  for 5 days at room temperature as above gives a species exhibiting a signal at  $\delta 8.83$  ppm ( $\text{CD}_2\text{Cl}_2$ ) in the proton NMR. NMR also displayed peaks which can be attributed to the  $-\text{C}_2\text{H}_5$  group ( $\delta 3.61$  (q), 2.1 (t) ppm). However, since purification was again futile one can not say with certainty that the species formed contains an ethoxy moiety. Again, the downfield signal could indicate an interstitial hydride; but since this signal is higher upfield it could indicate  $-\text{CH}$  formation. Other products observed are  $\text{H}_4\text{Ru}_4(\text{CO})_{12}$  and minor amounts of  $\text{H}_2\text{Ru}_4(\text{CO})_{13}$ .

VIII. STRUCTURE DETERMINATION OF  $\text{H}_2\text{Ru}_6(\text{CO})_{17}$ 

For X-ray examination and data collection, a suitable crystal of approximate dimensions 0.200 x 0.150 x 0.050 mm was mounted in a glass capillary. All X-ray data were collected at  $-40^\circ\text{C}$  on an Enraf-Nonius diffractometer with graphite-monochromated Mo K $\alpha$  radiation.

Table 2 gives crystallographic data for  $\text{H}_2\text{Ru}_6(\text{CO})_{17}$ . Unit cell parameters (a, b, c,  $\alpha$ ,  $\beta$ ,  $\gamma$ ) were obtained by least squares refinement of the angular settings ( $\phi$ ,  $\omega$ ,  $\kappa$ ) from 25 reflections, well-distributed in reciprocal space and lying in a  $2\theta$  range of  $24-30^\circ$ . Intensity data were collected in the  $\omega-2\theta$  scan mode with  $4 \leq 2\theta \leq 55^\circ$ . Four standard reflections were monitored and showed no significant decay. Data were corrected for Lorentz and polarization effects. The intensities were also corrected for absorption by using an empirical method based on the crystal orientation and measured  $\psi$  scans.

The structure was solved by a combination of the direct method MULTAN 11/82 [140] and the difference Fourier technique, and refined by full-matrix least squares. Analytical atomic scattering factors were used throughout the structure refinement with both the real and imaginary components of the anomalous dispersion included for all atoms. The heavy atoms first appeared in the E-map. Then the positions of the remaining atoms were determined from a Fourier synthesis which was phased on the metal atoms. Full-matrix least

squares refinement minimizing  $w(|F_o| - |F_c|)^2$  was carried out by using anisotropic thermal parameters. The weights were taken as  $w = [\sigma(I)^2 + (kI)^2]^{-1/2}$  where  $k = 0.04$  was chosen to make  $w\Delta F^2$  uniformly distributed in  $|F_o|$ . The full-matrix least squares refinement converged with  $R_f = \Sigma(|F_o| - |F_c|) / \Sigma |F_o|$  and  $R_{wf} = [\Sigma w(|F_o| - |F_c|)^2 / \Sigma |F_o|^2]^{1/2}$  equal to 0.028 and 0.032, respectively, and GOF = 0.989.

The capping hydrogens were located directly from the difference Fourier synthesis and are in agreement with other structures. [95-100] The positions and thermal parameters of the hydrogens were included in the least squares refinement. Final atomic positional and isotropic thermal parameters are given in Table 17.

#### IX. STRUCTURE DETERMINATION OF $[PPh_4]_2[Ru_6(CO)_{18}]$

For X-ray examination and data collection, a suitable crystal grown from MeOH/CH<sub>2</sub>Cl<sub>2</sub>/pentane was mounted in a glass capillary. All X-ray data were collected at 25°C on an Enraf-Nonius diffractometer with graphite-monochromated Mo K $\alpha$  radiation.

Table 5 gives crystallographic data for  $[PPh_4]_2[Ru_6(CO)_{18}]$ . Unit cell parameters (a, b, c,  $\alpha$ ,  $\beta$ ,  $\gamma$ ) were obtained by least squares refinement of the angular settings ( $\phi$ ,  $\omega$ ,  $\kappa$ ) from 25 reflections, well-distributed in reciprocal space and lying in a  $2\theta$  range of 24-30°. Intensity data were collected in the  $\omega$ -2 $\theta$  scan mode with  $4 \leq 2\theta \leq 40^\circ$ . Three standard reflections were monitored and showed moderate (4%) decay. Data were corrected for Lorentz and polarization and decay effects.

Table 17. Atomic Positional Parameters and Isothermal Parameters  
(and Esd's) for  $\text{H}_2\text{Ru}_6(\text{CO})_{17}$ .

<u>ATOM</u>	<u>X</u>	<u>Y</u>	<u>Z</u>	<u>B(iso)</u>
Ru(1)	0.70731(7)	0.25043(5)	0.15385(4)	1.53(1)
Ru(2)	0.96165(8)	0.50013(5)	0.21079(4)	1.98(1)
Ru(3)	0.74110(8)	0.02328(5)	0.21960(4)	2.00(1)
Ru(4)	0.98069(7)	0.27580(5)	0.28909(4)	1.59(1)
Ru(5)	0.61249(8)	0.16162(5)	0.32692(4)	1.93(1)
Ru(6)	0.72866(8)	0.41516(5)	0.32114(4)	1.90(1)
O(11)	0.9125(7)	0.2334(5)	0.0062(4)	3.2(1)
O(12)	0.3764(8)	0.0352(6)	0.0582(4)	3.7(2)
O(13)	0.5170(8)	0.4103(6)	0.0553(4)	4.2(1)
O(21)	1.2417(9)	0.7307(6)	0.3213(4)	4.6(2)
O(22)	0.8004(9)	0.6831(6)	0.1255(5)	4.6(2)
O(23)	1.1920(8)	0.5078(6)	0.0701(4)	3.8(1)
O(31)	0.8470(9)	-0.1573(6)	0.3368(4)	4.9(2)
O(32)	0.4211(9)	-0.2070(6)	0.1386(5)	5.0(2)
O(33)	0.9579(8)	-0.0325(6)	0.0867(4)	4.3(2)
O(41)	1.2731(8)	0.4976(5)	0.4055(4)	3.5(1)
O(42)	1.2256(7)	0.2488(6)	0.1639(4)	3.7(1)
O(43)	1.0912(8)	0.1130(6)	0.4239(4)	4.0(2)
O(51)	0.2412(8)	-0.0205(6)	0.2650(5)	4.1(2)
O(52)	0.3316(9)	-0.0012(7)	0.5290(4)	6.5(2)
O(56)	0.4676(8)	0.3092(6)	0.4603(4)	3.8(1)
O(61)	0.9553(8)	0.6354(6)	0.4562(4)	3.9(2)
O(62)	0.5129(8)	0.5768(5)	0.2588(4)	4.1(1)
C(11)	0.841(1)	0.2410(7)	0.0629(5)	2.3(2)
C(12)	0.506(1)	0.1055(7)	0.0994(5)	2.6(2)
C(13)	0.599(1)	0.3602(7)	0.0945(5)	2.6(2)
C(21)	1.135(1)	0.6426(7)	0.2808(5)	3.1(2)
C(22)	0.859(1)	0.6140(7)	0.1566(5)	2.9(2)

Table 17. Atomic Positional Parameters and Isothermal Parameters  
(and Esd's) for  $H_2Ru_6(CO)_{17}$  (cont.).

<u>ATOM</u>	<u>X</u>	<u>Y</u>	<u>Z</u>	<u>B(iso)</u>
C(23)	1.107(1)	0.5029(7)	0.1223(5)	2.9(2)
C(31)	0.807(1)	-0.0866(7)	0.2933(6)	3.0(2)
C(32)	0.538(1)	-0.1196(7)	0.1679(6)	2.9(2)
C(33)	0.874(1)	-0.0107(7)	0.1350(6)	3.1(2)
C(41)	1.160(1)	0.4233(7)	0.3590(5)	2.4(2)
C(42)	1.1296(9)	0.2590(7)	0.2082(5)	2.3(2)
C(43)	1.044(1)	0.1647(7)	0.3705(5)	2.5(2)
C(51)	0.384(1)	0.0458(7)	0.2895(5)	2.6(2)
C(52)	1.645(1)	1.0592(8)	0.4156(5)	3.6(2)
C(56)	0.544(1)	0.2936(8)	0.4071(5)	2.9(2)
C(61)	0.869(1)	0.5509(7)	0.4049(5)	2.6(2)
C(62)	0.597(1)	0.5167(7)	0.2845(5)	2.5(2)
H(1)	0.583(9)	0.281(7)	0.236(4)	2(2)*
H(2)	0.845(7)	0.300(5)	0.366(4)	1(1)*

Starred atoms were refined isotropically.

Anisotropically refined atoms are given in the form of the isotropic equivalent thermal parameter defined as:

$$(4/3) * [a^2 * \beta(1,1) + b^2 * \beta(2,2) + c^2 * \beta(3,3) + ab(\cos \gamma) * \beta(1,2) + ac(\cos \beta) * \beta(1,3) + bc(\cos \alpha) * \beta(2,3)]$$

The structure was solved by a combination of the direct method MULTAN 11/82 [140] and the difference Fourier technique, and refined by full-matrix least squares. Analytical atomic scattering factors were used throughout the structure refinement with both the real and imaginary components of the anomalous dispersion included for all atoms. The heavy atoms first appeared in the E-map. Then the positions of the remaining atoms were determined from a Fourier synthesis which was phased on the metal atoms.

Since the crystal structure had been previously determined by Shore and Hsu [102] and Johnson and Lewis, [85] further refinement was abandoned after all the atoms were refined isotropically. The  $R_F$  value had converged below 10% at this point.

#### X. STRUCTURE DETERMINATION OF $H_2RuOs_3(CO)_{13}$

For X-ray examination and data collection, a suitable crystal grown from pentane solution of approximate dimensions 0.300 x 0.350 x 0.275 mm was mounted in a glass capillary. All X-ray data were collected at 25°C on an Enraf-Nonius diffractometer with graphite-monochromated Mo  $K\alpha$  radiation.

Table 8 gives crystallographic data for  $H_2RuOs_3(CO)_{13}$ . Unit cell parameters (a, b, c,  $\alpha$ ,  $\beta$ ,  $\gamma$ ) were obtained by least squares refinement of the angular settings ( $\phi$ ,  $\kappa$ ,  $\omega$ ) from 25 reflections, well-distributed in reciprocal space and lying in a  $2\theta$  range of 24-30°. Intensity data were collected in the  $\omega$ - $2\theta$  scan mode with  $4 \leq 2\theta \leq 55^\circ$ . Three standard reflections were monitored and showed no significant decay; however, data were corrected for decay nonetheless. Data were also corrected

for Lorentz and polarization effects. The intensities were also corrected for absorption by using an empirical method based on the crystal orientation and measured  $\psi$  scans.

The structure was solved by a combination of the direct method MULTAN 11/82 [140] and the difference Fourier technique, and refined by full-matrix least squares. Analytical atomic scattering factors were used throughout the structure refinement with both the real and imaginary components of the anomalous dispersion included for all atoms. The heavy atoms first appeared on the E-map. Then the positions of the remaining atoms were determined from a Fourier synthesis which was phased on the metal atoms. Full-matrix least squares refinement minimizing  $w(|F_o| - |F_c|)^2$  was carried out by using anisotropic thermal parameters for all atoms except C11, C22, C42 and C44 which were refined isotropically. These atoms were so refined due to the appearance of negative anisotropic thermal parameters. The weights were taken as  $w = [\sigma(I)^2 + (kI)^2]^{-1/2}$  where  $k = 0.05$  was chosen to make  $w\Delta F^2$  uniformly distributed in  $|F_o|$ . The full-matrix least squares refinement converged with  $R_f = \Sigma(|F_o| - |F_c|) / \Sigma |F_o|$  and  $R_{wf} = [\Sigma w(|F_o| - |F_c|)^2 / \Sigma |F_o|^2]^{1/2}$  equal to 0.064 and 0.075, respectively, and GOF = 2.065. Final atomic positional and isotropic thermal parameters are given in Table 18.

## XI. STRUCTURE DETERMINATION OF [PPN][HRu<sub>6</sub>(CO)<sub>18</sub>]

For X-ray examination and data collection, a suitable crystal of approximate dimensions 0.250 x 0.275 x 0.325 mm was mounted in a glass

Table 18. Atomic Positional Parameters and Isothermal Parameters  
(and Esd's) for  $\text{H}_2\text{RuOs}_3(\text{CO})_{13}$ .

<u>ATOM</u>	<u>X</u>	<u>Y</u>	<u>Z</u>	<u>B(iso)</u>
Os(1)	0.17489(4)	0.2777(1)	0.59779(8)	2.87(2)
Os(2)	0.13991(4)	0.2195(1)	0.76263(8)	2.63(2)
Os(3)	0.10332(4)	0.4400(1)	0.61151(8)	2.94(2)
Ru(4)	0.08985(7)	0.1638(2)	0.5578(1)	2.14(4)
O(11)	0.2419(9)	0.511(3)	0.675(2)	8.0(9)
O(12)	0.2499(9)	0.085(3)	0.594(2)	7.6(8)
O(13)	0.1551(8)	0.366(2)	0.379(1)	4.9(6)
O(21)	0.198(1)	0.325(2)	0.971(2)	6.7(8)
O(22)	0.1639(9)	-0.077(2)	0.814(2)	6.4(7)
O(23)	0.0590(7)	0.167(2)	0.826(2)	6.0(6)
O(31)	0.165(1)	0.686(2)	0.673(2)	6.5(7)
O(32)	0.0323(9)	0.596(2)	0.663(2)	6.8(7)
O(33)	0.0706(8)	0.530(2)	0.390(1)	5.3(6)
O(41)	0.0478(9)	0.161(2)	0.322(2)	6.3(7)
O(42)	0.0049(9)	0.297(3)	0.573(2)	6.5(7)
O(43)	0.1558(9)	-0.050(2)	0.537(2)	6.6(7)
O(44)	0.045(1)	-0.089(3)	0.603(2)	11(1)
C(11)	0.217(1)	0.421(3)	0.648(2)	4.2(6)*
C(12)	0.222(1)	0.155(3)	0.598(2)	4.7(8)
C(13)	0.1604(9)	0.329(3)	0.460(2)	3.2(6)
C(21)	0.178(1)	0.288(3)	0.896(2)	4.3(7)
C(22)	0.153(1)	0.031(3)	0.790(2)	4.0(6)*
C(23)	0.089(1)	0.192(3)	0.801(2)	3.9(7)
C(31)	0.146(1)	0.592(3)	0.654(2)	3.4(7)
C(32)	0.058(1)	0.535(3)	0.643(2)	4.7(7)
C(33)	0.083(1)	0.492(2)	0.473(2)	3.5(7)

Table 18. Atomic Positional Parameters and Isothermal Parameters  
(and Esd's) for  $\text{H}_2\text{RuOs}_3(\text{CO})_{13}$  (cont.).

<u>ATOM</u>	<u>X</u>	<u>Y</u>	<u>Z</u>	<u>B(iso)</u>
C(41)	0.065(1)	0.164(3)	0.415(2)	3.9(7)
C(42)	0.041(1)	0.271(3)	0.570(2)	4.2(6)*
C(43)	0.135(1)	0.054(3)	0.547(2)	5.5(9)
C(44)	0.062(1)	0.011(3)	0.586(3)	4.9(7)*

Starred atoms were refined isotropically.

Anisotropically refined atoms are given in the form of the isotropic equivalent thermal parameter defined as:

$$(4/3) * [a^2 * \beta(1,1) + b^2 * \beta(2,2) + c^2 * \beta(3,3) + ab(\cos \gamma) * \beta(1,2) + ac(\cos \beta) * \beta(1,3) + bc(\cos \alpha) * \beta(2,3)]$$

capillary. All X-ray data were collected at  $-50^{\circ}\text{C}$  on an Enraf-Nonius diffractometer with graphite-monochromated Mo  $K\alpha$  radiation.

Table 13 gives crystallographic data for  $[\text{PPN}][\text{HRu}_6(\text{CO})_{18}]$ . Unit cell parameters ( $a$ ,  $b$ ,  $c$ ,  $\alpha$ ,  $\beta$ ,  $\gamma$ ) were obtained by least squares refinement of the angular settings ( $\phi$ ,  $\kappa$ ,  $\omega$ ) from 25 reflections, well-distributed in reciprocal space and lying in a  $2\theta$  range of  $24$ - $30^{\circ}$ . Intensity data were collected in the  $\omega$ - $2\theta$  scan mode with  $4 \leq 2\theta \leq 45^{\circ}$ . Three standard reflections were monitored and showed no significant decay. Data were corrected for Lorentz and polarization effects. The intensities were also corrected for absorption by using an empirical method based on the crystal orientation and measured  $\psi$  scans.

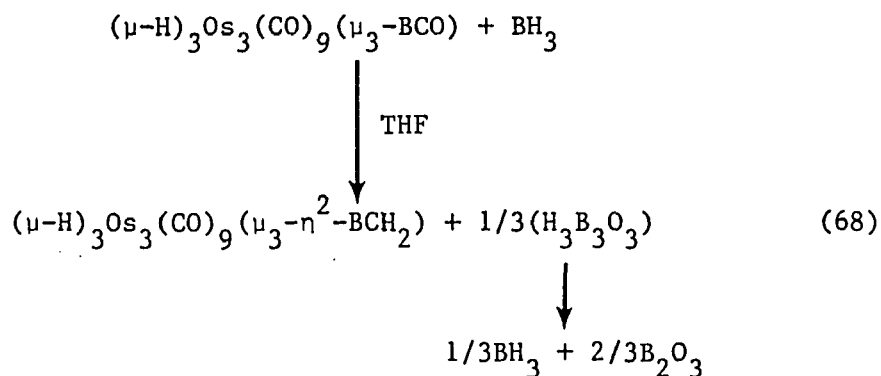
The structure was solved by a combination of the direct method MULTAN 11/82 [140] and the difference Fourier technique, and refined by full-matrix least squares. Analytical atomic scattering factors were used throughout the structure refinement with both the real and imaginary components of the anomalous dispersion included for all atoms. The heavy atoms first appeared in the E-map. Then the positions of the remaining atoms were determined from a Fourier synthesis which was phased on the metal atoms.

Since the crystal structure had been previously determined by Johnson and Lewis [84,86] further refinement was abandoned after refinement of the structure isotropically brought  $R_f$  below 10%. As with Johnson and Lewis, the interstitial hydride could not be located even after low temperature data collection.

## APPENDIX

### REACTION OF $\text{H}_2\text{Os}_3(\text{CO})_9\text{CCO}$ WITH $\text{B}_2\text{H}_6$

The thrust behind cluster chemistry is its connection to surface science and catalysis. Keeping this in mind, the cluster chemist always attempts to synthesize models for molecules on a metal surface. One of the key reactions in catalysis today is the conversion of CO to hydrocarbons. This idea was the premise on which the reduction of  $(\mu\text{-H})_3\text{Os}_3(\text{CO})_9(\mu_3\text{-BCO})$  with  $\text{BH}_3$  was carried out to form the triosmium borylidene carbonyl,  $(\mu\text{-H})_3\text{Os}_3(\text{CO})_9(\mu_3\text{-}\eta^2\text{-BCH}_2)$ . [159] (Equation 68)

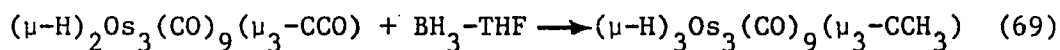


The borylidyne is reduced by the diborane to form the borylidene cluster. This reaction [159] is believed to occur through initial attack of  $\text{BH}_3$  on the oxygen of the  $\text{-BCO}$  unit followed by transfer of

two hydrides to the carbon atoms and subsequent elimination of HBO to form the borydene and  $H_3B_3O_3$  which then decomposes to  $B_2O_3$  and  $B_2H_6$ . [160]

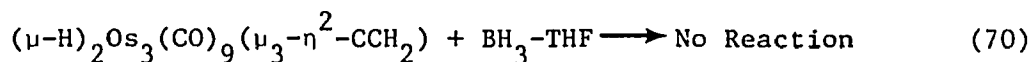
The borylidene is of interest due to its possible relationship to an intermediate which might form on a metal boride surface during the methanation of CO in the presence of a metal boride catalyst. The next logical question is: Could this reduction with  $BH_3$  be carried out using  $(\mu-H)_2Os_3(CO)_9(\mu_3-CCO)$  to model an intermediate on a metal carbide surface?

The triosmium ethylidyne cluster,  $(\mu-H)_3Os_3(CO)_9(\mu-CCH_3)$ , which has been previously reported by Deeming [154] is the resulting product when diborane is reacted at ambient temperature with the ketenylidene,  $(\mu-H)_2Os_3(CO)_9(\mu_3-CCO)$ . [98,161] (Equation 69)



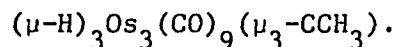
In the case of the ketenylidene, a two-fold reduction seems to be occurring to produce the ethylidyne rather than the vinylidene.

In an independent experiment, (Equation 70) diborane was reacted with the vinylidene under identical conditions as in the ketenylidene case; however, no reaction was observed to occur when followed by proton NMR.

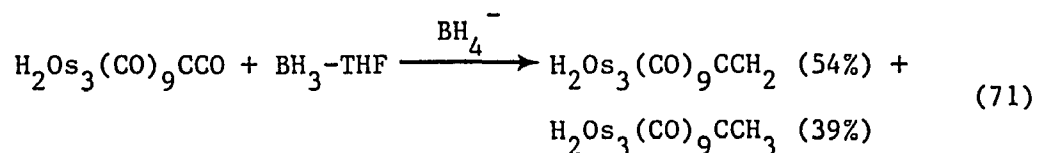


Thus the reduction of  $(\mu-H)_2Os_3(CO)_9(\mu_3-CCO)$  appears to proceed *via* a

concerted reduction mechanism involving  $\text{BH}_3$  coordination to the oxygen of the  $-\text{CCO}$  moiety as opposed to a two-step reduction to first form the vinylidene and then the final product,



However, it has been suggested by Shapley [162] that the source of diborane may affect the reaction outcome. He reports that if commercial  $\text{BH}_3\text{-THF}$ , containing ca. 5 mole %  $\text{NaBH}_4$  as a stabilizer, is employed the vinylidene,  $(\mu\text{-H})_2\text{Os}_3(\text{CO})_9(\mu_3\text{-}\eta^2\text{-CCH}_2)$  is observed in 54% yield. (Equation 71)



These results suggest that  $\text{BH}_4^-$  acts as a reducing agent forming the potential intermediate  $[\text{H}_2\text{Os}_3(\text{CO})_9\text{CCHO}]^-$  which may be involved in an "ionic" pathway leading to the formation of the observed product. [162] However, he later reports that in an independent reaction of  $[\text{H}_2\text{Os}_3(\text{CO})_9\text{CCHO}]^-$  with  $\text{BH}_3\text{-THF}$  no evidence for formation of either  $\text{H}_2\text{Os}_3(\text{CO})_9\text{CCH}_2$  or  $\text{H}_3\text{Os}_3(\text{CO})_9\text{CCH}_3$  was observed. [162]

Independent reactions of  $\text{H}_2\text{Os}_3(\text{CO})_9\text{CCO}$  in the presence of either commercial  $\text{BH}_3\text{-THF}$  or pure  $\text{B}_2\text{H}_6$  in THF, show no signs of  $[\text{HOs}_3(\text{CO})_9\text{CCHO}]^-$  or  $\text{H}_2\text{Os}_3(\text{CO})_9\text{CCH}_2$  when followed by proton NMR. The only product formed is  $\text{H}_3\text{Os}_3(\text{CO})_9\text{CCH}_3$ .

### A. Reaction of $\text{H}_2\text{Os}_3(\text{CO})_9\text{CCO}$ With Pure $\text{B}_2\text{H}_6$

In a typical reaction, an excess of  $\text{B}_2\text{H}_6$  (0.276 mmoles) was condensed into a THF solution of  $\text{H}_2\text{Os}_3(\text{CO})_9\text{CCO}$  (0.023 mmoles). This solution was stirred at room temperature for 12 hours. The volatiles were removed and the resulting yellow residue was purified by TLC (silica gel,  $\text{CH}_2\text{Cl}_2$ :hexane). The product was identified as  $\text{H}_3\text{Os}_3(\text{CO})_9\text{CCH}_3$  by comparison of its  $^1\text{H}$  NMR spectrum to that reported by Deeming [154] and Yesinowski and Bailey [163] and IR spectrum reported by Evans and McNulty. [164] The product was isolated in ca. 30% yield.  $^1\text{H}$  NMR ( $\text{CDCl}_3$ ,  $30^\circ\text{C}$ )  $\delta$ 4.54 (s,2H), -18.58 (s,3H) ppm; (Fig. 52) IR ( $\text{CHCl}_3$ )  $\nu_{\text{CO}}$  2077(m), 2068(m,sh), 2056(m), 2033(s,sh), 2021(s)  $\text{cm}^{-1}$ . (Fig. 53) The mass spectrum shows a parent ion peak which corresponds to the molecular formula  $^{12}_{11}\text{C}_{11}^{16}\text{H}_6^{192}\text{O}_9\text{Os}_3$   $m/z(\text{obsd})$  858,  $m/z(\text{calcd})$  858. The sequential loss of each of the nine carbonyls from the molecular ion was visible in the mass spectrum.

### B. NMR Reaction of $\text{H}_2\text{Os}_3(\text{CO})_9\text{CCO}$ With Pure $\text{B}_2\text{H}_6$ in THF

An NMR tube sealed to an adaptor and attached to the vacuum line was charged with a  $d_8$ -THF solution of  $\text{H}_2\text{Os}_3(\text{CO})_9\text{CCO}$  (0.0095 mmoles) and cooled to  $-196^\circ\text{C}$ . While at this temperature  $\text{B}_2\text{H}_6$  (0.0095 mmoles) was condensed onto the solution and the NMR tube sealed under vacuum. The NMR sample was warmed to room temperature and the first spectrum recorded after 10 minutes reaction time. The reaction was followed at room temperature by  $^1\text{H}$  and  $^{11}\text{B}$  NMR over a period of 16 hours. Conversion from  $\text{H}_2\text{Os}_3(\text{CO})_9\text{CCO}$  to  $\text{H}_3\text{Os}_3(\text{CO})_9\text{CCH}_3$  is approximately 50-

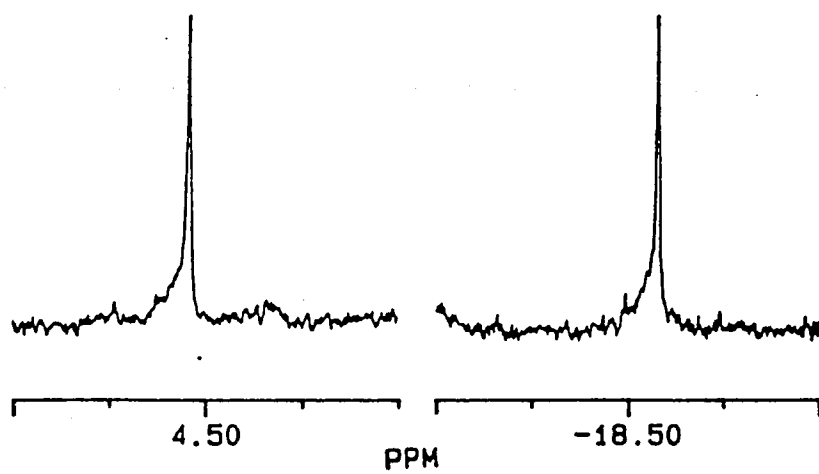


Figure 52. Proton NMR Spectrum of  $(\mu\text{-H})_3\text{Os}_3(\text{CO})_9(\mu_3\text{-CCH}_3)$ .

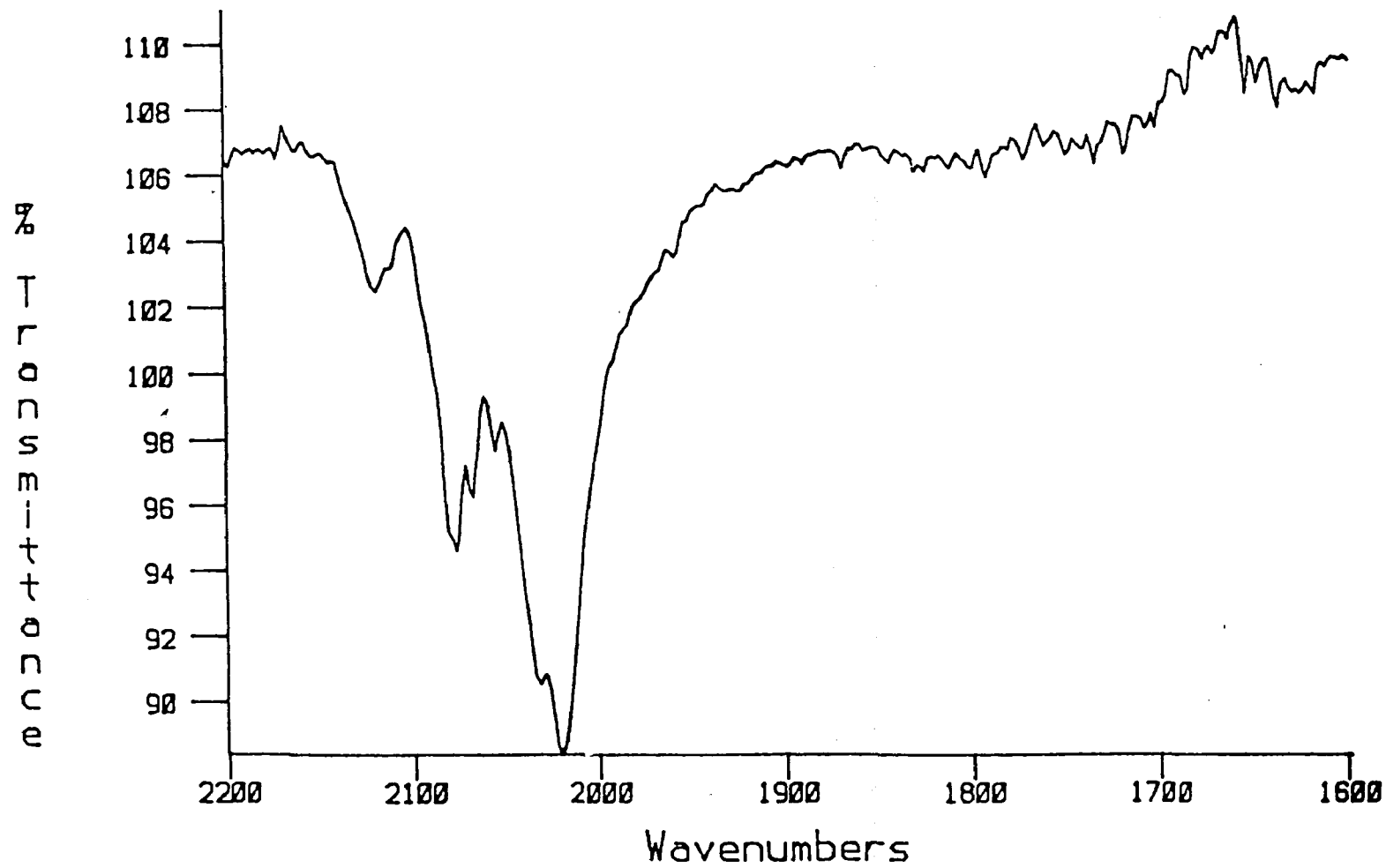


Figure 53. IR Spectrum of  $(\mu\text{-H})_3\text{Os}_3(\text{CO})_9(\mu_3\text{-CCH})_3$ .

55%. The boron-11 spectrum shows formation of a boron oxide species at  $\delta 4.1$  (t,  $J_{B-H} = 132$  Hz) ppm.

In a second NMR experiment,  $B_2H_6$  (0.012 mmoles) was reacted with  $H_2Os_3(CO)_9CCO$  (0.024 mmoles).  $^1H$  indicates formation of  $H_3Os_3(CO)_9CCH_3$  in approximately 25% yield after 16 hours and leveling off at 28% after 22 hours.

C. NMR Reaction of  $H_2Os_3(CO)_9CCO$  With Pure  $BH_3$ -THF in  $CH_2Cl_2$

An NMR tube sealed to an adaptor and attached to the vacuum line was charged with  $H_2Os_3(CO)_9CCO$  (0.0426 mmoles) in  $CD_2Cl_2$  (0.4 mL).  $B_2H_6$  (0.2130 mmoles) and THF (0.4295 mmoles) were condensed over and the tube cooled to  $-196^\circ C$  and sealed under vacuum. The NMR sample was warmed to room temperature and the first spectrum recorded after 5 minutes reaction time. The reaction was followed by  $^1H$  and  $^{11}B$  NMR over a period of 5 hours. During this time  $^1H$  NMR showed only  $H_3Os_3(CO)_9CCH_3$  formation. The  $^{11}B$  NMR showed formation of the previously observed oxide at  $\delta 4.1$  (t,  $J_{B-H} = 132$  Hz) ppm along with a new species exhibiting a septet at  $\delta 18.00$  (septet,  $J_{B-H} = 184$  Hz) ppm which upon proton decoupling collapses to a singlet.

D. NMR Reaction of  $H_2Os_3(CO)_9CCO$  With Commercial  $BH_3$ -THF in  $CH_2Cl_2$

$CD_2Cl_2$  (0.4 mL) and  $BH_3$ -THF (0.4 mL @ 1M, 0.4 mmol, ca. 5 mol %  $NaBH_4$  as stabilizer) were added to  $H_2Os_3(CO)_9CCO$  (0.0424 mmoles) under  $N_2$  in an NMR tube. The contents of the tube were frozen at  $-196^\circ C$  and the  $N_2$  purged from the system. The NMR tube was sealed under vacuum and then warmed to room temperature. The reaction was followed by  $^1H$

and  $^{11}\text{B}$  NMR over a period of 10 hours recording the first spectrum after 5 minutes of reaction time. During this time only the formation of  $\text{H}_3\text{Os}_3(\text{CO})_9\text{CCH}_3$  was observed.

E. Reaction of  $\text{H}_2\text{Os}_3(\text{CO})_9\text{CCH}_2$  With Pure  $\text{B}_2\text{H}_6$

An excess of  $\text{B}_2\text{H}_6$  (0.2758 mmoles) was condensed into a THF solution of  $\text{H}_2\text{Os}_3(\text{CO})_9\text{CCH}_2$  (0.0208 mmoles). The solution was then stirred at room temperature for 12 hours. The volatiles were removed and the residue dissolved in  $\text{CDCl}_3$ .  $^1\text{H}$  NMR showed no formation of  $\text{H}_3\text{Os}_3(\text{CO})_9\text{CCH}_3$  or other cluster species, only the starting vinylidene cluster.

F. NMR Reaction of  $\text{H}_2\text{Os}_3(\text{CO})_9\text{CCH}_2$  With Pure  $\text{B}_2\text{H}_6$  in THF.

$\text{B}_2\text{H}_6$  (0.0132 mmoles) was reacted with  $\text{H}_2\text{Os}_3(\text{CO})_9\text{CCH}_2$  (0.0132 mmoles) in a manner analogous to that described in the  $\text{H}_2\text{Os}_3(\text{CO})_9\text{CCO}$  case.  $^1\text{H}$  NMR indicated no formation of  $\text{H}_3\text{Os}_3(\text{CO})_9\text{CCH}_3$  after 12 hours at room temperature. No reaction was observed even after 1 week.

## REFERENCES

1. Cotton, F. A., *Quart. Rev. (Lond.)* 1966, 20, 389.
2. (a) Farrar, D. H.; Goudsmit, R. J., "Metal Clusters"; Moskowitz, M., Ed.; John Wiley & Sons: New York, 1986; 30-35; (b) Shore, S. G., "Rings, Clusters, and Polymers of the Main Group Elements"; Cowley, A. H., Ed.; ACS Symposium Series 232; Am. Chem. Soc.; 1983; 12; (c) Williams, P. D.; Curtis, M. D., *Inorg. Chem.* 1986, 25, 4562; (d) Cotton, F. A.; Wilkinson, G.; "Advances in Inorganic Chemistry A Comprehensive Text"; Wiley-Interscience: New York, 1980; 1178.
3. Muetterties, E. L.; Rhodin, T. N.; Band, E.; Brucker, C. F.; Pretzer, W. R., *Chem. Rev.* 1979, 79, 91.
4. Muetterties, E. L., *Chem. Soc. Rev.* 1982, 11, 283.
5. Muetterties, E. L., *Pure and Applied Chem.* 1982, 54, 83.
6. (a) Muetterties, E. L., *Angew. Chem. Int. Ed. Engl.* 1978, 17, 545; (b) Muetterties, E. L.; Krause, M. J., *Ibid* 1983, 22, 135.
7. Evans, J., *Chem. Soc. Rev.* 1981, 10, 159.
8. Calvert, R. B.; Shapley, J. R.; Schultz, A. J.; Williams, J. M.; Suib, S. L.; Stucky, G. D., *J. Am. Chem. Soc.* 1978, 100, 6240.
9. Thomas, M. G.; Beier, B. F.; Muetterties, E. L., *J. Am. Chem. Soc.* 1976, 98, 1296.
10. Smith, A. K.; Basset, J. M., *J. Mol. Catal.* 1977, 2, 229.
11. Deeba, J.; Gates, B. C., *J. Catal.* 1981, 67, 303.
12. Bailey, D. C.; Langer, S. H., *Chem. Rev.* 1981, 81, 109.
13. Doi, Y.; Yokota, A.; Miyake, J.; Soga, K., *Inorg. Chim. Acta* 1984, 90, L7.

14. Doi, Y.; Yokata, A.; Miyake, J.; Soga, K., *J. Chem. Soc., Chem. Commun.* 1984, 394.
15. Bentsen, J. G.; Wrighton, M. S., *Inorg. Chem.* 1984, 23, 512.
16. Liu, D. K.; Wrighton, M. S., *J. Am. Chem. Soc.* 1982, 104, 898.
17. Pierantozzi, R.; McQuade, K. J.; Gates, B. C.; Wolf, J.; Knoezinger, J.; Ruhmann, W., *J. Am. Chem. Soc.* 1979, 101, 5436.
18. Lieto, J.; Milstein, D.; Albright, R. L.; Minkiewicz, J. V.; Gates, B. C., *ChemTech* 1983, January, 46.
19. D'Ornelas, L.; Choplin, A.; Basset, J. M.; Hsu, L.-Y.; Shore, S. G., *Nouv. J. Chim.* 1985, 9, 155.
20. Psaro, R.; Ugo, R.; Zanderighi, G. M.; Besson, B.; Smith, A. K.; Basset, J. M., *J. Organomet. Chem.* 1981, 213, 215.
21. Smith, A. K.; Besson, B.; Basset, J. M.; Psaro, R.; Fusi, A.; Ugo, R., *J. Organomet. Chem.* 1980, 192, C31.
22. Hsu, L.-Y.; Shore, S. G.; D'Ornelas, L.; Choplin, A.; Basset, J. M., *Polyhedron* 1988, 7, 2399.
23. Besson, B.; Moraweck, B.; Basset, J. M.; Psaro, R.; Fusi, A.; Ugo, R., *J. Chem. Soc., Chem. Commun.* 1980, 569.
24. Odebunmi, E. O.; Matrana, B. A.; Datye, A. K.; Allard, L. F.; Jr.; Schwank, J.; Manogue, W. H.; Hayman, A.; Onuferko, J. H.; Knoezinger, H.; Gates, B. C., *J. Catal.* 1985, 95, 370.
25. (a) Collier, G.; Hunt, D. J.; Jackson, S. D.; Moyes, R. B.; Pickering, I. A.; Wells, R. B.; Simpson, A. F.; Whyman, R., *J. Catal.* 1983, 80, 154; (b) Hunt, D. J.; Jackson, S. D.; Moyes, R. B.; Wells, P. B.; Whyman, R., *Ibid.* 1984, 86, 333.
26. Ugo, R.; Psaro, R.; Zanderighi, G. M.; Basset, J. M.; Theolier, A.; Smith, A. K., "Fund. Res. Homo. Catal."; Tsutsui, M., Ed.; Vol. 3; Plenum Press: London, 1979.
27. Hughes, F.; Smith, A. K.; Taarit, Y. B.; Basset, J. M., *J. Chem. Soc., Chem. Commun.* 1980, 68.
28. Gladfelter, W. L.; Geoffroy, G. L., *Adv. Organomet. Chem.* 1980, 18, 207.
29. Anderson, J. R.; Elmers, P. S.; Howe, R. F.; Mainwaring, D. E., *J. Catal.* 1977, 50, 508.

30. Mason, R.; Mingos, D. M. P., *J. Organomet. Chem.* 1973, 50, 53.
31. Wade, K., *Chem. Ber.* 1975, 11, 177.
32. (a) Mingos, D. P. M., *Nature (Lond.)*, *Phys. Sci.* 1972, 236, 99; (b) Wade, K., *Adv. Inorg. Chem. Radiochem.* 1976, 18, 1.
33. Wade, K., "Transition Metal Clusters"; Johnson, B. G. F., Ed.; John Wiley & Sons: New York, 1980.
34. (a) Wade, K., *J. Chem. Soc.*, *Chem. Commun.* 1971, 792; (b) Williams, R. E., *Inorg. Chem.* 1971, 10, 210.
35. Lauher, J. W., *J. Am. Chem. Soc.* 1978, 100, 5305.
36. (a) Chini, R.; Heaton, B. T., *Top. Cur. Chem.* 1977, 71, 1; (b) Johnson, B. F. G., *J. Chem. Soc.*, *Chem. Commun.* 1976, 211.
37. Johnson, B. F. G., "Transition Metal Clusters"; Johnson, B. F. G., Ed.; John Wiley & Sons: New York, 1980.
38. Chini, P.; Longoni, G.; Albano, V. G., *Adv. Organomet. Chem.* 1976, 14, 285.
39. (a) Hoffman, R.; Schilling, B. E. R.; Bau, R.; Kaesz, H. D.; Mingos, D. M. P., *J. Am. Chem. Soc.* 1978, 100, 6088; (b) Green, J. C.; Mingos, D. M. P.; Sneddon, E. A., *J. Organomet. Chem.* 1980, 185, C20.
40. (a) Yawney, D. B. W.; Stone, F. G. A., *J. Chem. Soc. (A)*, 1969, 502; (b) Yawney, D. B. W.; Stone, F. G. A., *J. Chem. Soc.*, *Chem. Commun.* 1968, 619.
41. Fernandez, J. M.; Johnson, B. F. G.; Lewis, J.; Raithby, P. R., *J. Chem. Soc.*, *Dalton Trans.* 1981, 2250.
42. Johnson, B. F. G.; Johnston, R. D.; Lewis, J.; Williams, I. G., *J. Chem. Soc.*, *Chem. Commun.* 1968, 861.
43. (a) Eady, C. R.; Johnson, B. F. G.; Lewis, J., *J. Chem. Soc.*, *Dalton Trans.* 1975, 2606; (b) Eady, C. R.; Johnson, B. F. G.; Lewis, J., *J. Organomet. Chem.* 1972, 37, C39; (c) Reichert, B. E.; Sheldrick, G. M., *Acta Crystallogr.* 1977, B33, 173; (d) Eady, C. R.; Johnson, B. F. G.; Lewis, J.; Reichert, B. E.; Sheldrick, G. M., *J. Chem. Soc.*, *Chem. Commun.* 1976, 271; (e) Guy, J. J.; Sheldrick, G. M., *Acta Crystallogr.* 1978, B34, 1725.

44. (a) Eady, C. R.; Johnson, B. F. G.; Lewis, J., *J. Chem. Soc., Dalton Trans.* 1977, 838; (b) Johnson, B. F. G.; Johnston, R. D.; Lewis, J., *J. Chem. Soc. (A)* 1968, 2865.
45. Stone, F. G. A., "Inorganic Chemistry: Toward the 21st Century"; Chisholm, M. H., Ed.; ACS Symposium Series 211; Am. Chem. Soc.; 1983, 383-397.
46. Stone, F. G. A., "Organometallic Compounds Synthesis, Structure and Theory"; Shapiro, B. L., Ed.; Texas A&M Univ. Press: College Station, TX 1983.
47. Ashworth, T. A.; Howard, J. A. K.; Stone, F. G. A., *J. Chem. Soc., Chem. Commun.* 1979, 42.
48. Kennedy, S., Ph.D. Dissertation, The Ohio State Univ. 1982.
49. Jan, D.-Y., Ph.D. Dissertation, The Ohio State Univ. 1985.
50. (a) Plotkin, J. S.; Alway, D. G.; Weiserberger, C. R.; Shore, S. G., *J. Am. Chem. Soc.* 1980, 102, 6156; (b) Churchill, M. R.; Bueno, C.; Kennedy, S.; Bricker, J. C.; Plotkin, J. S.; Shore, S. G., *Inorg. Chem.* 1982, 21, 627; (c) Shore, S. G.; Hsu, W.-L.; Weisenberger, C. R.; Caste, M. L.; Churchill, M. R.; Bueno, C., *Organometallics* 1982, 1, 1405; (d) Shore, S. G.; Hsu, W.-L.; Churchill, J. R.; Bueno, C., *J. Am. Chem. Soc.* 1983, 105, 655; (e) Hsu, L.-Y.; Hsu, W.-L.; Jan, D.-Y.; Marshall, A. G.; Shore, S. G., *Organometallics* 1984, 3, 591; (f) Jan, D.-Y.; Hsu, W.-L.; Shore, S. G., *Inorganic Synthesis*, submitted for publication; (g) Shore, S. G.; Hsu, W.-L.; *US PATENT 4,515,728*; May 7, 1985; (h) Shore, S. G.; Jan, D.-Y.; Hsu, L.-Y.; Hsu, W.-L., *J. Am. Chem. Soc.* 1983, 105, 5923; (i) Shore, S. G.; Jan, D.-Y.; Hsu, W.-L.; Hsu, L.-Y.; Kennedy, S.; Huffman, J. C.; Wang, T.-C. L.; Marshall, A. G., *J. Chem. Soc., Chem. Commun.* 1984, 392.
51. Humphries, A. P.; Kaesz, H. D., *Progress in Inorg. Chem.* 1977, 25, 146.
52. Vargas, M. D.; Nicholls, J. N., *Adv. Inorg. Chem. Radiochem.* 1986, 30, 123.
53. Hieber, W.; Shubert, E. H., *Z. Allorg. Allg. Chem.* 1965, 338, 32.
54. Ruff, J. K., *Inorg. Chem.* 1968, 7, 1818.
55. Anders, U.; Graham, W. A. G., *J. Chem. Soc., Chem. Commun.* 1966, 291.

56. Hsu, L.-Y.; Bhattacharrya, J.; Shore, S. G., *Organometallics* 1985, 4, 1483.
57. Coffy, T. J.; Shore, S. G., submitted for publication.
58. Ruff, J. K.; White, R. P., Jr.; Dahl, L. F., *J. Am. Chem. Soc.* 1971, 93, 2159.
59. (a) Knight, J.; Mays, M. J., *J. Chem. Soc., Dalton Trans* 1972, 1022; (b) Knight, J.; Mays, J. J., *J. Chem. Soc., Chem. Commun.* 1971, 62; (c) Churchill, M. R.; Wormald, J.; Knight, J.; Mays, M. J., *J. Chem. Soc., Chem. Commun.* 1970, 458.
60. Steinhardt, R. C.; Gladfelter, W. L.; Harley, A. D.; Fox, J. R.; Geoffroy, G. L., *Inorg. Chem.* 1980, 19, 332.
61. Ceriotti, A.; Longoni, G.; Pergola, R. D.; Heaton, B. T.; Smith, D. O., *J. Chem. Soc., Dalton Trans.* 1983, 1433.
62. Heaton, B. T., submitted for publication.
63. Fumagalli, A.; Martinengo, S.; Ciani, G.; Marturano, G., *Inorg. Chem.* 1986, 25, 592.
64. Bhattacharrya, A. A.; Nagel, C. C.; Shore, S. G., *Organometallic* 1983, 2, 1187.
65. Bhattacharrya, A. A.; Shore, S. G., *Organometallics* 1983, 2, 1251.
66. Shore, S. G.; Bhattacharrya, A. A., *US PATENT 4,496,532*, Jan. 29, 1985.
67. Hayward, C.-M. T.; Shapley, J. R., *Inorg. Chem.* 1982, 21, 3816.
68. (a) Inkrott, K. E.; Shore, S. G., *Inorg. Chem.* 1979, 18, 2817; (b) Inkrott, K. S.; Shore, S. G., *J. Am. Chem. Soc.* 1978, 100, 3964; (c) Kennedy, S.; Alexander, J. J.; Shore, S. G., *J. Organomet. Chem.* 1981, 219, 385; (d) Johnson, B. F. G.; Lewis, J.; Raithby, P. R.; Suss, G., *J. Chem. Soc., Dalton Trans.* 1979, 1356; (e) Johnson, B. F. G.; Lewis, J.; Raithby, P. R.; Sheldrick, G. M.; Suss, G., *J. Organomet. Chem.* 1978, 162, 179; (f) Johnson, B. F. G.; Johnston, R. D.; Lewis, J.; Robinson, B. H.; Wilkinson, G., *J. Chem. Soc. (A)* 1968, 2856.
69. Venalaiene, T.; Pakkanen, T. A., *J. Organomet. Chem.* 1986, 316, 183.

70. (a) Geoffroy, G. L.; Gladfelter, W. L., *J. Am. Chem. Soc.* 1977, 99, 7565; (b) Geoffroy, G. L.; Gladfelter, W. L., *Ibid.* 1977, 99, 304.
71. Geoffroy, G. L.; Fox, J. R.; Burkhardt, E.; Foley, J. C.; Harley, A. D.; Rosen, R., *Inorganic Synthesis* 1982, 21, 57.
72. (a) Gladfelter, W. L.; Geoffroy, G. L., *Inorg. Chem.* 1980, 19, 2579; (b) Geoffroy, G. L.; Gladfelter, W. L., *J. Am. Chem. Soc.* 1977, 99, 6775; (c) Milone, L.; Aime, S.; Randall, E. W.; Rosenberg, E., *J. Chem. Soc., Chem. Commun.* 1975, 452.
73. Gilmore, C. J.; Woodward, P., *J. Chem. Soc., Chem. Commun.* 1970, 1463.
74. Hsu, L.-Y.; Bhattacharyya, A. A.; Shore, S. G., *Acta Crystallogr.* 1984, C40, 722.
75. Siriwardane, U., Ph.D. Dissertation, The Ohio State Univ. 1985.
76. Knox, S. A. R.; Koepke, J. W.; Andrews, M. A.; Kaesz, H. D., *J. Am. Chem. Soc.* 1975, 97, 3942.
77. (a) Gladfelter, W. L.; Fox, J. R.; Smegal, J. A.; Wood, T. G.; Geoffroy, G. L., *Inorg. Chem.* 1981, 20, 3223; (b) Fox, J. R.; Gladfelter, W. L.; Wood, T. G.; Smegal, J. A.; Foreman, T. K.; Geoffroy, G. L.; Tavanairpour, I.; Day, V. W.; Day, C. S., *Inorg. Chem.* 1981, 20, 3214; (c) Takusagawa, F.; Fumagalli, A.; Koetzle, T. F.; Steinmetz, G. R.; Rosen, R. P.; Gladfelter, W. L.; Geoffroy, G. L.; Bruck, M. A.; Bau, R., *Inorg. Chem.* 1981, 20, 3823; (d) Fox, J. R.; Gladfelter, W. L.; Geoffroy, G. L.; Tavanaiepour, I.; Abdel-Mequid, S.; Day, V. W., *Inorg. Chem.* 1981, 20, 3230; (e) Fox, J. R.; Gladfelter, W. L.; Geoffroy, G. L., *Inorg. Chem.* 1980, 19, 2574.
78. (a) Choplin, A.; Huang, L.; Basset, J. M.; Mathieu, R.; Siriwardane, U.; Shore, S. G., *Organometallics* 1986, 5, 1547; (b) Choplin, A.; Huang, L.; Theolier, A.; Gallezot, P.; Basset, J. M.; Siriwardane, U.; Shore, S. G.; Mathieu, R., *J. Am. Chem. Soc.* 1986, 108, 4224.
79. Furuya, F. R.; Gladfelter, W. L., *J. Chem. Soc., Chem. Commun.* 1986, 129.
80. Roberts, D. A.; Geoffroy, G. L., "Comprehensive Organometallic Chemistry"; Vol. 6; Pergamon Press: New York; 1982, Chap. 40.
81. (a) Parshall, G. W., *J. Am. Chem. Soc.* 1964, 86, 361; (b) Anders, U.; Graham, W. A. G., *J. Am. Chem. Soc.* 1967, 89, 539.

82. (a) Minot, C.; Criado-Sancho, M., *Nouv. J. Chim.* 1984, 8, 537;  
(b) Mingos, D. M. P., *Chem. Soc. Rev.* 1986, 15, 31.
83. (a) Hoffmann, R., *Science* 1981, 211, 995; (b) Hoffmann, R.,  
*Angew. Chem. Int. Ed. Engl.* 1982, 21, 711.
84. Eady, C. R.; Jackson, P. F.; Johnson, B. F. G.; Lewis, J.;  
Malatesta, M. C.; McPartlin, M.; Nelson, W. J. H., *J. Chem. Soc.,  
Dalton Trans.* 1980, 383.
85. Jackson, P. F.; Johnson, B. F. G.; Lewis, J.; McPartlin, M.;  
Nelson, W. J. H., *J. Chem. Soc., Chem. Commun.* 1979, 735.
86. Eady, C. R.; Johnson, B. F. G.; Lewis, J.; Malatesta, M. C.;  
Machin, P.; McPartlin, M., *J. Chem. Soc., Chem. Commun.* 1976,  
945.
87. Churchill, M. R.; Wormald, J., *J. Am. Chem. Soc.* 1971, 93, 5670.
88. Mason, R.; Thomas, K. M.; Mingos, D. M. P., *J. Am. Chem. Soc.*  
1973, 95, 3802.
89. Churchill, M. R.; Hollander, F. J.; Hutchinson, J. P., *Inorg.  
Chem.* 1977, 16, 2655.
90. Jackson, P. F.; Johnson, B. F. G.; Lewis, J.; McPartlin, J.;  
Nelson, W. J. H., *J. Chem. Soc., Chem. Commun.* 1978, 920.
91. Jenson, J. A.; Fjare, D. E.; Gladfelter, W. L., *Inorg. Chem.*  
1983, 22, 1250.
92. Churchill, J. R.; Hooander, F. J., *Inorg. Chem.* 1979, 18, 161.
93. Gilmore, G. J.; Woodward, P., *J. Chem. Soc. (A)* 1971, 3453.
94. Churchill, M. R.; Bueno, C.; Hsu, L.-Y.; Plotkin, J. S.; Shore,  
S. G., *Inorg. Chem.* 1982, 21, 1958.
95. Orpen, A. G.; Rivera, V.; Bryan, E. G.; Pippard, P.; Sheldrick,  
G. M., *J. Chem. Soc., Chem. Commun.* 1978, 723.
96. Churchill, M. R.; Wasserman, H. J., *Inorg. Chem.* 1980, 19, 239.
97. Churchill, M. R.; Li, Y.-J., *J. Organomet. Chem.* 1985, 291, 61.
98. Krause, J. A., MS Thesis, The Ohio State Univ. 1987.

99. (a) Williams, J.; Broach, R. W., *Inorg. Chem.* 1979, 18, 314; (b) Churchill, M. R.; Hollander, F. J.; Hutchinson, J. P., *Inorg. Chem.* 1977, 16, 2697.
100. (a) Churchill, M. R.; DeBoer, B. G., *Inorg. Chem.* 1977, 16, 878; (b) Johnson, B. F. G.; Lewis, J.; Kilty, P. A., *J. Chem. Soc. (A)* 1968, 2859.
101. Churchill, M. R.; DeBoer, B. G.; Rotella, F. J., *Inorg. Chem.* 1976, 15, 1843.
102. Shore, S. G.; Hsu, L.-Y., unpublished results.
103. Moss, J. R.; Graham, W. A. G., *J. Organomet. Chem.* 1970, 23, C23.
104. Graham, W. A. G.; Moss, J. R., *J. Organomet. Chem.* 1984, 270, 237.
105. Knight, J.; Mays, M. J., *J. Chem. Soc., Chem. Commun.* 1970, 1006.
106. Eadie, D. T.; Holden, H. D.; Johnson, B. F. G.; Lewis, J., *J. Chem. Soc., Dalton Trans.* 1984, 301.
107. Hsu, W.-L.; Shore, S. G., unpublished results.
108. Adams, R. D.; Babin, J. E.; Tasi, M., *Organometallics* 1988, 7, 219.
109. Burkhardt, E. W.; Geoffroy, G. L., *J. Organomet. Chem.* 1980, 198, 179.
110. Foulds, G. A.; Johnson, B. F. G.; Lewis, J.; Sorrell, R. M., *J. Chem. Soc., Dalton Trans.* 1986, 2515.
111. (a) Johnson, B. F. G.; Lewis, J.; Pippard, D. A., *J. Chem. Soc., Dalton Trans.* 1981, 407; (b) Tachikawa, M.; Shapley, J. R., *J. Organomet. Chem.* 1977, 124, C19; (c) Dawson, P. A.; Johnson, B. F. G.; Lewis, J.; Puga, J.; Raithby, P. R.; Rosales, M. J., *J. Chem. Soc., Dalton Trans.* 1982, 233.
112. Cotton, J. D.; Bruce, M. I.; Stone, F. G. A., *J. Chem. Soc. (A)* 1968, 2162.
113. Budge, J. R.; Scott, J. P.; Gates, B. C., *J. Chem. Soc., Chem. Commun.* 1983, 342.

114. Scott, J. P.; Budge, J. R.; Rheingold, A. L.; Gates, B. C., *J. Am. Chem. Soc.* 1987, 109, 7736.
115. Rheingold, A. L.; Gates, B. C.; Scott, J. P.; Budge, J. R., *J. Organomet. Chem.* 1987, 331, 81.
116. Churchill, M. R.; Hollander, F. J., *Inorg. Chem.* 1980, 19, 306.
117. Churchill, M. R.; Hollander, F. J., *Inorg. Chem.* 1979, 18, 843.
118. Glusker, J. P.; Trueblood, K. N., "Crystal Structure Analysis A Primer"; Second Edition; Oxford Univ. Press: New York, 1985.
119. Yawney, D. B. W.; Doedens, R. J., *Inorg. Chem.* 1972, 11, 838.
120. (a) Wei, C. H.; Dahl, L. F., *J. Am. Chem. Soc.* 1966, 88, 1821; (b) Wei, C. H.; Wilkes, G. R.; Dahl, L. F., *J. Am. Chem. Soc.* 1967, 89, 4792.
121. Owen, S. M., *Polyhedron* 1988, 7, 253.
122. McPartlin, M., *Polyhedron* 1984, 3, 1279.
123. (a) Mingos, D. M. P., *Acc. Chem. Res.* 1984, 17, 311; (b) Mingos, D. M. P., *J. Chem. Soc., Chem. Commun.* 1983, 706.
124. Basset, J. M.; Ugo, R., "Aspects of Homogeneous Catalysis"; Vol. 3; Ugo, R., Ed.; D. Reidel Publ. Co.: Boston, 1977; 145-147.
125. (a) Burton, J. J., *Cat. Rev.-Sci. Eng.* 1974, 9, 209; (b) Mader, S., *J. Vac. Sci. Technol.* 1971, 8, 247; (c) Hoare, M, R.; Pal, P., *J. Cryst. Growth* 1972, 17, 77; (d) Hoffmann, R.; Lipscomb, W. N., *J. Chem. Phys.* 1962, 36, 2179; (e) Prestridge, E. B.; Yates, D. J. C., *Nature* 1971, 234, 345.
126. Lavigne, G.; Kaesz, H. D., *J. Am. Chem. Soc.* 1984, 106, 4647.
127. (a) Hart, D. W.; Teller, R. G.; Wei, C.-Y.; Bau, R.; Longoni, G.; Campanella, S.; Chini, P.; Koetzle, T. F., *J. Am. Chem. Soc.* 1981, 103, 1458; (b) Hart, D. W.; Teller, R. G.; Wei, C.-Y.; Bau, R.; Longoni, G.; Campanella, S.; Chini, P.; Koetzle, T. F., *Angew. Chem. Int. Ed. Engl.* 1979, 18, 80.
128. Deeming, A. J., *Adv. Organometal Chem.* 1986, 26,1.
129. John, G. R.; Johnson, B. F. G.; Lewis, J., *J. Organomet. Chem.* 1979, 181, 143.

130. (a) Farrar, D. H.; Johnson, B. F. G.; Lewis, J.; Raithby, P. R.; Rosales, M. J., *J. Chem. Soc., Dalton Trans.* 1982, 2051;  
(b) Nicholls, J. N.; Farrar, D. H.; Jackson, P. F.; Johnson, B. F. G.; Lewis, J., *J. Chem. Soc., Dalton Trans.* 1982, 1395.
131. (a) Brown, H. C., "Hydroboration"; Benjamin: New York, 1962;  
(b) Brown, H. C., *Acc. Chem. Soc.* 1969, 2, 65.
132. Demitras, G. C.; Muetterties, E. L., *J. Am. Chem. Soc.* 1977, 99, 2796.
133. Keister, J., *J. Chem. Soc., Chem. Commun.* 1979, 214.
134. Keister, J. B.; Payne, M. W.; Muscatella, M. J., *Organometallics* 1983, 2, 219.
135. (a) Yeh, W.-Y.; Shapley, J. R.; Li, Y.-J.; Churchill, M. R., *Organometallics* 1985, 4, 767; (b) Gavens, P. D.; Mays, M. J., *J. Organomet. Chem.* 1978, 162, 389.
136. Churchill, M. R.; Beanan, L. R.; Wasserman, H. J.; Bueno, C.; Rahman, Z. A.; Keister, J. B., *Organometallics* 1983, 2, 1179.
137. Shriver, D. F.; Drezdson, M. A., "The Manipulation of Air-Sensitive Compounds"; Second Edition; Wiley-Interscience: New York, 1986.
138. Denton, D. L., Ph.D. Dissertation, The Ohio State Univ., 1973..
139. Payne, M. W., Ph.D. Dissertation, The Ohio State Univ., 1987.
140. SDP (Structure Determination Package); B. A. Frenz and Associates: College Station, TX, 1982, 1985.
141. Johnson, C. K., "ORTEP: A Fortran Thermal-Ellipsoid Plot Program for Crystal Structure Illustrations"; Oak Ridge National Laboratory: Oak Ridge, TN, 1965.
142. Hsu, L.-Y., "PSORTEP, A Fortran Thermal-Ellipsoid Crystal Structure Plot Program for the PS300 Series Terminal"; The Ohio State Univ.: Columbus, OH, 1988.
143. Enraf-Nonius CAD4 Diffractometer User's Manual; Enraf-Nonius Delft: Delft, The Netherlands, 1982, 1988.
144. Stout, G. H.; Jensen, L. H., "X-ray Structure Determination"; Macmillan: New York, 1968.
145. Gordon, A. J.; Ford, R. A., "A Chemist's Companion"; John Wiley & Sons: New York, 1972.

146. Nagel, C. C.; Bricker, J. C.; Alway, D. G.; Shore, S. G., *J. Organomet. Chem.* 1981, 219, C9.
147. Holmgren, J. S.; Shapley, J. R., *Organometallics* 1984, 3, 1322.
148. (a) Bartholomew, C. H.; Uken, A. H., *Applied Catal.* 1982, 4, 19;  
(b) Uken, A. H.; Bartholomew, C. H., *J. Catal.* 1960, 65, 402.
149. Keister, J. B.; Payne, M. W.; Muscatella, M. J., *Orgnaometallics* 1983, 2, 219.
150. Johnson, B. F. G.; Lewis, J.; Orpen, A. G.; Raithby, P. R., *J. Organomet. Chem.* 1979, 173, 187.
151. Shapley, J. R.; Cree-Uchiyama, J. E.; St. George, G. M., *J. Am. Chem. Soc.* 1983, 105, 140.
152. Bricker, J. C., Ph.D. Dissertation, The Ohio State Univ., 1983.
153. Nagel, C. C., Ph.D. Dissertation, The Ohio State Univ., 1981.
154. (a) Deeming, A. J.; Underhill, M., *J. Chem. Soc., Dalton Trans.* 1974, 1415; (b) Deeming, A. J.; Underhill, M., *J. Chem. Soc., Chem. Commun.* 1973, 277; (c) Keister, J. B.; Shapley, J. R., *J. Organomet. Chem.* 1975, 85, C29.
155. Shriver, D. F.; Sailor, M. J., personal communication.
156. Shapley, J. R.; Strickland, D. S.; St. George, G. M.; Churchill, M. R.; Bueno, C., *Organometallics* 1983, 2, 185.
157. Eady, C. R.; Johnson, B. F. G.; Lewis, J., *J. Chem. Soc., Dalton Trans.* 1977, 477.
158. Kaesz, H. D.; Knox, S. A. R.; Koepke, J. W.; Saillant, R. B., *J. Chem. Soc., Chem. Commun.* 1971, 477.
159. Jan, D.-Y.; Shore, S. G., *Organometallics* 1987, 6, 428.
160. Porter, R. D.; Gupta, S. K., *J. Phys. Chem.* 1964, 68, 280.
161. Krause, J. A.; Shore, S. G., manuscript in preparation.
162. Shapley, J. R., personal communication.
163. Yesinowski, J. P.; Bailey, D., *J. Organomet. Chem.* 1974, 65, C27.
164. Evans, J.; McNulty, G. S., *J. Chem. Soc., Dalton Trans.* 1984, 79.